E-ISSN 2587-0831

Indexed in PubMed Central and Web of Science - ESCI

European Journal of Breast Health

VOLUME: 22 • ISSUE: 3 • JULY 2026

EUROPEAN JOURNAL OF BREAST HEALTH

SENOLOGIC INTERNATIONAL SOCIETY
INTERNATIONAL SCHOOL OF SENOLOGY

NCBC
National Consortium of Breast Centers

European Journal of Breast Health is the official journal of the Turkish Federation of Breast Diseases Societies

The Senologic International Society (SIS) and the National Consortium of Breast Centers (NCBC) are the official supporters of the journal.

eurjbreasthealth.com

galenos

eurjbreasthealth.com

European Journal of Breast Health

Société Internacionale de Sénologie
Senologic International Society
Global Federation of Breast Healthcare Societies

SIS is the official supporter of the European Journal of Breast Health

TMHDF

European Journal of Breast Health is the official journal of the **Turkish Federation of Breast Diseases Societies**

Contact
Department of General Surgery,
İstanbul University İstanbul Faculty of Medicine, C Service Çapa / İstanbul
Phone/Fax : + 90 212 534 02 10

The European Journal of Breast Health indexed in PubMed Central, Web of Science-Emerging Sources Citation Index, Scopus, TUBITAK ULAKBIM TR Index, Embase, EBSCO, CINAHL, Türk Medline, CNKI and DOAJ.

galenos Publishing House

Publisher Contact
Address: Molla Gürani Mah. Kaçamak Sk. No: 21/1 34093 İstanbul, Türkiye
Phone: +90 (530) 177 30 97
E-mail: info@galenos.com.tr/yayin@galenos.com.tr
Web: www.galenos.com.tr

Publisher Certificate Number: 14521
Online Publication Date: July 2026
E-ISSN: 2587-0831
International scientific journal published quarterly.

European Journal of Breast Health

Editorial Advisory Board

European Journal of Breast Health

Aims and Scope

The European Journal of Breast Health (Eur J Breast Health) is an international, scientific, open access periodical published by independent, unbiased, and double-blinded peer-review principles journal. It is the official publication of the Turkish Federation of Breast Diseases Societies, and the Senologic International Society (SIS) is the official supporter of the journal.

The European Journal of Breast Health is published quarterly in January, April, July, and October. The publication language of the journal is English.

EJBH aims to be a comprehensive, multidisciplinary source and contribute to the literature by publishing manuscripts with the highest scientific level in the fields of research, diagnosis, and treatment of all breast diseases; scientific, biologic, social and psychological considerations, news and technologies concerning the breast, breast care and breast diseases.

The journal publishes original research articlesreviews, letters to the editor, brief correspondences, meeting reports, editorial summaries, observations, novel ideas, basic and translational research studies, clinical and epidemiological studies, treatment guidelines, expert opinions, commentaries, clinical trials and outcome studies on breast health, biology and all kinds of breast diseases, and very original case reports that are prepared and presented according to the ethical guidelines.

TOPICS within the SCOPE of EJBH concerning breast health, breast biology and all kinds of breast diseases:

Epidemiology, Risk Factors, Prevention, Early Detection, Diagnosis and Therapy, Psychological Evaluation, Quality of Life, Screening, Imaging Management, Image-guided Procedures, Immunotherapy, molecular Classification, Mechanism-based Therapies, Carcinogenesis, Hereditary Susceptibility, Survivorship, Treatment Toxicities, and Secondary Neoplasms, Biophysics, Mechanisms of Metastasis, Microenvironment, Basic and Translational Research, Integrated Treatment Strategies, Cellular Research and Biomarkers, Stem Cells, Drug Delivery Systems, Clinical Use of Anti-therapeutic Agents, Radiotherapy, Chemotherapy, Surgery, Surgical Procedures and Techniques, Palliative Care, Patient Adherence, Cosmesis, Satisfaction and Health Economic Evaluations.

The target audience of the journal includes specialists and medical professionals in surgery, oncology, breast health and breast diseases.

The editorial and publication processes of the journal are shaped in accordance with the guidelines of the International Committee of Medical Journal Editors (ICMJE), World Association of Medical Editors (WAME), Council of Science Editors (CSE), Committee on Publication Ethics (COPE), European Association of Science Editors (EASE), and National Information Standards Organization (NISO). The journal conforms with the Principles of Transparency and Best Practice in Scholarly Publishing (doaj.org/bestpractice).

The European Journal of Breast Health indexed in PubMed Central, Web of Science-Emerging Sources Citation Index, TUBITAK ULAKBIM TR Index, Embase, EBSCO, CINAHL, Scopus.

Submission Fee

The European Journal of Breast Health (Eur J Breast Health) has an open access to all articles published by itself and provides online free access as soon as it is published in the journal. We have published our journal for more than 15 years without any requests from you. But today, European Journal of Breast Health has had to charge you a low fee (150$) at the time of application to cover its increasing costs for services.

Open Access Policy

This journal provides immediate open and free access to its content on the principle that making research freely available to the public supports a greater global exchange of knowledge.

Open Access Policy is based on the rules of the Budapest Open Access Initiative (BOAI) http://www.budapestopenaccessinitiative.org/. By “open access” to peer-reviewed research literature, we mean its free availability on the public internet, permitting any users to read, download, copy, distribute, print, search, or link to the full texts of these articles, crawl them for indexing, pass them as data to software, or use them for any other lawful purpose, without financial, legal, or technical barriers other than those inseparable from gaining access to the internet itself. The only constraint on reproduction and distribution, and the only role for copyright in this domain, should be to give authors control over the integrity of their work and the right to be properly acknowledged and cited.

Contact: info@eurjbreasthealth.com

All expenses of the journal are covered by the Turkish Federation of Breast Diseases Societies and the Senologic International Society (SIS). Potential advertisers should contact the Editorial Office. Advertisement images are published only upon the Editor-in-Chief’s approval.

Publisher: Galenos Yayınevi

Address: Molla Gürani Mah. Kaçamak Sok. 21/1
Fındıkzade, Fatih, Istanbul, Türkiye

Phone : +90 (530) 177 30 97

E-mail : info@galenos.com.tr

Web : www.galenos.com.tr

European Journal of Breast Health

Instructions to Authors

The European Journal of Breast Health (Eur J Breast Health) is an international, open access, online-only periodical published in accordance with the principles of independent, unbiased, and double-blinded peer-review.

The journal is owned by Turkish Federation of Breast Diseases Societies and affiliated with Senologic International Society (SIS), and it is published quarterly on January, April, July, and October. The publication language of the journal is English. The target audience of the journal includes specialists and medical professionals in general surgery and breast diseases.

The editorial and publication processes of the journal are shaped in accordance with the guidelines of the International Council of Medical Journal Editors (ICMJE), the World Association of Medical Editors (WAME), the Council of Science Editors (CSE), the Committee on Publication Ethics (COPE), the European Association of Science Editors (EASE), and National Information Standards Organization (NISO). The journal conforms to the Principles of Transparency and Best Practice in Scholarly Publishing (doaj.org/bestpractice).

Originality, high scientific quality, and citation potential are the most important criteria for a manuscript to be accepted for publication. Manuscripts submitted for evaluation should not have been previously presented or already published in an electronic or printed medium. The journal should be informed of manuscripts that have been submitted to another journal for evaluation and rejected for publication. The submission of previous reviewer reports will expedite the evaluation process. Manuscripts that have been presented in a meeting should be submitted with detailed information on the organization, including the name, date, and location of the organization.

Manuscripts submitted to the European Journal of Breast Health will go through a double-blind peer-review process. Each submission will be reviewed by at least two external, independent peer reviewers who are experts in their fields in order to ensure an unbiased evaluation process. The editorial board will invite an external and independent editor to manage the evaluation processes of manuscripts submitted by editors or by the editorial board members of the journal. The Editor in Chief is the final authority in the decision-making process for all submissions.

An approval of research protocols by the Ethics Committee in accordance with international agreements (World Medical Association Declaration of Helsinki "Ethical Principles for Medical Research Involving Human Subjects," amended in October 2013, www.wma.net) is required for experimental, clinical, and drug studies and for some case reports. If required, ethics committee reports or an equivalent official document will be requested from the authors. For manuscripts concerning experimental research on humans, a statement should be included that shows that written informed consent of patients and volunteers was obtained following a detailed explanation of the procedures that they may undergo. For studies carried out on animals, the measures taken to prevent pain and suffering of the animals should be stated clearly. Information on patient consent, the name of the ethics committee, and the ethics committee approval number should also be stated in the Materials and Methods section of the manuscript. It is the authors' responsibility to protect the patients' anonymity carefully. For photographs that may reveal the identity of the patients, signed releases of the patient or their legal representative should be enclosed.

All submissions are screened by a similarity detection software (iThenticate by CrossCheck).

In the event of alleged or suspected research misconduct, e.g., plagiarism, citation manipulation, and data falsification/fabrication, the Editorial Board will follow and act in accordance with COPE guidelines.

Each individual listed as an author should fulfill the authorship criteria recommended by the International Committee of Medical Journal Editors

(ICMJE - www.icmje.org). The ICMJE recommends that authorship be based on the following 4 criteria:

1. Substantial contributions to the conception or design of the work; or the acquisition, analysis, or interpretation of data for the work; AND

2. Drafting the work or revising it critically for important intellectual content; AND

3. Final approval of the version to be published; AND

4. Agreement to be accountable for all aspects of the work in ensuring that questions related to the accuracy or integrity of any part of the work are appropriately investigated and resolved.

In addition to being accountable for the parts of the work he/she has done, an author should be able to identify which co-authors are responsible for specific other parts of the work. In addition, authors should have confidence in the integrity of the contributions of their co-authors.

All those designated as authors should meet all four criteria for authorship, and all who meet the four criteria should be identified as authors. Those who do not meet all four criteria should be acknowledged in the title page of the manuscript.

The European Journal of Breast Health requires corresponding authors to submit a signed and scanned version of the Copyright Transfer and Acknowledgement of Authorship Form (available for download through www.eurjbreasthealth.com) during the initial submission process in order to act appropriately on authorship rights and to prevent ghost or honorary authorship. If the editorial board suspects a case of "gift authorship," the submission will be rejected without further review. As part of the submission of the manuscript, the corresponding author should also send a short statement declaring that he/she accepts to undertake all the responsibility for authorship during the submission and review stages of the manuscript.

European Journal of Breast Health requires and encourages the authors and the individuals involved in the evaluation process of submitted manuscripts to disclose any existing or potential conflicts of interests, including financial, consultant, and institutional, that might lead to potential bias or a conflict of interest. Any financial grants or other support received for a submitted study from individuals or institutions should be disclosed to the Editorial Board. To disclose a potential conflict of interest, the ICMJE Potential Conflict of Interest Disclosure Form should be filled in and submitted by all contributing authors. Cases of a potential conflict of interest of the editors, authors, or reviewers are resolved by the journal's Editorial Board within the scope of COPE and ICMJE guidelines.

The Editorial Board of the journal handles all appeal and complaint cases within the scope of COPE guidelines. In such cases, authors should get in direct contact with the editorial office regarding their appeals and complaints. When needed, an ombudsperson may be assigned to resolve cases that cannot be resolved internally. The Editor in Chief is the final authority in the decision-making process for all appeals and complaints.

When submitting a manuscript to the European Journal of Breast Health, authors accept to assign the copyright of their manuscript to Turkish Federation of Breast Diseases Societies. If rejected for publication, the copyright of the manuscript will be assigned back to the authors. European Journal of Breast Health requires each submission to be accompanied by a Copyright Transfer and Acknowledgement of Authorship Form (available for download at www.eurjbreasthealth.com). When using previously published content, including figures, tables, or any other material in both print and electronic formats, authors must obtain permission from the copyright holder. Legal, financial and criminal liabilities in this regard belong to the author(s).

Statements or opinions expressed in the manuscripts published in European Journal of Breast Health reflect the views of the author(s) and not the opinions of the editors, the editorial board, or the publisher; the editors, the editorial board, and the publisher disclaim any responsibility or liability for such materials. The final responsibility in regard to the published content rests with the authors.

European Journal of Breast Health

Instructions to Authors

Submission Fee

The European Journal of Breast Health (Eur J Breast Health) has an open access to all articles published by itself and provides online free access as soon as it is published in the journal. We have published our journal for more than 15 years without any requests from you. But today, your journal has had to charge you a low fee (100$) at the time of application to cover its increasing costs for services.

The services provided in this context are the provision of systems for editors and authors, editorial work, provision of article designs, the establishment of indexing links, provision of other publishing services and support services.

You can take a look at the unbiased article evaluation process here. If you find a problem with the open access status of your article or licensing, you can contact editor@eurjbreasthealth.com

After your submission to the Eur J Breast Health evaluation system, the submission fees are collected from you or through your fund provider, institution or sponsor.

Eur J Breast Health regularly reviews the fees of submission fees and may change the fees for submission fees. When determining the costs for Eur J Breast Health submission fees, it decides according to the following developments.

- Quality of the journal,
- Editorial and technical processes of the journal,
- Market conditions,
- Other revenue streams associated with the journal

You can find the submission fees fee list here.

Article type	Price
Original articles	$150
Editorial comment	Free of charge
Review article (No application fee will be charged from invited authors)	$150
Case report	$150
Letter to the editor	Free of charge
Images in clinical practices	Free of charge
Current opinion	Free of charge
Systematic review	$150

When and How do I pay?

After the article is submitted to the Eur J Breast Health online evaluation system, an email regarding payment instructions will be sent to the corresponding author.

The editorial review process will be initiated after the payment has been made for the article.

There are two options to purchase the submission fee:

1- Making a remittance

The payment is needed to be made to the account number below. While purchasing the submission fee, please indicate your article manuscript title in the payment description section.

Account no/IBAN: TR49 0011 1000 0000 0098 1779 82 (TL)
TR17 0011 1000 0000 0098 5125 29 (USD)
TR73 0011 1000 0000 0098 5125 88 (EUR)

Account name: Meme Hastalıkları Dernekleri Federasyonu İktisadi İşletmesi

Branch code (QNB Finans Bank Cerrahpaşa): 1020

Swift code: FNNBTRISOPS

NOTE: All authors must pay the bank wire fee additionally. Otherwise, the deducted amount of the submission fee is requested from the author.

2- Virtual POS method (Credit card payment with 3D Secure)

The payment link will be sent to you for your purchase. You can contact us if you have further questions in this regard.

If you believe payment instructions are not in your email contact us via the email addresses **payment@eurjbreasthealth.com** and **journalpay@tmhdf.org.tr**

Refund policy:

The Eur J Breast Health will refund the overpayments of the submission fees for the same article or in case of multiple payments by the authors and financiers as free submission fees payment code to be used in the submission fees system.

Withdrawal of the article; There is no refund for articles whose editorial review has started in the Eur J Breast Health system. You can view article retraction policies here.

Returning the article to the author; The European Journal of Breast Health will refund the submission fees with a coupon code if the article is returned to the author. Using this code, authors can use the submission fees of different articles without making a new payment. You can view article return policies here.

Rejecting or accepting the article; Eur J Breast Health does not refund any submission fees for articles whose editorial process has started, and the process has been completed.

MANUSCRIPT PREPARATION

The manuscripts should be prepared in accordance with ICMJE-Recommendations for the Conduct, Reporting, Editing, and Publication of Scholarly Work in Medical Journals (updated in December 2019 - http://www.icmje.org/icmje-recommendations). Authors are required to prepare manuscripts in accordance with the CONSORT guidelines for randomized research studies, STROBE guidelines for observational original research studies, STARD guidelines for studies on diagnostic accuracy, PRISMA guidelines for systematic reviews and meta-analysis, ARRIVE guidelines for experimental animal studies, and TREND guidelines for non-randomized public behaviour.

Manuscripts can only be submitted through the journal's online manuscript submission and evaluation system, available at www.eurjbreasthealth.com. Manuscripts submitted via any other medium will not be evaluated.

Manuscripts submitted to the journal will first go through a technical evaluation process where the editorial office staff will ensure that the manuscript has been prepared and submitted in accordance with the journal's guidelines. Submissions that do not conform to the journal's guidelines will be returned to the submitting author with technical correction requests.

Authors are required to submit the following:

- Copyright Transfer and Acknowledgement of Authorship Form, and
- ICMJE Potential Conflict of Interest Disclosure Form (should be filled in by all contributing authors)

during the initial submission. These forms are available for download at www.eurjbreasthealth.com.

Preparation of the Manuscript

Title page: A separate title page should be submitted with all submissions, and this page should include:

European Journal of Breast Health

Instructions to Authors

• The full title of the manuscript as well as a short title (running head) of no more than 50 characters,

• Name(s), affiliations, and highest academic degree(s) of the author(s),

• Grant information and detailed information on the other sources of support,

• Name, address, telephone (including the mobile phone number) and fax numbers, and email address of the corresponding author,

• Acknowledgment of the individuals who contributed to the preparation of the manuscript but who do not fulfill the authorship criteria.

Abstract: An English abstract should be submitted with all submissions except for Letters to the Editor. The abstract of Original Articles should be structured with subheadings (Objective, Materials and Methods, Results, and Conclusion). Please check Table 1 below for word count specifications.

Keywords: Each submission must be accompanied by a minimum of three to a maximum of six keywords for subject indexing at the end of the abstract. The keywords should be listed in full without abbreviations. The keywords should be selected from the National Library of Medicine, Medical Subject Headings database (https://www.nlm.nih.gov/mesh/MBrowser.html).

Key Points: All submissions except letters to the editor should be accompanied by 3 to 5 "key points" which should emphasize the most noteworthy results of the study and underline the principle message that is addressed to the reader. This section should be structured as itemized to give a general overview of the article. Since "Key Points" targeting the experts and specialists of the field, each item should be written as plain and straightforward as possible.

Manuscript Types

Original Articles: This is the most important type of article since it provides new information based on original research. The main text of original articles should be structured with "Introduction", "Materials and Methods", "Results", "Discussion and Conclusion" subheadings. Please check Table 1 for the limitations for Original Articles.

Statistical analysis to support conclusions is usually necessary. Statistical analyses must be conducted in accordance with international statistical reporting standards (Altman DG, Gore SM, Gardner MJ, Pocock SJ. Statistical guidelines for contributors to medical journals. Br Med J 1983: 7; 1489-93). Information on statistical analyses should be provided with a separate subheading under the Materials and Methods section,and the statistical software that was used during the process must be specified.

Units should be prepared in accordance with the International System of Units (SI).

Editorial Comments: Editorial comments aim to provide a brief critical commentary by reviewers with expertise or with high reputation in the topic of the research article published in the journal. Authors are selected and invited by the journal to provide such comments. Abstract, Keywords, and Tables, Figures, Images, and other media are not included.

Review Articles: Reviews prepared by authors who have extensive knowledge on a particular field and whose scientific background has been translated into a high volume of publications with a high citation potential are welcomed. These authors may even be invited by the journal. Reviews should describe, discuss, and evaluate the current level of knowledge of a topic in clinical practice and should guide future studies. The main text should contain Introduction, Clinical and Research Consequences, and Conclusion sections. Please check Table 1 for the limitations for Review Articles.

Case Reports: There is limited space for case reports in the journal and reports on rare cases or conditions that constitute challenges in diagnosis and treatment, those offering new therapies or revealing knowledge not included in the literature, and interesting and educative case reports are accepted for publication. The text should include "Introduction", "Case Presentation", "Discussion and Conclusion" subheadings. Please check Table 1 for the limitations for Case Reports.

Letters to the Editor: This type of manuscript discusses important parts, overlooked aspects, or lacking parts of a previously published article. Articles on subjects within the scope of the journal that might attract the readers' attention, particularly educative cases, may also be submitted in the form of a "Letter to the Editor." Readers can also present their comments on the published manuscripts in the form of a "Letter to the Editor." Abstract, Keywords, and Tables, Figures, Images, and other media should not be included. The text should be unstructured. The manuscript that is being commented on must be properly cited within this manuscript.

Images in Clinical Practices: Our journal accepts original high-quality images related to the cases that we come across during clinical practices, that cite the importance or infrequency of the topic, make the visual quality stand out and present important information that should be shared in academic platforms. Titles of the images should not exceed 10 words. Images can be signed by no more than 3 authors. Figure legends are limited to 200 words, and the number of figures is limited to 3. Video submissions will not be considered.

Current Opinion: Current Opinion provides readers with a commentary of either recently published articles in the European Journal of Breast Health or some other hot topic selected articles. Authors are selected and invited by the journal for such commentaries. This type of article contains three main sections titled as Background, Present Study, and Implications. Authors are expected to describe the background of the subject/study briefly, critically discuss the present research, and provide insights for future studies.

Table 1. Limitations for each manuscript type

Type of manuscript	Word limit	Abstract word limit	Reference limit	Table limit	Figure limit
Original Article	3500	250 (Structured)	30	6	7 or tatal of 15 images
Review Article	5000	250	50	6	10 or total of 20 images
Case Report	1000	200	15	No tables	10 or total of 20 images
Letter to the Editor	500	No abstract	5	No tables	No media
Current Opinion	300	No abstract	5	No tables	No media

Tables

Tables should be included in the main document, presented after the reference list, and they should be numbered consecutively in the order they are referred to within the main text. A descriptive title must be placed above the tables. Abbreviations used in the tables should be defined below the tables by footnotes (even if they are defined within the main text). Tables should be created using the "insert table"

Instructions to Authors

command of the word processing software,and they should be arranged clearly to provide easy reading. Data presented in the tables should not be a repetition of the data presented within the main text but should be supporting the main text.

Figures and Figure Legends

Figures, graphics, and photographs should be submitted as separate files (in TIFF or JPEG format) through the submission system. The files should not be embedded in a Word document or the main document. When there are figure subunits, the subunits should not be merged to form a single image. Each subunit should be submitted separately through the submission system. Images should not be labeled (a, b, c, etc.) to indicate figure subunits. Thick and thin arrows, arrowheads, stars, asterisks, and similar marks can be used on the images to support figure legends. Like the rest of the submission, the figures too should be blind. Any information within the images that may indicate an individual or institution should be blinded. The minimum resolution of each submitted figure should be 300 DPI. To prevent delays in the evaluation process, all submitted figures should be clear in resolution and large in size (minimum dimensions: 100 × 100 mm). Figure legends should be listed at the end of the main document.

All acronyms and abbreviations used in the manuscript should be defined at first use, both in the abstract and in the main text. The abbreviation should be provided in parentheses following the definition.

When a drug, product, hardware, or software program is mentioned within the main text, product information, including the name of the product, the producer of the product, and city and the country of the company (including the state if in USA), should be provided in parentheses in the following format: "Discovery St PET/CT scanner (General Electric, Milwaukee, WI, USA)"

All references, tables, and figures should be referred to within the main text, and they should be numbered consecutively in the order they are referred to within the main text.

Limitations, drawbacks, and the shortcomings of original articles should be mentioned in the Discussion section before the conclusion paragraph.

References

While citing publications, preference should be given to the latest, most up-to-date publications. If an ahead-of-print publication is cited, the DOI number should be provided. Authors are responsible for the accuracy of references. Journal titles should be abbreviated in accordance with the journal abbreviations in Index Medicus/ MEDLINE/PubMed. All authors should be listed if an article has six or less authors; it should not be represented by "et al." in articles. Arabic numbers in parentheses. References published in PubMed should have a PMID: xxxxxx at the end of it, which should be stated in parenthesis. The reference styles for different types of publications are presented in the following examples.

Journal Article: Little FB, Koufman JA, Kohut RI, Marshall RB. Effect of gastric acid on the pathogenesis of subglottic stenosis. Ann Otol Rhinol Laryngol 1985; 94:516-519. (PMID: 4051410)

Book Section: Suh KN, Keystone JS. Malaria and babesiosis. Gorbach SL, Barlett JG, Blacklow NR, editors. Infectious Diseases. Philadelphia: Lippincott Williams; 2004.p.2290-308.

Books with a Single Author: Sweetman SC. Martindale the Complete Drug Reference. 34th ed. London: Pharmaceutical Press; 2005.

Editor(s) as Author: Huizing EH, de Groot JAM, editors. Functional reconstructive nasal surgery. Stuttgart-New York: Thieme; 2003.

Conference Proceedings: Bengisson S. Sothemin BG. Enforcement of data protection, privacy and security in medical informatics. In: Lun KC, Degoulet P, Piemme TE, Rienhoff O, editors. MEDINFO 92. Proceedings of the 7th World Congress on Medical Informatics; 1992 Sept 6-10; Geneva, Switzerland. Amsterdam: North-Holland; 1992. pp.1561-5.

Scientific or Technical Report: Cusick M, Chew EY, Hoogwerf B, Agrón E, Wu L, Lindley A, et al. Early Treatment Diabetic Retinopathy Study Research Group. Risk factors for renal replacement therapy in the Early Treatment Diabetic Retinopathy Study (ETDRS), Early Treatment Diabetic Retinopathy Study Kidney Int: 2004. Report No: 26.

Thesis: Yılmaz B. Ankara Üniversitesindeki Öğrencilerin Beslenme Durumları, Fiziksel Aktiviteleri ve Beden Kitle İndeksleri Kan Lipidleri Arasındaki Ilişkiler. H.Ü. Sağlık Bilimleri Enstitüsü, Doktora Tezi. 2007.

Manuscripts Accepted for Publication, Not Published Yet: Slots J. The microflora of black stain on human primary teeth. Scand J Dent Res. 1974.

Epub Ahead of Print Articles: Cai L, Yeh BM, Westphalen AC, Roberts JP, Wang ZJ. Adult living donor liver imaging. Diagn Interv Radiol. 2016 Feb 24. doi: 10.5152/dir.2016.15323. [Epub ahead of print].

Manuscripts Published in Electronic Format: Morse SS. Factors in the emergence of infectious diseases. Emerg Infect Dis (serial online) 1995 Jan-Mar (cited 1996 June 5): 1(1): (24 screens). Available from: URL: http:/ www.cdc.gov/ncidodlElD/cid.htm.

REVISIONS

When submitting a revised version of a paper, the author must submit a detailed "Response to the reviewers" that states point by point how each issue raised by the reviewers has been covered and where it can be found (each reviewer's comment, followed by the author's reply and line numbers where the changes have been made) as well as an annotated copy of the main document. Revised manuscripts must be submitted within 30 days from the date of the decision letter. If the revised version of the manuscript is not submitted within the allocated time, the revision option may be cancelled. If the submitting author(s) believe that additional time is required, they should request this extension before the initial 30-day period is over.

Accepted manuscripts are copy-edited for grammar, punctuation, and format. Once the publication process of a manuscript is completed, it is published online on the journal's webpage as an ahead-of-print publication before it is included in its scheduled issue. A PDF proof of the accepted manuscript is sent to the corresponding author,and their publication approval is requested within 2 days of their receipt of the proof.

Editor in Chief: Prof. Vahit ÖZMEN

Address: Department of General Surgery, İstanbul University İstanbul Faculty of Medicine, Çapa, İstanbul

Phone : +90 (212) 534 02 10

Fax : +90 (212) 534 02 10

E-mail : editor@eurjbreasthealth.com

Web : www.eurjbreasthealth.com

Publisher: Galenos Yayınevi

Address: Molla Gürani Mah. Kaçamak Sok. 21/1
Fındıkzade, Fatih, Istanbul, Türkiye

Phone : +90 (530) 177 30 97

E-mail : info@galenos.com.tr

Web : www.galenos.com.tr

European Journal of Breast Health

Contents

European Journal of Breast Health

Contents

REVIEW

European Journal of BREAST HEALTH

DOI: 10.4274/ejbh.galenos.2026.2026-1-2
Eur J Breast Health 2026;22(3):240-247

Next-Generation Therapeutic Targets in Triple-Negative Breast Cancer

Kalsoom Mohammed Saleem[1], Mahira Firudin Amirova[2], Javanshir Ali Rahimov[3], Khaleddin Novruz Musayev[4], Ellada Eldar Huseynova[2], Nigar Veli Melikova[2]

[1]Department of Pharmaceutical Sciences, Riphah International University Faculty of Medicine, Islamabad, Pakistan
[2]Department of Biochemistry, Azerbaijan Medical University Faculty of Public Health, Baku, Azerbaijan
[3]Department of Epidemiology and Biostatistics, Azerbaijan Medical University Faculty of Medicine, Baku, Azerbaijan
[4]Department of II Surgery, Azerbaijan Medical University Faculty of Medicine, Baku, Azerbaijan

ABSTRACT

Triple-negative breast cancer (TNBC) lacks estrogen and progesterone receptors, and estrogen receptor/progesterone receptor/human epidermal growth factor receptor 2 expression, and is associated with early relapse, visceral metastasis, and limited targeted options. High-throughput profiling supports TNBC as a collection of molecularly distinct diseases with exploitable vulnerabilities across DNA-damage response, cell-cycle control, receptor tyrosine kinase signaling, metabolism, and anti-tumor immunity. Clinically, immune checkpoint blockade has shifted standards of care in selected settings, and biomarker enrichment is increasingly central to trial design. In parallel, DNA repair-directed approaches, including poly(ADP-ribose) polymerase inhibitors in BRCA1/2-mutant and homologous recombination–deficient tumors, are being extended through rational combinations that intensify replication stress (e.g., ataxia telangiectasia and Rad3-related protein, WEE1, or checkpoint kinase 1 inhibition) to deepen responses and delay resistance. Additional candidate targets, including androgen receptor-driven disease biology, epidermal growth factor receptor, fibroblast growth factor receptor, vascular endothelial growth factor receptor signaling, and emerging antibody-drug conjugate antigens highlight the importance of matching therapy to subtype and tumor microenvironment context. Metabolic reprogramming (glycolysis, fatty-acid oxidation/synthesis, and amino-acid use) intersects with therapy resistance and may provide complementary combination opportunities. In this study, we synthesize recent advances in actionable TNBC pathways, summarize key preclinical and clinical evidence, and propose a pragmatic framework for biomarker-led combinations that integrate DNA repair, cell-cycle, metabolic, and immune vulnerabilities.

Keywords: Triple-negative breast cancer (TNBC); precision oncology; DNA damage response; cell-cycle/mitotic targets; metabolic reprogramming; immunotherapy; antibody-drug conjugates

KEY POINTS

- Triple-negative breast cancer (TNBC) is aggressive, heterogeneous, and lacks estrogen receptor/progesterone receptor/human epidermal growth factor receptor 2, so targeted options are limited.
- Next-generation targets matter because profiling reveals distinct TNBC subgroups with actionable vulnerabilities.

Corresponding Author: Mahira Firudin Amirova MD;
E-mail: gerayelmira@gmail.com **ORCID:** orcid.org/0000-0001-5598-6995
Received: 13.01.2026 **Accepted:** 25.02.2026 **Epub:** 30.03.2026 **Available Online Date:** 17.06.2026
Cite this article as: Saleem KM, Amirova MF, Rahimov JA, Musayev KN, Huseynova EE, Melikova NV. Next-generation therapeutic targets in triple-negative breast cancer. Eur J Breast Health. 2026;22(3):240-247

- Poly(ADP-ribose) polymerase (PARP) inhibitors work best in BRCA1/2-mutated and other homologous recombination deficiency (HRD) TNBC, and research is expanding beyond classic HRD.
- Pairing PARP inhibition with ataxia telangiectasia and Rad3-related protein, WEE1, or checkpoint kinase 1 inhibitors can raise replication stress and create synthetic lethality.
- These replication-stress combinations may also help overcome or delay treatment resistance.
- Cell-cycle and mitotic regulators like CDC25 and aurora kinase A are druggable nodes that disrupt abnormal proliferation.
- Protein-stability and oncogenic drivers such as heat shock protein 90, mouse double minute 2 homolog/MDM2 binding protein, and metadherin support survival and metastasis and may be biomarker-linked targets.
- Receptor tyrosine kinase targeting (epidermal growth factor receptor, fibroblast growth factor receptor, vascular endothelial growth factor receptor) can benefit selected TNBC patients when guided by biomarkers.
- Immunotherapy with programmed cell death protein 1/programmed death-ligand 1 (PD-L1) inhibitors improves outcomes in PD-L1-positive TNBC, and combination approaches aim to deepen responses.
- The best path forward is biomarker-driven, rational combinations that integrate DNA repair, cell-cycle, metabolic, and immune vulnerabilities.

Introduction

Breast cancer remains a major global health burden, with hundreds of thousands of deaths annually and persistent disparities in outcomes across regions and populations (1). Contemporary epidemiology underscores both the scale of the problem and the importance of sustained investment in early detection and improved systemic therapy (2, 3). Triple-negative breast cancer (TNBC) is defined clinically by the absence of estrogen receptor, progesterone receptor, and estrogen receptor (ER)/progesterone receptor (PR)/human epidermal growth factor receptor 2 (HER2). Although this definition is operationally useful, it encompasses multiple biologically distinct diseases that differ in immune infiltration, metastatic tropism, and therapy sensitivity. TNBC accounts for roughly 10–20% of breast cancers and is associated with higher rates of early relapse and visceral metastasis compared with hormone receptor-positive disease (4). Because surgery and endocrine therapy and HER2-directed therapy are ineffective (5), systemic management historically relied on chemotherapy, with newer targeted and immune-based strategies now expanding options, due to which we focus on next-generation therapeutic vulnerabilities in TNBC and the practical logic for combination regimens. We emphasize DNA-damage response and replication stress, cell-cycle and checkpoint dependence, growth factor and nuclear receptor signaling, inflammatory and stem-like programs that enable metastasis and drug resistance, and metabolic reprogramming as an adjunct target space. Throughout, we highlight biomarker contexts that can help match patients to therapies and prioritize the most actionable combinations for clinical translation (6-8).

Materials and Methods

Literature search was conducted in databases including PubMed/MEDLINE, Scopus, and Web of Science using key words "triple negative breast cancer", "targeted therapy", "precision therapy", "drug resistance", "metastasis". Target/pathway terms aligned with the review scope [poly(ADP-ribose) polymerase (PARP), p53, epidermal growth factor receptor (EGFR), fibroblast growth factor receptor, PI3K/AKT/mammalian target of rapamycin (mTOR), immune checkpoint etc.]. Studies were included if they include clinical trials, *in vitro*/*in vivo* studies providing mechanistic support for a target's role in TNBC biology or systematic reviews or meta-analyses used primarily to contextualize clinical efficacy/safety trends. Exclusion criteria included non-TNBC breast cancer studies without extractable TNBC subgroup data or articles lacking primary data, and reports with insufficient methodological detail to interpret findings.

Results

TNBC Heterogeneity and the Evolving Treatment Landscape

Despite progress, TNBC management remains constrained by three recurring challenges: rapid emergence of resistance, limited durability of response in metastatic disease, and treatment-related toxicities that restrict intensification. Even when immune checkpoint blockade or targeted therapy is indicated, most regimens still rely on chemotherapy backbones that contribute neuropathy, myelosuppression, fatigue, and cumulative organ toxicities. Consequently, many reviews emphasize a shift from empiric escalation toward precision combination strategies that use biomarkers to select patients who can benefit from targeted agents while allowing chemotherapy de-escalation when deep responses occur (7-9). A practical implication is that target selection in TNBC often means selecting a combination rather than a single agent. Because the disease frequently uses parallel pathways [receptor tyrosine kinase (RTK) signaling, checkpoint dependence, inflammatory loops, and metabolic adaptation] to maintain survival, therapeutic programs that inhibit only one node are commonly bypassed. Drug development frameworks therefore prioritize identifying dominant dependencies in a given tumor state, pairing agents with complementary mechanisms (e.g., DNA damage plus checkpoint inhibition), and using on-treatment biomarkers to confirm that the intended pathway is suppressed *in vivo* (6, 10). TNBC heterogeneity has practical implications for therapy selection. Molecular subtyping

efforts consistently identify basal-like phenotypes enriched for DNA repair and cell-cycle abnormalities, as well as immune-enriched tumors and androgen receptor-driven subgroups that resemble luminal programs despite ER/PR negativity (11, 12). Clinically useful biomarkers now include germline/somatic *BRCA1/2* alterations, homologous recombination deficiency (HRD)-associated features, and immune markers such as programmed death-ligand 1 (PD-L1) expression and tumor-infiltrating lymphocytes. Guideline-based care increasingly integrates biomarker-driven strategies alongside chemotherapy, particularly in high-risk early-stage and metastatic settings (9, 13). Immune checkpoint blockade has shifted standards of care for selected patients. Atezolizumab combined with nab-paclitaxel has been reviewed as an approach for PD-L1-positive metastatic TNBC, with ongoing efforts to refine patient selection, sequencing, and management of immune-related adverse events (14, 15). More broadly, programmed cell death protein 1 (PD-1)/PD-L1 targeting in breast cancer is supported by an expanding clinical evidence base, and multiple lines of investigation aim to deepen and prolong responses through rational combinations (13, 16). At the same time, the therapeutic pipeline is broadening. Reviews of TNBC drug discovery emphasize DNA repair targeting, kinase pathway inhibitors, and emerging immune and antibody-based platforms as key growth areas (6, 10, 17). In particular, antibody engineering has enabled bispecific formats that can redirect immune effector functions or engage multiple tumor antigens, potentially overcoming pathway redundancy and tumor escape mechanisms (17).

DNA as Target: Repair Path, Replication Stress, and Synthetic Lethality in TNBC Cells

Platinum chemotherapy provides a clinically familiar example of DNA damage exploitation in TNBC, and it is often considered in HR- deficient or highly proliferative tumors. The rationale is conceptually aligned with PARP inhibition: both approaches increase DNA lesions that require high-fidelity repair. However, platinum sensitivity is not synonymous with HRD, and clinical benefit can vary depending on tumor subtype, prior exposure, and drug tolerance. For this reason, contemporary strategies frequently combine DNA crosslinking agents with targeted checkpoint inhibitors rather than relying on cytotoxic DNA damage alone (6, 18). Epigenetic modulation can also intersect with DNA repair targeting. Histone deacetylase (HDAC) inhibition may alter chromatin accessibility, transcription of repair genes, and replication stress responses. In TNBC cells, the HDAC inhibitor suberoylanilide hydroxamic acid has been reported to enhance the activity of PARP inhibitor olaparib, suggesting a potential strategy for sensitization in tumors where PARP inhibition alone is insufficient (4, 19). More recently, discovery-oriented work has described dual targeting of G-quadruplex structures and HDAC activity as a novel approach to disrupt proliferation and increase DNA damage burden (20). When considering these combinations, two principles are especially important. First, combinations should be built around a specific failure mode, e.g., restoring HR, checkpoint adaptation, or transcriptional rewiring rather than combining agents solely because each has modest single-agent activity. Second, the biomarker strategy should anticipate toxicity since multi-agent DNA damage and checkpoint regimens can increase hematologic adverse events, so early-phase development must establish schedules that preserve exposure while maintaining tolerability (7, 8). Defects in HR repair create a synthetic lethal opportunity for PARP inhibition. In HR-deficient tumors, PARP inhibition both impairs single-strand break repair and increases replication-associated lesions that evolve into unrepaired double-strand breaks, driving selective tumor cell death (6). However, resistance can emerge through restoration of HR function, replication fork protection, altered PARP trapping, or rewiring of cell-cycle checkpoints. Accordingly, a major thrust of next-generation therapy is to combine PARP inhibition with agents that amplify replication stress or prevent DNA damage tolerance. Checkpoint and replication-stress targeting provides a mechanistic route to deepen PARP responses. Ataxia telangiectasia and Rad3-related (ATR) protein kinase is involved in the DNA damage response and a master regulator of replication stress signaling, coordinating fork stabilization and S/G2 checkpoint enforcement. In phosphatase and tensin homolog (PTEN)-deficient breast cancers, ATR targeting has been proposed as a personalized therapy strategy, with preclinical evidence supporting increased DNA damage and vulnerability to DNA repair disruption (21). Similarly, WEE1 G2 checkpoint kinase inhibition can force premature mitotic entry, converting accumulated DNA lesions into mitotic catastrophe. Co-targeting DNA repair and checkpoint control has shown synergistic effects in TNBC models with Cyclin E or *BRCA1* alterations (22, 23). Clinical translation of replication-stress combinations is underway. One example is berzosertib (an ATR inhibitor) combined with cisplatin in advanced TNBC, evaluated in a phase 1b setting. Such regimens aim to exploit the reliance of highly proliferative tumors on checkpoint signaling when exposed to DNA crosslinking agents (18). These approaches also illustrate key implementation questions: identifying predictive biomarkers (e.g., HRD, PTEN loss, high replication stress signatures) and managing overlapping toxicities, including myelosuppression and fatigue.

DNA repair intersects with immune regulation. PARP inhibition has been reported to upregulate PD-L1 expression and increase cancer-associated immunosuppression, providing a biologic rationale for combining PARP inhibitors with checkpoint blockade (24). Depending on context, this PD-L1 increase could represent an adaptive immune-evasion response that becomes therapeutically actionable when PD-1/PD-L1 is blocked. Thus, replication-stress therapies may serve dual roles in direct

cytotoxicity through DNA damage and indirect immune modulation that enhances checkpoint inhibitor responsiveness.

Cell Cycle Checkpoint Targets in TNBC

Checkpoint dependence is not only a consequence of genomic instability; it can also be a compensatory adaptation to oncogene-driven hyperproliferation. In such states, tumor cells tolerate replication stress by engaging ATR-CHK1 (checkpoint kinase 1) signaling, enforcing G2/M arrest, and activating transcriptional programs that buffer damage. WEE1 and polo-like kinase 1 (PLK1) represent complementary nodes where WEE1 maintains G2 control, while PLK1 drives mitotic progression. Therefore, combinations that perturb both checkpoint enforcement and mitotic execution may be particularly effective when paired with DNA damage induction (22, 23, 25). Mutant p53 biology also links to inflammatory and RTK signaling. Mutant p53 can influence cytokine pathways and transcriptional outputs that promote invasion and survival, which may explain why mutant p53 targeting is viewed as a cross-cutting strategy that can affect both tumor-intrinsic growth and microenvironmental interactions (26). From a translational perspective, identifying mutant p53-dependent transcriptional states and mapping them to druggable dependencies, such as cyclin-dependent kinase 7 (CDK7) can create a more actionable precision framework than attempting universal p53 restoration (27). Beyond DNA repair, TNBC frequently depends on cell-cycle checkpoints and transcriptional programs that compensate for genomic instability. WEE1 inhibition represents one checkpoint-directed strategy, and preclinical work suggests synergy with capecitabine by increasing DNA damage and limiting repair capacity (23). PLK1 is another mitotic regulator implicated in TNBC; immunohistochemical studies in triple-negative breast carcinoma support PLK1 as a plausible therapeutic target and potential biomarker for aggressive biology (25). The p53 pathway is particularly relevant because tumor protein p53 (TP53) is mutated in a large fraction of TNBC. Comprehensive genetic profiling in triple-negative tumors has documented frequent TP53 alterations alongside other actionable changes, reinforcing the importance of pathway-based targeting strategies (28). Mutant p53 has been proposed as a novel therapeutic target in metastatic breast cancer, both because mutant p53 can gain pro-oncogenic functions and because p53 pathway disruption can create exploitable dependencies on alternative checkpoints (26). An emerging concept is to target mutant-p53 dependency rather than attempting direct p53 reactivation in every setting. For example, CDK7 inhibition has been explored as a way to exploit the transcriptional addiction of mutant p53-dependent TNBC cells, emphasizing that transcriptional regulation can be as critical as classical kinase signaling in sustaining tumor growth (27). These ideas complement checkpoint and DNA repair therapies: by reducing transcription of survival programs or DNA damage response genes, transcriptional inhibitors may lower the threshold for apoptosis when tumors are exposed to replication stress.

Growth Factor Signaling Molecules as Target for TNBC Treatment

RTK biology in TNBC is best understood as a signaling network rather than a single driver. EGFR can promote downstream mitogen-activated protein kinase and phosphatidyl inositol 3-kinase (PI3K) pathway activation, while MET proto-oncogene (cMET) provides a bypass route that preserves proliferative signaling under EGFR blockade. Accordingly, combinatorial approaches may include dual RTK inhibition, RTK inhibition plus PI3K/AKT/mTOR suppression, or RTK inhibition plus chemotherapy to increase tumor cell kill before adaptive reprogramming occurs (29, 30). Seven-in-absentia homologue (SIAH) pathway activity has been proposed as a functional readout of persistent EGFR/K-rat sarcoma family (RAS) signaling, which may be particularly relevant for identifying tumors that remain pathway-dependent despite chemotherapy exposure. If validated prospectively, such pathway activity markers could help stratify patients for RTK- or pathway-directed intensification, and could provide an on-treatment measure of whether resistance is emerging through pathway reactivation (31).

Angiogenesis inhibition occupies a similar niche: it is rarely sufficient as monotherapy but may contribute meaningful benefit in combinations that improve drug delivery, reduce hypoxia-driven adaptation, or reshape immune infiltration. Mechanistic reviews of anti-vascular endothelial growth factor (VEGF) therapy emphasize that the most effective use cases may be those where vascular normalization or immune-vascular interactions are explicitly targeted rather than expecting angiogenesis blockade to eradicate tumor cells directly (32). RTK signaling remains a major vulnerability for subsets of TNBC, but single-agent RTK inhibition has often been limited by pathway redundancy and compensatory signaling. EGFR is frequently expressed in TNBC, and combinations of antibodies to EGFR have inhibited TNBC models in preclinical work, supporting the premise that multi-epitope blockade or combination with cytotoxic agents can improve efficacy (29). Resistance mechanisms highlight why network-level strategies are required. cMET activation has been associated with EGFR-directed therapy resistance in TNBC, suggesting that dual RTK targeting or downstream pathway suppression may be needed to prevent bypass signaling (33). More recently, persistent activation of the EGFR/K-RAS/SIAH pathway has been linked to chemoresistance and early relapse in TNBC, reinforcing the importance of identifying durable pathway readouts (e.g., SIAH activity) that can track oncogenic signaling under treatment pressure (31). Downstream signaling inhibitors are therefore central to the next-generation landscape. The

PI3K/AKT/mTOR axis regulates growth, survival, and metabolism and is commonly altered or activated in TNBC through multiple upstream inputs. Drug discovery reviews emphasize both the promise and challenge of pathway inhibition, including feedback activation, metabolic adaptation, and toxicity that can limit dose intensity (30). Combination logic often pairs PI3K/AKT/mTOR pathway inhibitors with chemotherapy, RTK targeting, or immunotherapy to reduce adaptive signaling and increase tumor cell kill. Angiogenesis contributes to tumor growth and metastasis through VEGF receptor signaling, which can also shape immune contexture by influencing vascular permeability and immune cell trafficking. Recent reviews of anti-VEGF therapy in breast cancer summarize key molecular targets and therapeutic strategies, supporting continued exploration of angiogenesis inhibitors in biomarker-defined settings and rational combinations (32).

Inflammatory Signaling in TNBC, STAT3 Dependence and Cancer Stemness

The signal transducer and activator of transcription 3 (STAT3)-linked mechanisms also suggest a rationale for multi-layer targeting. For example, tumors that show leptin receptor (LEPR)-STAT3 dependence at hematological and neurological expressed 1-like protein (HN1L)-high states could, in principle, be co-targeted at the cytokine receptor level (to reduce upstream activation) and at downstream survival nodes such as PI3K/AKT/mTOR or checkpoint signaling, particularly when therapy exposure increases inflammatory cues from the microenvironment (30, 34). Similarly, cancer stem cell (CSC)-directed sensitization strategies illustrated by dasatinib-mediated chemosensitization may be most effective when coupled to a second agent that eradicates the bulk tumor population. This "two-compartment" logic (bulk tumor cytotoxicity plus CSC suppression) aligns with the clinical observation that initial responses can be followed by relapse driven by residual resistant clones or stem-like populations (4, 7, 34-36).

Inflammatory signaling supports TNBC progression by promoting proliferation, invasion, immune suppression, and therapy resistance. Interleukin-6 (IL-6)/STAT3 signaling is a recurrent theme: multiple TNBC regulators converge on STAT3 activation, which can sustain stem-like features and chemotherapy resistance. Mechanistically, gametogenetin-binding protein has been reported to suppress TNBC aggressiveness by inhibiting IL-6/STAT3 signaling activation, highlighting that negative regulators of STAT3 can function as tumor suppressors (37). Conversely, *HN1L* gene has been implicated in promoting TNBC stem cells through a LEPR-STAT3 pathway, linking inflammatory cues to stemness and metastatic potential (34). Pharmacologic disruption of IL-6/STAT3 signaling is therefore an active area of investigation. Bazedoxifene has been described as an IL-6/glycoprotein 130 kDa (GP130) inhibitor with activity in TNBC models, supporting GP130 as a druggable node in inflammatory signaling (38). These approaches may complement immunotherapy: By reducing cytokine-driven immune suppression and stem-like persistence, STAT3 pathway inhibition could improve both chemotherapy sensitivity and immune-mediated tumor clearance.

CSC phenotypes are linked to relapse and metastasis in TNBC, and CSC-directed strategies often overlap with inflammatory and RTK signaling. Dasatinib, a proto-oncogene tyrosine-protein kinase (SRC)-family kinase inhibitor, has been shown to sensitize TNBC cells to chemotherapy by targeting CSCs, exemplifying a sensitization approach that is not primarily cytotoxic as monotherapy but can amplify standard regimens (35). More broadly, reviews of CSC targeting in TNBC emphasize that successful translation will require robust CSC biomarkers and endpoints that capture residual disease biology (36).

Metabolic Reprogramming in TNBC Microenvironmental Context

Metabolic targeting is increasingly viewed as a way to constrain adaptability rather than to produce immediate tumor regression in all patients. Because metabolic pathways support multiple resistance phenotypes-drug efflux, antioxidant defense, and survival under hypoxia-metabolic interventions may be particularly useful as partners for DNA damage, RTK, or immune therapies. For instance, PI3K/AKT/mTOR signaling regulates glucose uptake and anabolic growth, so pathway inhibition can indirectly reshape metabolic state; conversely, tumors may compensate for pathway inhibition by switching fuel sources or increasing oxidative metabolism (30, 39). Serine biosynthesis illustrates how a relatively narrow metabolic vulnerability can connect to broad phenotypes such as metastasis. When phosphoserine aminotransferase 1 (PSAT1) is required for invasive behavior, targeting serine pathway enzymes may suppress dissemination even if primary tumor proliferation is only modestly affected. This supports a broader strategy: matching metabolic inhibitors to clinically relevant phenotypes (metastasis risk, stem-like persistence) and measuring endpoints beyond short-term tumor shrinkage (36, 40). Metabolic reprogramming enables TNBC cells to survive fluctuating nutrient supply, oxidative stress, and therapy-induced damage. A comprehensive review of metabolic remodeling in TNBC highlights glycolysis, mitochondrial adaptation, lipid metabolism, and amino-acid utilization as interconnected vulnerabilities that also influence immune function and drug resistance (39). Importantly, metabolic dependencies vary by subtype and microenvironment; therefore, metabolic targeting is most likely to succeed when guided by biomarkers such as pathway enzyme expression, metabolite signatures, or transcriptional programs. Metabolism also connects systemic physiology to tumor behavior. Adipokines and adiponectin-related signaling

have been investigated in relation to estrogen receptor-negative and triple-negative subtypes, suggesting that host metabolic state can shape tumor biology and potentially therapy response (41). While such associations do not immediately specify a drug target, they reinforce a practical point: metabolic and inflammatory context can influence the effectiveness of targeted and immune therapies, and should be considered in trial stratification and covariate adjustment. Specific metabolic enzymes can mediate invasion and metastasis. For example, selective loss of PSAT1 has been reported to inhibit invasion, migration, and experimental metastasis in TNBC, positioning serine biosynthesis as a candidate vulnerability in metabolically dependent tumors (42). Because metabolic interventions can have systemic effects, careful dose optimization and patient selection will be important, particularly when metabolic targeting is combined with chemotherapy or immunotherapy.

Emerging Platforms and Combination Design Principles

A useful way to operationalize combination selection is to map each patient's tumor to a small set of dominant liabilities and then choose combinations that cover complementary failure modes. Examples include HRD/BRCA-altered or high replication stress tumors: PARP ± ATR/WEE1, with optional checkpoint blockade when immune markers are present (18, 22, 24). In RTK/pathway-dependent tumors, EGFR/RTK-directed therapy plus downstream PI3K/AKT/mTOR suppression or chemotherapy is appropriate (29, 30, 33). In STAT3/CSC-enriched tumors, GP130/STAT3 targeting plus CSC sensitization to chemotherapy, with careful immune monitoring should be used (35, 38).

Because TNBC is clinically managed across distinct disease states (neoadjuvant, adjuvant, metastatic), the optimal endpoint also differs. In early-stage disease, pathologic complete response and event-free survival can be sensitive to intensification strategies. In metastatic disease, durable disease control and quality of life are paramount, and toxicity-limited regimens may need sequential rather than simultaneous combinations. These trade-offs argue for adaptive clinical trial designs that allow response-guided therapy modification and incorporate patient-reported outcomes alongside molecular biomarkers (7, 8, 13). Antibody engineering is enabling next-generation platforms that can complement small-molecule and cytotoxic strategies. Bispecific antibodies offer opportunities to co-engage immune cells and tumor antigens or to block multiple signaling inputs simultaneously, potentially reducing pathway redundancy and adaptive resistance (17). In parallel, new delivery and targeting strategies including peptide-derived agents continue to expand the druggable space in TNBC. For instance, gap junction protein connexin 26-derived cell-penetrating peptides have been used to target homeobox transcription factor, a stemness-associated factor NANOG and focal adhesion kinase (FAK, also called PTK2). FAK, illustrating a mechanism-driven strategy that links stemness programs to focal adhesion signaling (43). Combination design is increasingly informed by mechanistic complementarity: pair DNA damage with checkpoint blockade to convert damage into lethal events (22, 23), combine pathway inhibitors to prevent bypass signaling (31, 33), integrate immune modulation when tumor antigens and immune infiltration are present (13, 16), and target stem-like persistence or inflammatory loops to reduce relapse risk (34, 36). Early-phase clinical development of multi-agent regimens, such as kinase inhibition combined with immunotherapy and chemotherapy, demonstrates the feasibility of multi-node targeting but also emphasizes the need for toxicity-aware sequencing and adaptive dosing (44).

In practice, biomarker integration is the key enabling factor. Candidate biomarkers include: BRCA/HRD status (for PARP and replication-stress therapies), PTEN loss or high replication stress signatures (for ATR/WEE1 strategies), PD-L1 and immune gene signatures (for checkpoint blockade), and STAT3 pathway activity markers (for IL-6/GP130 or LEPR–STAT3 targeting). Developing trial designs that allow therapy adaptation based on early molecular response using circulating tumor DNA or serial biopsy may help reduce overtreatment while preserving efficacy (7, 8).

Conclusion

TNBC is a heterogeneous clinical entity that demands biologically guided therapy. Recent progress reflects two complementary trends: better matching of patients to therapies using biomarkers (e.g., PD-L1, HRD) and increasing use of rational combinations that anticipate resistance and exploit synthetic lethal interactions. Replication-stress strategies (ATR/WEE1/CHK pathways), RTK and downstream signaling blockade (EGFR/cMET/PI3K), inflammatory and stemness targeting (STAT3/CSC programs), and metabolic adjunct therapies together form a coherent next-generation toolkit. Continued advances will depend on integrating these tools into adaptive, biomarker-led clinical strategies that maximize durable control while minimizing cumulative toxicity.

Footnotes

Authorship Contributions

Concept: K.M.S., M.F.A., J.A.R., K.N.M., E.E.H., N.V.M.; Design: K.M.S., M.F.A., J.A.R., K.N.M., E.E.H., N.V.M.; Data Collection or Processing: K.M.S., M.F.A., J.A.R., K.N.M., E.E.H., N.V.M.; Analysis or Interpretation: K.M.S., M.F.A., J.A.R., K.N.M., E.E.H., N.V.M.; Writing: K.M.S., M.F.A., J.A.R., K.N.M., E.E.H., N.V.M.

Conflict of Interest: No conflict of interest declared by the authors.

Financial Disclosure: The authors declare that this study received no financial disclosure.

References

1. Aliyeva HN, Amirova MF, Melikova NV, Guliyeva FE, Hasanov VM, Rahimov JA. Diagnostic algorithm for clarifying intraductal papilloma without galactography. World of Medicine and Biology. 2025; 3: 256-260. [Crossref]
2. Siegel RL, Miller KD, Fuchs HE, Jemal A. Cancer statistics, 2022. CA Cancer J Clin. 2022; 72: 7-33. (PMID: 35020204) [Crossref]
3. Menon G, Alkabban FM, Ferguson T. Breast cancer. 2024. In: StatPearls [Internet]. Treasure Island (FL): StatPearls Publishing; 2025 Jan. (PMID: 29493913) [Crossref]
4. Park Y, Moriyama A, Kitahara T, Yoshida Y, Urita T, Kato R. Triple-negative breast cancer and poly(ADP-ribose) polymerase inhibitors. Anticancer Agents Med Chem. 2012; 12: 672-677. (PMID: 22263793) [Crossref]
5. Akhundova JN, Amirova MF, Lymph nodes morphological changes and breast cancer subtypes in prediction of metastases. World of Medicine and Biology. 2024; 4: 15-19. [Crossref]
6. Gupta GK, Collier AL, Lee D, Hoefer RA, Zheleva V, Siewertsz van Reesema LL, et al. Perspectives on triple-negative breast cancer: current treatment strategies, unmet needs, and potential targets for future therapies. Cancers (Basel). 2020; 12: 2392. (PMID: 32846967) [Crossref]
7. Mehanna J, Haddad FG, Eid R, Lambertini M, Kourie HR. Triple-negative breast cancer: current perspective on the evolving therapeutic landscape. Int J Womens Health. 2019; 11: 431-437. (PMID: 31447592) [Crossref]
8. Obidiro O, Battogtokh G, Akala EO. Triple negative breast cancer treatment options and limitations: future outlook. Pharmaceutics. 2023; 15: 1796. (PMID: 37513983) [Crossref]
9. Trayes KP, Cokenakes SEH. Breast cancer treatment. Am Fam Physician. 2021; 104: 171-178. (PMID: 34383430) [Crossref]
10. Nakhjavani M, Hardingham JE, Palethorpe HM, Price TJ, Townsend AR. Druggable molecular targets for the treatment of triple negative breast cancer. J Breast Cancer. 2019; 22: 341-361. (PMID: 31598336) [Crossref]
11. Bianchini G, Balko JM, Mayer IA, Sanders ME, Gianni L. Triple-negative breast cancer: challenges and opportunities of a heterogeneous disease. Nat Rev Clin Oncol. 2016; 13: 674-690. (PMID: 27184417) [Crossref]
12. Yin L, Duan JJ, Bian XW, Yu SC. Triple-negative breast cancer molecular subtyping and treatment progress. Breast Cancer Res. 2020; 22: 61. (PMID: 32517735) [Crossref]
13. Ren Y, Song J, Li X, Luo N. Rationale and clinical research progress on PD-1/PD-L1-based immunotherapy for metastatic triple-negative breast cancer. Int J Mol Sci. 2022; 23: 8878. (PMID: 36012144) [Crossref]
14. Kagihara JA, Andress M, Diamond JR. Nab-paclitaxel and atezolizumab for the treatment of PD-L1-positive, metastatic triple-negative breast cancer: review and future directions. Expert Rev Precis Med Drug Dev. 2020; 5: 59-65. (PMID: 32190733) [Crossref]
15. Kang C, Syed YY. Atezolizumab (in combination with Nab-Paclitaxel): a review in advanced triple-negative breast cancer. Drugs. 2020; 80: 601-607. (PMID: 32248356) [Crossref]
16. Planes-Laine G, Rochigneux P, Bertucci F, Chrétien AS, Viens P, Sabatier R, et al. PD-1/PD-L1 targeting in breast cancer: the first clinical evidences are emerging. A literature review. Cancers (Basel). 2019; 11: 1033. (PMID: 31336685) [Crossref]
17. Dees S, Ganesan R, Singh S, Grewal IS. Bispecific antibodies for triple negative breast cancer. Trends Cancer. 2021; 7: 162-173. (PMID: 33041246) [Crossref]
18. Telli ML, Tolaney SM, Shapiro GI, Middleton M, Lord SR, Arkenau HT, et al. Phase 1b study of berzosertib and cisplatin in patients with advanced triple-negative breast cancer. NPJ Breast Cancer. 2022; 8: 45. (PMID: 35393425) [Crossref]
19. Min A, Im SA, Kim DK, Song SH, Kim HJ, Lee KH, et al. Histone deacetylase inhibitor, suberoylanilide hydroxamic acid (SAHA), enhances anti-tumor effects of the poly (ADP-ribose) polymerase (PARP) inhibitor olaparib in triple-negative breast cancer cells. Breast Cancer Res. 2015; 17: 33. (PMID: 25888415) [Crossref]
20. Jiang XC, Tu FH, Wei LY, Wang BZ, Yuan H, Yuan JM, et al. Discovery of a novel G-quadruplex and histone deacetylase (HDAC) dual-targeting agent for the treatment of triple-negative breast cancer. J Med Chem. 2022; 65: 12346-12366. (PMID: 36053318) [Crossref]
21. Al-Subhi N, Ali R, Abdel-Fatah T, Moseley PM, Chan SYT, Green AR, et al. Targeting ataxia telangiectasia-mutated- and Rad3-related kinase (ATR) in PTEN-deficient breast cancers for personalized therapy. Breast Cancer Res Treat. 2018; 169: 277-286. (PMID: 29396668) [Crossref]
22. Chen X, Yang D, Carey JPW, Karakas C, Albarracin C, Sahin AA, et al. Targeting replicative stress and DNA repair by combining PARP and Wee1 kinase inhibitors is synergistic in triple negative breast cancers with cyclin E or *BRCA1* alteration. Cancers (Basel). 2021; 13: 1656. (PMID: 33916118) [Crossref]
23. Pitts TM, Simmons DM, Bagby SM, Hartman SJ, Yacob BW, Gittleman B, et al. Wee1 inhibition enhances the anti-tumor effects of capecitabine in preclinical models of triple-negative breast cancer. Cancers (Basel). 2020; 12: 719. (PMID: 32204315) [Crossref]
24. Jiao S, Xia W, Yamaguchi H, Wei Y, Chen MK, Hsu JM, et al. PARP inhibitor upregulates PD-L1 expression and enhances cancer-associated immunosuppression. Clin Cancer Res. 2017; 23: 3711-3720. (PMID: 28167507) [Crossref]
25. Salama ME, Khairy DA. Polo-like kinase 1(PLK1) immunohistochemical expression in triple negative breast carcinoma: a probable therapeutic target. Asian Pac J Cancer Prev. 2021; 22: 3921-3925. (PMID: 34967572) [Crossref]
26. Synnott NC, Murray A, McGowan PM, Kiely M, Kiely PA, O'Donovan N, et al. Mutant p53: a novel target for the treatment of patients with triple-negative breast cancer? Int J Cancer. 2017; 140: 234-246. (PMID: 27615392) [Crossref]
27. Peng J, Yang M, Bi R, Wang Y, Wang C, Wei X, et al. Targeting mutated p53 dependency in triple-negative breast cancer cells through CDK7 inhibition. Front Oncol. 2021; 11: 664848. (PMID: 34109118) [Crossref]
28. Jouali F, El Ansari FZ, Marchoudi N, Barakat A, Zmaimita H, Samlali H, et al. *EGFR*, *BRCA1*, *BRCA2* and *TP53* genetic profile in Moroccan triple negative breast cancer cases. Int J Mol Epidemiol Genet. 2020; 11: 16-25. (PMID: 32714499) [Crossref]
29. Ferraro DA, Gaborit N, Maron R, Cohen-Dvashi H, Porat Z, Pareja F, et al. Inhibition of triple-negative breast cancer models by combinations of antibodies to EGFR. Proc Natl Acad Sci U S A. 2013; 110: 1815-1820. (PMID: 23319610) [Crossref]
30. Khan MA, Jain VK, Rizwanullah M, Ahmad J, Jain K. PI3K/AKT/mTOR pathway inhibitors in triple-negative breast cancer: a review on drug discovery and future challenges. Drug Discov Today. 2019; 24: 2181-2191. (PMID: 31520748) [Crossref]
31. Tang AH, Hoefer RA, Guye ML, Bear HD. Persistent EGFR/K-RAS/SIAH pathway activation drives chemo-resistance and early tumor relapse in triple-negative breast cancer. Cancer Drug Resist. 2022; 5: 691-702. (PMID: 36176751) [Crossref]
32. Zhang M, Liu J, Liu G, Xing Z, Jia Z, Li J, et al. Anti-vascular endothelial growth factor therapy in breast cancer: molecular pathway, potential targets, and current treatment strategies. Cancer Lett. 2021; 520: 422-433. (PMID: 34389434) [Crossref]
33. Sohn J, Liu S, Parinyanitikul N, Lee J, Hortobagyi GN, Mills GB, et al. cMET activation and EGFR-directed therapy resistance in triple-negative breast cancer. J Cancer. 2014; 5: 745-753. (PMID: 25368674) [Crossref]

34. Liu Y, Choi DS, Sheng J, Ensor JE, Liang DH, Rodriguez-Aguayo C, et al. HN1L promotes triple-negative breast cancer stem cells through LEPR-STAT3 pathway. Stem Cell Reports. 2018; 10: 212-227. (PMID: 29249663) [Crossref]

35. Tian J, Raffa FA, Dai M, Moamer A, Khadang B, Hachim IY, et al. Dasatinib sensitises triple negative breast cancer cells to chemotherapy by targeting breast cancer stem cells. Br J Cancer. 2018; 119: 1495-1507. (PMID: 30482914) [Crossref]

36. Park SY, Choi JH, Nam JS. Targeting cancer stem cells in triple-negative breast cancer. Cancers (Basel). 2019; 11: 965. (PMID: 31324052) [Crossref]

37. Liu J, Liu L, Yagüe E, Yang Q, Pan T, Zhao H, et al. GGNBP2 suppresses triple-negative breast cancer aggressiveness through inhibition of IL-6/STAT3 signaling activation. Breast Cancer Res Treat. 2019; 174: 65-78. (PMID: 30450530) [Crossref]

38. Tian J, Chen X, Fu S, Zhang R, Pan L, Cao Y, et al. Bazedoxifene is a novel IL-6/GP130 inhibitor for treating triple-negative breast cancer. Breast Cancer Res Treat. 2019; 175: 553-566. (PMID: 30852762) [Crossref]

39. Sun X, Wang M, Wang M, Yu X, Guo J, Sun T, et al. Metabolic reprogramming in triple-negative breast cancer. Front Oncol. 2020; 10: 428. (PMID: 32296646) [Crossref]

40. Roshanian Bakhsh M, Peymani M, Rouhi L, Ghaedi K. *PSAT1* gene as a biomarker for targeting triple negative breast cancer in presence of rapamycin. Nucleosides Nucleotides Nucleic Acids. 2022; 41: 166-182. Erratum in: Nucleosides Nucleotides Nucleic Acids. 2025: 1. (PMID: 35038970) [Crossref]

41. Llanos AAM, Lin Y, Chen W, Yao S, Norin J, Chekmareva MA, et al. Immunohistochemical analysis of adipokine and adipokine receptor expression in the breast tumor microenvironment: associations of lower leptin receptor expression with estrogen receptor-negative status and triple-negative subtype. Breast Cancer Res. 2020; 22: 18. (PMID: 32046756) [Crossref]

42. Metcalf S, Dougherty S, Kruer T, Hasan N, Biyik-Sit R, Reynolds L, et al. Selective loss of phosphoserine aminotransferase 1 (PSAT1) suppresses migration, invasion, and experimental metastasis in triple negative breast cancer. Clin Exp Metastasis. 2020; 37: 187-197. (PMID: 31630284) [Crossref]

43. Mulkearns-Hubert EE, Esakov Rhoades E, Ben-Salem S, Bharti R, Hajdari N, Johnson S, et al. Targeting NANOG and FAK via Cx26-derived cell-penetrating peptides in triple-negative breast cancer. Mol Cancer Ther. 2024; 23: 56-67. (PMID: 37703580) [Crossref]

44. Chen L, Jiang YZ, Wu SY, Wu J, Di GH, Liu GY, et al. Famitinib with camrelizumab and Nab-Paclitaxel for advanced immunomodulatory triple-negative breast cancer (FUTURE-C-plus): an open-label, single-arm, phase II trial. Clin Cancer Res. 2022; 28: 2807-2817. (PMID: 35247906) [Crossref]

ORIGINAL ARTICLE

European Journal of BREAST HEALTH

DOI: 10.4274/ejbh.galenos.2025.2025-10-10
Eur J Breast Health 2026;22(3):248-260

Expression and Survival Analysis Show High Mobility Group (HMG) Family as Prognostic Biomarkers in Breast Cancer

Ehtesham Ahmed Shariff[1], Ahmed Azharuddin[1], Rateb Abu-Zaid[1], Ahmed Al-Wathinani[1], Eid Basheer Alenazy[2], Raiyan Ehtesham Ahmed Sharieff[3]

[1]Department of Emergency Medical Services, Faculty of EMS, Prince Sultan Bin Abdulaziz College for Emergency Medical Services, King Saud University, Riyadh, Saudi Arabia
[2]Laboratories and Medical Technology (Technical Laboratory), King Saud University Medical City, Riyadh, Saudi Arabia
[3]College of Medicine, Alfaisal University, Riyadh, Saudi Arabia

ABSTRACT

Objective: High-mobility group (HMG) protein families are critical regulators of chromatin structure and gene expression in breast cancer. This study systematically evaluates their expression patterns, genetic interactions, and clinical relevance.

Materials and Methods: Expression profiles of HMG proteins were analyzed using mRNA data from gene expression profiling interactive analysis 2. We performed protein-level validation using the Human Protein Atlas. Prognostic significance was assessed through survival analysis, while genetic alterations were mapped using cBioPortal. Pathway enrichment and protein-protein interactions were explored with EnrichR and Search Tool for the retrieval of interacting genes/proteins, respectively. Associations with p53 mutation status were investigated using University of Alabama at Birmingham Cancer Data Analysis Portal.

Results: HMGA1 emerged as a central driver in triple-negative breast cancer (TNBC), forming a transcriptional complex with FOXM1 that activated VEGFA-mediated angiogenesis, which correlated withwas associated with poor patient survival. In contrast, HMGA2 overexpression was paradoxically associated with favorable outcomes despite promoting tumor angiogenesis. HMGB1 regulation was linked to genomic instability and metastasis, yet it showed potential protective effects in survival analyses. HMGB2 independently predicts poor prognosis in large tumors, and HMGB3 correlates with aggressive progression. HMGB4, though expressed at low levels, is associated with improved survival in early-stage patients. HMGN1 and HMGN4 promoted tumor growth, while HMGN2 suppressed proliferation and induced apoptosis, highlighting its therapeutic potential.

Conclusion: HMG proteins exhibit context-dependent roles in breast cancer, with HMGA1, HMGB2-3, and HMGN1/4 driving tumors, while HMGA2, HMGB1, HMGB4, and HMGN2 show protective or paradoxical effects. These findings position HMG proteins as both biomarkers and therapeutic targets, particularly HMGA1 in TNBC angiogenesis and HMGN2 in the induction of apoptosis.

Keywords: Breast cancer; HMG family; survival analysis; prognostic markers; mRNA expression

Corresponding Author: Ehtesham Ahmed Shariff MD;
E-mail: esharieff@ksu.edu.sa **ORCID:** orcid.org/0000-0001-6847-3961
Received: 22.10.2025 **Accepted:** 09.12.2025 **Available Online Date:** 17.06.2026
Cite this article as: Shariff EA, Azharuddin A, Abu-Zaid R, Al-Wathinani A, Alenazy EB, Sharieff REA. Expression and survival analysis show high mobility group (HMG) family as prognostic biomarkers in breast cancer. Eur J Breast Health. 2026;22(3):248-260

KEY POINTS

- HMGA1 drives angiogenesis via FOXM1/VEGFA, which is associated with poor prognosis.
- HMGA2 paradoxically promotes angiogenesis, yet correlates with improved survival.
- HMGB1 up genomic instability/metastasis but may protect survival.
- HMGB2 promote tumour size/stage and HMGB3 signal advanced disease.
- HMGN1/HMGN4 promote tumour growth and HMGN2 inhibits proliferation and induces apoptosis.

Introduction

Breast cancer remains one of the most prevalent cancers among women worldwide and is a leading cause of cancer-related mortality (1). The complexity of breast cancer, characterized by its heterogeneous nature and varying responses to treatment, necessitates the identification of reliable prognostic markers (2). Early detection and accurate prognostic assessments are vital for improving survival rates and tailoring therapeutic strategies (3). Research has demonstrated that specific high mobility group (HMG) proteins are differentially expressed in breast cancer tissues compared with normal breast tissue, suggesting their involvement in tumorigenesis and progression (4).

HMG proteins are a diverse family of chromatin-associated proteins that play crucial roles in regulating gene expression, DNA repair, and cell proliferation (5). This family includes several members, each exhibiting distinct functions that contribute to cellular processes and tumor biology. HMGA (HMGA1, HMGA2) proteins show differentiation of embryonic and adult stem cells (6). HMGB proteins (HMGB1, HMGB2, HMGB3, HMGB4), first studied in yeast, have become central to cancer biology research. They regulate DNA repair and gene expression and drive cellular processes that promote tumour progression (7). HMG nucleosome-binding (HMGN) proteins, particularly HMGN1 and HMGN2, regulate chromatin accessibility and transcription factor binding in ameloblast differentiation. Their down-regulation accelerates ameloblast maturation and enamel deposition, highlighting their role in modulating gene expression, which may also influence cancer progression (8). HMGN3 promotes cancer progression by repressing epithelial regulatory genes in cholangiocarcinoma (CCA), with its high expression associated with metastasis (9). HMGN4 promotes thyroid cancer by altering gene expression, downregulating tumor suppressors, and increasing tumorigenicity (10).

In the context of breast cancer, these proteins have garnered attention due to their potential as prognostic biomarkers that can inform treatment decisions and predict patient outcomes.

The prognostic significance of HMG proteins in breast cancer is underscored by their associations with various clinical outcomes (11). Elevated levels of certain HMGA2 proteins have been associated with poor prognosis, whereas elevated levels of other HMGA2 proteins correlate with favourable outcomes (12).

Molecular cancer biomarkers, including those from the HMG protein family, serve as measurable indicators of cancer risk, presence, and patient prognosis (13). Their utility extends to risk assessment, screening, diagnosis, and monitoring of treatment responses. As the landscape of breast cancer treatment evolves, the integration of molecular biomarkers into clinical practice becomes increasingly important for personalized patient care (14).

Despite increasing recognition of the involvement of HMG proteins in oncogenesis, their specific contributions to breast cancer remain insufficiently defined. Existing omics-based studies have largely focused on individual gene signatures or pathway-level analyses, leaving the expression dynamics and prognostic relevance of HMG family members underexplored. Given their established roles in chromatin remodelling, transcriptional regulation, and tumour progression, HMG proteins represent promising yet under-investigated candidates for systematic evaluation in breast cancer. This study addresses this gap by integrating multi-omics datasets to comprehensively characterize HMG protein expression patterns across breast cancer subtypes and to assess their prognostic implications. By highlighting subtype-specific associations and utilizing large-scale online databases, we aim to identify novel biomarkers that could refine prognostic stratification. These biomarkers may also inform therapeutic strategies, thereby advancing precision oncology in breast cancer.

Materials and Methods

Gene Expression Patterns and Prognostic Evaluation of the HMG Family

We evaluated the mRNA expression levels of HMG proteins in breast cancer patients. This was performed using the gene expression profiling interactive analysis 2 (GEPIA) platform (http://gepia.cancer-pku.cn/) (15). Additionally, we performed a differential expression analysis based on pathological stages, considering a *p*-value of less than 0.01 significant. To confirm the correlation between mRNA and protein levels, we analyzed

HMG protein levels using the Human Protein Atlas database (https://www.proteinatlas.org/). We assessed the prognostic importance of HMG proteins using the Kaplan-Meier Plotter, which integrates survival data from Gene Expression Omnibus, European Genome-Phenome Archive, and the Cancer Genome Atlas (TCGA) for 943 breast cancer patients (16). To analyze overall survival (OS), progression-free survival (PFS), and post-progression survival (PPS), we categorized samples into high- and low-expression groups based on median expression levels. A univariate Cox regression analysis was conducted, adjusting for pathological grade, clinical stage, and TP53 mutation status. A *p*-value <0.05 was considered statistically significant.

Genetic Alteration Frequencies of HMG Family Proteins

We used the cBioPortal (http://www.cbioportal.org) for in breast cancer patients. This included selecting genomic profiles of HMG family members, focusing on mutations, copy-number alterations, and mRNA expression. The data obtained were used for further analysis and research.

Functional Enrichment Analysis of the HMG Family

We conducted a cancer hallmarks enrichment analysis of *HMG* genes linked to OS in human solid tumors. Additionally, we performed biological enrichment analysis, specifically for gene ontology (GO) terms and Reactome 2022 pathways, on HMG family members using EnrichR (17-20). These approaches helped us understand the role of *HMG* genes in biological processes.

Protein-Protein Interactions Analysis of HMG Family Members

To explore potential interactions among our genes of interest, we used the search tool for the retrieval of interacting genes (STRING) database (21). This tool identifies known and predicted protein-protein interactions from various sources, including experimental data and text mining. The gene list was input into STRING, and a confidence score threshold of 0.4 was applied to retain high-confidence interactions.

Gene Expression Analysis in Relation to p53 Mutation Status

We analyzed gene expression levels in relation to p53 mutation status using the University of Alabama at Birmingham Cancer Data Analysis Portal web tool (22, 23). This tool accesses gene expression data from TCGA database, allowing stratification by clinical and molecular characteristics, including tumor stage and p53 mutation status. We examined the data for statistically significant differences in expression levels between wild-type and mutant p53 samples. Gene expression levels were reported as transcripts per million (TPM) and visualized with box plots.

Ethical Statement

The data in this paper were sourced solely from an open-access database. We did not collect data directly from patients or interfere with their treatment. Therefore, ethical approval was not required for this study.

Results

HMG Proteins mRNA Expression Levels in Breast Cancer Patients

We examined the mRNA levels of HMG proteins in breast cancer patients. Our analysis using GEPIA revealed that the mRNA levels of HMGA1, HMGB1, HMGB2, HMGB3, HMGN1, HMGN2, HMGN3, and HMGN4 were significantly higher in breast cancer tissues compared with normal breast tissues (Figure 1). In contrast, HMGA2 exhibited moderate expression, while HMGB4 showed very low expression in cancer tissues (Figure 1). Furthermore, we investigated the expression of HMG proteins across different stages of breast cancer. We found that the mRNA levels of HMGA1, HMGB1, HMGB2, HMGB3, HMGN1, HMGN2, HMGN3, and HMGN4 differed significantly across tumor stages. However, the expression levels of HMGA2 and HMGB4 did not differ significantly across these stages (Figure 2). This suggests that certain HMG proteins may play distinct roles at different stages of cancer progression.

Prognostic Significance of HMG Proteins mRNA Expression Levels

The prognostic value of HMG proteins' mRNA levels in breast cancer patients was assessed using the Kaplan-Meier plotter. The results indicated that high mRNA levels of HMGA2, HMGB1, HMGB2, HMGB4, HMGN2, and HMGN4 were associated with better OS. Conversely, high levels of HMGA1, HMGB3, HMGN1, and HMGN3 correlated with poorer OS (Figure 3). The statistical analysis revealed significant differences among the HMGA, HMGB, and HMGN groups, highlighting the prognostic importance of these proteins. Additionally, high expression levels of HMGB1, HMGB4, HMGA2, and HMGN3, or low expression levels of HMGA1, HMGB2, HMGB3, HMGN1, HMGN2, and HMGN4, were correlated with favorable PFS (Figure 4). Patients exhibiting high expression levels of HMGB1 and HMGN2 showed favorable PPS. In contrast, high levels of HMGA1, HMGA2, HMGB2, HMGB3, HMGB4, HMGN1, HMGN3, and HMGN4 were associated with unfavorable PPS (Figure 5). These findings underscore the potential of HMG proteins as prognostic biomarkers in breast cancer.

The cancer hallmark overrepresentation table provided valuable insights into the roles of specific genes in various cancer hallmarks (Table 1). Among the hallmarks analyzed, sustaining proliferative signaling showed a notable association with HMGB1; however, the high *p*-value of 0.93429 indicates that its contribution to this hallmark may not be statistically significant. In contrast, genome instability presented a more compelling association: HMGB1 involvement exhibited an odds ratio of 3.01, suggesting a potential role in promoting genomic

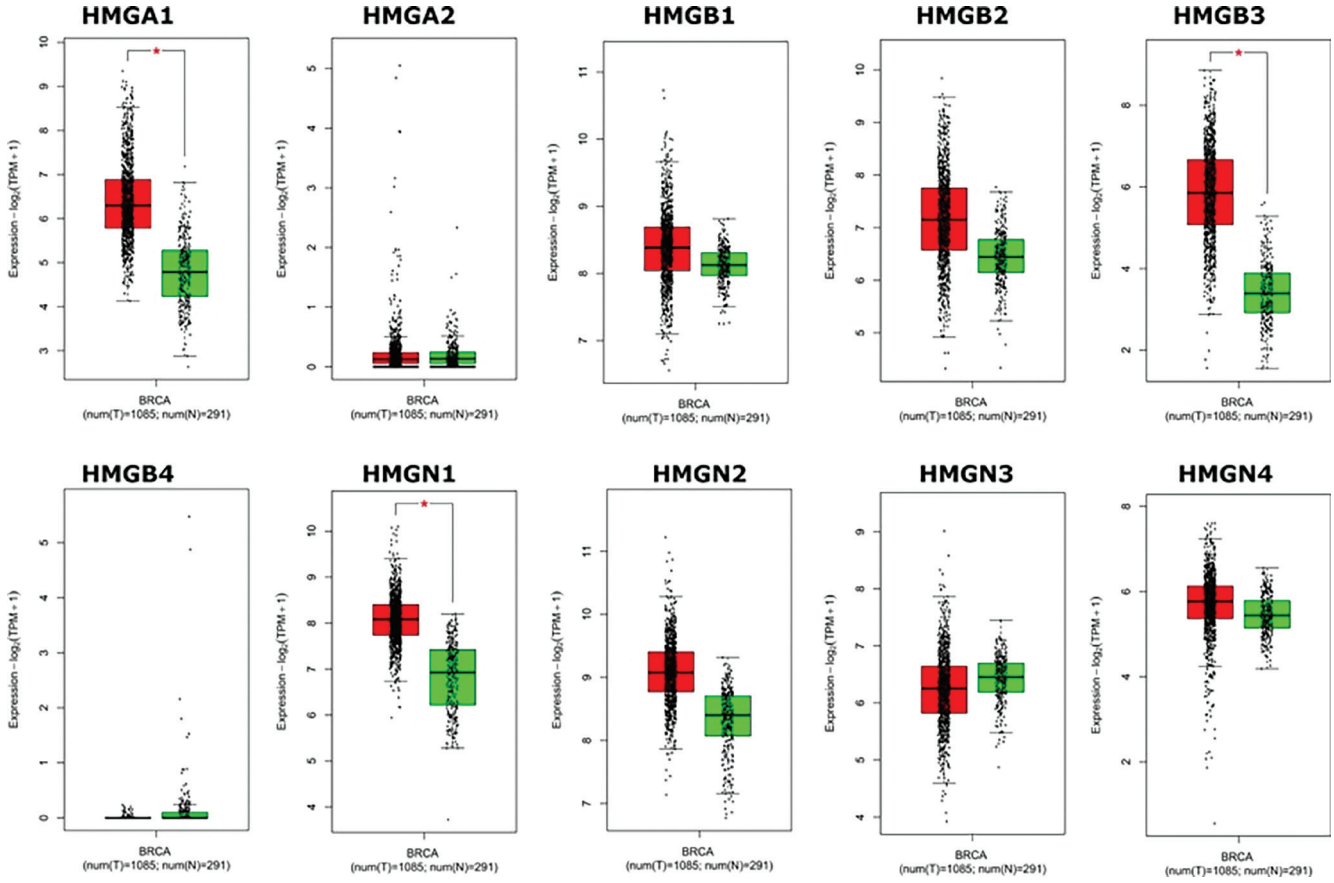

Figure 1. Differential mRNA expression patterns of HMG protein family members in BRCA tumor *vs*. normal tissue. Comparison of mRNA expression levels for HMG protein family members in breast cancer patients from TCGA dataset (n = 1085 tumors *vs*. 291 normal samples). Asterisks (*) indicate statistically significant differences (p<0.05) in expression between tumor (T) and normal (N) tissues. Proteins HMGA1/2, HMGB1–4, and HMGN1–4 demonstrate varied expression patterns across different HMG subgroups

HMG: High-mobility group; BRCA: Breast cancer; TCGA: The Cancer Genome Atlas; HMGN: HMG nucleosome-binding; TPM: Transcripts per million

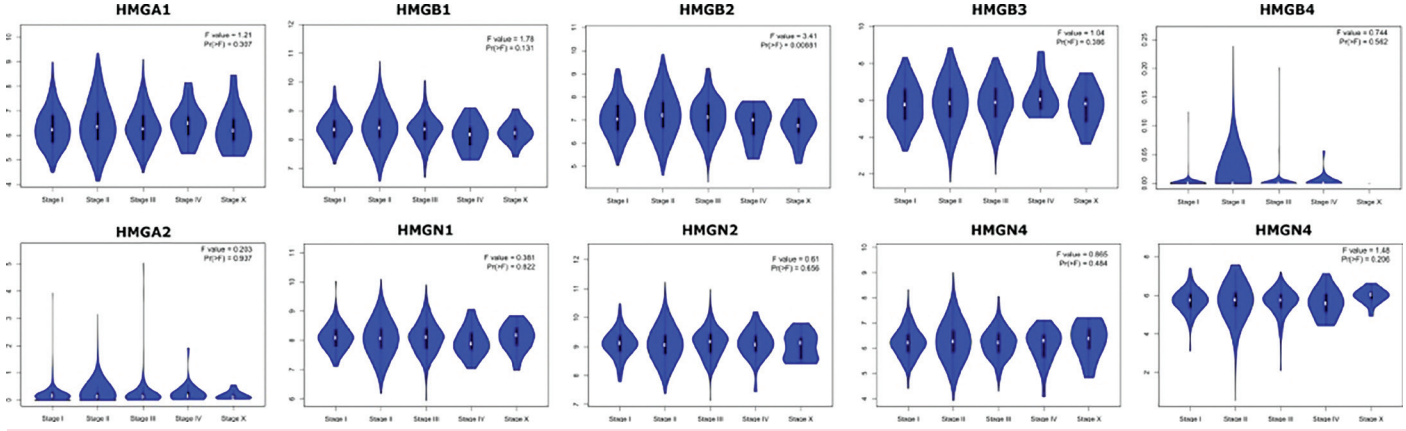

Figure 2. Stage-specific mRNA expression patterns of HMG proteins in breast cancer progression. Box plots were generated to compare HMG family mRNA expression across breast cancer progression stages (I-IV, X) in TCGA data, revealing stage-dependent variations in HMGA1/2, HMGB1–4, and HMGN1–4 subgroups. Notable findings include that HMGN4 shows significant stage-dependent expression (F = 3.41, p = 0.0088), whereas most members show non-significant trends (p>0.05)

HMG: High-mobility group; TCGA: The Cancer Genome Atlas; HMGN: HMG nucleosome-binding

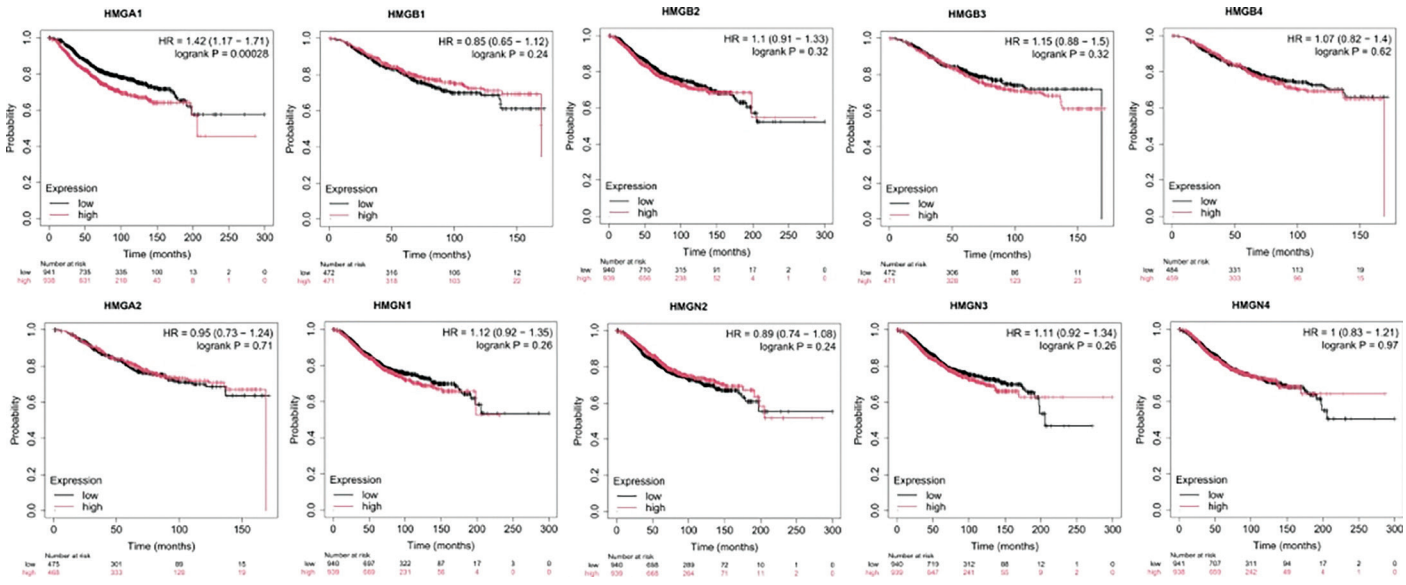

Figure 3. Survival analysis of HMG protein family mRNA expression in breast cancer patients. Kaplan-Meier survival analysis of HMG family mRNA [$\log_2$(TPM+1)] in the TCGA breast cancer cohort (n = 1,878) identifies HMGN1 as a key prognostic marker (HR = 1.42, p = 0.00028), with non-significant trends for HMGA4 (p = 0.62) and HMGB2 (p = 0.32). Log-rank test applied; group sizes shown

HMG: High-mobility group; TCGA: The Cancer Genome Atlas; HMGN: HMG nucleosome-binding; TPM: Transcripts per million; HR: Hazard ratio

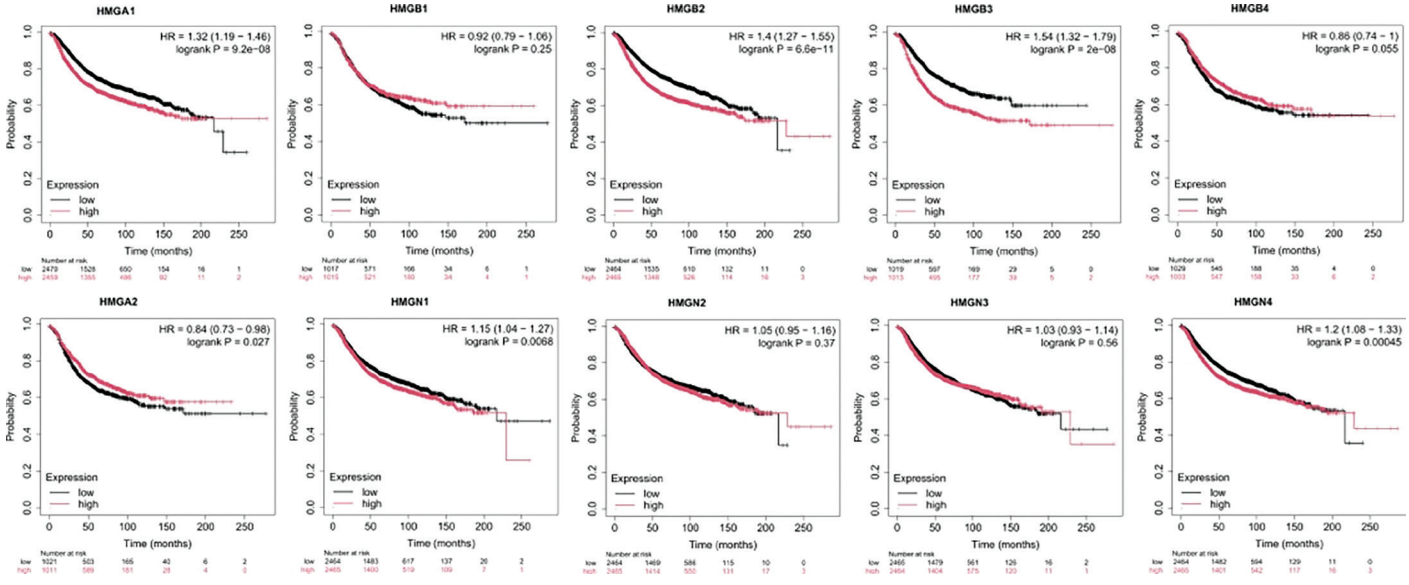

Figure 4. Prognostic impact of HMG family mRNA expression on breast cancer outcomes. Kaplan-Meier analysis of PFS among 2,465 TCGA breast cancer patients identifies divergent prognostic roles of HMG family members. HMGA1 and HMGN1 are associated with favorable outcomes, whereas HMGN4, HMGB4, and HMGN3 are associated with poorer prognosis; HMGN4 shows the strongest adverse prognostic effect. Non-significant trends are observed for HMGB2 and HMGA2

HMG: High-mobility group; TCGA: The Cancer Genome Atlas; HMGN: HMG nucleosome-binding; PFS: Progression-free survival

alterations that could drive cancer progression. The hallmark "evading growth suppressors" revealed notable interactions with HMGA1, HMGA2, and HMGB1, indicating that these genes may collectively contribute to bypassing regulatory mechanisms that typically inhibit cell proliferation. The odds ratio of 1.66 suggests a moderate association, reinforcing the idea that these genes could play a synergistic role in tumorigenesis. Sustained angiogenesis, critical for tumor growth, is associated with HMGA2, which has an odds ratio of 2.82, suggesting its significant involvement in promoting blood vessel formation to support tumor nourishment. HMGA2 and HMGB1 have been linked to the hallmark of tissue invasion and metastasis. Their involvement suggests a potential mechanism by which cancer cells invade surrounding tissues and spread to distant sites. The hallmarks of evading immune destruction, tumor-promoting inflammation, and resisting cell death did not significantly overlap with the analyzed genes. This absence of association suggests that these pathways may not be directly modulated by the genes under investigation

Prognostic Roles of HMG Proteins in Patients with Different Clinicopathological Features

This study examined the prognostic significance of HMG protein levels in breast cancer patients with varying clinicopathological features. We assessed the correlation of HMG protein expression with tumor stage and TP53 mutation status. We specifically investigated the expression levels of HMG proteins in relation to p53 mutation status, comparing wild-type and mutant p53 samples. Gene expression levels, quantified as TPM, were visualized using box plots, as presented in Figure 6. Notably, HMG proteins from all groups (HMGA, HMGB, and HMGN) exhibited elevated expression levels in p53-mutant samples, whereas the *HMGB4* gene was not expressed. This suggests that HMG proteins may have distinct roles based on p53 mutation status.

When stratified by cancer grade, the results showed (Table 2) that elevated levels of HMGB2, HMGB4, and HMGN1 mRNA were associated with better OS in patients with grade II disease. Conversely, high levels of HMGB4 and HMGN2 were linked to better OS in patients with grade I and grade III disease, while HMGB1 was associated with poor survival in grade I. High expression levels of all HMG proteins, except HMGB4, were associated with poor OS in stage I patients. This highlights the complexity of HMG protein roles in different cancer grades and stages.

HMG Family Genetic Alterations in Breast Cancer Patients

We evaluated the genetic alterations in the HMG family in breast cancer using cBioPortal. The frequency of gene alterations was

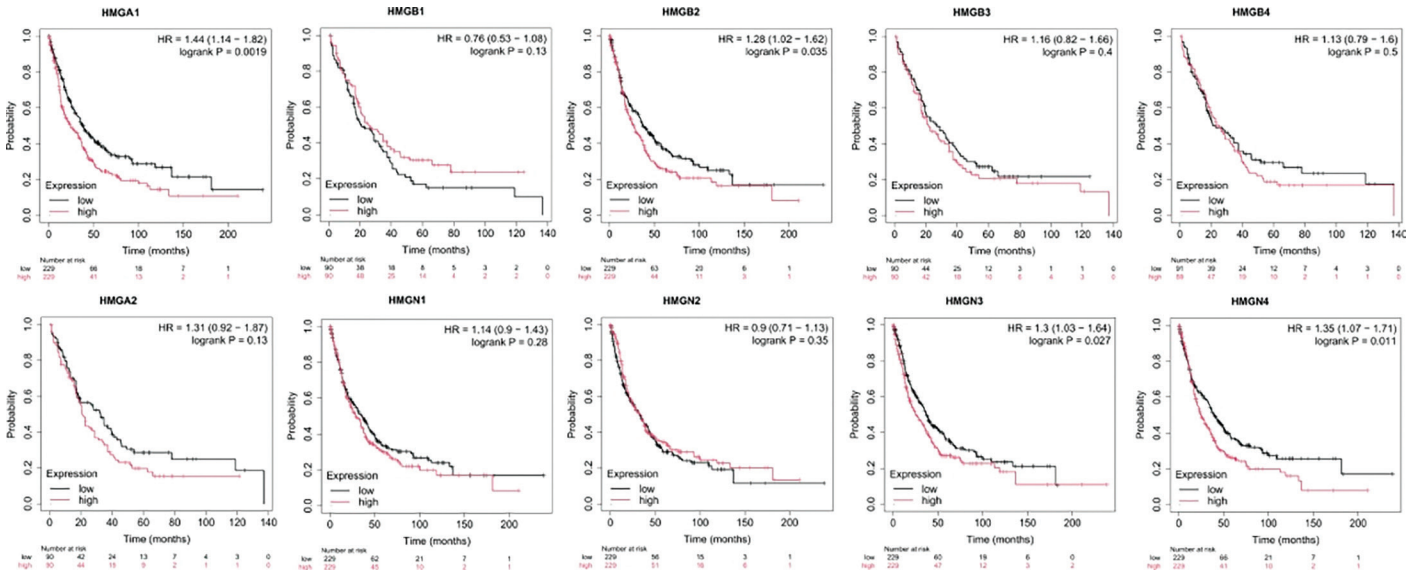

Figure 5. Post-progression survival analysis of HMG protein family mRNA expression in breast cancer. Kaplan-Meier curves showing post-progression survival outcomes stratified by mRNA expression levels of HMGA1/2, HMGB1–4, and HMGN1–4 in TCGA breast cancer cohort. Significant associations were observed for HMGN4 (HR = 1.35, 95% CI: 1.07–1.71, $p = 0.011$), HMGN2 (HR = 1.28, 95% CI: 1.02–1.62, $p = 0.035$), and HMGB1 (HR = 1.44, 95% CI: 1.14–1.82, $p = 0.0019$). Trends include HMGA4 (HR = 1.13, $p = 0.5$), and HMGB3 shows a statistically non-significant association (HR = 1.16, $p = 0.40$). The analysis was performed using the log-rank test with a median expression cut-off. Numbers at risk are shown for the low- and high-expression groups. Time scale: 0–200 months post-progression

HMG: High-mobility group; TCGA: The Cancer Genome Atlas; HMGN: HMG nucleosome-binding; HR: Hazard ratio; CI: Confidence interval

Table 1. HMG protein associations with cancer hallmark pathways

Cancer hallmark	Overlap	*p*-value	Adjusted *p*-value	Odds ratio	Hallmark *vs.* hallmark	Genes
Sustaining proliferative signaling	1/3574	0.93429	0.93429	0.5	0.39	*HMGB1*
Genome instability	1/747	0.4001	0.70848	3.01	1.88	*HMGB1*
Evading growth suppressors	3/3288	0.38067	0.70848	1.66	1.28	*HMGA2; HMGB1; HMGA1*
Evading immune destruction	0/1	Nan	1.0	Nan	0.0	Nan
Sustained angiogenesis	1/796	0.42041	0.70848	2.82	1.77	*HMGA2*
Tissue invasion and metastasis	2/2318	0.47232	0.70848	1.61	1.21	*HMGA2; HMGB1*
Tumor-promoting inflammation	0/1	Nan	1.0	Nan	0.0	Nan
Resisting cell death	1/1941	0.74997	0.89996	1.06	0.73	*HMGA2*
Reprogramming energy metabolism	0/1	Nan	1.0	Nan	0.0	Nan
Replicative immortality	0/1	Nan	1.0	Nan	0.0	Nan

Comprehensive enrichment analysis reveals heterogeneous involvement of HMG proteins across cancer hallmarks, though none reach statistical significance after multiple testing correction (FDR-adjusted $p>0.7$). The strongest raw associations were observed in evading growth suppressors (*HMGA1/HMGA2/HMGB1*; OR = 1.66) and tissue invasion and metastasis (OR = 1.61), while genome instability (OR = 3.01) and sustained angiogenesis (OR = 2.82) exhibited elevated risk trends. Five hallmarks, including immune evasion and metabolic reprogramming, showed no linkages to *HMG* genes

HMG: High-mobility group; FDR: False discovery rate; OR: Odds ratio

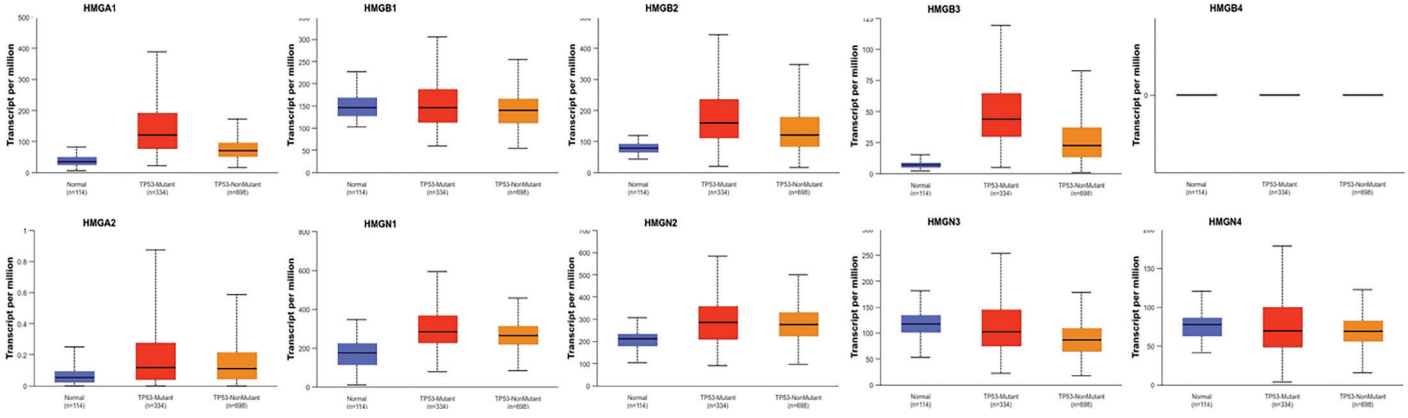

Figure 6. Differential expression patterns of HMG proteins by TP53 mutation status in breast cancer. Box plots comparing mRNA expression levels [$\log_2$ (TPM+1)] of HMGA1/2, HMGB1–4, and HMGN1–4 across normal breast tissue (n = 114), TP53-mutant (n = 334), and TP53-non-mutant (n = 698) tumors in TCGA cohort. HMGA1 (2.1-fold, mutant *vs.* non-mutant), HMGA2 (3.3-fold), and HMGB2 (1.8-fold) show upregulation in TP53-mutant tumors

HMG: High-mobility group; TCGA: The Cancer Genome Atlas; HMGN: HMG nucleosome-binding; TPM: Transcripts per million

measured as $\log_2$ values of the mutation count, ranging from 1 to 2. It includes mutations, amplifications, deep deletions, structural variants, and multiple alterations in TCGA datasets (Figure 7). *HMG* genes exhibited a high frequency of amplification, followed by mutations and deep deletions. Structural variants and multiple alterations occurred less frequently. The percentages of genetic alterations in specific *HMG* genes varied from <1.0% to 2.0% (e.g., HMGA1: 1.0%; HMGA2: 2.0%; HMGB1: 2.0%; HMGB2: 1.0%; HMGB3: 1.0%; HMGB4: <1.0%; HMGN1: 2.0%; HMGN2: <1.0%; HMGN3: <1.0%; HMGN4: 1.0%), with amplification being the most common alteration observed (Figure 8). We also assessed the prognostic roles of HMG in breast cancer patients with or without alterations. However, no significant correlation was found between the presence of alterations and OS or PFS in breast cancer patients (p-values: 0.140 and 0.112, respectively). Nonetheless, the unaltered group showed a favorable correlation with disease-free survival. The STRING database was used to construct a network of HMGs and closely interacting genes, demonstrating the intricate relationships between these proteins (Figure 8).

Table 2. Overall survival of breast cancer patients with different clinicopathological features and secretoglobin expression levels

Secretoglobin family	Clinicopathological features	Cases	HR	*p*-value
	Grades			
HMGA1	I	113	1.17	0.547
	II	243	1.07	0.529
	III	481	0.99	0.913
HMGA2	I	113	1.43	0.507
	II	243	1.25	0.371
	III	481	0.82	0.197
HMGB1	I	113	0.98	0.965
	II	243	0.80	0.380
	III	481	1.01	0.972
HMGB2	I	113	1.47	0.139
	II	243	1.27	**0.030**
	III	481	1.06	0.539
HMGB3	I	113	0.97	0.948
	II	243	1.23	0.417
	III	481	0.91	0.516
HMGB4	I	113	0.38	**0.093**
	II	243	0.43	**0.001**
	III	481	1.09	0.579
HMGN1	I	113	1.31	0.287
	II	243	1.21	**0.085**
	III	481	1.09	0.374
HMGN2	I	113	0.95	0.832
	II	243	1.03	0.776
	III	481	0.80	**0.016**
HMGN3	I	113	0.87	0.583
	II	243	1.08	0.479
	III	481	0.92	0.391
HMGN4	I	113	0.99	0.959
	II	243	0.94	0.559
	III	481	1.15	0.130

Survival analysis was used to evaluate the *p*-value. Bold font highlights the statistical significance of the difference; HR: Hazard ratio; HMG: High mobility group

Functional Enrichment Analysis of HMGs in Breast Cancer Patients

We utilized EnrichR to conduct enrichment analyses for GO Biological Process 2023, GO cellular component 2023, GO molecular function 2023, and Reactome 2022 on HMGs. The findings revealed that biological processes associated with HMGs were enriched in several categories, including protein-DNA complexes, chromatin organization, DNA conformation and topological changes, regulation of DNA binding, V(D)J recombination, regulation of stem cell proliferation, heterochromatin formation, and regulation of DNA-templated transcription (Table 3). The GO cellular component analysis indicated that HMGs primarily function in the nucleus, membrane-bounded intracellular organelles, and chromosomes, including heterochromatin and condensed nuclear chromosomes (Table 3). Molecular function enrichment analysis showed that HMGs are involved in DNA bending, formation of secondary structures and four-way junctions, and other critical processes.

The analysis found that the Reactome pathway associated with HMGs was enriched for several processes, including apoptosis induced DNA fragmentation, apoptotic execution phase, DNA damage/telomere stress induced senescence, APOBEC3G mediated resistance to human immunodeficiency virus type 1, two-long terminal repeat circle formation, programmed cell death, and integration of provirus (Table 3). These findings highlight the multifaceted roles of HMG proteins in breast cancer biology.

Discussion and Conclusion

HMGA1 is a master regulator in the progression of triple-negative breast cancer (TNBC), forming a complex with FOXM1 to enhance transcriptional activity of genes such as VEGFA, which promotes angiogenesis. Their co-expression correlates with poor patient prognosis, suggesting that targeting the HMGA1/FOXM1 interaction may be a viable therapeutic strategy (24). Our results showed significantly elevated HMGA1 mRNA levels in breast cancer tissues compared to normal tissues, indicating its potential role as an oncogene. Its association with poor OS in patients suggests that HMGA1 may contribute to tumor aggressiveness and progression. The involvement of HMGA1 in evading growth suppressors highlights its potential mechanism for bypassing regulatory pathways that typically inhibit cell proliferation. Given its prominent role in tumorigenesis, HMGA1 may serve as a critical biomarker for aggressive breast cancer phenotypes.

While HMGA2 exhibited moderate expression levels, its association with favorable survival outcomes indicates a complex role in breast cancer. The protein's involvement in sustained angiogenesis suggests it may facilitate tumor growth by promoting blood vessel formation. A study shows that HMGA2 is overexpressed in breast cancer, promoting cell proliferation, migration, and invasion while protecting against apoptosis. It also contributes to the acquisition of cancer stem cell features, suggesting that targeting HMGA2 may effectively impede breast cancer progression (25). This duality in function, acting as a promoter of angiogenesis while correlating with improved survival, necessitates further research to clarify its role in different tumor contexts and stages.

HMGB1 was significantly upregulated in breast cancer tissues and was strongly associated with genomic instability, suggesting a role

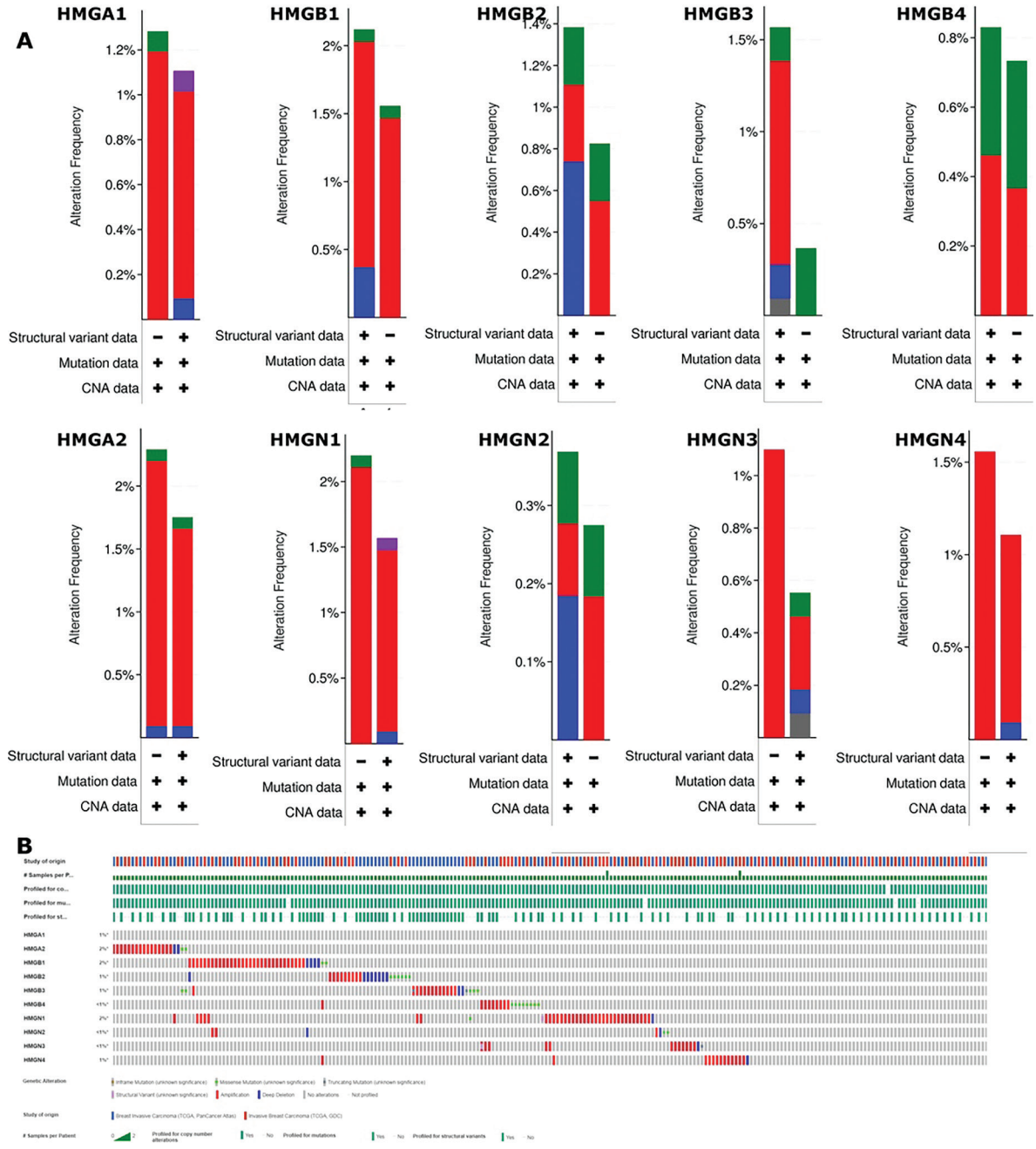

Figure 7. Genomic landscape of HMG protein family alterations in breast cancer. Analysis of 1,098 TCGA breast cancer patients reveals low yet patterns of genetic alterations in HMG-family genes. HMGA1 (2%) and HMGB2 (1.5%) show the highest alteration rates, and HMGA1 amplifications and HMGB3 deletions are the predominant copy-number changes. Structural variants in HMGN2/3 are rare (<0.5%), while HMGA2 mutations co-occur with TP53 alterations. Data integration from the TCGA PanCancer and GDC cohorts employs color-coded visualization (amplifications = red, deletions = blue) and platform-specific profiling indicators (+/– symbols)

HMG: High-mobility group; TCGA: The Cancer Genome Atlas; HMGN: HMG nucleosome-binding; GDC: Genomic data commons; CNA: Copy number alteration

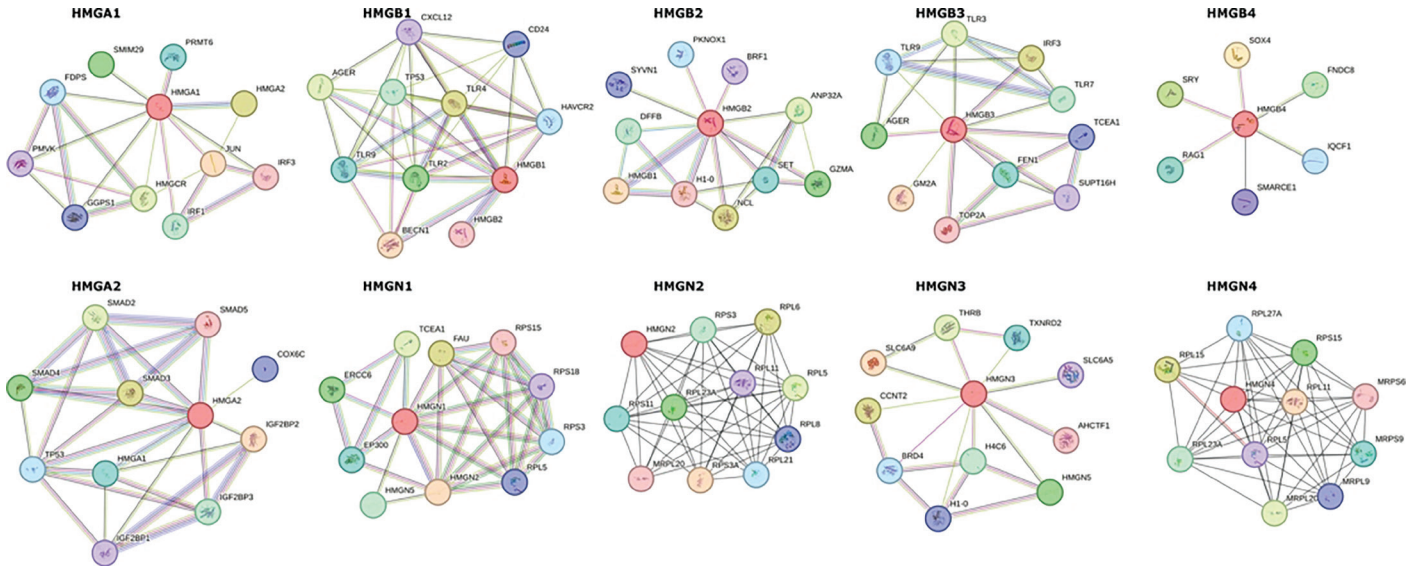

Figure 8. Protein interaction network of HMG family members in breast cancer biology. STRING analysis of HMG proteins reveals three core modules: (1) immune regulation via HMGB1/2-TLRs (2/3/4/9) and interferon genes; (2) chromatin remodeling through HMGA1/2-SMAD2–5/TP53 interactions; and (3) ribosome biogenesis linking HMGN1–4 to RPL/RPS proteins. Cross-cluster connections include HMGA1-DNA repair (*FEN1/ERCC6*) and HMGB4-cholesterol biosynthesis (*HMGCR/FDPS*)

HMG: High-mobility group; HMGN: HMG nucleosome-binding; STRING: Search tool for the retrieval of interacting genes/proteins; TLRs: Toll-like receptors; RPL/RPS: Ribosomal protein, large subunit/small subunit

Table 3. Gene ontology and pathways enrichment analysis of secretoglobin in breast cancer

Category	Term	*p*-value	*q*-value	Overlap genes
GO biological process 2023				
GOTERM_BP	Protein-DNA complex organization (GO: 0071824)	1.172228e-13	2.215510e-11	[*HMGN4, HMGB2, HMGA2, HMGN2, HMGN3, HMGN1*]
GOTERM_BP	Chromatin organization (GO: 0006325)	1.098989e-09	1.038544e-07	[*HMGN4, HMGB2, HMGA2, HMGN2, HMGN3, HMGN1*]
GOTERM_BP	DNA conformation change (GO: 0071103)	1.975326e-08	1.244455e-06	[*HMGB2, HMGB3, HMGB1*]
GOTERM_BP	DNA geometric change (GO: 0032392)	3.628342e-07	1.714392e-05	[*HMGB2, HMGB3, HMGB1*]
GOTERM_BP	Regulation of DNA binding (GO: 0051101)	1.538445e-06	5.815322e-05	[*HMGB2, HMGA2, HMGB1*]
GO cellular component 2023				
GOTERM_CC	Nucleus (GO: 0005634)	0.000011	0.000183	[*HMGN4, HMGA1, HMGB2, HMGA2, HMGB1, HMGN2, HMGN3, HMGB4, HMGN1*]
GOTERM_CC	Intracellular membrane-bounded organelle (GO: 0043231)	0.000040	0.000318	[*HMGN4, HMGA1, HMGB2, HMGA2, HMGB1, HMGN2, HMGN3, HMGB4, HMGN1*]
GOTERM_CC	Chromosome (GO: 0005694)	0.000062	0.000332	[*HMGB2, HMGA2, HMGB1*]
GOTERM_CC	Heterochromatin (GO: 0000792)	0.000261	0.001045	[*HMGA1, HMGA2*]
GOTERM_CC	Condensed chromosome (GO: 0000793)	0.000392	0.001255	[*HMGB2, HMGB1*]

Table 3. Continued

Category	Term	*p*-value	*q*-value	Overlap genes
GOTERM_CC	Nuclear chromosome (GO: 0000228)	0.046507	0.106379	[*HMGA2*]
GO molecular function 2023				
GOTERM_MF	DNA binding, bending (GO: 0008301)	2.918490e-17	1.109026e-15	[*HMGA1, HMGB2, HMGA2, HMGB3, HMGB1, HMGB4*]
GOTERM_MF	DNA secondary structure binding (GO: 0000217)	2.230118e-12	4.237225e-11	[*HMGA1, HMGB2, HMGA2, HMGB3, HMGB1*]
GOTERM_MF	Four-way junction DNA binding (GO: 0000400)	5.022899e-08	4.771754e-07	[*HMGB2, HMGB3, HMGB1*]
GOTERM_MF	Supercoiled DNA binding (GO: 0097100)	2.248131e-06	1.708580e-05	[*HMGB2, HMGB1*]
Reactome pathway 2022				
Reactome-2022	Apoptosis induced DNA fragmentation R-HSA-140342	0.000017	0.000869	[*HMGB2, HMGB1*]
Reactome-2022	Formation of senescence-associated heterochromatin foci R-HSA-2559584	0.000030	0.000869	[*HMGA1, HMGA2*]
Reactome-2022	Apoptotic execution phase R-HSA-75153	0.000294	0.005594	[*HMGB2, HMGB1*]
Reactome-2022	DNA damage/telomere stress induced senescence R-HSA-2559586	0.000405	0.005776	[*HMGA1, HMGA2*]
Reactome-2022	Cellular senescence R-HSA-2559583	0.002915	0.027539	[*HMGA1, HMGA2*]

GO: Gene ontology; GOTERM: Gene ontology term; BP: Biological process; CC: Cellular component; MF: Molecular function

in promoting genomic alterations that drive cancer progression. Notably, high levels of HMGB1 were linked to better overall and PFS, indicating its potential as a protective factor in breast cancer. HMGB1 enhances breast cancer metastasis by activating fibroblasts through the receptor for advanced glycation end products/aerobic glycolysis pathway. High HMGB1 expression in migratory cancer cells leads to increased fibroblast activation, which subsequently promotes tumor cell metastasis (26). Its involvement in evading growth suppressors further emphasizes its critical role in tumor biology, making it a promising candidate for therapeutic targeting.

HMGB2 is overexpressed in breast cancer tissues and correlates with larger tumor size and advanced stage. Its expression serves as an independent prognostic factor, promoting tumor growth and aerobic glycolysis by regulating lactate dehydrogenase B and fructose-1,6-bisphosphatase 1 (27). Findings show that the expression of HMGB2 is significantly higher in breast cancer tissues, and it is associated with favorable survival outcomes in certain tumor grades. Its role in chromatin organization and DNA binding suggests that HMGB2 may influence gene expression patterns critical for tumor development. The complex relationship between HMGB2 expression and patient survival underscores the need for further investigation into its functional mechanisms in breast cancer.

Similar to HMGB1 and HMGB2, HMGB3 was found to be upregulated in breast cancer tissues. However, its association with poor OS indicates that it may contribute to tumor progression. The role of HMGB3 in chromatin dynamics and gene regulation positions it as a key player in the molecular landscape of breast cancer. HMGB3 expression correlates positively with aggressive cancer features and negatively with hormone receptor status. Knockdown of HMGB3 promotes cancer cell proliferation and enhances sensitivity to chemotherapy (28). Understanding its specific contributions to tumor biology could reveal novel therapeutic strategies.

HMGB4 was expressed at very low levels in breast cancer tissues, yet its expression was associated with improved survival in certain patient subsets. This suggests that HMGB4 might have a protective role in early-stage disease. The lack of significant expression in advanced tumors indicates that it may not be a

primary driver of tumorigenesis but could still provide insights into tumor biology and patient prognosis.

HMGN1 expression was significantly elevated in breast cancer tissues and was associated with poorer OS. Its role in chromatin remodeling and transcriptional regulation suggests that HMGN1 may facilitate oncogenic processes. The association with unfavorable survival outcomes highlights the need for further exploration of its functional mechanisms and its potential as a therapeutic target. Previous studies have shown that HMGN1 regulates chromatin structure and tumour immunityto more than 147 proteins. These reported changes include effects on histone activity, stress pathways, and immune responses (29). The study shows HMGN1's critical role in cancer cell function and suggests potential avenues for therapeutic exploration based on proteomic analysis.

HMGN2 significantly inhibits proliferation and migration of Michigan Cancer Foundation-7 breast cancer cells and promotes apoptosis. *In vivo* studies using a mouse model demonstrated that administration of HMGN2 reduced tumor growth and increased apoptotic cell counts (30). Our findings show that increased expression of HMGN2 in breast cancer was associated with favorable survival outcomes in specific tumor grades. Its involvement in chromatin structure and transcriptional regulation positions it as a potential modulator of gene expression in cancer. The contrasting survival associations indicate that HMGN2 may play context-dependent roles in tumor biology.

HMGN3 was found to have elevated expression levels in breast cancer tissues, correlating with poor OS. Its role in chromatin dynamics suggests that it may influence gene expression patterns critical for tumor progression. The association with unfavorable survival outcomes emphasizes the need for further research to elucidate its precise role in breast cancer biology. HMGN3 has not been directly studied in breast cancer but has been highlighted for its role in CCA. It shows increased expression in CCA compared to hepatocellular carcinoma, suggesting both its potential as a diagnostic marker for CCA and its involvement in tumor invasion, which is influenced by transforming growth factor beta signaling (31).

HMGN4 is highly expressed in TNBC and regulates cell proliferation both *in vitro* and *in vivo*. It interacts with the signal transducer and activator of transcription 3 (STAT3) pathway, forming a feedback loop that promotes TNBC cell growth (32). Our study reported that HMGN4 exhibited increased expression in breast cancer tissues, but HMGN4 expression did not show a clear correlation with survival outcomes. Its involvement in chromatin organization and DNA binding indicates that it may regulate gene expression. Further studies are needed to clarify its functional significance in breast cancer and its potential as a prognostic marker.

This study highlights the diverse roles of HMG proteins (HMGA, HMGB, and HMGN) in breast cancer biology and prognosis. HMGA1 correlates with poor survival, underscoring its potential as a therapeutic target. HMGA2, despite being associated with favourable outcomes, promotes angiogenesis and tumour progression, reflecting its complex dual role. HMGB1 appears protective, as it is linked to improved survival, yet it simultaneously facilitates metastasis, whereas HMGB2 and HMGB3 are associated with aggressive disease features. HMGB4, expressed at low levels, may confer benefits in early-stage tumours. Among HMGN proteins, elevation of HMGN1 predicts poor prognosis, suggesting therapeutic relevance, whereas HMGN2 demonstrates anti-proliferative and pro-apoptotic effects. HMGN3 may contribute to progression, and HMGN4, highly expressed in TNBC, interacts with STAT3 signalling, though; its prognostic impact remains unclear. Collectively, these findings emphasize the translational potential of HMG proteins as biomarker panels for prognostic stratification and as therapeutic targets for pathway-specific interventions. Future validation through multi-cohort studies, functional assays, and clinical trials will be essential to establish their clinical utility and advance precision oncology in breast cancer.

Ethics

Ethics Committee Approval: Therefore, ethical approval was not required for this study.

Informed Consent: Informed consent from individuals was not required.

Footnotes

Authorship Contributions

Surgical and Medical Pracites: E.A.S., A.A., R.A.Z., A.A.W., E.B.A., R.E.A.S.; Concept: E.A.S., A.A.; Design: E.A.S., A.A., R.A.Z.; Data Collection and/or Processing: R.A.Z., A.A.W., E.B.A., R.E.A.S.; Analysis and/or Interpretation: E.A.S., A.A., R.A.Z., A.A.W., R.E.A.S.; Literature Search: E.A.S., A.A., R.A.Z., A.A.W., E.B.A., R.E.A.S.; Writing: E.A.S., A.A., R.A.Z., R.E.A.S.

Conflict of Interest: The authors have no conflicts of interest to declare.

Financial Disclosure: The authors declared that this study has received no financial support.

References

1. Kim J, Harper A, McCormack V, Sung H, Houssami N, Morgan E, et al. Global patterns and trends in breast cancer incidence and mortality across 185 countries. Nat Med. 2025; 31: 1154-1162. (PMID: 39994475) [Crossref]
2. Popa MT, Noditi A, Peleaæã TM, Stoleru S, Blidaru A. Breast cancer: a heterogeneous pathology. Prognostic and predictive factors – a narrative review. Chir [Internet]. 2025 Jan 1 [cited 2025 Jun 29]; 120: 32-47. [Crossref]
3. Chen L, Kong X, Wang Z, Wang X, Fang Y, Wang J. Pre-treatment systemic immune-inflammation index is a useful prognostic indicator in patients with breast cancer undergoing neoadjuvant chemotherapy. J Cell Mol Med. 2020; 24: 2993-3021. (PMID: 31989747) [Crossref]

4. Mallik R, Kundu A, Chaudhuri S. High mobility group proteins: the multifaceted regulators of chromatin dynamics. Nucleus. 2018; 61. [Crossref]

5. Chen J, Li H, Huang Y, Tang Q. The role of high mobility group proteins in cellular senescence mechanisms. Front Aging. 2024; 5: 1486281. (PMID: 39507236) [Crossref]

6. Parisi S, Piscitelli S, Passaro F, Russo T. HMGA Proteins in stemness and differentiation of embryonic and adult stem cells. Int J Mol Sci. 2020; 21: 362. (PMID: 31935816) [Crossref]

7. Lamas-Maceiras M, Vizoso-Vázquez Á, Barreiro-Alonso A, Cámara-Quílez M, Cerdán ME. Thanksgiving to yeast, the HMGB proteins history from yeast to cancer. Microorganisms. 2023; 11: 993. (PMID: 37110415) [Crossref]

8. He B, Kram V, Furusawa T, Duverger O, Chu EY, Nanduri R, et al. Epigenetic regulation of ameloblast differentiation by HMGN proteins. J Dent Res. 2024; 103: 51-61. (PMID: 37950483) [Crossref]

9. Sorin S, Kubota S, Hamidi S, Yokomizo-Nakano T, Vaeteewoottacharn K, Wongkham S, et al. HMGN3 represses transcription of epithelial regulators to promote migration of cholangiocarcinoma in a SNAI2-dependent manner. FASEB J. 2022; 36: e22345. (PMID: 35635715) [Crossref]

10. Kugler J, Postnikov YV, Furusawa T, Kimura S, Bustin M. Elevated HMGN4 expression potentiates thyroid tumorigenesis. Carcinogenesis. 2017; 38: 391-401. (PMID: 28186538) [Crossref]

11. Kroemer G, Kepp O. Radiochemotherapy-induced elevations of plasma HMGB1 levels predict therapeutic responses in cancer patients. Oncoimmunology. 2021; 10: 2005859. (PMID: 34858731) [Crossref]

12. Ma Q, Ye S, Liu H, Zhao Y, Zhang W. The emerging role and mechanism of HMGA2 in breast cancer. J Cancer Res Clin Oncol. 2024; 150: 259. (PMID: 38753081) [Crossref]

13. Huang BF, Tzeng HE, Chen PC, Wang CQ, Su CM, Wang Y, et al. HMGB1 genetic polymorphisms are biomarkers for the development and progression of breast cancer. Int J Med Sci. 2018; 15: 580-586. (PMID: 29725248) [Crossref]

14. Lee HJ, Kim JY, Song IH, Park IA, Yu JH, Ahn JH, et al. High mobility group B1 and N1 (HMGB1 and HMGN1) are associated with tumor-infiltrating lymphocytes in HER2-positive breast cancers. Virchows Arch. 2015; 467: 701-709. (PMID: 26445971) [Crossref]

15. Tang Z, Kang B, Li C, Chen T, Zhang Z. GEPIA2: an enhanced web server for large-scale expression profiling and interactive analysis. Nucleic Acids Res. 2019; 47: W556-W560. (PMID: 31114875) [Crossref]

16. Győrffy B. Survival analysis across the entire transcriptome identifies biomarkers with the highest prognostic power in breast cancer. Comput Struct Biotechnol J. 2021; 19: 4101-4109. (PMID: 34527184) [Crossref]

17. Cerami E, Gao J, Dogrusoz U, Gross BE, Sumer SO, Aksoy BA, et al. The cBio cancer genomics portal: an open platform for exploring multidimensional cancer genomics data. Cancer Discov. 2012; 2: 401-404. Erratum in: Cancer Discov. 2012; 2: 960. (PMID: 22588877) [Crossref]

18. Chen EY, Tan CM, Kou Y, Duan Q, Wang Z, Meirelles GV, et al. Enrichr: interactive and collaborative HTML5 gene list enrichment analysis tool. BMC Bioinformatics. 2013; 14: 128. (PMID: 23586463) [Crossref]

19. Kuleshov MV, Jones MR, Rouillard AD, Fernandez NF, Duan Q, Wang Z, et al. Enrichr: a comprehensive gene set enrichment analysis web server 2016 update. Nucleic Acids Res. 2016; 44: W90-W97. (PMID: 27141961) [Crossref]

20. Xie Z, Bailey A, Kuleshov MV, Clarke DJB, Evangelista JE, Jenkins SL, et al. Gene set knowledge discovery with enrichr. Curr Protoc. 2021; 1: e90. (PMID: 33780170) [Crossref]

21. Szklarczyk D, Gable AL, Nastou KC, Lyon D, Kirsch R, Pyysalo S, et al. The STRING database in 2021: customizable protein-protein networks, and functional characterization of user-uploaded gene/measurement sets. Nucleic Acids Res. 2021; 49: D605-D612. Erratum in: Nucleic Acids Res. 2021; 49: 10800. (PMID: 33237311) [Crossref]

22. Chandrashekar DS, Bashel B, Balasubramanya SAH, Creighton CJ, Ponce-Rodriguez I, Chakravarthi BVSK, et al. UALCAN: a portal for facilitating tumor subgroup gene expression and survival analyses. Neoplasia. 2017; 19: 649-658. (PMID: 28732212) [Crossref]

23. Chandrashekar DS, Karthikeyan SK, Korla PK, Patel H, Shovon AR, Athar M, et al. UALCAN: an update to the integrated cancer data analysis platform. Neoplasia. 2022; 25: 18-27. (PMID: 35078134) [Crossref]

24. Zanin R, Pegoraro S, Ros G, Ciani Y, Piazza S, Bossi F, et al. HMGA1 promotes breast cancer angiogenesis supporting the stability, nuclear localization and transcriptional activity of FOXM1. J Exp Clin Cancer Res. 2019; 38: 313. (PMID: 31311575) [Crossref]

25. Mansoori B, Duijf PHG, Mohammadi A, Najafi S, Roshani E, Shanehbandi D, et al. Overexpression of HMGA2 in breast cancer promotes cell proliferation, migration, invasion and stemness. Expert Opin Ther Targets. 2020; 24: 255-265. (PMID: 32172636) [Crossref]

26. Chen Y, Cai L, Guo X, Li Z, Liao X, Zhang X, et al. HMGB1-activated fibroblasts promote breast cancer cells metastasis via RAGE/aerobic glycolysis. Neoplasma. 2021; 68: 71-78. (PMID: 33030958) [Crossref]

27. Fu D, Li J, Wei J, Zhang Z, Luo Y, Tan H, et al. HMGB2 is associated with malignancy and regulates Warburg effect by targeting LDHB and FBP1 in breast cancer. Cell Commun Signal. 2018; 16: 8. (PMID: 29463261) [Crossref]

28. Zhou X, Zhang Q, Liang G, Liang X, Luo B. Overexpression of HMGB3 and its prognostic value in breast cancer. Front Oncol. 2022; 12: 1048921. (PMID: 36620553) [Crossref]

29. Mehnert M, Li W, Wu C, Salovska B, Liu Y. Combining rapid data independent acquisition and CRISPR gene deletion for studying potential protein functions: a case of HMGN1. Proteomics. 2019; 19: e1800438. (PMID: 30901150) [Crossref]

30. Fan B, Shi S, Shen X, Yang X, Liu N, Wu G, et al. Effect of HMGN2 on proliferation and apoptosis of MCF-7 breast cancer cells. Oncol Lett. 2019; 17: 1160-1166. Retraction in: Oncol Lett. 2025; 29: 259. (PMID: 30655878) [Crossref]

31. Sorin S, Pokaew N, Vaeteewoottacharn K, Waraasawapati S, Pairojkul C, Sashida G, et al. Overexpression of HMGN3 nucleosome binding protein is associated with tumor invasion and TGF-β expression in cholangiocarcinoma. ScienceAsia. 2022; 48: 518-523. [Crossref]

32. Mou J, Xu X, Wang F, Kong W, Chen J, Ren J. HMGN4 plays a key role in STAT3-mediated oncogenesis of triple-negative breast cancer. Carcinogenesis. 2022; 43: 874-884. (PMID: 35792800) [Crossref]

ORIGINAL ARTICLE

European Journal of BREAST HEALTH

DOI: 10.4274/ejbh.galenos.2025.2025-11-2
Eur J Breast Health 2026;22(3):261-269

Cost of Breast Cancer Treatment by Comorbidity in Dubai, the United Arab Emirates: A Retrospective Data Analytical Approach

Meenu Mahak Soni[1], Noora Almulla[2], Heba Mohammed Mamdouh[3,4]

[1]Department of Health Economics and Insurance Policies, Dubai Health Authority, Dubai, United Arab Emirates
[2]Department of Health Insurance Providers Permits, Dubai Health Authority, Dubai, United Arab Emirates
[3]Department of Family Health, Alexandria University, Alexandria, Egypt
[4]Department of Data Analysis, Research and Studies, Dubai Health Authority, Dubai, United Arab Emirates

ABSTRACT

Objective: Breast cancer is the most common malignancy among women in Dubai, yet the economic burden of its treatment remains understudied. This study aimed to estimate the direct medical costs of breast cancer care in Dubai in 2024 and to examine variations by encounter type, comorbidity burden, and provider setting.

Materials and Methods: A retrospective cross-sectional analysis of insurance claims was conducted for January-December 2024. Breast cancer cases were identified using International Classification of Diseases, 10th revision, clinical modification codes, and comorbidity burden was assessed using the Charlson comorbidity index (CCI). Costs were analyzed by encounter type (outpatient, inpatient, day case) and by provider setting (clinic/center versus hospital). A Tweedie generalized linear model was applied to evaluate the effect of comorbidities and service characteristics on costs.

Results: A total of 8,967 patients (mean age 51.8 years) with 81,248 claims were identified. Outpatient visits constituted 86% of encounters and accounted for 81% of total expenditure (USD 48.7M). Inpatient admissions accounted for 6% of encounters and had the highest mean cost per patient (USD 10,808). The total expenditure was USD 60.0M. Costs increased significantly with comorbidity severity: patients with CCI ≥5 incurred 6.4-fold higher costs compared to those without comorbidities ($p<0.0001$). Hospital-based care increased costs by 16%, and pharmacy claims contributed an additional 31% to expenditures.

Conclusion: Breast cancer treatment in Dubai imposes a substantial economic burden, largely driven by outpatient services, hospital-based care, and medication costs. Comorbidity significantly increases expenditures. These findings highlight the importance of integrated, risk-stratified care pathways and sustainable strategies to optimize resource allocation for breast cancer management in the United Arab Emirates.

Keywords: Treatment cost; breast cancer; comorbidity; Dubai; United Arab Emirates

Corresponding Author: Meenu Mahak Soni MD; MBBS,MSc;
E-mail: mschandersoni@dha.gov.ae **ORCID:** orcid.org/0009-0003-0795-5387

Received: 23.11.2025 **Accepted:** 21.12.2025 **Available Online Date:** 17.06.2026
Cite this article as: Soni MM, Almulla N, Mamdouh HM. Cost of breast cancer treatment by comorbidity in Dubai, the United Arab Emirates: a retrospective data analytical approach. Eur J Breast Health. 2026;22(3):261-269

KEY POINTS

- Breast cancer is the most common malignancy among women globally and in the United Arab Emirates. While costs have been studied in high-income countries, there is limited evidence on the economic burden in Dubai, particularly with respect to comorbidity burden and healthcare setting.
- This study provides the first comprehensive claims-based cost analysis of breast cancer in Dubai. Outpatient services accounted for most spending, but inpatient admissions and higher Charlson comorbidity index scores substantially increased per-patient costs, with severe comorbidities increasing costs more than sixfold. The findings highlight the importance of risk-stratified integrated care pathways and pharmaceutical cost management. They provide evidence to policymakers and insurers in Dubai to support the design of sustainable oncology financing, the prioritization of outpatient management where feasible, and the implementation of value-based purchasing strategies.

Introduction

Breast cancer is the most frequently diagnosed cancer among women worldwide (1). Nearly one in four cancer diagnoses is breast cancer. In 2020, there were 2.3 million global incidents and 685,000 deaths as a result (2). Early detection, screening programs, and newer treatment options have led to improved overall outcomes, particularly in earlier stages of treatment, where these improvements are most evident (3, 4). Despite improved outcomes, breast cancer continues to have a significant clinical and economic impact on healthcare systems globally (5, 6).

The economic burden of breast cancer has been examined thoroughly in high-income countries, where direct medical costs are estimated to be in the billions and are highly influenced by stage at diagnosis, comorbidity burden, age cohort, and type of services utilized (7-9). Economic evaluations are instrumental in guiding healthcare policy decisions, promoting equitable access to care, and ensuring the sustainability of breast cancer care (5). In general, inpatient admissions and targeted therapy have been repeatedly examined as major cost drivers, although the age cohorts demonstrate different cost distributions due to comorbidity profiles and treatment strategies (10-12). In particular, comorbidities significantly increase the economic burden of breast cancer treatment, resulting in higher healthcare costs for patients (13). For instance, researchers have shown that after adjusting for comorbid conditions, the annual difference in total healthcare cost for recently diagnosed breast cancer patients can be substantial, reaching tens of thousands of dollars per patient (14).

Across the Middle East and North Africa, breast cancer accounts for a considerable proportion of cancer diagnoses among females, often occurring at younger ages and at more advanced stages than in Western populations (15, 16). Specifically, in the United Arab Emirates (UAE), breast cancer is the most common malignancy among women, accounting for approximately 38% of all cancers in women (17).

Some published studies on the incidence and treatment modalities of breast cancer can be found in the UAE (18-20). However, literature detailing the economic burden of breast cancer on the healthcare systems in Dubai, UAE, regarding service type, comorbidity burden, and age cohort cannot be found. This knowledge gap limits the ability of health policymakers and private-sector insurers to understand the economic burden of breast cancer and to develop financing models that are sustainable and that effectively allocate resources within Dubai's health care system.

In our efforts to fill this gap, the present study utilized retrospective claims data from Dubai to estimate the direct medical costs of breast cancer for 2024. Costs were examined by type of service (outpatient, day-case, and inpatient care) and by comorbidity, assessed using the Charlson comorbidity index (CCI). The results will provide policymakers, insurers, and healthcare providers with important information regarding the economic burden of breast cancer in Dubai, and will contribute to evidence-based planning and cost-effective care delivery.

Materials and Methods

Study Design

A cross-sectional retrospective study was conducted using eClaimLink, the electronic platform that records all claim transactions under Dubai-based health insurance policies. This system contains information on the services utilized, the type of healthcare facility where services were delivered, and the associated costs.

All claims related to breast cancer patients, identified by International Classification of Diseases 10th revision (ICD-10), clinical modification codes as the primary diagnosis, were extracted for the period from January to December 2024 using structured query language. The dataset contained information on length of stay (LOS), comorbid conditions, encounter type, services rendered, provider setting (clinic, center, pharmacy, or hospital), net claimed amounts, and demographic variables, such as age. Data on breast cancer stage were not available; therefore, costs could not be analyzed according to disease stage.

Clinical factors, including comorbidities given their influence on medical expenditures, were measured using ICD-10 codes.

Comorbidity burden was assessed using the CCI. The CCI is a validated measure that lists 23 chronic conditions (plus others) and directly indicates those conditions (21). Based on the CCI

score, the severity of comorbidity was categorized into three grades: mild, with CCI scores of 1–2; moderate, with CCI scores of 3–4; and severe, with CCI scores ≥5. The CCI assigned weights to secondary medical conditions, and the score was calculated. The two analytical scenarios were applied: a base scenario in which the CCI was calculated excluding "any malignancy" and "any metastatic solid tumor," thereby isolating the effect of non-cancer comorbidities. An alternative scenario is when CCI is calculated to include malignancy and metastasis, reflecting the full disease burden when cancer-related conditions are incorporated. This dual specification enabled a comparison of how comorbidity influenced costs, depending on whether cancer itself was included in the index.

Variables

Data on the sociodemographic variables were missing, and only patient age was obtained directly from the records. An outpatient encounter was defined as a visit to a healthcare facility for diagnosis or treatment that did not result in admission. An inpatient encounter was defined as an admission involving at least one overnight stay in the healthcare facility (22). A day-case encounter was defined as an admission in which the patient received care and was discharged on the same day without an overnight stay (23).

The primary outcome was the direct medical cost of breast cancer care, calculated as the net claimed amount submitted to insurers for claims in which breast cancer was recorded only as the primary diagnosis. Independent variables included comorbidity status (CCI score), encounter type (outpatient, day case, inpatient), and provider type (clinic/center, hospital, pharmacy). To define the cost of care related to breast cancer treatment, inpatient visit costs were identified by searching for hospitalizations with ICD-10 codes C50.0–C50.9 (24).

To calculate the average cost, we measured the total annual healthcare spending for each eligible patient on breast cancer-related services, including inpatient admissions, day case and outpatient visits, and medications. All costs were converted from UAE Dirhams (AED) to US$ using the official US dollar conversion rate (1 US dollar = 3.673 AED).

Statistical Analysis

Data cleaning and analysis were performed using R software. Descriptive statistics were first calculated, including the total cost of breast cancer treatment, the average cost per patient per year, with standard deviation (SD), and the percentage distribution of costs by type of admission. Treatment costs were also stratified by comorbidity status (presence *vs.* absence of comorbidity).

To account for the highly skewed and zero-inflated pattern of cost data, regression analysis was performed using a Tweedie generalized linear model (25, 26) with a log link function. The baseline category was defined as patients with no comorbidity (CCI = 0) who were receiving outpatient care at clinics or centers. The model predictors included CCI score, type of encounter (reference: outpatient), provider type (reference: clinic/center), and selected interaction effects between encounter type and provider type. We did not include age in the primary specification because age was inconsistently recorded at the claim level in our data extract, which risked introducing measurement error; furthermore, age and CCI were strongly correlated in our cohort, and exploratory models suggested that including both led to instability and counterintuitive signs without improving model fit. All tests were two-sided, with a p-value < 0.05 indicating statistical significance.

Ethical standards were applied throughout this study as per Dubai Health Authority guidelines and regulations. The Dubai Scientific Research Ethics Committee at the Dubai Health Authority waived ethical approval in such cases because the study used secondary data and did not involve human participants.

Results

A total of 8,967 breast cancer patients were included, with a mean age of 51.8 years (SD: 8.6).The majority (88%) were aged 40–64 years. A total of 81,248 claims were recorded, with 43% of patients having more than five claims. Most encounters were outpatient (86%), followed by day-case (8%) and inpatient admissions (6%). The CCI was 0 in 92% of patients, 1–2 in 0.4%, 3–4 in 5%, and ≥5 in 0.1%. Overall, 694 patients had one or more comorbidities (excluding any malignancy or metastasis); the most common were hypertension (98%) and diabetes (77%) (Table 1).

The total direct medical expenditure for breast cancer patients in Dubai in 2024 amounted to USD 60.0 million. Outpatient encounters accounted for the majority of spending (USD 48.7 million; 81%), with a mean annual cost per patient of USD 5,520 (SD: 13,884). Inpatient encounters contributed USD 6.3 million (11%), with an annual mean cost of USD 10,808 (SD: 14,243), representing the highest average cost across encounter types. Day-case encounters accounted for USD 5.0 million (8%), with an annual mean cost of USD 5,696 (SD: 10,662) (Table 2).

In analyses stratified by comorbidity, cost patterns differed depending on how the CCI was specified. Under the base scenario (CCI excluding "any malignancy" and "metastasis"), mean costs were modestly higher in patients with non-cancer comorbidities, and differences were statistically significant for outpatient care (USD 7,604 *vs.* USD 5,345; $p = 0.0003$) but not for inpatient care (USD 15,906 *vs.* USD 10,236; $p = 0.283$) or day case encounters (USD 5,097 *vs.* USD 5,764; $p = 0.514$). In contrast, under the alternative scenario (CCI including "any malignancy" and "metastasis"), the comorbidity group accounted for virtually

Table 1. Summary statistics for breast cancer patients in Dubai, 2024

Variables	Patients	
	n	%
Overall study population	8,967	
Age in years (mean ± SD)	51.8±8.6	
18–39	664	7%
40–64	7,877	88%
65+	427	5%
Categorize by claim count		
Claim count of 1	2,235	25%
2 to 3	1,870	21%
4 to 5	1,034	12%
>5	3,828	43%
Categorize by encounter type		
Outpatient	8,819	86%
Inpatient	585	6%
Day case	880	8%
Baseline risk score-CCI[1]		
0	8,273	92%
1–2	652	7%
3–4	37	0.4%
5+	5	0.1%
Comorbidities		
Yes	694	
CVD[2]	22	3.2%
Renal disease	31	4%
Rheumatic disease	35	5%
CHF[3]	43	6%
Asthma	60	9%
COPD[4]	71	10%
Diabetes uncomplicated	312	45%
Diabetes complicated	225	32%
Hypertension	683	98%
Metastasis		
Yes	1,325	15%

[1]: Charlson comorbidity index; [2]: Cardiovascular disease; [3]: Congestive heart failure; [4]: Chronic obstructive pulmonary disease; SD: Standard deviation

all expenditure and exhibited consistently higher mean costs across settings: outpatient (USD 5,895 *vs.* USD 885; $p<0.0001$), inpatient (USD 10,928 *vs.* USD 7,720; $p = 0.0012$), and day case (USD 5,721 *vs.* USD 4,240; $p = 0.0205$). These findings indicate that when cancer-related disease burden is incorporated into the comorbidity construct, the incremental cost associated with comorbidity becomes substantial and statistically robust across all encounter types, with the largest absolute difference observed in outpatient care (Table 3).

To examine the role of comorbidity severity, patients were classified into three CCI groups (1–2, 3–4, and ≥5) and costs were compared across encounter types under both scenarios (Table 4). The analysis revealed a progressive increase in costs across encounter types in both scenarios, though the strength of association varied. In base scenario, cost tended to rise with higher CCI, but statistically significance was limited particularly for the ≥5 group, where small numbers constrained interpretation. In contrast, the alternative scenario demonstrated a clear and statistically robust gradient. Outpatient costs increased from USD 4,215 (CCI: 1–2) to USD 5,823 (CCI: 3–4) and USD 14,000 (CCI ≥5; $p<0.005$). Inpatient mean costs followed a similar pattern (USD 10,020 to 8,424 to 13,744; $p = 0.02$ from 3–4 *vs.* ≥5), while day case costs rose from USD 4,913 to USD 3,943 and USD 7,331 respectively ($p = 0.003$ from 3-4 *vs.* ≥5). These findings underscore the substantial cost burden associated with advanced comorbidities when cancer-related conditions are included in the index.

To address the weaker significance in the base scenario and to more precisely estimate the independent effects of comorbidity, we performed multivariable regression (Table 5).

The regression analysis identified several factors with significant multiplicative effects on breast cancer treatment costs (Table 5). When using outpatient at clinic/center with CCI = 0 as the reference, a graded association between non-cancer comorbidity and higher spending was observed.

Compared with CCI = 0, CCI 1–2 was associated with a 16% increase in costs [ratio: 1.16; 95% confidence interval (CI): 1.00–1.34; $p = 0.03$], while CCI 3–4 was directionally higher, but not statistically significant (ratio: 1.46; 95% CI: 0.88–2.44; $p = 0.141$). Patients with CCI ≥5 experienced a marked rise—approximately 6.45-fold higher costs (ratio: 6.44; 95% CI: 2.62–15.84; $p<0.0001$).

Relative to the reference encounter, day case care was associated with a 57% increase in costs (ratio: 1.57; 95% CI: 1.33–1.84; $p<0.0001$) and inpatient care was associated with nearly a threefold increase (ratio: 2.90; 95% CI: 2.44–3.45; $p<0.0001$).

By provider setting, care delivered in hospitals was associated with 16% higher costs (ratio: 1.158; 95% CI: 1.030–1.302; $p = 0.014$) and pharmacy claims were associated with 31% higher costs (ratio: 1.311; 95% CI: 1.146–1.499; $p<0.0001$) compared with clinic/center. The model's baseline mean cost was 3,142 USD (95% CI: 2,830–3,489).

These regression estimates are further visualized in Figure 1, which provides a graphical representation of the multiplicative effects and their confidence intervals.

Table 2. Distribution of breast cancer treatment costs by encounter type in Dubai, 2024

Encounter type	*n*	Total (USD)	Mean (USD)	SD	%
Outpatient	(8819)	48,683,546	5,520	13,884	81%
Inpatient	(585)	6,322,425	10,808	14,243	11%
Day case	(880)	5,012,297	5,696	10,662	8%

N: Number of breast cancer patients; Mean: Annual mean treatment cost per patient in US dollars (USD); SD: Standard deviation. Percentages represent each encounter type's share of total annual breast cancer treatment expenditure

Table 3. Distribution of breast cancer treatment cost by presence of comorbidity in Dubai, 2024

Base scenario-CCI excludes any malignancy and metastasis									
	Comorbidity-no				Comorbidity-yes				
Encounter type	*n*	Total (USD)	Mean (USD)	SD	*n*	Total (USD)	Mean (USD)	SD	*p*-value
Out-patient	(**8,134**)	43,475,096	5,345	13,700	(**685**)	5,208,450	7,604	15,767	0.0003
In-patient	(**526**)	5,383,943	10,236	6,659	(**59**)	938,483	15,906	40,148	0.283
Day case	(**790**)	4,553,610	5,764	10,842	(**90**)	458,687	5,097	8,956	0.514
Alternative scenario-CCI includes any malignancy and metastasis									
	Comorbidity-no				Comorbidity-yes				
Encounter type	*n*	Total (USD)	Mean (USD)	SD	*n*	Total (USD)	Mean (USD)	SD	*p*-value
Out-patient	(**659**)	583,370	885	2,816	(**8,160**)	48,100,176	5,895	14,346	<0.0001
In-patient	(**22**)	169,837	7,720	3,394	(**563**)	6,152,589	10,928	14,491	0.0012
Day case	(**15**)	63,600	4,240	1,889	(**865**)	4,948,697	5,721	10,750	0.0205

N: Number of breast cancer patients; Mean: Annual mean treatment cost per patient; SD: Standard deviation; CCI: Charlson comorbidity index. The "base scenario" defines comorbidity using CCI scores that exclude "any malignancy" and "metastasis," whereas the "alternative scenario" includes these conditions. *p*-values correspond to two-sided tests comparing the mean annual treatment costs between patients with and without comorbidity within each encounter type (Statistical significance was defined as $p<0.05$)

Table 4. Distribution of breast cancer treatment cost according to Charlson's comorbidity index classification

Base scenario-CCI excludes any malignancy and metastasis													
	Charlson index 1–2				Charlson index 3–4				Charlson index ≥5				*p*-value
Encounter type	*n*	Total (USD)	Mean (USD)	SD	*n*	Total (USD)	Mean (USD)	SD	*n*	Total (USD)	Mean (USD)	SD	
Out-patient	(**646**)	4,900,559	7,586	15,943	(**35**)	307,058	8,773	13,100	(**4**)	833	208	216	0.0005[a]
In-patient	(**54**)	529,353	9,803	5,733	(**4**)	94,347	23,587	7,562	(**1**)	314,783	314,783	-	0.0328[b]
Day case	(**84**)	429,620	5,115	9,168	(**5**)	27,682	5,536	6,079	(**1**)	1,384	1,384	-	0.8900[a,c]
Alternative scenario-CCI includes any malignancy and metastasis													
	Charlson index 1–2				Charlson index 3–4				Charlson index ≥5				*p*-value
Encounter type	*n*	Total (USD)	Mean (USD)	SD	*n*	Total (USD)	Mean (USD)	SD	*n*	Total (USD)	Mean (USD)	SD	
Out-patient	(**6385**)	26,913,622	4,215	10,178	(**448**)	2,608,921	5,823	13,116	(**1327**)	18,577,633	14,000	25,106	<0.005[a]
In-patient	(**380**)	3,807,616	10,020	5,500	(**32**)	269,577	8,424	4,884	(**151**)	2,075,396	13,744	26,344	0.020[d]
Day case	(**510**)	2,505,499	4,913	9,664	(**47**)	185,331	3,943	5,731	(**308**)	2,257,867	7,331	12,700	0.003[d]

N: Number of breast cancer patients; Mean: Annual mean treatment cost per patient; SD: Standard deviation; CCI: Charlson comorbidity index. CCI categories are presented as 1–2, 3–4, and ≥5.

p-value column:

[a]: *p*-value from an overall comparison of mean annual costs across the three CCI categories (1–2, 3–4, ≥5) within the encounter type and scenario.

[b]: *p*-value from a pairwise comparison between CCI 1–2 and CCI 3–4; the CCI ≥5 category ($n<2$) was excluded from this test.

[c]: In rows where CCI ≥5 has $n<2$, estimates should be interpreted with caution due to sparse data.

[d]: *p*-value from a pairwise comparison between CCI 3–4 and CCI ≥5. (Statistical significance was defined as $p<0.05$)

Table 5. Generalized linear regression analysis of the predictors of costs of treatment in patients with breast cancer, Dubai

Variable	Cost ratio	95% CI	*p*-value
Intercept	3142	2830–3489	<0.0001
CCI band (no cancer items)			
CCI band 1–2	1.16	1.00–1.34	0.0373
CCI band 3–4	1.46	0.88–2.44	0.1405
CCI band ≥5	6.44	2.62–15.84	<0.0001
Encounter type			
Day case	1.57	1.33–1.84	<0.0001
Inpatient	2.90	2.45–3.45	<0.0001
Provider type			
Hospital	1.16	1.03–1.30	0.0143
Pharmacy	1.31	1.14–1.49	<0.0001

Cost ratios are exponentiated coefficients from a Tweedie generalized linear model with a log link, where the dependent variable is total annual breast cancer treatment cost (USD). For each categorical predictor, the reported cost ratios compare the listed category with its reference group: CCI = 0 (no comorbidity); outpatient encounter = clinic/center; and provider type = clinic/center. CCI: Charlson comorbidity index, constructed here by excluding "any malignancy" and "metastasis" to isolate non-cancer comorbidity. CI: Confidence interval. The *p*-values are from two-sided Wald tests of the null hypothesis that the cost ratio equals 1.00 (Statistical significance was defined as $p<0.05$)

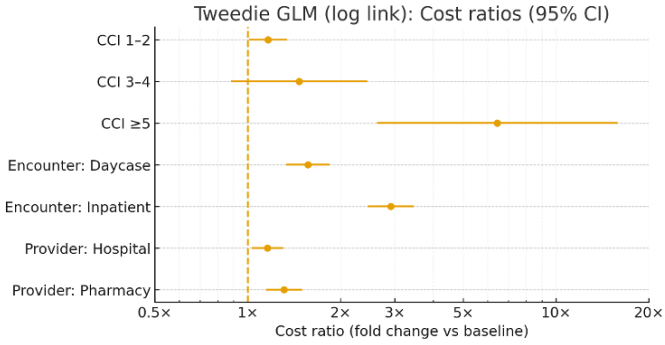

Figure 1. Forest plot of multiplicative effects on breast cancer treatment costs, Dubai, 2024

CCI: Charlson comorbidity index; CI: Confidence interval; GLM: Generalized linear model

Discussion and Conclusion

This research presents what is reportedly among the first comprehensive examinations of breast cancer treatment costs in Dubai, yielding some important findings. The analysis of claims revealed considerable heterogeneity in service use, with almost 50% of patients having incurred more than five claims and one-quarter having incurred only a single claim. This heterogeneity likely reflects variations in treatment intensity, follow-up regimen, and complications related to the disease, and supports the impression that a small proportion of patients account for a large share of the total use of services. Such patterns highlight the value of developing strategies that focus on high-user groups to limit costs, as they will account for the largest share of overall system utilization costs. Consistent with our findings, researchers from the UAE reported variability in healthcare utilization patterns in Dubai (27) especially during the pandemic. With potentially significant economic implications, cost analyses are important for assessing breast cancer interventions and informing healthcare practice and policy.

According to the present findings, comorbidity significantly affects the cost of treating breast cancer in Dubai. In the base scenario, excluding malignancy and metastasis, the annual mean outpatient cost for patients with comorbidity was USD 7,604 (versus USD 5,345 in patients without comorbidity, $p = 0.0003$), and the mean inpatient and day case costs did not differ between patients with and without comorbidity. When malignancy and metastasis were added to the data from the CCI, the cost difference was significant across all types of encounters. In regression modeling, patients in the highest severity category (CCI ≥5) experienced 6.4 times increased cost compared to patients without comorbidity. The gradient effect illustrates the burden of coexisting cancer and related chronic diseases, which require more complex and intensive management. This is consistent with prior evidence from international studies that have reported that higher CCI scores are associated with increased hospitalizations, longer LOS, and increased overall costs of cancer care (28-31). These findings reinforce the methodological value of systematically including comorbidity in cost-effectiveness studies of breast cancer. Prior studies have shown that cost estimates differ considerably depending on comorbidity specifications, particularly when cancer-related conditions are included and classified using the CCI (32-34).

Overall, these findings provide additional support for viewing comorbidity as more than a clinical predictor of outcomes, rather as an essential contributing factor to an increased economic burden in cancer populations.

The location of care had a significant effect on breast cancer costs in Dubai. Most services were provided in outpatient encounters (86% of all claims, representing USD 48.7 million, or 81% of total costs), with an annual mean cost of care of USD 5,520 per patient. Inpatient admissions comprised only 6% of encounters but accounted for a large share of total costs, with a mean cost per patient of USD 10,808, almost double that of outpatient or day-case care. According to the multivariable regression analysis of costs in this sample, inpatient care was associated with a threefold increase in costs crude ratio (CR): 2.90, 95% CI: 2.45–3.45], and day-case services were associated with a 57% increase in costs (CR: 1.56, 95% CI: 1.33–1.84). When care was provided in a hospital, compared with care in a clinic or featured center, there was a 16% increased cost burden. These patterns were more common among patients with comorbidities, as they were managed in the hospital more often because of greater clinical complexity and a higher need for multidisciplinary interventions; some patients also required monitoring. Previous research has reported a similar finding among breast cancer patients: those with greater CCI scores incur disproportionately high hospital-based healthcare expenditure, largely because of longer inpatient stays, more complications, and an increased need for specialist services (29, 35). On the other hand, patients with low or no comorbidities had more frequent outpatient or ambulatory care visits and significantly lower costs per episode of care. This dual effect—in which comorbidity increases overall economic burden and drives care toward more costly hospital encounters—has also been reflected in other health system assessments (36, 37). This highlights the need for risk-stratified care pathways that incorporate comorbidity status into clinical decision-making, thereby allowing patients with multimorbidity to transition safely into a low-cost outpatient environment without compromising quality of care.

The current results revealed that the cost of medications was a significant driver of overall treatment costs in breast cancer care in Dubai. Pharmacy (medication claims) was independently associated with a 31% increase in overall costs (ratio: 1.31; 95% CI: 1.15–1.49), indicating the substantial contribution of medications to the economic burden of treatment. Patients with higher CCI scores were particularly affected because they were more likely to need antihypertensives, antidiabetics, and cardioprotective drugs to treat chronic conditions such as hypertension, diabetes, and cardiovascular disease, in addition to oncologic therapy. Overall, the combined effect associated with the need for dual treatment resulted in substantial increases in medication costs. These findings align with international evidence demonstrating that breast cancer patients with multimorbidity require substantially greater volumes of supportive medication addition to standard cancer therapies, such as endocrine treatments and targeted biologics (28-30, 38, 39). This dual challenge of oncology and non-oncology prescriptions not only does it create increased direct medical costs but it also complicates the long-term cost-sharing burden between patients and health systems. These findings highlight the need for holistic strategies in managing pharmaceutical costs that account for interactions among medications prescribed for comorbidities and for cancer management. Incorporating comorbidity status into these approaches may provide an additional targeted method to facilitate access to needed therapies in multimorbid populations with breast cancer.

The greatest strength of this study is the use of a comprehensive claims database, which enables the study to include the fully insured population of breast cancer patients in Dubai. This provides a comprehensive view of the patients' healthcare interactions. Therefore, we can explore the cost drivers in detail through medical encounters, care settings, and comorbidities, and link possible cost drivers within one large, real-world patient group. The dual specification of the CCI is also a strength, as it allows for evaluation of both non-cancer and all-inclusive comorbidity burdens, thereby providing methodological contributions that enhance the interpretability of cost variation. The use of a Tweedie generalized linear model strengthened the analysis by appropriately modeling the skewed distribution of the cost data, thereby improving estimates.

Study Limitations

However, some limitations need to be recognized. The lack of clinical information, including tumor stage, tumor biology, or treatment intent, made it difficult to categorize costs by disease severity or specific treatment pathway. Because diagnostic codes are used to capture the prevailing comorbidities, the true prevalence of these comorbidities may be underestimated. Additionally, some of the age data were missing or incomplete and therefore had to be excluded because the models could not handle an incomplete age variable, and demographic risk factors were therefore not included in some regression models. Our analysis was limited to direct medical costs obtained from insurance claims files and eClaimLink; indirect costs (out-of-pocket costs or expenditures outside of eClaimLink) and non-financial problems (such as loss of productivity and quality of life) were not included in the financial burden analysis. Because the analysis was cross-sectional, we cannot infer causality from the observed associations; it is possible that the associations simply reflect another underlying case mix or provider practice patterns for the patient cohort, which were either not available in the data or not fully captured. In this analysis, may slightly

underestimate breast cancer care costs because costs for which breast cancer was listed as a secondary or tertiary diagnosis were often not considered.

This study provides the first comprehensive assessment of breast cancer treatment costs in Dubai, stratified by comorbidity, offering novel insights into local cost drivers. Outpatient services accounted for most encounters and overall spending; however, inpatient admissions, though less frequent, generated substantially higher per-patient costs. The CCI demonstrated a consistent escalation in costs across care settings, with the greatest impact observed in hospital-based encounters. Medication expenditures also emerged as significant contributors, particularly among patients managing treatments for both cancer and chronic diseases.

These findings underscore the importance of systematically incorporating comorbidity measures into health economic analyses, as they meaningfully alter cost estimates and highlight key drivers of financial burden. By filling a critical evidence gap in the UAE, this study illustrates how localized cost-of-illness data can inform insurance design, service prioritization, and sustainable oncology financing, consistent with other international studies. For policymakers and insurers, these results highlight the need for integrated care models that address comorbidities and expand risk-stratified pathways to safely transition patients toward lower-cost outpatient settings. Strategies to manage pharmaceutical spending should also be implemented, including formulary optimization and value-based purchasing. Future research should extend this work by linking claim-based cost estimates with survival and quality-of-life outcomes, thereby supporting value-based, patient-centered cancer care in Dubai, the UAE.

Ethics

Ethics Committee Approval: The Dubai Scientific Research Ethics Committee at the Dubai Health Authority waived ethical approval in such cases because the study used secondary data and did not involve human participants.

Informed Consent: Informed consent from individuals was not required.

Footnotes

Authorship Contributions

Surgical and Medical Practices: M.M.S., N.A.A., H.M.M.; Concept: M.M.S.; Design: M.M.S.; Data Collection and/or Processing: M.M.S.; Analysis and/or Interpretation: M.M.S., H.M.M.; Literature Search: M.M.S., N.A.A., H.M.M.; Writing: M.M.S., N.A.A., H.M.M.

Conflict of Interest: The authors have no conflicts of interest to declare.

Financial Disclosure: The authors declared that this study has received no financial support.

References

1. Bray F, Ferlay J, Soerjomataram I, Siegel RL, Torre LA, Jemal A. Global cancer statistics 2018: GLOBOCAN estimates of incidence and mortality worldwide for 36 cancers in 185 countries. CA Cancer J Clin. 2018; 68: 394-424. Erratum in: CA Cancer J Clin. 2020; 70: 313. (PMID: 30207593) [Crossref]
2. Sung H, Ferlay J, Siegel RL, Laversanne M, Soerjomataram I, Jemal A, et al. Global cancer statistics 2020: GLOBOCAN estimates of incidence and mortality worldwide for 36 cancers in 185 countries. CA Cancer J Clin. 2021; 71: 209-249. (PMID: 33538338) [Crossref]
3. Waks AG, Winer EP. Breast cancer treatment: a review. JAMA. 2019; 321: 288-300. (PMID: 30667505) [Crossref]
4. Cardoso F, Kyriakides S, Ohno S, Penault-Llorca F, Poortmans P, Rubio IT, et al E; ESMO Guidelines Committee. Electronic address: clinicalguidelines@esmo.org. Early breast cancer: ESMO clinical practice guidelines for diagnosis, treatment and follow-up†. Ann Oncol. 2019; 30: 1194-1220. Erratum in: Ann Oncol. 2019; 30: 1674. Erratum in: Ann Oncol. 2021; 32: 284. (PMID: 31161190) [Crossref]
5. Yabroff KR, Lund J, Kepka D, Mariotto A. Economic burden of cancer in the United States: estimates, projections, and future research. Cancer Epidemiol Biomarkers Prev. 2011; 20: 2006-2014. (PMID: 21980008) [Crossref]
6. Mariotto AB, Etzioni R, Hurlbert M, Yabroff KR, Shao Y, Feuer EJ, et al. Estimating the cost of cancer care in the United States: past, present, and future. J Natl Cancer Inst. 2017; 109: djw159. [Crossref]
7. Brown ML, Lipscomb J, Snyder C. The burden of illness of cancer: economic cost and quality of life. Annu Rev Public Health. 2001; 22: 91-113. (PMID: 11274513) [Crossref]
8. Luengo-Fernandez R, Leal J, Gray A, Sullivan R. Economic burden of cancer across the European Union: a population-based cost analysis. Lancet Oncol. 2013; 14: 1165-1174. (PMID: 24131614) [Crossref]
9. Lee KS, Chang HS, Lee SM, Park EC. Economic burden of cancer in Korea during 2000-2010. Cancer Res Treat. 2015; 47: 387-398. (PMID: 25672582) [Crossref]
10. Yabroff KR, Davis WW, Lamont EB, Fahey A, Topor M, Brown ML, et al. Patient time costs associated with cancer care. J Natl Cancer Inst. 2007; 99: 14-23. (PMID: 17202109) [Crossref]
11. de Oliveira C, Weir S, Rangrej J, Krahn MD, Mittmann N, Hoch JS, et al. The economic burden of cancer care in Canada: a population-based cost study. CMAJ Open. 2018; 6: E1-E10. (PMID: 29301745) [Crossref]
12. Guy GP Jr, Ekwueme DU, Yabroff KR, Dowling EC, Li C, Rodriguez JL, et al. Economic burden of cancer survivorship among adults in the United States. J Clin Oncol. 2013; 31: 3749-3757. (PMID: 24043731) [Crossref]
13. Edwards BK, Noone AM, Mariotto AB, Simard EP, Boscoe FP, Henley SJ, et al. Annual report to the nation on the status of cancer, 1975-2010, featuring prevalence of comorbidity and impact on survival among persons with lung, colorectal, breast, or prostate cancer. Cancer. 2014; 120: 1290-1314. (PMID: 24343171) [Crossref]
14. Fu AZ, Jhaveri M. Healthcare cost attributable to recently-diagnosed breast cancer in a privately-insured population in the United States. J Med Econ. 2012; 15: 688-694. (PMID: 22397589) [Crossref]
15. El Saghir NS, Charara RN, Kreidieh FY, Eaton V, Litvin K, Farhat RA, et al. Global practice and efficiency of multidisciplinary tumor boards: results of an American Society of Clinical Oncology International survey. J Glob Oncol. 2015; 1: 57-64. (PMID: 28804774) [Crossref]
16. Ibrahim AS, Khaled HM, Mikhail NN, Baraka H, Kamel H. Cancer incidence in egypt: results of the national population-based cancer registry program. J Cancer Epidemiol. 2014;2014:437971. (PMID: 25328522) [Crossref]
17. United Arab Emirates Ministry of Health and Prevention. Cancer incidence in United Arab Emirates Annual Report 2019. Dubai: MOHAP; 2020. [Crossref]

18. Al-Awadhi A, Iqbal F, Kourie HR, Al-Shamsi HO. Breast cancer in the UAE. In: Al-Shamsi HO, editor. Cancer Care in the United Arab Emirates. Singapore: Springer Nature; 2024:417-434. [Crossref]

19. Elobaid Y, Aamir M, Grivna M, Suliman A, Attoub S, Mousa H, et al. Breast cancer survival and its prognostic factors in the United Arab Emirates: a retrospective study. PLoS One. 2021; 16: e0251118. (PMID: 33951102) [Crossref]

20. Al-Shamsi HO, Abdelwahed N, Al-Awadhi A, Albashir M, Abyad AM, Rafii S, et al. Breast cancer in the United Arab Emirates. JCO Glob Oncol. 2023; 9: e2200247. (PMID: 36608306) [Crossref]

21. Charlson ME, Pompei P, Ales KL, MacKenzie CR. A new method of classifying prognostic comorbidity in longitudinal studies: development and validation. J Chronic Dis. 1987; 40: 373-83. (PMID: 3558716) [Crossref]

22. What is in-patient vs. out-patient healthcare? 2022. Available online: https://www.now-health.com/en/blog/what-is-inpatient-vs-out-patient-healthcare. Last accessed 10.09.2025. [Crossref]

23. Zahir K, Bhandary R. Day case surgery. Surgery (Oxford). 2022; 40: 796-801. [Crossref]

24. ICD10data.com. ICD-10-CM Diagnosis Code of Malignant neoplasm of breast 2025 ICD-10-CM Diagnosis Code C50-C50.9. Available online: https://www.icd10data.com/ICD10CM/Codes/C00-D49/C50-C50/C50-. Date accessed: September 8, 2025. [Crossref]

25. Jørgensen B. Exponential dispersion models. Journal of the Royal Statistical Society Series B: Statistical Methodology. 1987; 49: 127-145. [Crossref]

26. Dunn PK, Smyth GK. Series evaluation of Tweedie exponential dispersion model densities. Statistics and Computing. 2005; 15: 267-280. [Crossref]

27. Soni MM, Mamdouh HM, Suliman EA. Impact of COVID-19 pandemic on utilization of healthcare services and spending patterns in Dubai, United Arab Emirates: a cross-sectional study. Healthcare (Basel). 2024; 12: 473. (PMID: 38391849) [Crossref]

28. Land LH, Dalton SO, Jensen MB, Ewertz M. Impact of comorbidity on mortality: a cohort study of 62,591 Danish women diagnosed with early breast cancer, 1990-2008. Breast Cancer Res Treat. 2012; 131: 1013-1020. (PMID: 22002567) [Crossref]

29. Ng HS, Vitry A, Koczwara B, Roder D, McBride ML. Patterns of comorbidities in women with breast cancer: a Canadian population-based study. Cancer Causes Control. 2019; 30: 931-941. (PMID: 31280456) [Crossref]

30. Yoon SJ, Kim EJ, Seo HJ, Oh IH. The association between Charlson comorbidity index and the medical care cost of cancer: a retrospective study. Biomed Res Int. 2015; 2015: 259341. (PMID: 26347086) [Crossref]

31. Søgaard M, Thomsen RW, Bossen KS, Sørensen HT, Nørgaard M. The impact of comorbidity on cancer survival: a review. Clin Epidemiol. 2013; 5(Suppl 1): 3-29. (PMID: 24227920) [Crossref]

32. Hall WH, Ramachandran R, Narayan S, Jani AB, Vijayakumar S. An electronic application for rapidly calculating Charlson comorbidity score. BMC Cancer. 2004; 4: 94. (PMID: 15610554) [Crossref]

33. Sarfati D, Koczwara B, Jackson C. The impact of comorbidity on cancer and its treatment. CA Cancer J Clin. 2016; 66: 337-350. (PMID: 26891458) [Crossref]

34. de Groot V, Beckerman H, Lankhorst GJ, Bouter LM. How to measure comorbidity. A critical review of available methods. J Clin Epidemiol. 2003; 56: 221-229. (PMID: 12725876) [Crossref]

35. Patnaik JL, Byers T, Diguiseppi C, Denberg TD, Dabelea D. The influence of comorbidities on overall survival among older women diagnosed with breast cancer. J Natl Cancer Inst. 2011; 103: 1101-1111. (PMID: 21719777) [Crossref]

36. Warren JL, Yabroff KR, Meekins A, Topor M, Lamont EB, Brown ML. Evaluation of trends in the cost of initial cancer treatment. J Natl Cancer Inst. 2008; 100: 888-897. (PMID: 18544740) [Crossref]

37. Jagsi R, Jiang J, Momoh AO, Alderman A, Giordano SH, Buchholz TA, et al. Complications after mastectomy and immediate breast reconstruction for breast cancer: a claims-based analysis. Ann Surg. 2016; 263: 219-227. (PMID: 25876011) [Crossref]

38. Neugut AI, Subar M, Wilde ET, Stratton S, Brouse CH, Hillyer GC, et al. Association between prescription co-payment amount and compliance with adjuvant hormonal therapy in women with early-stage breast cancer. J Clin Oncol. 2011; 29: 2534-2542. (PMID: 21606426) [Crossref]

39. Tefferi A, Kantarjian H, Rajkumar SV, Baker LH, Abkowitz JL, Adamson JW, et al. In support of a patient-driven initiative and petition to lower the high price of cancer drugs. Mayo Clin Proc. 2015; 90: 996-1000. (PMID: 26211600) [Crossref]

ORIGINAL ARTICLE

European Journal of BREAST HEALTH

DOI: 10.4274/ejbh.galenos.2026.2025-9-15
Eur J Breast Health 2026;22(3):270-278

Personalized Treatment Outcomes in Idiopathic Granulomatous Mastitis: A Retrospective Study of Ninety-Two Patients

Rashad Jafarov[1], Altay Aliyev[2], Iqbal Babazade[3], Rena Abdullayeva[4], Khayala Sharifova[5], Nihad Asadov[1], Elgun Samedov[6]

[1]Department of Rheumatology, Central Military Hospital of the Ministry of Defence, Baku, Azerbaijan
[2]Department of Oncology, Liv Bona Dea Hospital, Baku, Azerbaijan
[3]Military Medical Faculty, Azerbaijan Medical University, Baku, Azerbaijan
[4]Department of Gynecology, Universal Hospital, Baku, Azerbaijan
[5]Department of Radiology, Azerbaijan State Advanced Training Institute for Doctors named after A. Aliyev, Baku, Azerbaijan
[6]Department of General Surgery, Liv Bona Dea Hospital, Baku, Azerbaijan

ABSTRACT

Objective: Idiopathic granulomatous mastitis (IGM) is a rare benign inflammatory breast disease with a high risk of relapse. The study objective was to evaluate relapse predictors and treatment outcomes in a large cohort of IGM patients.

Materials and Methods: We retrospectively analyzed female patients diagnosed with IGM (2018–2024) at the Central Military Hospital, Baku. Diagnosis was confirmed by core needle biopsy. Patients were managed with systemic therapy (corticosteroids and/or immunosuppressants) when clinically indicated; local measures (e.g., aspiration/drainage, intralesional steroid) were used selectively in localized disease. Relapse was defined as reappearance of clinical or radiological findings after remission. Univariable and multivariable logistic regression models were applied to identify independent predictors.

Results: The cohort consisted of 92 patients. Relapse occurred in 22/85 methotrexate-treated patients (25.9%), with most relapses occurring between the third and fifth months. No relapse events were observed in the azathioprine subgroup (n = 7). However, this finding should be considered observational only due to the small numbers and zero-event data. In multivariable analysis, erythrocyte sedimentation rate (ESR) >20 mm/h (and angiotensin converting enzyme >52 U/L, where applicable) were associated with relapse, whereas apparent associations with tumor necrosis factor alpha inhibitors and cyclosporine likely reflect confounding by indication because these agents were used as rescue therapy in refractory/relapsing disease. Elevated ESR was also associated with prolonged treatment duration (p = 0.006).

Conclusion: A structured and individualized treatment approach may contribute to favorable clinical outcomes in patients with IGM. Observed relapse patterns support the importance of risk-adapted management rather than a uniform therapeutic strategy. Given the retrospective design and limited subgroup sizes, these findings should be interpreted cautiously and considered hypothesis-generating. Prospective, multicenter studies are required to validate relapse-associated factors and optimize treatment strategies.

Keywords: Idiopathic granulomatous mastitis; relapse; immunosuppressive therapy; methotrexate; azathioprine; risk-adapted treatment

Corresponding Author: Rashad Jafarov MD,
E-mail: dr.jafarov@gmail.com **ORCID:** orcid.org/0009-0000-9631-209X

Received: 17.11.2025 **Accepted:** 21.01.2026 **Epub:** 18.03.2026 **Available Online Date:** 17.06.2026

Cite this article as: Jafarov R, Aliyev A, Babazade I, Abdullayeva R, Sharifova K, Asadov N, et al. Personalized treatment outcomes in idiopathic granulomatous mastitis: a retrospective study of ninety-two patients. Eur J Breast Health. 2026;22(3):270-278

KEY POINTS

- Idiopathic granulomatous mastitis.
- Relapse.
- Immunosuppressive therapy.
- Methotrexate.
- Azathioprine.

Introduction

Idiopathic granulomatous mastitis (IGM) is a rare, chronic, and benign inflammatory breast disease, first described in 1972 (1). It predominantly affects women of reproductive age, most commonly occurring within the first five years postpartum, typically between the ages of 30 and 45 years (2). Rarely, IGM occurs in men and postmenopausal women (3). The exact etiology of the disease remains unclear; however, several factors, such as autoimmune processes, hormonal influences, pregnancy, lactation, use of oral contraceptives, and hyperprolactinemia are believed to play a role in its pathogenesis (4).

The involvement of autoimmune mechanisms is supported by the favorable response of IGM to corticosteroids and immunosuppressive agents (5). Furthermore, the common presence of extra-mammary inflammatory manifestations, such as erythema nodosum and arthritis, further supports the hypothesis of immune-mediated pathology (6). Histologically, IGM is characterized by non-caseating granulomas predominantly affecting the breast lobules, often accompanied by microabscesses (7). Given its granulomatous nature, infectious etiologies, such as tuberculosis, fungal infections, sarcoidosis, and granulomatosis with polyangiitis must be considered in the differential diagnosis. Biopsy confirmation is mandatory (8).

Clinically, IGM typically presents as a palpable breast mass, often accompanied by pain, erythema, nipple retraction, and occasionally the formation of fistulous tracts (9). Axillary lymphadenopathy may also be observed, which can complicate differentiation from malignant tumors (10). The disease course is variable, with recurrence rates ranging from 5% to 50% (11). Due to its chronic and recurrent nature, long-term follow-up is necessary (12).

Management strategies for IGM remain controversial, and no consensus exists regarding the optimal treatment approach (13). Therapeutic options include corticosteroids, immunosuppressive agents, including methotrexate and azathioprine, antibiotics, and surgical intervention (14). While some studies suggest that surgical excision may be associated with higher recurrence rates, others advocate for a multimodal approach that incorporates systemic therapy (15). The aim of this study was to identify clinical and laboratory predictors of relapse in IGM and evaluate the effectiveness of a structured, individualized treatment strategy.

Materials and Methods

This retrospective study was conducted at the Rheumatology Department Outpatient Clinic of the Central Military Hospital of the Ministry of Defence between 2018 and 2024. Female patients who were either referred with a diagnosis of IGM or were newly diagnosed in our clinic were included. The mean follow-up duration was more than one year, allowing assessment of treatment response and early recurrence but late relapses may have been missed due to the chronic course of IGM. The diagnosis of IGM was histopathologically confirmed by findings of granulomatous inflammation consistent with mastitis, including epithelioid histiocytes, Langhans-type giant cells, and lymphocytic infiltration.

Ethical approval was obtained from the Ethics Committee of Liv Bona Dea, Baku Hospital (approval no: BDP-2023/174, date: 02.11.2024).

Inclusion criteria comprised patients with IGM confirmed by a tru-cut biopsy performed due to a breast mass. Serological profiles including anti-nuclear antibodies (ANA), anti-neutrophil cytoplasmic antibodies (ANCA), rheumatoid factor (RF), angiotensin converting enzyme (ACE), erythrocyte sedimentation rate (ESR), and C-reactive protein (CRP) were analyzed to exclude other granulomatous diseases such as sarcoidosis, autoimmune, and vasculitic conditions. ANA positivity was defined as titers ≥1:160, and ACE levels >52 U/L were considered elevated. All data were retrospectively extracted from the hospital's electronic medical records system. To assess relapse predictors, univariate and multivariate binary logistic regression models were constructed using clinical and treatment variables, including ESR, CRP, immunosuppressant use, and age. Statistical significance was defined as $p<0.05$.

Demographic data included patient age, age at diagnosis, the interval (in months) between symptom onset and diagnosis, and time since last childbirth. Comorbidities were also recorded and included type 2 diabetes mellitus, coronary artery disease, other organ-specific or systemic conditions and heart failure.

Clinical evaluation included characteristics of the breast masses, including painful/painless, erythema, discharge, abscess, appearance, recurrent abscesses, unilateral/bilateral lesions, lesions ≥5 cm in diameter, and laterality of breast involvement. Laboratory and imaging data included ESR >20 mm/h, CRP ≥5 mg/L, and ACE >52 U/L. Baseline ultrasound was used to document mass size ≥5 cm. ANA, ANCA, and RF tests were performed for all patients.

All patients initially presented to the general surgery outpatient clinic and were then referred to rheumatology. Initial treatments, including surgical interventions (abscess drainage or mass excision, without distinction), were recorded.

Recurrence was defined as the reappearance of clinical or radiological signs of disease following a period of complete remission lasting at least 4 weeks. Number of recurrences, time to first and second recurrence (in months), and treatment modalities during recurrence (antibiotics, steroids, methotrexate, azathioprine) were documented.

Treatment Strategy

Treatment was individualized based on clinical disease activity. Treatment decisions were individualized based on disease extent, inflammatory activity (ESR/CRP), symptom severity, and patient factors (including lactation). Because non-severe IGM can be managed with a de-escalation approach, observation, and/or local therapies (e.g., ultrasound-guided aspiration/drainage and intralesional corticosteroid injection) were considered as initial management for mild, well-localised disease, before resorting to systemic immunosuppression. Systemic therapy was reserved for clinically active, extensive, progressive, or refractory disease, or when symptoms significantly affected quality of life. When systemic therapy was used, oral prednisolone (0.5–1 mg/kg/day) was initiated during the active inflammatory phase and tapered according to clinical response and tolerability. Once clinical stability was achieved, steroids were tapered over approximately 4 weeks. Dose selection was individualized and adjusted according to clinical response and tolerability.

Patients were pragmatically stratified into mild, moderate, and severe categories based on lesion size, inflammatory markers (ESR/CRP), and symptom severity to guide treatment intensity.

- Mild: Localized disease with normal or minimally elevated ESR/CRP and minimal clinical inflammation.
- Moderate: Symptomatic inflammatory disease and/or moderate elevations in ESR/CRP.
- Severe: Marked inflammatory activity (elevated ESR/CRP), extensive disease and/or lesion diameter ≥5 cm, or complicated disease (e.g., abscess/fistula).

This stratification was used as a center-specific practical tool and does not represent a validated consensus classification.

Stratification into mild, moderate, and severe forms was based on a combination of lesion size, CRP/ESR levels, and severity of clinical symptoms. This stratification enabled a personalized treatment approach. To reduce cumulative corticosteroid exposure, a steroid-sparing immunosuppressant (most commonly methotrexate in this cohort) was introduced in patients requiring prolonged steroids, those with extensive disease, or those with relapse. In refractory or relapsing cases, tumor necrosis factor aplha (TNF-α) inhibitors (adalimumab) and cyclosporine were used. Patients were monitored monthly with clinical and laboratory assessments, and treatment doses were adjusted based on response. The pragmatic stepwise, risk-adapted treatment pathway used in our centre is summarized in Figure 1.

Treatment Modalities

1. Corticosteroid Therapy: Prednisolone was used as systemic therapy for patients with clinically active inflammatory disease and tapered in parallel with clinical improvement. In relapse, a previously effective dose could be reintroduced temporarily while steroid-sparing therapy was optimized.

2. Immunosuppressive Therapy: Methotrexate (85 patients) and azathioprine (7 patients) were used. Azathioprine was used in selected postpartum/breastfeeding patients when methotrexate was not preferred. Azathioprine was used in selected postpartum/breastfeeding patients when methotrexate was not preferred. Refractory and relapsing cases were managed with TNF-α inhibitors (adalimumab) and cyclosporine.

3. Antibiotic Therapy: Administered when an infectious component was confirmed.

4. Combination Therapy: Two main combinations were used. In patients treated with biological agents (adalimumab, cyclosporine), infection markers, liver function, and complete blood counts were closely monitored. Screening for hepatitis and latent tuberculosis (purified protein derivative or Quantiferon) was performed. No serious infections requiring hospitalization were documented in the available records; however, adverse events were not systematically captured in this retrospective dataset, so toxicity may be underestimated. Routine monitoring during systemic immunosuppression included clinical assessment and periodic laboratory testing (complete blood count and liver function tests), with infection screening prior to biologic therapy as described.

- Methotrexate + Cyclosporine (200 mg/day for 4–6 months)
- Methotrexate + Adalimumab (40 mg every other week)

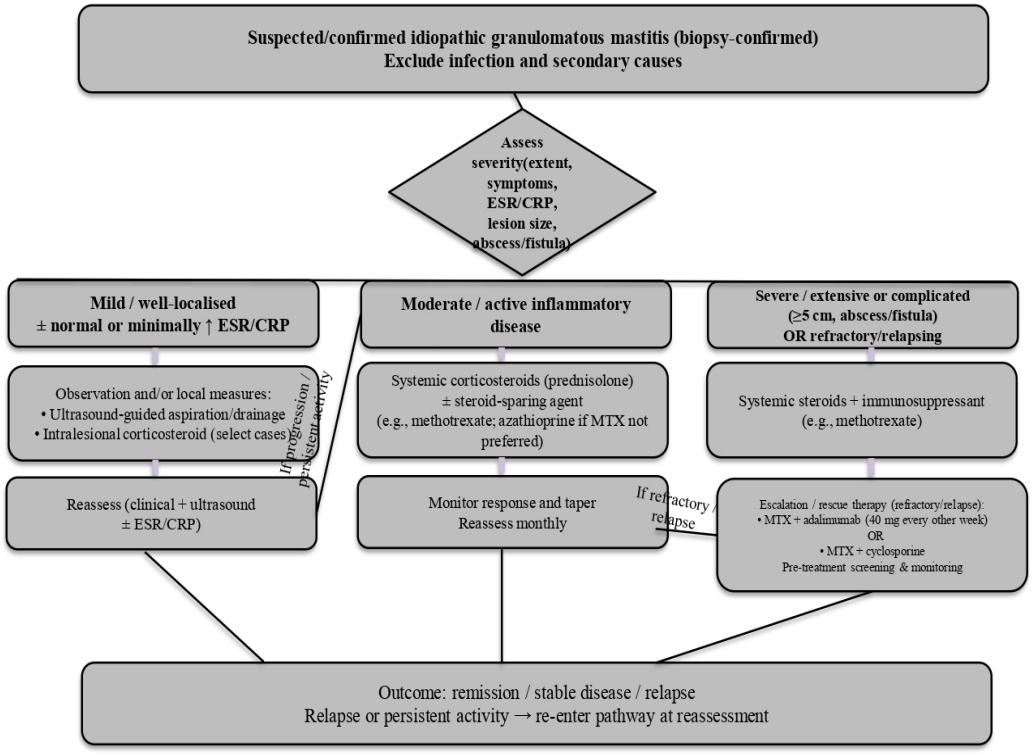

Figure 1. Treatment algorithm (pragmatic, stepwise, risk-adapted). Pragmatic stepwise, risk-adapted treatment pathway used in our centre. Mild, well-localised disease may be managed initially with observation and/or local therapies, whereas systemic immunosuppression is reserved for clinically active, extensive, progressive, or refractory disease. Escalation (e.g., adalimumab or cyclosporine) was used as rescue therapy in relapsing/refractory cases

ESR: Erythrocyte sedimentation rate; CRP: C-reactive protein; OR: Odds ratio; MTX: Methotrexate

Corticosteroid duration varied according to disease activity and response. In patients with persistent or relapsing disease, tapering was slowed and/or a steroid-sparing immunosuppressant was optimized. The primary outcome was defined as disease recurrence, determined by the reappearance of clinical or radiological findings after achieving complete or partial remission. Secondary outcomes included time to recurrence and treatment response (remission, stable disease, or progression). In cases where clinical improvement was not satisfactory, the steroid dose was increased again to regain disease control.

Statistical Analysis

All statistical analyses were performed using IBM SPSS Statistics for Windows, version 29 (SPSS Inc., Chicago, Illinois). Descriptive statistics for continuous variables are presented as mean ± standard deviation or median (minimum-maximum), and categorical variables as frequencies (n) and percentages (%). The Kolmogorov-Smirnov and Shapiro-Wilk tests were used to assess normality of continuous variables. Depending on distribution, independent t-test or Mann-Whitney U test was applied for group comparisons. For categorical variables, Pearson's chi-square or Fisher's exact test (when expected cell values were <5) was used.

To evaluate associations with recurrence and treatment duration, univariable and multivariable logistic regression models were applied. Variables entered into the regression model included age, ESR, CRP, lesion size, laterality, and immunosuppressant use (methotrexate, azathioprine, TNF-α inhibitors, cyclosporine, corticosteroids, surgical intervention). Odds ratios with 95% confidence intervals were calculated. Linear regression was used for continuous outcome variables. Correlation analyses employed Pearson or Spearman tests, depending on data type. A two-tailed p-value <0.05 was considered statistically significant. In subgroups with limited event counts (e.g., azathioprine), multivariate regression was restricted.

Results

Data from 92 patients were analyzed. The mean age of patients was 36.10±9.63 years. The average treatment duration was 9.84±4.70 months, reflecting the typical course of therapy. In

terms of comorbitities, five patients had thyroid dysfunction, five had hypertension, and two had diabetes mellitus. However, these comorbidities did not show any significant effect on treatment duration or relapse rates, likely due to the younger age distribution of the cohort. ANA positivity was detected in 4 (4.35%) patients and RF in 1 (1.1%) patient. Of the 85/92 (92.4%) patients treated with methotrexate, 22 experienced a relapse (25.9%), primarily occurring between the third and fifth month of treatment. A comparison of clinical, laboratory, and treatment characteristics between recurrent and non-recurrent IGM patients is summarized in Table 1. All relapses were observed in the methotrexate group. None of the 7 patients treated with

Table 1. Comparison of clinical, laboratory, and treatment characteristics between recurrent and non-recurrent IGM patients

Variable	IGM recurrence - no (n/%)	IGM recurrence - yes (n/%)	*p*-value
Total patients	70 (76.1%)	22 (23.9%)	-
Baseline characteristics			
Age (mean ± SD)	36.10±9.63	36.10±9.63	>0.05
Time from symptom onset to diagnosis (months)	Not specified	Not specified	-
Clinical features			
Presence of mass	70 (100%)	22 (100%)	-
Painful mass	50 (71.4%)	18 (81.8%)	-
Redness	32 (45.7%)	10 (45.4%)	-
Discharge	27 (38.5%)	9 (40.9%)	-
Fistula	5 (7.1%)	3 (13.6%)	-
Nipple retraction	10 (14.3%)	5 (22.7%)	-
Cellulitis	4 (5.7%)	2 (9.1%)	-
Erythema nodosum	6 (8.5%)	2 (9.1%)	-
Recurrent abscess	Not specified	Not specified	-
Unilateral lesion	61 (87.1%)	18 (81.8%)	-
Mass ≥5 cm on initial ultrasound	18 (26%)	8 (36%)	-
Laboratory findings			
ESR >20 mm/h	21 (30%)	10 (45%)	0.023
CRP ≥5 mg/L	26 (37%)	8 (36%)	0.056
ACE >52 U/L	10 (14%)	4 (18%)	-
Prolactin (mean)	Not specified	Not specified	>0.05
Risk factors			
Comorbidities	10 (14%)	5 (23%)	-
Stress factor	30 (43%)	9 (41%)	-
Oral contraceptive use	7 (10%)	2 (9%)	-
Menopause	3 (4.3%)	1 (4.5%)	-
Breast trauma	Not specified	Not specified	-
Treatment & follow-up			
Initial steroid use	70 (100%)	22 (100%)	-
Initial methotrexate use	63 (90%)	22 (100%)	0.473
Initial azathioprine use	7 (10%)	0 (0%)	0.494
TNF-α inhibitor use	0 (0%)	17 (77.3%)	-
Methotrexate + cyclosporine	0 (0%)	5 (22.7%)	-
Combination therapy (any)	0 (0%)	22 (100%)	-
Follow-up status	Not specified	Not specified	-

ESR: Erythrocyte sedimentation rate; CRP: C-reactive protein; IGM: Idiopathic granulomatous mastitis; ACE: Angiotensin converting enzyme; TNF-α: Tumor necrosis factor alpha; SD: Standard deviation

azathioprine experienced a relapse but this was not different from the relapse rate in the methotrexate group ($p = 0.494$). Among the 22 relapsing patients, 5 received methotrexate + cyclosporine (200 mg/day, for 4–6 months), and 17 received methotrexate + adalimumab (40 mg every other week).

Correlation analyses identified the following associations. No statistically significant correlation was found between relapse and use of methotrexate ($r = 0.076$, $p = 0.473$) or azathioprine ($r = 0.072$, $p = 0.494$). A significant positive correlation was found between relapse and treatment duration ($r = 0.422$, $p<0.001$), suggesting that relapses are associated with prolonged therapy, possibly due to repeated clinical and radiologic recurrence. No correlation was found between patient age and treatment duration. A significant weak positive correlation was identified between ESR and treatment duration ($r = 0.246$, $p = 0.023$), suggesting that elevated ESR is associated with longer treatment periods. However, there was no correlation between CRP and treatment duration ($F = 1.638$, $p = 0.056$), showing a trend without significance. No significant correlation was found between treatment duration and other immunosuppressive (methotrexate, azathioprine, TNF-α inhibitors, cyclosporine) or antibiotic therapies.

To further explore the effect of laboratory variables on treatment duration, one-way ANOVA analyses were performed This indicated a statistically significant difference in treatment duration across ESR groups ($F = 2.172$, $p = 0.006$), suggesting that higher ESR levels are associated with longer treatment periods. However, CRP showed ($F = 1.638$, $p = 0.056$), a trend toward association with treatment duration, but this did not reach statistical significance.

Overall, the findings suggest that clinical or radiologic relapse after achieving remission is significantly associated with extended treatment durations. Elevated ESR was associated with longer treatment duration and relapse status. In contrast, factors such as age, surgical intervention, and various immunosuppressive or antibiotic regimens did not show a statistically significant effect on treatment duration. These findings provide important insights for optimizing relapse risk assessment and patient monitoring strategies in clinical practice.

In the multivariable logistic regression model, ESR >20 mm/h, TNF-α inhibitor use, and cyclosporine treatment showed statistical associations with relapse status (Table 2). These treatment-related associations should be interpreted cautiously because TNF-α inhibitors and cyclosporine were used as rescue therapy in refractory/relapsing disease (confounding by indication). No relapse events were observed in the azathioprine subgroup but the small sample size was very small and there were zero-event data. Table 3 illustrates the distribution of relapse onset over time, showing a peak between the third and fifth months after treatment initiation.

Table 2. Logistic regression model showing variables associated with relapse status

Variable	OR	95% CI	*p*-value
ESR >20 mm/h	2.45	1.10–5.46	0.023
CRP ≥5 mg/L	1.95	0.98–4.22	0.056
TNF-α inhibitor	4.87	1.70–13.90	<0.001
Cyclosporine	3.85	1.48–10.03	0.006
Azathioprine	-	-	0.494 (no relapses observed)
Age	0.98	0.93–1.03	0.398
Surgical intervention	1.55	0.82–2.91	0.184
ACE >52 U/L	2.26	1.12–4.53	0.010

TNF-α inhibitors and cyclosporine were used as rescue therapy in relapsing/refractory cases; therefore, their statistical associations with relapse should be interpreted cautiously due to confounding by indication, TNF-α: Tumor necrosis factor alpha; OR: Odds ratio; CI: Confidence interval; ESR: Erythrocyte sedimentation rate; CRP: C-reactive protein

Table 3. Time distribution of relapse occurrence following initiation of treatment, with clustering between 3rd and 5th months

Variable	Association (OR)	95% CI	*p*-value
ESR >20 mm/h	2.32	1.01–5.34	0.048
TNF-α inhibitor	4.12	1.38–12.30	0.011
Cyclosporine	3.44	1.22–9.76	0.019
ACE >52 U/L	2.05	0.98–4.29	0.060 (borderline significance)

TNF-α: Tumor necrosis factor alpha; OR: Odds ratio; CI: Confidence interval; ACE: Angiotensin converting enzyme; ESR: Erythrocyte sedimentation rate

Discussion and Conclusion

Our findings indicate that the personalized and phased treatment protocol we implemented resulted in a relapse rate of only 25.9% in patients with IGM. This relapse rate falls within the lower range of rates reported in the international literature, which range from 20% to 47.5% (16). Several retrospective studies have reported even higher relapse rates, between 35% and 50%, highlighting the tendency of IGM to relapse frequently during its natural course (17). These differences support the effectiveness of our individualized approach in routine clinical practice.

The low relapse rate likely reflects the structured, multi-phase treatment protocol. Common challenges frequently reported include premature tapering of corticosteroids, delayed initiation of biological therapies, and inadequate follow-up (18). In contrast, our center applied a pragmatic, stepwise approach in which systemic therapy was generally reserved for clinically active or extensive disease, and steroid-sparing agents were used to reduce cumulative corticosteroid exposure when prolonged treatment was required, followed by gradual tapering and long-term immunosuppressive support using methotrexate or azathioprine (19). Despite the small sample size the azathioprine subgroup exhibited zero relapse events. Therefore, this observation should be considered exploratory and not interpreted as evidence of superior efficacy. In steroid-refractory or relapsing cases, biologic agents (e.g., adalimumab) and cyclosporine were used only as rescue therapy in refractory/relapsing disease, and observed outcomes should be interpreted in the context of the presence of confounding by indication (20).

In the methotrexate group (n = 85), the relapse rate was 25.9% (n = 22) and tended to occur between three and five months of therapy. This highlights the importance of careful steroid dose adjustment and sustained immunosuppressive therapy (21). Recent efforts have aimed to standardize clinical classification and improve comparability across IGM cohorts. A consensus study has proposed a practical clinical classification framework, and a Pittsburgh classification-based treatment algorithm has also been presented, emphasizing stepwise escalation from observation/local measures to systemic immunosuppression for severe or refractory disease. Our mild/moderate/severe stratification overlaps conceptually with these emerging frameworks but was applied retrospectively and should be regarded as a center-specific pragmatic approach rather than a validated consensus classification (22, 23).

Prospective studies comparing methotrexate- and azathioprine-based regimens are warranted to clarify relative efficacy and safety (24).

Despite the favorable relapse outcomes observed in this cohort, systemic immunosuppressive therapy carries an inherent risk of overtreatment, particularly in patients with mild disease or limited inflammatory activity. Therefore, treatment intensity should be carefully individualized, balancing potential benefits against systemic adverse effects. Risk-adapted decision-making remains essential in the management of IGM.

Local treatment modalities, including intralesional corticosteroid injections and surgical drainage, represent valid therapeutic options in selected patients with localized disease. The limited use of these approaches in the present cohort reflects institutional practice patterns rather than a recommendation against local therapies. Treatment selection should remain individualized, incorporating both systemic and local strategies when clinically appropriate.

Combination therapies applied in refractory and relapsing cases also yielded meaningful clinical outcomes. The regimens of methotrexate + cyclosporine (200 mg/day for 4–6 months) and methotrexate + adalimumab (40 mg every other week) resulted in early positive clinical and laboratory responses from the first month of treatment, although these observations should again be interpreted cautiously due to the retrospective design (25). These results align with a recent report supporting the promising role of TNF-α inhibitors in granulomatous inflammatory diseases, including IGM (26).

Moreover, our study adopted a stringent definition of relapse, considering only those recurrences that occurred after complete clinical and radiological remission. The therapeutic strategy was guided by a structured and stepwise protocol: For non-severe localized disease, observation and/or local measures may be appropriate as initial management, with systemic immunosuppression reserved for clinically active, extensive, progressive, or refractory disease, and the introduction of combination therapy (methotrexate + cyclosporine or adalimumab) only in cases of relapse (27). Monthly monitoring and individualized steroid tapering were central to relapse prevention. In contrast, many studies classify any clinical fluctuation as relapse, potentially inflating relapse rates and limiting comparability (28). Unlike many previous reports limited to univariate or descriptive analyses, our study employed multivariate regression, which allowed us to explore variables statistically associated with relapse in this retrospective cohort. This methodological strength enhances the reliability of our conclusions. The relatively low relapse rate in our cohort compared with previous reports further highlights the potential value of our structured treatment strategy. The relapse clustering between months 3 and 5 may relate to steroid tapering dynamics, reinforcing the need for immunosuppressive maintenance.

We also observed a statistically significant association between ESR and treatment duration. The observed associations between relapse status and the use of TNF-α inhibitors or cyclosporine

should be interpreted with caution. These agents were not initiated as first-line therapies but were introduced after relapse as rescue treatments for refractory disease. Therefore, their statistical association with relapse reflects confounding by indication rather than a causal or predictive effect. This highlights the inherent limitations of retrospective analyses when interpreting treatment-related regression outcomes. There may be benefit in measuring ESR when monitoring treatment response and relapse risk. This finding reinforces the established role of systemic inflammation in the clinical course of IGM but may also indicate poor control of the inflammatory response or may simply indicate continued non-specific inflammation from some unidentified cause or confounder (29).

Although prolactin has been hypothesized as a contributing factor in IGM, our study did not find a significant association between prolactin levels and recurrence, consistent with findings from previous research (30). Surgical intervention, while sometimes necessary, was associated with a tendency toward higher relapse rates in our small subset of surgically treated patients, aligning with other studies emphasizing the risks of surgery without concurrent immunosuppression (31).

Ultimately, our study illustrated the complexity of IGM management. There is no universally superior treatment approach. Rather, individualized, multimodal strategies tailored to each patient's clinical presentation and disease severity appear to yield optimal results. Future research should prioritize randomized controlled trials and long-term follow-up studies to refine therapeutic algorithms and improve patient outcomes (32).

Study Limitations

This study is limited by its retrospective design and relatively small subgroup sizes, which restricted some multivariate comparisons. Larger, prospective studies are required to validate these predictors.

The retrospective design of this study also prevents causal inference and is subject to incomplete data capture and indication bias. In addition, the median follow-up duration of only 14.3 months may be insufficient to detect late relapses, given the chronic and recurrent nature of IGM. Additionally, this was a single-center cohort with a postpartum/breastfeeding-enriched population, which may limit generalizability to broader or non-endemic settings. Therefore, long-term disease control and durability of remission could not be fully assessed. Adverse events related to corticosteroids, methotrexate, azathioprine, and biologic agents were not systematically graded or quantified due to the retrospective nature of the study. Consequently, the true incidence of treatment-related toxicity may be underestimated. Future prospective studies with standardized safety reporting are needed to better define the risk-benefit profile of systemic immunosuppressive therapies in IGM.

This study demonstrated that a structured and individualized treatment approach may contribute to favorable clinical outcomes in patients with IGM. The observed relapse patterns highlight the importance of risk-adapted management strategies rather than a uniform therapeutic algorithm. However, given the retrospective design, limited subgroup sizes, and follow-up duration, the present findings should be interpreted cautiously and require further validation. Prospective, multicenter studies are warranted to validate relapse-associated factors and to define the optimal balance between systemic and local treatment modalities.

Ethics

Ethics Committee Approval: Ethical approval was obtained from the Ethics Committee of Liv Bona Dea, Baku Hospital (approval no: BDP-2023/174, date: 02.11.2024).

Informed Consent: Retrospective study.

Acknowledgments

We extend our sincere appreciation to the patients and their families for their invaluable participation in this study. We also wish to thank the clinical and administrative staff of the Rheumatology Department at the Central Military Hospital for their support during data collection and follow-up. Furthermore, we are grateful to the statistical review team for their guidance in validating the findings.

Footnotes

Authorship Contributions

Concept: R.J., A.A., I.B., R.A., K.S., N.A., E.S.; Design: R.J., A.A., I.B., R.A., K.S., N.A., E.S.; Data Collection or Processing: R.J., A.A., I.B., R.A., K.S., N.A., E.S.; Analysis or Interpretation: R.J., A.A., I.B., R.A., K.S., N.A., E.S.; Literature Search: R.J., A.A., I.B., R.A., K.S., N.A., E.S.; Writing: R.J., A.A., I.B., R.A., K.S., N.A., E.S.

Conflict of Interest: No conflict of interest was declared by the authors.

Financial Disclosure: The authors declared that this study received no financial support.

References

1. Kessler E, Wolloch Y. Granulomatous mastitis: a lesion clinically simulating carcinoma. Am J Clin Pathol. 1972; 58: 642-646. (PMID: 4674439) [Crossref]
2. Barreto DS, Sedgwick EL, Nagi CS, Benveniste AP. Granulomatous mastitis: etiology, imaging, pathology, treatment, and clinical findings. Breast Cancer Res Treat. 2018; 171: 527-534. (PMID: 29971624) [Crossref]
3. Pereira J, Alves F, Ferreira F, Vasconcelos de Matos L, Massena A, Martins A. Liquid biopsies in progressing metastatic colorectal cancer- application and their therapeutic implications according to the RAS status. Cureus. 2020; 12: e7035. (PMID: 32211268) [Crossref]

4. Benson JR, Dumitru D. Idiopathic granulomatous mastitis: presentation, investigation and management. Future Oncol. 2016; 12: 1381-1394. (PMID: 27067146) [Crossref]

5. Ringsted S, Friedman M. A rheumatologic approach to granulomatous mastitis: a case series and review of the literature. Int J Rheum Dis. 2021; 24: 526-532. (PMID: 33523600) [Crossref]

6. Uysal E, Soran A, Sezgin E; Granulomatous Mastitis Study Group. Factors related to recurrence of idiopathic granulomatous mastitis: what do we learn from a multicentre study? ANZ J Surg. 2018; 88: 635-639. (PMID: 28749045) [Crossref]

7. Maione C, Palumbo VD, Maffongelli A, Damiano G, Buscemi S, Spinelli G, et al. Diagnostic techniques and multidisciplinary approach in idiopathic granulomatous mastitis: a revision of the literature. Acta Biomed. 2019; 90: 11-15. (PMID: 30889150) [Crossref]

8. Kiyak G, Dumlu EG, Kilinc I, Tokaç M, Akbaba S, Gurer A, et al. Management of idiopathic granulomatous mastitis: dilemmas in diagnosis and treatment. BMC Surg. 2014; 14: 66. (PMID: 25189179) [Crossref]

9. Wolfrum A, Kümmel S, Theuerkauf I, Pelz E, Reinisch M. Granulomatous mastitis: a therapeutic and diagnostic challenge. Breast Care (Basel). 2018; 13: 413-418. (PMID: 30800035) [Crossref]

10. Akbulut S, Yilmaz D, Bakir S. Methotrexate in the management of idiopathic granulomatous mastitis: review of 108 published cases and report of four cases. Breast J. 2011; 17: 661-668. (PMID: 21951547) [Crossref]

11. Azizi A, Prasath V, Canner J, Gharib M, Sadat Fattahi A, Naser Forghani M, et al. Idiopathic granulomatous mastitis: management and predictors of recurrence in 474 patients. Breast J. 2020; 26: 1358-1362. (PMID: 32249491) [Crossref]

12. Skandarajah A, Marley L. Idiopathic granulomatous mastitis: a medical or surgical disease of the breast? ANZ J Surg. 2015; 85: 979-982. (PMID: 25424519) [Crossref]

13. Martinez-Ramos D, Simon-Monterde L, Suelves-Piqueres C, Queralt-Martin R, Granel-Villach L, Laguna-Sastre JM, et al. Idiopathic granulomatous mastitis: a systematic review of 3060 patients. Breast J. 2019; 25: 1245-1250. (PMID: 31273861) [Crossref]

14. Nguyen MH, Molland JG, Kennedy S, Gray TJ, Limaye S. Idiopathic granulomatous mastitis: case series and clinical review. Intern Med J. 2021; 51: 1791-1797. (PMID: 34713960) [Crossref]

15. Sheybani F, Sarvghad M, Naderi H, Gharib M. Treatment for and clinical characteristics of granulomatous mastitis. Obstet Gynecol. 2015; 125: 801-807. (PMID: 25751209) [Crossref]

16. Zhou F, Liu L, Liu L, Yu L, Wang F, Xiang Y, et al. Comparison of conservative versus surgical treatment protocols in treating idiopathic granulomatous mastitis: a meta-analysis. Breast Care (Basel). 2020; 15: 415-420. (PMID: 32982653) [Crossref]

17. Altintoprak F, Kivilcim T, Ozkan OV. Aetiology of idiopathic granulomatous mastitis. World J Clin Cases. 2014; 2: 852-858. (PMID: 25516860) [Crossref]

18. Cadena-Semanate RE, Estrella-Tapia LF, Contreras-Yametti FI, Contreras-Yametti JE, Salazar-Molina RD. Adalimumab in a patient with refractory idiopathic granulomatous mastitis: a case report. Breast J. 2021; 27: 99-102. (PMID: 33142352) [Crossref]

19. Pandey TS, Mackinnon JC, Bressler L, Millar A, Marcus EE, Ganschow PS. Idiopathic granulomatous mastitis--a prospective study of 49 women and treatment outcomes with steroid therapy. Breast J. 2014; 20: 258-266. (PMID: 24673796) [Crossref]

20. Chiu LW, Goodwin K, Vohra P, Amerson E. Cystic neutrophilic granulomatous mastitis regression with the tumor necrosis factor-α inhibitor, adalimumab. Eur J Breast Health. 2021; 18: 94-101. (PMID: 35059598) [Crossref]

21. Aghajanzadeh M, Hassanzadeh R, Alizadeh Sefat S, Alavi A, Hemmati H, Esmaeili Delshad MS, et al. Granulomatous mastitis: presentations, diagnosis, treatment and outcome in 206 patients from the north of Iran. Breast. 2015; 24: 456-460. (PMID: 25935828) [Crossref]

22. Emiroglu M, Akcan A, Velidedeoglu M, Girgin S, Aytac O, Canturk NZ, et al. Diagnosis, approach, and clinical classification of idiopathic granulomatous mastitis: consensus report. Breast Care (Basel). 2024; 19: 243-251. (PMID: 39439860) [Crossref]

23. Aytac H, Nazli M, Ozbas S, Yigit B, Tokocin M, Mendelson E, et al. (2025, May 12). The idiopathic granulomatous mastitis treatment algorithm based on the Pittsburgh classifications (Abstract No. 69.03) [Conference abstract]. Academic Surgical Congress (ASC) 2025 Abstracts. [Crossref]

24. Senol K, Ozsen M, Gokalp G, Tolunay S, Tasdelen MI. Efficacy of azathioprine in reducing recurrence in idiopathic granulomatous mastitis. Sci Rep. 2025; 15: 7391. (PMID: 40033068) [Crossref]

25. Lermi N, Ekin A, Yağız B, Yıldırım F, Albayrak F, Sunkak S, et al. Idiopathic granulomatous mastitis: TNFi effectivity in a retrospective inception cohort. Clin Rheumatol. 2025; 44: 2553-2560. (PMID: 40314853) [Crossref]

26. Kehribar DY, Duran TI, Polat AK, Ozgen M. Effectiveness of methotrexate in idiopathic granulomatous mastitis treatment. Am J Med Sci. 2020; 360: 560-565. (PMID: 32635989) [Crossref]

27. Gürüler E, Şenol K. The recurrence outcome with respect to treatment choices in idiopathic granulomatous mastitis: a retrospective cohort study with 10-year single-center experience. Asian Journal of Surgery, 2025. [Crossref]

28. Tekgöz E, Çolak S, Çinar M, Yilmaz S. Treatment of idiopathic granulomatous mastitis and factors related with disease recurrence. Turk J Med Sci. 2020; 50: 1380-1386. (PMID: 32394683) [Crossref]

29. Lermi N, Ekin A, Ocak T, Bozkurt ZY, Ötegeçeli MA, Yağız B, et al. What predicts the recurrence in ıdiopathic granulomatous mastitis? Clin Rheumatol. 2023; 42: 2491-2500. (PMID: 37301771) [Crossref]

30. Bani-Hani KE, Yaghan RJ, Matalka II, Shatnawi NJ. Idiopathic granulomatous mastitis: time to avoid unnecessary mastectomies. Breast J. 2004; 10: 318-322. (PMID: 15239790) [Crossref]

31. Kok KY, Telisinghe PU. Granulomatous mastitis: presentation, treatment and outcome in 43 patients. Surgeon. 2010; 8: 197-201. (PMID: 20569938) [Crossref]

32. Atak T, Sagiroglu J, Eren T, Ali Özemir I, Alimoglu O. Strategies to treat idiopathic granulomatous mastitis: retrospective analysis of 40 patients. Breast Dis. 2015; 35: 19-24. (PMID: 24989362) [Crossref]

ORIGINAL ARTICLE

European Journal of BREAST HEALTH

DOI: 10.4274/ejbh.galenos.2026.2026-1-3
Eur J Breast Health 2026;22(3):279-284

Redefining Margin Assessment in Breast Conservation Surgery: Surgeon-Performed Intraoperative Ultrasound as a Reliable Alternative to Radiologic and Mammographic Assessment

Tabrej Alam[1], Arvind Baghel[1], Devashish Mishra[2], Ranu Tiwari Mishra[3], Shyam Ji Rawat[4], Sanjay Kumar Yadav[1], Dhananjaya Sharma[1]

[1]Department of Surgery, NSCB Medical College, Jabalpur, India
[2]Department of Radiology, NSCB Medical College, Jabalpur, India
[3]Department of Pathology, NSCB Medical College, Jabalpur, India
[4]Department of Radiotherapy, NSCB Medical College, Jabalpur, India

ABSTRACT

Objective: Accurate intraoperative margin assessment during breast-conserving surgery (BCS) is essential to minimize re-excision and preserve cosmesis. In resource-constrained settings, advanced imaging and frozen section analysis are often unavailable, and surgeons frequently rely on visual-tactile judgment. This study compared the diagnostic accuracy of surgeon-performed intraoperative specimen ultrasound (IOSpUS-S), radiologist-performed specimen ultrasound (IOSpUS-R), specimen mammography, and gross inspection against final histopathology.

Materials and Methods: This prospective study included 40 patients with early breast cancer undergoing wide local excision at a tertiary centre in central India. Each excised specimen was evaluated intraoperatively, *ex vivo*, by gross inspection, IOSpUS (surgeon and radiologist), and specimen mammography. Diagnostic parameters, including sensitivity, specificity, positive predictive value (PPV), negative predictive value (NPV), accuracy, and correlation with the final histopathological margins, were calculated. Receiver operating characteristic analysis was performed to determine discriminative performance.

Results: Both surgeon- and radiologist-performed IOSpUS achieved identical diagnostic performance: sensitivity 100%, specificity 100.0%, PPV 100.0%, NPV 97.5%, and accuracy 97.6%. Specimen mammography showed similar results, whereas gross inspection had zero sensitivity but 100% specificity, with an overall accuracy of 95.0%. The mean histopathological margin width was 13.2±3.7 mm. IOSpUS showed a strong correlation with histopathology ($r = 0.87$ for surgeon-performed and $r = 0.83$ for radiologist-performed; $p<0.001$). Only one patient (2.5%) had a close margin that was correctly identified by both IOSpUS modalities and mammography, but was missed on gross inspection.

Conclusion: Surgeon-performed IOSpUS provides real-time, workflow-efficient intraoperative margin assessment, with diagnostic performance comparable to that of radiologist-performed ultrasound and specimen mammography in this prospective cohort. In low-resource environments, gross examination, though less sensitive, remains a viable adjunct when imaging facilities are limited. A combined approach has the potential to reduce re-excision by supporting intraoperative decision-making.

Keywords: Breast cancer; intraoperative ultrasound; specimen mammography; margin assessment; gross examination; low-resource setting

Corresponding Author: Sanjay Kumar Yadav MD;
E-mail: sky1508@gmail.com **ORCID:** orcid.org/0000-0002-0682-4970

Received: 06.01.2026 **Accepted:** 05.02.2026 **Epub:** 24.04.2026 **Available Online Date:** 17.06.2026

Cite this article as: Alam T, Baghel A, Mishra D, Mishra RT, Rawat SJ, Yadav SK, et al. Redefining margin assessment in breast conservation surgery: surgeon-performed intraoperative ultrasound as a reliable alternative to radiologic and mammographic assessment. Eur J Breast Health. 2026;22(3):279-284

KEY POINTS

- Surgeon-performed intraoperative specimen ultrasound (IOSpUS-S) is oncologically reliable: It demonstrates diagnostic accuracy and margin correlation equivalent to radiologist-performed ultrasound and specimen mammography, validating surgeons as effective real-time margin assessors during breast-conserving surgery.
- Workflow efficiency without diagnostic compromise: IOSpUS-S significantly reduces intraoperative time and dependency on radiology services, enabling immediate margin-directed decision-making without loss of accuracy, critical in high-volume and resource-limited settings.
- Gross inspection alone is insufficient but remains a pragmatic adjunct: while gross examination has poor sensitivity for close/positive margins, its high specificity supports its role as a supplementary tool where imaging is unavailable, especially when combined with surgeon-performed ultrasound.

Introduction

Breast cancer is the most common malignancy among women worldwide and remains a major health burden in India (1, 2). Wide local excision (WLE) is an integral part of breast-conserving surgery (BCS) for early breast cancer, as it aims to remove the tumor completely while preserving breast shape and cosmesis (3, 4). The adequacy of surgical margins is crucial in preventing local recurrence, and positive margins often require re-excision or mastectomy, procedures that adversely affect both oncological and cosmetic outcomes (5, 6). Several intraoperative techniques have been developed to evaluate margins and reduce reoperation rates (7-10). Traditionally, specimen mammography has been used, particularly in cases of ductal carcinoma *in situ* (DCIS) (11, 12). Radiologist-performed specimen ultrasound (IOSpUS-R) has been employed to evaluate soft-tissue tumors more accurately than mammography; however, it requires specimen transfer and radiology input, which can prolong the operative workflow (13-16).

Surgeon-performed intraoperative specimen ultrasound (IOSpUS-S) has emerged as a pragmatic alternative, particularly in settings where dependence on radiologists, frozen section facilities, or dedicated imaging infrastructure limits real-time decision-making (17-19). This approach has the potential to reduce re-excisions, operative delays, and costs, particularly in resource-constrained settings. In low- and middle-income countries, the resources required for advanced intraoperative imaging are scarce, and breast cancer surgery often relies on the surgeon's experience and visual-tactile judgment. Gross examination of excised specimens, though simple and cost-neutral, is inherently subjective and hence is considered to have limited ability to detect close margin involvement (16, 20, 21). The present study was therefore undertaken to compare the diagnostic performance of gross examination, specimen mammography, radiologist-performed *ex vivo* (IOSpUS-R), and surgeon-performed *ex vivo* (IOSpUS-S) against final histopathology, the gold standard.

Materials and Methods

This prospective observational study was conducted in the Department of Surgery, Netaji Subhash Chandra Bose Medical College, Jabalpur (MP), India, over 18 months (August 2023 to December 2024). Ethical approval was obtained from the Netaji Subhash Chandra Bose Medical College Jabalpur Institutional Ethics Committee (approval no: IEC/2023/7335-143, date: 18.08.2023), and informed consent from all participants were obtained. This prospective study included 40 consecutive patients with biopsy-proven invasive breast carcinoma undergoing WLE. Patients with pure DCIS, multifocal or multicentric disease, prior neoadjuvant chemotherapy, or non-mass lesions with calcification-dominant imaging were excluded.

All patients underwent standard preoperative mammography and ultrasound for localization and surgical planning. During surgery, WLE was performed with adequate margins in accordance with oncological principles. Each excised specimen was assessed intraoperatively using four margin-assessment methods. First, gross examination and surgeon-performed *ex vivo* ultrasound were carried out in the operating room using a portable high-frequency ultrasound probe to examine the specimen and assess margin status. Second, specimens were evaluated using radiologist-performed *ex vivo* ultrasound after transfer to the radiology department. Third, specimen mammography was performed to assess for calcifications and to evaluate margin clearance.

The findings of each modality were documented and compared with the final histopathology, which served as the gold standard; a close margin was defined as tumor not on the inked margin, with the closest margin measuring <2 mm. The primary outcome was the sensitivity, specificity, positive predictive value (PPV), and negative predictive value (NPV) of each imaging modality. Interobserver agreement between surgeon-performed and radiologist-performed ultrasound was also assessed. The radiologist was not informed of the surgeon's ultrasound interpretation. The final histopathological assessment was performed, blinded to all intraoperative margin assessments. While complete blinding of the surgeon to the specimen was not feasible, bias was mitigated using a standardized scanning protocol and predetermined cut-off values for close margins.

Statistical Analysis

Data were analyzed using an Excel spreadsheet and MedCalc Statistical Software (MedCalc Software Ltd., Ostend, Belgium).

Continuous variables were expressed as mean ± standard deviation, while categorical data were presented as frequencies and percentages. Diagnostic performance parameters, including sensitivity, specificity, PPV, NPV, and overall accuracy, were calculated for each intraoperative modality using final histopathology as the gold standard. Exact 95% confidence intervals (CIs) for sensitivity and specificity were computed using the Wilson score method without continuity correction. Comparative analyses between modalities were performed using the chi-square (χ^2) test or Fisher's exact test as appropriate. Correlations between margin distance measured by intraoperative methods and final histopathological margins were analyzed using the Pearson correlation coefficient(r); the strength of association was interpreted as follows: r = 0.00–0.30 (weak), 0.31–0.70 (moderate), and >0.70 (strong).

Diagnostic performance across modalities was further assessed by constructing receiver operating characteristic (ROC) curves, and the area under the curve (AUC) was calculated, along with its standard error and 95% CI, to evaluate discriminatory ability. All tests were two-sided, and statistical significance was set at p<0.05.

Table 1. Demographic and clinical profile of patients

Variable	Category	Frequency (%)
Age	**Mean ± SD (range)**	**42.65±13.36 (32–70)**
Occupation	Homemakers Others	93% 7%
Menopausal status	Postmenopausal Premenopausal	18 (45%) 22 (55%)
Clinical stage	I II	6 (15%) 34 (85%)
Molecular subtype	A+B Her 2 enriched TNBC	18 (45%) 10 (25%) 12 (30%)

TNBC: Triple-negative breast cancer; SD: Standard deviation

Results

Patient Characteristics

Forty consecutive patients with breast cancer undergoing WLE were included. The mean age was 49±9 years (range 32–68). All lesions were invasive ductal carcinomas; the mean tumor diameter on final histopathology was 2.4±0.8 cm (Table 1).

Margin Assessment and Diagnostic Performance

Each excised specimen was evaluated intraoperatively by gross inspection, IOSpUS-S, radiologist-performed intraoperative specimen ultrasound (IOSpUS-R), and specimen mammography. Final histopathology served as the reference standard. The sensitivity of IOSpUS-S and IOSpUS-R was 100.0% (95% CI: 21–100); specificity was 100.0% (95% CI: 88.8–100); PPV was 100%; NPV was 97.5%; and overall accuracy was 97.6%. Specimen mammography yielded comparable performance metrics: sensitivity 100.0% (95% CI: 21.1–100); specificity 100.0% (95% CI: 88.8–100); PPV 100%; NPV 97.5%; and accuracy 97.6%. Gross inspection missed the only close-margin case in this cohort; therefore, its sensitivity could not be reliably estimated (0.0%, 95% CI: 0–37.9), and overall accuracy was 95.0% (95% CI: 83.1–99.4). There was no statistically significant difference between IOUS-R and IOUS-S (p = 0.99); however, both outperformed gross inspection (p<0.05, χ^2 test) (Table 2).

Figure 1 depicts the ROC curves comparing diagnostic performance among modalities. Both surgeon- and radiologist-performed margin assessments showed near-identicalnearly identical curves with AUC = 0.90. Specimen mammography demonstrated moderate discrimination (AUC = 0.84), whereas gross inspection aligned closely with the reference line (AUC = 0.50).

Margin Distance Correlation

The mean histopathological margin width was 13.2±3.7 mm. Measurements obtained with surgeon-performed IOSpUS-S correlated strongly with histopathology (r = 0.87, p<0.001),while radiologist-performed IOSpUS-R also demonstrated high

Table 2. Diagnostic performance of intraoperative margin assessment modalities (n = 40)

Modality	TP	FP	TN	FN	Sensitivity (%)	Specificity (%)	AUC	95% CI	PPV (%)	NPV (%)	Accuracy (%)
IOSpUS-R	1	0	39	0	100.0	100.0	0.90	0.83–0.98	100.0	97.5	97.6
IOSpUS-S	1	0	39	0	100.0	100.0	0.90	0.83–0.98	100.0	97.5	97.6
Specimen mammography	1	0	39	0	100.0	100.0	0.84	0.73–0.95	100.0	97.5	97.6
Gross inspection	0	0	39	1	0.0	100.0	0.50	0.34–0.65	-	95.0	95.0
Combined (gross+IOSpUS-S)	1	0	39	0	100.0	100.0	-	-	100.0	97.5	97.6

TP: True positives; FP: False positives; TN: True negatives; FN: False negatives; AUC: Area under curve; PPV: Positive predictive value; NPV: Negative predictive value; IOSpUS-S: Intraoperative specimen ultrasonography-surgeon; IOSpUS-R: Intraoperative specimen ultrasonography-radiologist; CI: Confidence interval

correlationalso correlated strongly with histopathology (r = 0.83, $p<0.001$). Specimen mammography showed a moderate correlation ($r = 0.68$, $p = 0.04$), whereas gross inspection showed a poor correlation ($r = 0.41$, $p = 0.12$) (Table 3).

Re-Excision Rate and Operative Workflow

Final histopathology confirmed that a single patient (2.5%) had a positive margin. This margin was accurately detected intraoperatively by both IOUS modalities and specimen mammography, but was missed on gross inspection, resulting in one false-negative case that was re-excised in the same sitting, under the same anaesthesia. The overall re-excision rate was 2.5%. The mean additional intraoperative time for IOSpUS-S evaluation was 5.8±1.9 minutes, significantly shorter than that for IOSpUS-R and specimen mammography (16 +/– 2 min and 14.2±2.6 minutes respectively, $p<0.001$). No intraoperative complications or workflow interruptions were encountered.

Discussion and Conclusion

In this study of 40 patients undergoing WLE, we found that surgeon-performed and radiologist-performed *ex vivo* intraoperative ultrasound achieved excellent specificity and an overall diagnostic accuracy of 97.6% in margin assessment, with both modalities detecting the single close/positive margin that was missed by gross inspection. Importantly, gross visual inspection, despite its low sensitivity, maintained perfect specificity, highlighting that in settings lacking imaging infrastructure, careful gross margin assessment may still offer a pragmatic fallback. In resource-limited settings, where intraoperative imaging or frozen-section analysis is unavailable, gross inspection by an experienced breast surgeon remains a practical adjunct to reduce re-excision rates. Specimen ultrasound is technically less demanding than *in vivo* breast ultrasound and can be adopted by breast surgeons after focused training. The use of a standardized protocol further minimizes operator dependency and enhances reproducibility.

Figure 1. Depicts the receiver operating characteristic curves comparing diagnostic performance among modalities

Table 3. Correlation between intraoperative margin assessment modalities and final histopathological margin width

Modality	Correlation coefficient (r)	*p*-value
Surgeon-performed (IOSpUS-S)	0.87	0.0003
Radiologist-performed (IOSpUS-R)	0.83	0.0005
Specimen mammography	0.68	0.037
Gross inspection	0.41	0.118

IOSpUS-S: Intraoperative specimen ultrasonography-surgeon; IOSpUS-R: Intraoperative specimen ultrasonography-radiologist

Ex vivo intraoperative ultrasound has been increasingly validated as an effective technique to reduce positive margins and re-excision rates. A systematic review and meta-analysis analyzingof palpable infiltrating ductal breast cancers demonstrated that *ex vivo* IOUS guidance was significantly associated with higher rates of clear lumpectomy margins (odds ratio: ~2.3) compared to palpation or wire-guided surgery (18, 19, 22). Our results are consistent with this trend: *ex vivo* IOUS can reliably detect margin compromise with minimal operative delay.

On the other hand, gross intraoperative margin assessment (i.e., visual and tactile inspection of the specimen surface) has historically been considered inferior to imaging- or pathology-based intraoperative methods. However, a recent study evaluated the performance of gross intraoperative assessment and found that its use could contribute meaningfully to reducing re-excisions (20). Authors reported modest sensitivity but acceptable specificity and cautioned that performance is operator-dependent. Similarly, Hoekstra et al. (23) examined a registry dataset and concluded that gross margin examination reduced re-excision rates among invasive breast cancer BCS cohorts. Our experience accords with these findings: although our gross inspection missed one close margin, the inspection's perfect specificity suggests that a positive result is reliably predictive and can help triage which margins require further evaluation. When combined with surgeon-performed IOUS, gross examination could help prioritize suspicious zones for imaging or re-excision, thereby optimizing workflow.

Study Limitations

Nevertheless, our study has limitations. The present study should be interpreted in light of its small sample size and low event rate, as there was only one close-margin case. Consequently, diagnostic performance estimates should be considered exploratory and hypothesis-generating rather than definitive. Second, our results stem from a single institution with experienced surgeons and radiologists; performance might be lower in less-experienced

hands. Third, this was a controlled setting; in busy clinical environments, additional time, coordination, or fatigue could affect IOUS performance. Fourth, we did not evaluate long-term local recurrence, cosmetic outcomes, or cost-effectiveness. All lesions in this study were mass-forming invasive carcinomas. The applicability of IOSpUS to pure DCIS or calcification-dominant lesions remains limited; specimen mammography continues to play a critical role.

Despite these limitations, our study has several strengths: we directly compared surgeon- and radiologist-performed IOUS with both specimen mammography and gross assessment in the same cohort, providing an internal control. The real-time integration of surgeon-performed IOSpUS-S demonstrates practical feasibility without disrupting operative flow.

Surgeon-performed IOSpUS provides real-time and workflow-efficient intraoperative margin assessment, with diagnostic performance comparable to radiologist-performed ultrasound and specimen mammography in this prospective cohort. In low-resource environments, gross examination though less sensitive remains a viable adjunct when imaging facilities are limited. A combined approach has the potential to reduce re-excision and may support intraoperative decision-making aimed at reducing re-excision.

Ethics

Ethics Committee Approval: Ethical approval was obtained from the Netaji Subhash Chandra Bose Medical College Jabalpur Institutional Ethics Committee (approval no: IEC/2023/7335-143, date: 18.08.2023).

Informed Consent: Informed consent from all participants were obtained.

Acknowledgement

The authors acknowledge support from the Multidisciplinary Research Unit, NSCBMC, Department of Health Research.

Footnotes

Authorship Contributions

Surgical and Medical Pracites: T.A., S.K.Y., A.B., D.M., S.J.R., R.M., D.S.; Concept: T.A., S.K.Y., A.B., D.M., S.J.R., R.M., D.S.; Design: T.A., S.K.Y., A.B., D.M., S.J.R., R.M., D.S.; Data Collection and/or Processing: T.A., S.K.Y., A.B., D.M., S.J.R., R.M., D.S.; Analysis and/or Interpretation: T.A., S.K.Y., A.B., D.M., S.J.R., R.M., D.S.; Literature Search: T.A., S.K.Y., A.B., D.M., S.J.R., R.M., D.S.; Writing: T.A., S.K.Y., A.B., D.M., S.J.R., R.M., D.S.

Conflict of Interest: The authors have no conflicts of interest to declare.

Financial Disclosure: The authors declared that this study has received no financial support.

References

1. Arnold M, Morgan E, Rumgay H, Mafra A, Singh D, Laversanne M, et al. Current and future burden of breast cancer: global statistics for 2020 and 2040. Breast. 2022; 66: 15-23. (PMID: 36084384) [Crossref]
2. Kulothungan V, Ramamoorthy T, Sathishkumar K, Mohan R, Tomy N, Miller GJ, et al. Burden of female breast cancer in India: estimates of YLDs, YLLs, and DALYs at national and subnational levels based on the national cancer registry programme. Breast Cancer Res Treat. 2024; 205: 323-332. (PMID: 38433127) [Crossref]
3. Yadav SK, S A, Johri G, Shekhar S, Sharma D. Oncoplastic breast surgery in low-resource settings: feasibility, adoption and outcomes of local perforator flaps. Indian J Surg Oncol. 2026; 17: 36-40. (PMID: 41641424) [Crossref]
4. Clough KB, Kaufman GJ, Nos C, Buccimazza I, Sarfati IM. Improving breast cancer surgery: a classification and quadrant per quadrant atlas for oncoplastic surgery. Ann Surg Oncol. 2010; 17: 1375-1391. (PMID: 20140531) [Crossref]
5. Houssami N, Macaskill P, Marinovich ML, Morrow M. The association of surgical margins and local recurrence in women with early-stage invasive breast cancer treated with breast-conserving therapy: a meta-analysis. Ann Surg Oncol. 2014; 21: 717-730. (PMID: 24473640) [Crossref]
6. Pop CF, Ortega C, Lecomte M, Kristanto P, Khaled C, De Neubourg F, et al. Impact of margin distance on recurrence and survival following breast-conserving surgery after neoadjuvant systemic therapy. NPJ Breast Cancer. 2025; 11: 45. (PMID: 40389463) [Crossref]
7. Hwang ES, Beitsch P, Blumencranz P, Carr D, Chagpar A, Clark L, et al; INSITE study team. Clinical impact of intraoperative margin assessment in breast-conserving surgery with a novel pegulicianine fluorescence-guided system: a nonrandomized controlled trial. JAMA Surg. 2022; 157: 573-580. (PMID: 35544130) [Crossref]
8. Jong LS, Veluponnar D, Geldof F, Sanders J, Guimaraes MDS, Vrancken Peeters MTFD, et al. Toward real-time margin assessment in breast-conserving surgery with hyperspectral imaging. Sci Rep. 2025; 15: 9556. (PMID: 40108280) [Crossref]
9. Pradipta AR, Tanei T, Morimoto K, Shimazu K, Noguchi S, Tanaka K. Emerging technologies for real-time intraoperative margin assessment in future breast-conserving surgery. Adv Sci (Weinh). 2020; 7: 1901519. (PMID: 32382473) [Crossref]
10. Maloney BW, McClatchy DM, Pogue BW, Paulsen KD, Wells WA, Barth RJ. Review of methods for intraoperative margin detection for breast conserving surgery. J Biomed Opt. 2018; 23: 1-19. (PMID: 30369108) [Crossref]
11. Lin C, Wang KY, Chen HL, Xu YH, Pan T, Chen YD. Specimen mammography for intraoperative margin assessment in breast conserving surgery: a meta-analysis. Sci Rep. 2022; 12: 18440. (PMID: 36323863) [Crossref]
12. Mariscotti G, Durando M, Pavan LJ, Tagliafico A, Campanino PP, Castellano I, et al. Intraoperative breast specimen assessment in breast conserving surgery: comparison between standard mammography imaging and a remote radiological system. Br J Radiol. 2020; 93: 20190785. (PMID: 32101449) [Crossref]
13. Wang Y, Ebuoma L, Saksena M, Liu B, Specht M, Rafferty E. Clinical evaluation of a mobile digital specimen radiography system for intraoperative specimen verification. AJR Am J Roentgenol. 2014; 203: 457-462. (PMID: 25055285) [Crossref]
14. Tan KY, Tan SM, Chiang SH, Tan A, Chong CK, Tay KH. Breast specimen ultrasound and mammography in the prediction of tumour-free margins. ANZ J Surg. 2006; 76: 1064-1067. (PMID: 17199691) [Crossref]
15. Butler-Henderson K, Lee AH, Price RI, Waring K. Intraoperative assessment of margins in breast conserving therapy: a systematic review. Breast. 2014; 23: 112-119. (PMID: 24468464) [Crossref]

16. Dowling GP, Hehir CM, Daly GR, Hembrecht S, Keelan S, Giblin K, et al. Diagnostic accuracy of intraoperative methods for margin assessment in breast cancer surgery: a systematic review & meta-analysis. Breast. 2024; 76: 103749. (PMID: 38759577) [Crossref]

17. Colakovic N, Zdravkovic D, Skuric Z, Mrda D, Gacic J, Ivanovic N. Intraoperative ultrasound in breast cancer surgery-from localization of non-palpable tumors to objectively measurable excision. World J Surg Oncol. 2018; 16: 184. (PMID: 30205823) [Crossref]

18. Pan H, Wu N, Ding H, Ding Q, Dai J, Ling L, et al. Intraoperative ultrasound guidance is associated with clear lumpectomy margins for breast cancer: a systematic review and meta-analysis. PLoS One. 2013; 8: e74028. (PMID: 24073200) [Crossref]

19. Ferrucci M, Milardi F, Passeri D, Cagol M, Del Bianco P, Grossi U, et al. Intraoperative ultrasound-guided breast-conserving surgery: a performance analysis on the basis of novel cancer lesion classification and patients' cosmetic satisfaction. Surgery. 2025; 180: 109037. (PMID: 39823651) [Crossref]

20. Nunez A, Jones V, Schulz-Costello K, Schmolze D. Accuracy of gross intraoperative margin assessment for breast cancer: experience since the SSO-ASTRO margin consensus guidelines. Sci Rep. 2020; 10: 17344. (PMID: 33060797) [Crossref]

21. St John ER, Al-Khudairi R, Ashrafian H, Athanasiou T, Takats Z, Hadjiminas DJ, et al. Diagnostic accuracy of intraoperative techniques for margin assessment in breast cancer surgery: a meta-analysis. Ann Surg. 2017; 265: 300-310. (PMID: 27429028) [Crossref]

22. Armani A, Borst J, Douglas, S. Goldharber N, Taj R, Blair SL. Intraoperative margin trials in breast cancer. Curr Breast Cancer Rep. 2022; 14: 65-74. [Crossref]

23. Hoekstra S, Stoller D, Raef H. Does gross margin examination reduce re-excision rate in breast conservation for invasive carcinoma? CALLER review. Eur J Breast Health. 2020; 16: 198-200. (PMID: 32656520) [Crossref]

ORIGINAL ARTICLE

European Journal of BREAST HEALTH

DOI: 10.4274/ejbh.galenos.2026.2025-11-11
Eur J Breast Health 2026;22(3):285-293

Safety and Early Outcomes of Immediate Autologous Breast Reconstruction in Advanced Breast Cancer: An Indian Experience

Meenu Jose[1], Shivani Sable[1], Tabassum Wadasadawala[1], Rajiv Sarin[1], Rima Pathak[1], Revathy Krishnamurthy[1], Shalaka Joshi[2], Vinaykant Shankhdhar[3], Dushyant Jaiswal[3], Saumya Mathews[3], Mayur Mantri[3]

[1]Tata Memorial Centre, Homi Bhabha National Institute, Department of Radiation Oncology, Mumbai, India
[2]Tata Memorial Centre, Homi Bhabha National Institute, Department of Surgical Oncology, Mumbai, India
[3]Tata Memorial Centre, Homi Bhabha National Institute, Department of Plastic and Reconstructive Surgery, Mumbai, India

ABSTRACT

Objective: Post-mastectomy breast reconstruction improves body image and quality of life for women with breast cancer. Most adverse events emerge within the first 90 days and may contribute to long-term morbidity. This study prospectively evaluated the incidence and predictors of early complications following immediate autologous breast reconstruction in women with locally advanced breast cancer.

Materials and Methods: Prospective data from a randomized controlled trial (CTRI/2017/01/007745) involving women undergoing immediate autologous whole breast reconstruction were analysed. Breast and donor-site complications were recorded and graded using Clavien-Dindo classification over 0–30 and 31–90 days. Univariate and multivariate analyses were performed to identify risk factors.

Results: A total of 160 patients were included. The mean age was 37±7 years; body mass index (BMI) was 25.7±4.6; 25.6% had comorbidities. Deep inferior epigastric perforator (DIEP) flaps accounted for 85% of reconstructions. Within 0–30 days, 45% developed primary-site complications; 33% developed donor-site complications. At 31–90 days, primary-site complications were reduced to 15%, and donor-site complications to 13%. Re-exploration was required in 11%; however, no flap loss was observed. Univariate analysis showed age >37, BMI ≥25, diabetes, multiple comorbidities, any comorbidity, and DIEP increased primary-site complication risk and BMI ≥25 and DIEP predicted donor-site events. Multivariate analysis confirmed multiple comorbidities and DIEP as predictors of primary-site complications, while BMI ≥25 and DIEP predicted donor-site complications. As DIEP flaps predominated, in our patients technique-based comparisons should be interpreted cautiously.

Conclusion: Immediate autologous whole-breast reconstruction in patients with advanced breast cancer undergoing multimodal therapy, including intensive chemotherapy and radiotherapy, resulted in a high overall complication rate but no reconstructive failures, highlighting the need for a selective, individualized approach with comprehensive preoperative counselling and shared decision-making.

Keywords: Surgical complications; breast reconstruction; breast cancer; acute complications; autologous reconstruction

Corresponding Author: Tabassum Wadasadawala MD
E-mail: twadasadawala@actrec.gov.in **ORCID:** orcid.org/0000-0003-2167-420X

Received: 11.12.2025 **Accepted:** 01.03.2026 **Available Online Date:** 17.06.2026
Cite this article as: Jose M, Sable S, Wadasadawala T, Sarin R, Pathak R, Krishnamurthy R, et al. Safety and early outcomes of immediate autologous breast reconstruction in advanced breast cancer: an Indian experience. Eur J Breast Health. 2026;22(3):285-293

KEY POINTS

- Early complications were common but manageable, with no flap failures or delays in adjuvant treatment, underscoring clinical safety.
- Higher body mass index and multiple comorbidities emerged as the most significant predictors of postoperative complications.
- Immediate autologous breast reconstruction can be safely performed in selected patients with advanced breast cancer who are undergoing multimodal therapy (chemotherapy and radiotherapy).

Introduction

While breast reconstruction has become widely accepted and accessible in high-income countries (1), its adoption remains limited in low- and middle-income countries (LMIC). For women in LMICs the choice between breast conservation surgery and mastectomy is often challenging. Limited knowledge about the safety of breast-conserving surgery, financial barriers, and concerns regarding the potential side effects of radiotherapy often lead patients to favour mastectomy.

Ideally, every woman undergoing a mastectomy should be offered options for breast reconstruction. However, lack of expertise, lack of thorough knowledge about the nuances of integration of local and systemic therapy, and lack of preoperative counselling about surgical morbidity influence patient confidence in making informed decisions. Early complications (defined as within the first 90 days post-surgery) can have an adverse effect on the long-term aesthetic outcome. Identifying and managing perioperative complications is therefore crucial to improving outcomes and enhancing patient satisfaction and psychological recovery.

Immediate breast reconstruction (IBR) is a desirable option for women undergoing mastectomy in LMIC setting (2). Identifying risk factors for complications is crucial for optimizing patient-reported outcomes. Identifying an individual at high-risk allows health care providers to exercise caution when selecting patients for reconstruction, to discuss reconstruction options with patients and to tailor perioperative assessments.

This study aims to assess factors associated with complications among patients undergoing immediate autologous breast reconstruction at a resource-constrained LMIC referral centre. It will provide an opportunity for shared decision-making regarding surgical care for patients with locally advanced disease who are receiving multimodality treatment including intensive chemotherapy, targeted therapy, and radiotherapy.

Materials and Methods

The study was approved by Tata Memorial Centre Ethics Committee-I (approval number: 1683, date: 12.05.2016) and registered in Clinical Trials Registry-India (CTRI/2017/01/007745); the trial completed accrual between 2016 and 2024. The trial accrued patients with invasive breast cancer who underwent immediate autologous whole-breast reconstruction following mastectomy and were randomized to receive adjuvant radiotherapy with either conventional fractionation (50 Gy in 25 fractions) or moderate hypofractionation (40 Gy in 15 fractions). This article evaluates 90-day surgical complications among patients enrolled in this trial, assessing both the reconstructed breast and the donor site; this assessment is one of the trial's secondary endpoints.

Study Population

Patients diagnosed with locally advanced invasive breast cancer (stage II–IV, oligometastatic disease treated with curative intent) who were planned for mastectomy followed by immediate autologous whole-breast reconstruction were accrued at a single centre for this open-label randomised controlled trial.

Surgical Details

Primary autologous reconstruction is preferred amongst our cohort of patients due to various factors such as extent of skin resection, cost of a staged procedure, distance from place of treatment etc. The body morphology of South Asian patients makes the lower abdomen a favourable donor site for autologous reconstruction. Hence, most of our patients undergo the deep inferior epigastric perforator (DIEP) flap reconstruction. Other donor sites are evaluated only when the abdominal donor site is inadequate or the patient is nulliparous. None of the patients had an implant-based reconstruction.

Data Collection

Demographic, clinical, and treatment data for all patients were maintained prospectively. Demographics included age, comorbidities, and body mass index (BMI). Surgical variables included flap type, pedicle status, flap weight, and reconstruction time. The incidence and severity of morbidity at the recipient and donor sites were recorded separately for all patients. All events, regardless of severity, were captured independently during 0–30 days and 31–90 days. Patients who experienced multiple complications were identified, and the percentage of each complication type was calculated separately for both the recipient and donor sites. Complications at recipient and donor sites were recorded for the 0–30-day and 31–90-day periods, and cumulative complication rates were reported for the entire 90-day postoperative period.

Definition of Surgical Morbidity

Surgical morbidity was assessed using the Clavien-Dindo scoring system based on the type and severity of intervention required to manage them (3). The Clavien-Dindo classification categorizes complications into five grades (I–V): Grade I represents complications requiring only medical treatment (antiemetics, antipyretics, analgesics, diuretics, electrolytes, and physiotherapy); grade II refers to complications requiring pharmacological treatment (drugs other than those used for grade I); grade III involves complications requiring surgical, endoscopic, or radiological intervention(IIIa for local anaesthesia and IIIb for general anaesthesia); grade IV refers to life-threatening complications requiring intensive care; and grade V indicates death. Complications of breast surgery include seroma, wound infection, necrosis, and bleeding. If multiple complications developed in a single patient, the worst grade was recorded.

Follow-up Schedule

All scheduled and unscheduled visits within 90 days of surgery were captured, and the reasons were recorded. All events of readmissions and reoperations for the management of complications at both the recipient and donor sites were captured and grouped into three time points: 0–30 days, 30–90 days, and 0–90 days.

Statistical Analysis

Descriptive statistics were used to summarize demographic and clinical characteristics, as well as postoperative outcomes. Continuous variables were summarized using mean and standard deviation, whereas categorical variables were expressed as frequencies and percentages. The incidence data for various complications for 0–30 days, 30–90 days, and 0–90 days were reported separately for the recipient and donor sites.

Univariate and multivariate logistic regression analyses were conducted over the 0–90-day period to identify factors associated with wound-related complications. Odds ratios (OR), 95% confidence intervals, and *p*-values were reported. Variables with $p<0.2$ in univariate analysis were included in multivariate models to adjust for confounders. All analyses were carried out using R version 4.5.0.

Results

A total of 160 patients were analysed. The demographic and clinical characteristics are summarized in Table 1. The mean age of the patients was 37±7 years, and the mean BMI was 25.65±4.59. Twelve patients (7.5%) had multiple comorbidities, with hypertension and diabetes being the most common. The types of flaps included DIEP flap, transverse rectus abdominis myocutaneous flap, anterolateral thigh flap, and latissimus dorsi flap. The majority (85%) of patients underwent IBR using the DIEP-flap. All patients who received chemotherapy and targeted therapy in the form of neoadjuvant and/or adjuvant treatment and adjuvant radiotherapy had locally advanced disease. Most patients had T3-T4 disease (72.5%). Neoadjuvant

Table 1. Demographic data

Demographics	Overall (number/percent)
Age (mean SD)	37.3±7.1
Comorbidities*	
No comorbidities	119 (74.3%)
Diabetes mellitus	17 (10.6%)
Hypertension	14 (8.75%)
Tuberculosis	6 (3.75%)
Thyroid disorders	20 (12.5%)
Bronchial asthma	2 (1.25%)
BMI	
Normal weight (18.5–24.9)	77 (48.2%)
Overweight (25.0–29.9)	58 (36.2%)
Obese (≥30)	25 (15.6%)
Laterality	
Right	76 (47.5%)
Left	84 (52.5%)
T stage	
T1,T2	44 (27.5%)
T3,T4	116 (72.5%)
Chemotherapy	
Neoadjuvant chemotherapy	83 (51.9%)
Surgery between 2 regimens of chemotherapy	57 (35.6%)
Adjuvant chemotherapy	20 (12.5%)
Type of reconstruction	
DIEP#	136 (85%)
LD# flap	13 (8.1%)
Others**	11 (6.9%)
Pedicle status, n (%)	
Single pedicle	146 (91.2%)
Bipedicle	14 (8.8%)
Flap weight (grams) (mean ± SD)	704±244
Reconstruction time (mean ± SD)	6 hrs 30 minutes ±1 hour

*includes patients with multiple comorbidities, hence the total number of complications do not sum up to the total number of patients.

**others included flaps based on TRAM, superior gluteal artery based, and ALT flap

#: DIEP: Deep inferior epigastric perforator; LD: Latissimus dorsi; BMI: Body mass index; SD: Standard deviation; TRAM: Transverse rectus abdominus myocutaneous flap; ALT: Anterolateral thigh

chemotherapy (NACT) was offered to 83 (51.9%) patients, adjuvant chemotherapy to 20 (12.5%), and surgery was performed between the two regimens in 57 (35.6%) patients. Patients received various chemotherapy regimens, most commonly anthracycline-cyclophosphamide combinations followed by taxane-based therapy, administered in the neoadjuvant and/or adjuvant settings. In human epidermal growth factor receptor 2-positive patients, trastuzumab was added to the taxane regimen, whereas in those with triple-negative breast cancer, platinum agents were combined with taxanes. In patients receiving NACT (n = 83), 79 (95%) started radiotherapy within 90 days of surgery, with a median time to radiotherapy of 50 days [interquartile range (IQR) 40–64]. In the remaining 4 patients, radiotherapy was delayed by more than 90 days. Two of them had wound complications; one reported late for radiotherapy; and one developed local chest wall recurrence. Among patients receiving adjuvant chemotherapy, all started chemotherapy within 90 days post-surgery, with a median of 28 days (IQR: 21–42). For these patients, the median time from the last chemotherapy cycle to initiation of radiotherapy was 29 days (IQR: 21–38.5). The distribution of dose fractionation was 48.5% in the conventional arm and 49.4% in the test arm. Three patients did not receive radiotherapy because they developed metastatic disease.

Morbidity at the Primary Site

During the 0–30-day period, flap complications occurred in 72 patients (45%), decreasing to 15% in the 31–90-day period. Overall, in the 0–30-day period, the most frequent complication was wound infection (n = 53, 73.6%). The majority (n = 46, 87%) of wound infections were classified as Clavien-Dindo grade III complications, and one was a grade IV complication. Partial necrosis was seen in 23 patients (31.9%), and seroma in 16 patients (22%). Twelve patients had multiple complications, including infection, seroma, and necrosis. In the 31–90-day period, 24 patients (15%) reported complications. Wound infection remained the most common complication (83.3%) (Table 2).

During the initial 30-day postoperative period, 10 (6.25%) patients required readmission primarily due to wound infections; an additional 8 (5.0%) patients required readmission between days 31 and 90, also predominantly for wound infections (Table 3). In nine patients, infections were caused by Methicillin-resistant *Staphylococcus aureus* (MRSA), with three of them also showing growth of other organisms, such as *Klebsiella*, *Pseudomonas*, and *Enterobacter*. The rest of the patients had non-MRSA growth. Additionally, eighteen patients (11.25%) required re-exploration on the first post-operative day, primarily due to venous insufficiency, but there were no flap failures. Overall, complications were more frequent and more severe in the early period. The overall complication rate at the primary site during the 0–90-day period was 46.8% (75 patients), of which 93.4% were grade III (Table 3).

Morbidity at the Donor Site

Donor site complications occurred in 52 patients (32.5%) during the initial 30 days, decreasing to 21 patients (13.8%) in the 31–90-day period. Wound infection was the most common complication at the donor site during both the 0–30-day and 31–90-day postoperative periods (Table 4). Five patients had multiple complications, including a combination of infection, seroma, and necrosis. Only 8 (5%) patients required readmission in the 0–30 days, and 6 (3.7%) patients required readmission in the 31–90 days for donor-related complications. Infection with MRSA was the most common reason for readmission in both periods. The overall complication rate was 36.8% (59 patients) during the 0–90-day period; 86.4% were grade III (Table 3).

Univariate Analysis

The factors analysed included age, BMI, obesity, presence of diabetes mellitus, other comorbidities, type of chemotherapy regimen, and reconstruction technique. Patients older than 37 had significantly higher odds of primary site complications (OR = 2.22, p = 0.014) compared with younger patients. Higher BMI ≥25 (OR = 2.06, p = 0.025), presence of diabetes alone (OR = 3.05, p = 0.046) or multiple comorbidities (OR = 3.67, p = 0.018) or any comorbidity (OR=2.48, p=0.015) was associated with increased

Table 2. Morbidity at primary site

Clavien-Dindo grade*	Wound infection		Necrosis		Seroma	
	0–30 d (n, %)	31–90 d (n, %)	0–30 d (n, %)	31–90 d (n, %)	0–30 d (n, %)	31–90 d (n, %)
Grade I	3 (5.7)	1 (4.2)	2 (8.7)	1 (25)	4 (25)	0 (0)
Grade II	3 (5.7)	3 (12.5)	1 (4.35)	0 (0)	0 (0)	0 (0)
Grade IIIa	38 (71.7)	15 (62.5)	15 (65.2)	3 (75)	10 (62.5)	2 (100)
Grade IIIb	8 (15)	5 (20.8)	4 (17.4)	0 (0)	2 (12.5)	0 (0)
Grade IV	1 (1.9)	0 (0)	1 (4.35)	0 (0)	0 (0)	0 (0)
Total cases	**53 (100)**	**24 (100)**	**23 (100)**	**4 (100)**	**16 (100)**	**2 (100)**

*Includes patients with multiple conditions such as wound infection, necrosis, seroma reported as per worst grade

complications. Non-DIEP reconstruction was associated with a lower OR for developing complications (OR = 0.32, $p = 0.025$). For donor site, higher BMI ≥25 was significantly associated with increased complication rate (OR = 2.56, $p = 0.005$) and non-DIEP reconstructions had lower OR for complication rate (OR = 0.25, $p = 0.017$). Age >37, the presence of multiple comorbidities or any comorbidity, and NACT were associated with an increased risk of complications, but the associations were not statistically significant (Table 5 and Table 6).

Multivariate Analysis

At the primary site, the presence of multiple comorbidities and DIEP reconstruction were significantly associated with higher complication rates on multivariate analysis. At the donor site, higher BMI and DIEP reconstruction were significantly associated with higher complication rates (Table 5 and Table 6). As DIEP flaps constituted the majority of reconstructions (85%), the non-DIEP comparison group was relatively small and heterogeneous, which may limit the robustness of technique-based comparisons.

Table 3. Breast and donor site complications 0–90 days

Complications	Breast (N–75)*	Donor site (N–59)*
Wound infection	68 (42.4%)	69 (43.1%)
Seroma	18 (11.3%)	-
Necrosis	22 (13.75%)	2 (1.2%)
Hematoma	-	2 (1.2%)
Clavien-Dindo grading#		
Grade I	1 (1.3%)	2 (2.7%)
Grade II	4 (5.3%)	6 (8%)
Grade IIIa	59 (78.7%)	44 (58.7%)
Grade IIIb	11 (14.7%)	7 (9.3%)
Grade IV	1 (1.3%)	1 (1.6%)
Re-exploration day 1	18 (11.25%)	2 (1.2%)
Re-admission		
0–30 days	10 (6.25%)	8 (5%)
31–90 days	8 (5%)	6 (3.7%)

*Due to the occurrence of multiple complications in some patients, the total number of complications do not sum up to the total number of patients.

#: For patients with multiple complications, a higher Clavien-Dindo grade is assigned based on the most severe complication

Discussion and Conclusion

Despite the well-recognized benefits of breast reconstruction, uptake remains low in India and similar LMIC settings. A previous study from our institution reported an acceptance rate of only 27% and showed that the interest of patients in delayed reconstruction was low (2). A Central India survey of 192 patients found that none opted for post-mastectomy reconstruction over two years, preferring to avoid additional surgery despite its psychological benefits (4). Additionally, considering limited resources, expertise, and costs, there was a preference for immediate autologous reconstruction over implant-based reconstruction.

In LMIC contexts, perioperative complications after whole breast reconstruction carry greater implications—disrupting cancer adjuvant treatment schedules, affecting body image, increasing healthcare costs, and potentially straining limited resources. Documentation of complications is, therefore, a critical quality-of-care measure. To our knowledge, this is the only prospective Indian study with a reasonable sample size to evaluate early surgical complications at both flap and donor sites after immediate autologous reconstruction in patients with locally advanced breast cancer receiving multimodality treatment in the form of chemotherapy and radiotherapy and to identify risk factors. Previous Indian studies, both prospective (5) and retrospective (6), had much smaller cohorts and did not analyse risk factors.

In the present study, complications of the reconstructed breast occurred in 46.8% of patients , and donor-site complications occurred in 36.8% of patients, within 90 days. These rates fall within the upper range of those reported in international series of immediate autologous breast reconstruction, in which

Table 4. Morbidity at donor site

Clavien-Dindo grade*	Wound infection		Necrosis		Seroma		Hematoma	
	0–30 d (n, %)	31–90 d (n, %)	0–30 d (n, %)	31–90 d (n, %)	0–30 d (n, %)	31–90 d (n, %)	0–30 d (n, %)	31–90 d (n, %)
Grade I	7 (12.1)	0 (0)	0 (0)	0 (0)	0 (0)	0 (0)	0 (0)	0 (0)
Grade II	6 (10.3)	3 (11.1)	0 (0)	0 (0)	1 (33.3)	0 (0)	0 (0)	0 (0)
Grade IIIa	36 (62.0)	19 (70.4)	1 (50)	0 (0)	2 (66.7)	0 (0)	0 (0)	0 (0)
Grade IIIb	8 (13.8)	5 (18.5)	1 (50)	0 (0)	0 (0)	1 (100)	2 (100)	0 (0)
Grade IV	1 (1.7)	0 (0)	0 (0)	0 (0)	0 (0)	0 (0)	0 (0)	0 (0)
Total cases	**58 (100)**	**27 (100)**	**2 (100)**	**0 (100)**	**3 (100)**	**1 (100)**	**2 (100)**	**0 (100)**

*Combined complications include patients with multiple conditions such as wound infection, necrosis, seroma reported as per worst grade

overall complication rates of approximately 30–40% have been reported (7-9).

Wound infection was the most frequent complication in this study, accounting for the majority of early adverse events. The observed infection rate 42% at primary site, 43% at donor site was higher than that reported in large Western prospective cohorts such as the Mastectomy Reconstruction Outcomes Consortium, where infection rates of approximately 4–10% have been documented (8, 9). This difference is likely multifactorial and may reflect the higher prevalence of obesity and diabetes in our population, the advanced stage of disease requiring more frequent use of NACT, and differences in perioperative and post-discharge wound care practices. Similar associations between metabolic comorbidities and increased infection risk have been consistently reported in prior studies (10-13). The rates of partial flap necrosis and seroma formation observed were comparable to those reported in other microsurgical breast reconstruction series, where minor necrosis and seroma were among the most frequent non-infectious adverse events (7, 14).

Re-exploration was required in 11.2% of patients, most commonly due to venous insufficiency. This rate is comparable to published microsurgical series reporting re-exploration rates between 7% and 12% (14, 15). Beugels et al. (14) reported a lower re-exploration rate of approximately 7% in their retrospective cohort of DIEP flap reconstructions. Emergency re-exploration has been shown to be associated with a higher risk of subsequent

Table 5. Univariate and multivariate analysis for complications at primary site at 0-90 days

Characteristic	n	Event n	Univariate OR* (95% CI*)	*p*-value	Multivariate OR* (95% CI*)	*p*-value
Age						
≤37 (ref)	87	33	-	-	-	-
>37	73	42	**2.22 (1.18–4.22)**	**0.014**	1.93 (1.00–3.80)	0.053
BMI						
<25 (ref)	77	29	-	-	-	-
≥25	83	46	**2.06 (1.10–3.90)**	**0.025**	-	-
Obesity (BMI ≥30)						
No (ref)	137	65	-	-	-	-
Yes	23	10	0.85 (0.34–2.07)	0.724	-	-
Diabetes mellitus						
No (ref)	143	63	-	-	-	-
Yes	17	12	**3.05 (1.07–9.99)**	**0.046**	-	-
Multiple comorbidities						
No (ref)	141	61	-	-	-	-
Yes	19	14	**3.67 (1.33–11.9)**	**0.018**	**3.56 (1.16–12.8)**	**0.035**
Any comorbidity						
No (ref)	119	49	-	-	-	-
Yes	41	26	**2.48 (1.20–5.25)**	**0.015**	-	-
Neoadjuvant chemotherapy received						
No (ref)	20	8	-	-	-	-
Yes	140	67	1.38 (0.54–3.71)	0.511	-	-
Chemotherapy regimen						
Neoadjuvant (ref)	83	42	-	-	-	-
Sandwich	57	25	0.76 (0.39–1.50)	0.433	-	-
Adjuvant	20	8	0.65 (0.23–1.74)	0.396	-	-
Type of reconstruction						
DIEP# (ref)	136	69	-	-	-	-
Other flaps	24	6	**0.32 (0.11–0.82)**	**0.025**	**0.28 (0.09–0.73)**	**0.014**

*OR: Odds ratio; CI: Confidence interval; BMI: Body mass index

#: DIEP: Deep inferior epigastric perforator

Table 6. Univariate and multivariate analysis for complications at donor site at 0-90 days.

Characteristic	n	Event n	Univariate OR* (95% CI*)	*p*-value	Multivariate OR* (95% CI*)	*p*-value
Age						
≤37 (ref)	87	30	-	-	-	-
>37	73	34	1.66 (0.88–3.15)	0.121	-	-
BMI						
<25 (ref)	77	22	-	-	-	-
≥25	83	42	2.56 (1.34–4.99)	**0.005**	2.25 (1.16–4.47)	**0.018**
Obesity (BMI ≥30)						
No (ref)	137	55	-	-	-	-
Yes	23	9	0.96 (0.38–2.34)	0.927	-	-
Diabetes mellitus						
No (ref)	143	54	-	-	-	-
Yes	17	10	2.35 (0.85–6.83)	0.101	-	-
Multiple comorbidities						
No (ref)	141	53	-	-	-	-
Yes	19	11	2.28 (0.87–6.24)	0.096	2.44 (0.88–7.22)	0.092
Any comorbidity						
No (ref)	119	43	-	-	-	-
Yes	41	21	1.86 (0.91–3.83)	0.091	-	-
Neoadjuvant chemotherapy received						
No (ref)	20	6	-	-	-	-
Yes	140	58	1.65 (0.62–4.89)	0.333	-	-
Chemotherapy regimen						
Neoadjuvant (ref)	83	33	-	-	-	-
Sandwich	57	25	1.18 (0.60–2.35)	0.629	-	-
Adjuvant	20	6	0.65 (0.21–1.80)	0.421	-	-
Type of reconstruction						
#DIEP (ref)	136	60	-	-	-	-
Other flaps	24	4	0.25 (0.07–0.71)	**0.017**	0.26 (0.07–0.78)	**0.025**

*OR: Odds ratio; CI: Confidence interval; BMI: Body mass index

#: DIEP: Deep inferior epigastric perforator

postoperative infection, which may partially explain the infection burden observed in our study (16).

Notably, no cases of total flap loss were observed in the present cohort. This finding aligns with contemporary reports demonstrating flap survival rates exceeding 95% in experienced centres (15, 17). The absence of flap loss is particularly reassuring given the high-risk nature of this population, characterized by locally advanced disease and exposure to chemotherapy and radiotherapy. This underscores the importance of meticulous microsurgical technique, close postoperative monitoring, and early intervention when vascular compromise is suspected.

Donor-site morbidity occurred in 36.8% of patients, predominantly due to wound infection and seroma formation. This pattern mirrors finding of multi-institutional studies of abdominally based free flaps, where donor-site complications range from 20–40% and are strongly influenced by BMI and metabolic comorbidities (18-20). Our early donor-site infection rate (8.1% within 30 days) falls within the range reported in contemporary series (20).

Higher BMI and multiple comorbidities emerged as independent predictors of postoperative morbidity in our study. This observation is consistent with a substantial body of literature demonstrating obesity and diabetes as major risk factors for both

recipient- and donor-site complications following autologous breast reconstruction (10-13, 18, 19). Although abundant donor tissue may be technically advantageous in obese patients (12), our data suggest that when BMI exceeds 25 kg/m², the risk of postoperative complications rises significantly. These findings reinforce the importance of incorporating patient-related risk factors into preoperative counselling and shared decision-making.

Chemotherapy sequencing remains an important consideration in LMICs, where high patient volumes and limited operating room availability may lead to unavoidable delays in surgical scheduling. Our study found no increased complication risk with neoadjuvant or adjuvant chemotherapy, aligning with some but not all literature (15, 21, 22).

Compared to Western data, our patient population is younger (mean age 37 *vs.* 47–53 years) (8, 9, 23), with locally advanced disease, has exclusively undergone immediate autologous reconstruction, and presents a different comorbidity profile. In contrast, implant-based reconstruction is the dominant approach in high-income countries (1, 8, 9).

Globally, pooled data suggest that reconstruction increases surgical complications compared with mastectomy alone (24). Our planned matched-pair analysis will compare 90-day morbidity between patients undergoing mastectomy alone and those undergoing mastectomy with reconstruction in India.

Study Limitations

While our prospective single-centre design strengthens the validity of the findings, limitations include a modest sample size and the absence of a mastectomy-only comparator group. Additionally, the association between DIEP reconstruction and higher complication rates should be interpreted cautiously, given the marked predominance of DIEP flaps and the small, heterogeneous non-DIEP subgroup. The observed association may be confounded by factors such as case complexity, higher BMI, and multiple comorbidities. Nonetheless, our results provide valuable region-specific data, informing clinicians and patients about the morbidity profile of immediate autologous breast reconstruction in an Asian LMIC context. The findings highlight the need for individualized patient counselling, optimization of comorbidities, and improved perioperative care pathways-essential for the safe adoption of reconstruction in resource-constrained environments.

Although there was no flap loss or delay in adjuvant therapy, the high overall complication rate highlights the need for a selective, individualized approach, with comprehensive preoperative counselling and shared decision-making. These complication rates should be interpreted in the context of multimodal oncologic treatment, including radiotherapy and chemotherapy. Higher BMI and comorbidities emerged as key predictors of post-operative morbidity, underscoring the importance of careful patient selection. Taken together, these findings support the short-term surgical safety of immediate autologous whole-breast reconstruction in patients with advanced breast cancer who are undergoing multimodal therapy in low- and middle-income settings.

Ethics

Ethics Committee Approval: The study was approved by Tata Memorial Centre Ethics Committee-I (approval number: 1683, date: 12.05.2016) and registered in Clinical Trials Registry-India (CTRI/2017/01/007745)

Informed Consent: All patients were counselled followed by accrual after signing of informed consent form.

Footnotes

Authorship Contributions

Surgical and Medical Practices: M.J., S.S., T.W., R.S., R.P., R.K., S.J., V.S., D.J., S.M., M.M.; Concept: M.J., S.S., T.W., R.S., R.P., R.K., S.J., V.S., D.J., S.M., M.M.; Design: M.J., S.S., T.W., R.S., R.P., R.K., S.J., V.S., D.J., S.M., M.M.; Data Collection or Processing: M.J., S.S., T.W.; Analysis or Interpretation: M.J., S.S., T.W.; Literature Search: M.J., S.S., T.W., S.J.; Writing: M.J., S.S., T.W., S.J., S.M.

Conflict of Interest: No conflict of interest was declared by the authors.

Financial Disclosure: The authors declared that this study received no financial support.

References

1. Albornoz CR, Bach PB, Mehrara BJ, Disa JJ, Pusic AL, McCarthy CM, et al. A paradigm shift in U.S. Breast reconstruction: increasing implant rates. Plast Reconstr Surg. 2013; 131: 15-23. (PMID: 23271515) [Crossref]
2. Nair NS, Penumadu P, Yadav P, Sethi N, Kohli PS, Shankhdhar V, et al. Awareness and acceptability of breast reconstruction among women with breast cancer: a prospective survey. JCO Glob Oncol. 2021; 7: 253-260. (PMID: 33571006) [Crossref]
3. Panhofer P, Ferenc V, Schütz M, Gleiss A, Dubsky P, Jakesz R, et al. Standardization of morbidity assessment in breast cancer surgery using the Clavien Dindo Classification. Int J Surg. 2014; 12: 334-339. (PMID: 24486930) [Crossref]
4. Shrivastava R, Gupta A, Bharath S, Yadav SK, Agarwal P, Sharma D, et al. Unveiling perceptions regarding post mastectomy breast reconstruction: a questionnaire-based survey of patients from central India. World J Surg. 2024; 48: 2058-2063. (PMID: 39019650) [Crossref]
5. Marwah A, Chandrappa AB, Vasudevan S, Rao AYNY, Sreekumar D, Shetty P, et al. Outcomes of deep inferior epigastric artery perforator (DIEP) flap in indian population-a prospective single-institute study. Indian J Plast Surg. 2024; 57: 106-115. (PMID: 38774736) [Crossref]
6. Pai E, Kumar T. Whole breast reconstruction in developing India: a cancer surgeon's experience with the pedicled transverse rectus abdominis (TRAM) flap. Indian J Surg Oncol. 2022; 13: 826-833. (PMID: 36687247) [Crossref]
7. Jimenez RB, Packowski K, Horick N, Rosado N, Chinta S, Koh DJ, et al. The timing of acute and late complications following mastectomy and implant-based reconstruction. Ann Surg. 2023; 278: e203-e208. (PMID: 35837894) [Crossref]

8. Wilkins EG, Hamill JB, Kim HM, Kim JY, Greco RJ, Qi J, et al. Complications in postmastectomy breast reconstruction: one-year outcomes of the mastectomy reconstruction outcomes consortium (MROC) study. Ann Surg. 2018; 267: 164-170. (PMID: 27906762) [Crossref]

9. Balasubramanian I, Harding T, Boland MR, Ryan EJ, Geraghty J, Evoy D, et al. The impact of postoperative wound complications on oncological outcomes following immediate breast reconstruction for breast cancer: a meta-analysis. Clin Breast Cancer. 2021; 21: e377-e387. (PMID: 33451964) [Crossref]

10. Willoughby LI, D'Abbondanza JA, Baltzer HL, Mahoney JL, Musgrave MA. Body mass index impacts infection rates in immediate autogenous breast reconstruction. Breast Cancer Res Treat. 2019; 175: 765-773. (PMID: 30937658) [Crossref]

11. Panayi AC, Agha RA, Sieber BA, Orgill DP. Impact of obesity on outcomes in breast reconstruction: a systematic review and meta-analysis. J Reconstr Microsurg. 2018; 34: 363-375. (PMID: 29510420) [Crossref]

12. Klement KA, Hijjawi JB, LoGiudice JA, Alghoul M, Omesiete-Adejare P. Microsurgical breast reconstruction in the obese: a better option than tissue expander/implant reconstruction? Plast Reconstr Surg. 2019; 144: 539-546. (PMID: 31460996) [Crossref]

13. Escobar-Domingo MJ, Bustos VP, Kim EJ, Campbell T, Fanning JE, Foppiani JA, et al. The impact of metabolic syndrome in breast reconstruction decision-making and postoperative outcomes: a nationwide analysis. J Plast Reconstr Aesthet Surg. 2024; 89: 21-29. (PMID: 38128370) [Crossref]

14. Beugels J, Bod L, van Kuijk SMJ, Qiu SS, Tuinder SMH, Heuts EM, et al. Complications following immediate compared to delayed deep inferior epigastric artery perforator flap breast reconstructions. Breast Cancer Res Treat. 2018; 169: 349-357. (PMID: 29399731) [Crossref]

15. Mehrara BJ, Santoro TD, Arcilla E, Watson JP, Shaw WW, Da Lio AL. Complications after microvascular breast reconstruction: experience with 1195 flaps. Plast Reconstr Surg. 2006; 118: 1100-1109. (PMID: 17016173) [Crossref]

16. Bucataru A, Balasoiu M, Ghenea AE, Zlatian OM, Vulcanescu DD, Horhat FG, et al. Factors contributing to surgical site infections: a comprehensive systematic review of etiology and risk factors. Clin Pract. 2023; 14: 52-68. (PMID: 38248430) [Crossref]

17. Musmann RJ, Andree C, Munder B, Hagouan M, Janku D, Daniels M, et al. Secondary solution for breast reconstruction following total DIEP flap loss: a single-center experience after 3270 DIEP flaps. J Plast Reconstr Aesthet Surg. 2024; 92: 11-25. (PMID: 38489983) [Crossref]

18. Fisher MH, Ohmes LB, Yang JH, Le E, Colakoglu S, French M, et al. Abdominal donor-site complications following autologous breast reconstruction: a multi-institutional multisurgeon study. J Plast Reconstr Aesthet Surg. 2024; 90: 88-94. (PMID: 38364673) [Crossref]

19. Vyas RM, Dickinson BP, Fastekjian JH, Watson JP, DaLio AL, Crisera CA. Risk factors for abdominal donor-site morbidity in free flap breast reconstruction. Plast Reconstr Surg. 2008; 121: 1519-1526. (PMID: 18453973) [Crossref]

20. Huang H, Lu Wang M, Chen Y, Chadab TM, Vernice NA, Otterburn DM. A machine learning approach to predicting donor site complications following DIEP flap harvest. J Reconstr Microsurg. 2024; 40: 70-77. (PMID: 37040876) [Crossref]

21. Warren Peled A, Itakura K, Foster RD, Hamolsky D, Tanaka J, Ewing C, et al. Impact of chemotherapy on postoperative complications after mastectomy and immediate breast reconstruction. Arch Surg. 2010; 145: 880-885. (PMID: 20855759) [Crossref]

22. Song J, Zhang X, Liu Q, Peng J, Liang X, Shen Y, et al. Impact of neoadjuvant chemotherapy on immediate breast reconstruction: a meta-analysis. PLoS One. 2014; 9: e98225. (PMID: 24878776) [Crossref]

23. Santosa KB, Qi J, Kim HM, Hamill JB, Pusic AL, Wilkins EG. Effect of patient age on outcomes in breast reconstruction: results from a multicenter prospective study. J Am Coll Surg. 2016; 223: 745-754. (PMID: 27806906) [Crossref]

24. Zeng CY, Qiu YY, Li JY, Huang JH, Bai XS, Han XL, et al. Locally advanced breast cancer patients should be cautious about the immediate breast reconstruction after mastectomy: a pooling analysis of safety and efficacy. World J Surg Oncol. 2024; 22: 165. (PMID: 38918808) [Crossref]

ORIGINAL ARTICLE

European Journal of BREAST HEALTH

DOI: 10.4274/ejbh.galenos.2026.2025-12-7
Eur J Breast Health 2026;22(3):294-306

Outcomes of Chest Wall Perforator Flaps for Partial Breast Reconstruction: A Single-Center, Single-Surgeon Experience

Waleed Burhamah[1], Unnati Shah[2], Karisma Sharma[3], Caroline Xiangmei[3], Iqbal Javeria[2]

[1]Department of Plastic Surgery, University Hospitals Birmingham NHS Foundation Trusts, Birmingham, United Kingdom
[2]Sandwell and West Birmingham NHS Trusts, Birmingham, United Kingdom
[3]University Hospitals Birmingham NHS Foundation Trusts, Birmingham, United Kingdom

ABSTRACT

Objective: Achieving clear margins in breast-conserving surgery (BCS) can result in significant tissue loss, particularly in women with small breast volumes or large tumours. Oncoplastic BCS aims to ensure an oncologically safe resection with superior cosmetic outcomes. Chest wall perforator flaps (CWPFs) offer a muscle-sparing, volume-replacement option in BCS. This study reports a single-centre, single-surgeon experience using CWPFs for partial breast reconstruction.

Materials and Methods: A retrospective cohort study was conducted, including all women who underwent wide local excision followed by reconstruction with a CWPF between 2023 and 2025. Demographic, tumour, treatment, and outcome variables were collected from electronic records.

Results: Fifty-five patients (median age 52) underwent CWPF reconstruction, most commonly with lateral intercostal artery perforator flaps (n = 48, 87.3%). Two (n = 2, 3.6%) patients had wound breakdown postoperatively, requiring return to theatre for re-suturing. Our margin re-excision rate was 9.1% (n = 5), and 3.6% of patients (n = 2) required completion mastectomy because final histology identified more extensive disease than preoperative imaging had indicated. No partial or complete flap losses were observed. Two patients (n = 2, 3.6%) required secondary lipofilling sessions for aesthetic purposes.

Conclusion: CWPFs are a reliable, safe, and aesthetically favourable option for partial breast reconstruction, particularly in women with small to moderate breast volumes and minimal ptosis. Rates of complications, flap loss, and re-excision were low and comparable to those reported in the existing literature. Further prospective multi-centre studies that include patient-reported outcomes are warranted to assess long-term satisfaction.

Keywords: Breast reconstruction; breast conserving surgery; oncoplastic breast surgery; chest wall perforator flaps

Corresponding Author: Waleed Burhamah MB BCh BAO (NUI, RCSI) (Hons) MRCS;
E-mail: waleedburhamah1994@gmail.com **ORCID:** orcid.org/0000-0001-7707-2043

Received: 24.12.2025 **Accepted:** 08.03.2026 **Available Online Date:** 17.06.2026
Cite this article as: Burhamah W, Shah U, Sharma K, Xiangmei C, Javeria I. Outcomes of chest wall perforator flaps for partial breast reconstruction: a single-center, single-surgeon experience. Eur J Breast Health. 2026;22(3):294-306

KEY POINTS

- Chest wall perforator flaps (CWPFs) are an oncologically safe and an aesthetically favourable option for partial breast reconstruction.
- In women with small-to-moderate breast volumes and minimal ptosis, we report low complication rates.
- Most complications are managed non-operatively.
- The use of CWPF can avoid symmetrizing surgery.

Introduction

Achieving oncologically safe margins in breast cancer surgery often necessitates the removal of a considerable volume of breast tissue, which can lead to postoperative deformities, particularly in women with small breasts or large tumours. Breast-conserving surgery (BCS) has become the standard approach for early-stage breast cancer, aiming to maintain breast aesthetics while ensuring comparable oncological safety to mastectomy, especially when combined with adjuvant radiotherapy (1-3).

The advent of oncoplastic BCS (OPBCS) has expanded the potential for breast preservation following wide local excision. By integrating plastic surgical principles, OPBCS allows for improved cosmetic outcomes without compromising oncological safety (3-10). These procedures can be broadly categorized into volume displacement techniques, such as therapeutic mammoplasty, and volume replacement techniques utilizing local or regional autologous tissue flaps (6).

In patients with small breast volumes, excision of more than 20% of breast tissue often results in unsatisfactory cosmetic outcomes, making volume displacement techniques less suitable. In such cases, volume replacement approaches offer distinct advantages by restoring the breast's contour and volume while minimizing the need for contralateral symmetrizing procedures (10, 11). One effective strategy involves the use of chest wall perforator flaps (CWPFs). Their use is secondary to advances in understanding of the chest wall vascular anatomy; this has facilitated the development of several muscle-sparing reconstructive options based on perforator vessels. First described by Hamdi et al. (12), CWPFs are fascio-adipo-cutaneous pedicled flaps that preserve muscle integrity while providing reliable tissue coverage. Variants of CWPFs now include the thoracodorsal artery perforator (TDAP), lateral intercostal artery perforator (LICAP), lateral thoracic artery perforator (LTAP), anterior intercostal artery perforator (AICAP), and medial intercostal artery perforator (MICAP) flaps (9, 12, 13).

This is a single-centre, single-surgeon experience which aims to report outcomes of CWPFs in partial breast reconstruction, contributing to the current literature by extending our understanding of the utility, safety, and efficacy of CWPFs in breast-conserving surgery.

Materials and Methods

Study Design, Participants and Data Collection

This single-centre, retrospective cohort study included all women who underwent surgery for breast cancer, involving a wide local excision followed by breast reconstruction using a CWPF, performed by a single surgeon between 2023 and 2025. Patient details were retrieved from the hospital electronic patient record system, and relevant clinical data were extracted from clinic letters, operation notes, radiology and histology reports, and multidisciplinary team outcomes. This study is exempt from ethical approval due to the observational retrospective nature of the study design.

The study is registered with the hospital's Clinical Effectiveness Team (ID 3392).

The collected variables included patient demographics [age, smoking status, medical comorbidities, body mass index (BMI), bra size, cup size, presence or absence of ptosis], tumour factors [laterality, location, focality, histology, radiological dimensions, estrogen receptor (ER), progesterone receptor (PR), and human epidermal growth factor receptor 2 (HER2) status], treatment factors (type of flap, neoadjuvant and/or adjuvant treatment, lymph node procedures, gross tumour size, use of intra-operative drains), and, finally, outcome measures (complications, return to theatre, completion mastectomy rates, need for margin re-excision, and recurrence). Patients were followed up in a consultant-led clinic after the procedure; furthermore, our oncological surveillance is in line with the current follow-up policy set by the UK National Health Service. Patients receive annual bilateral mammograms for at least the first five years, followed by reversion to the 3-yearly National Health Screening programme for women aged 50–70.

Surgical Technique

All operations were performed by a single oncoplastic breast consultant surgeon. Chest wall perforator vessels were identified using a handheld Doppler device preoperatively. Cases were either performed as a single-stage procedure following wide local excision (Table 1) or performed following a previous wide local excision (WLE) necessitating further margin re-excision and reconstruction with CWPF (Table

Table 1. Summarizes baseline demographics and clinical characteristics by flap type. Continuous variables are summarised as median (IQR), and categorical variables are summarised as n (%)

Variable	Group	Total (*n* = 55)	LICAP (*n* = 48)	AICAP (*n* = 2)	MICAP (*n* = 3)	LTAP (*n* = 2)	*p*-value
Presentation	Symptomatic	29 (52.7%)	25 (52.1%)	1 (50.0%)	1 (33.3%)	2 (100.0%)	0.939
	Screening	26 (47.3%)	23 (10.4%)	1 (50.0%)	2 (66.7%)	0 (0.0%)	0.939
Age [median (IQR)]		52.0 (45.5, 58.0)	52.0 (45.0, 58.0)	59.5 (55.8, 63.2)	57.0 (52.0, 59.5)	43.5 (41.2, 45.8)	0.317
BMI kg/m^2 [median (IQR)]		27.2 (24.6, 32.2)	28.0 (24.5, 32.5)	29.7 (27.4, 32.0)	26.6 (24.9, 29.1)	25.0 (24.9, 25.1)	0.722
Comorbidities	Yes	21 (38.2%)	19 (39.6%)	2 (100.0%)	0 (0.0%)	0 (0.0%)	0.095
	No	34 (61.8%)	29 (60.4%)	0 (0.0%)	3 (100.0%)	2 (100.0%)	
Smoking	Yes	6 (10.9 %)	6 (12.5%)	0 (0.0%)	0 (0.0%)	0 (0.0%)	0
	No	49 (89.1 %)	42 (87.5%)	2 (100.0%)	3 (100.0%)	2 (100.0%)	
Bra size [median (IQR)]		36.0 (34.0, 38.0)	36.0 (34.0, 38.0)	37.0 (36.5, 37.5)	34.0 (34.0, 35.0)	34.0 (34.0, 34.0)	0.302
Cup size	A	2 (3.6%)	2 (4.2%)	0 (0.0%)	0 (0.0%)	0 (0.0%)	0.954
	B	12 (21.8%)	9 (18.8%)	1 (50.0%)	2 (66.7%)	0 (0.0%)	
	C	17 (30.9%)	17 (31.3%)	0 (0.0%)	0 (0.0%)	0 (0.0%)	
	D	17 (31%)	14 (33.2%)	1 (50.0%)	0 (0.0%)	2 (100.0%)	
	DD	4 (7.3%)	3 (6.2%)	0 (0.0%)	1 (33.3%)	0 (0.0%)	
	E	1 (1.8%)	1 (2.1%)	0 (0.0%)	0 (0.0%)	0 (0.0%)	
	F	1 (1.8%)	1 (2.1%)	0 (0.0%)	0 (0.0%)	0 (0.0%)	
	G	1 (1.8%)	1 (2.1%)	0 (0.0%)	0 (0.0%)	0 (0.0%)	
Ptosis	No	23 (41.8%)	20 (41.7%)	1 (50.0%)	2 (66.7%)	0 (0.0%)	0.292
	1	24 (43.6%)	20 (41.7%)	1 (50.0%)	1 (33.3%)	2 (100.0%)	
	2	5 (9.1%)	5 (10.4%)	0 (0.0%)	0 (0.0%)	0 (0.0%)	
	3	3 (5.5%)	3 (6.2%)	0 (0.0%)	0 (0.0%)	0 (0.0%)	
Tumour factors							
Side	Left	29 (52.7%)	25 (52.1%)	1 (50.0%)	2 (66.7%)	1 (50.0%)	0.968
	Right	26 (47.3%)	23 (47.9%)	1 (50.0%)	1 (33.3%)	1 (50.0%)	
Histology	NST	32 (58.2%)	28 (58.3%)	1 (50.0%)	2 (66.7%)	1 (50.0%)	0.002
	IDC	8 (14.5%)	7 (14.6%)	1 (50.0%)	0 (0.0%)	0 (0.0%)	
	LGDCIS	3 (5.5%)	3 (6.2%)	0 (0.0%)	0 (0.0%)	0 (0.0%)	
	ILC	8 (14.5%)	8 (16.7%)	0 (0.0%)	0 (0.0%)	0 (0.0%)	
	HGDCIS	3 (5.5%)	2 (4.2%)	0 (0.0%)	1 (33.3%)	0 (0.0%)	
	LCIS	1 (1.8%)	0 (0.0%)	0 (0.0%)	0 (0.0%)	1 (50.0%)	
Focality	Multifocal	22 (40.0%)	20 (41.7%)	1 (50.0%)	0 (0.0%)	1 (50.0%)	0.873
	Unifocal	33 (60.0%)	28 (58.3%)	1 (50.0%)	3 (100.0%)	1 (50.0%)	
Quadrant	UOQ	45 (81.8%)	42 (87.5%)	1 (50.0%)	0 (0.0%)	2 (100.0%)	0
	LOQ	5 (9.1%)	5 (10.4%)	0 (0.0%)	0 (0.0%)	0 (0.0%)	
	LIQ	5 (9.1%)	1 (2.1%)	1 (50.0%)	3 (100.0%)	0 (0.0%)	
	UIQ	0 (0.0%)	0 (0.0%)	0 (0.0%)	0 (0.0%)	0 (0.0%)	
Radiological dimensions (mm) [median (IQR)]		25.0 (22.0, 33.5)	25.5 (22.0, 32.8)	25.0 (25.0, 25.0)	18.0 (14.5, 27.0)	38.0 (33.0, 43.0)	0.465
Tumour size (mm) [median (IQR)]		33.0 (24.0, 50.5)	31.5 (24.0, 50.2)	35.0 (27.5, 42.5)	38.0 (19.0, 42.0)	58.0 (57.0, 59.0)	0.3

Table 1. continued

Variable	Group	Total (n = 55)	LICAP (n = 48)	AICAP (n = 2)	MICAP (n = 3)	LTAP (n = 2)	p-value
Specimen weight (g) [median (IQR)]		63.0 (34.6, 105.0)	63.4 (35.2, 100.5)	105.5 (70.2, 140.8)	27.7 (25.4, 48.9)	97.5 (69.7, 125.2)	0.513
ER	Yes	50 (90.9%)	44 (91.7%)	2 (100.0%)	2 (66.7%)	2 (100.0%)	0.463
	No	5 (9.1%)	4 (8.3%)	0 (0.0%)	1 (33.3%)	0 (0.0%)	
PR	Yes	50 (90.9%)	44 (91.7%)	2 (100.0%)	2 (66.7%)	2 (100.0%)	0.463
	No	5 (9.1%)	4 (8.3%)	0 (0.0%)	1 (33.3%)	0 (0.0%)	
HER2	No	48 (87.3%)	41 (85.4%)	2 (100.0%)	3 (100.0%)	2 (100.0%)	0.76
	Yes	7 (12.7%)	7 (14.6%)	0 (0.0%)	0 (0.0%)	0 (0.0%)	
Treatment factors							
Primary *vs.* secondary flap	Primary flap	50 (90.9%)	44 (91.7%)	2 (100.0%)	2 (66.7%)	2 (100.0%)	0.463
	Secondary flap	5 (9.1%)	4 (8.3%)	0 (0.0%)	1 (33.3%)	0 (0.0%)	
NACT	No	50 (90.9%)	43 (89.6%)	2 (100.0%)	3 (100.0%)	2 (100.0%)	0.849
	Yes	5 (9.1%)	5 (10.4%)	0 (0.0%)	0 (0.0%)	0 (0.0%)	
Primary node surgery	SLNB	36 (65.4%)	31 (64.6%)	2 (100.0%)	2 (66.7%)	1 (50.0%)	0.626
	ANC	16 (29.1%)	15 (31.2%)	0 (0.0%)	0 (0.0%)	1 (50.0%)	
	None	3 (5.5%)	2 (4.2%)	0 (0.0%)	1 (33.3%)	0 (0.0%)	
Radiotherapy	Yes	49 (89.1%)	43 (89.6%)	1 (50.0%)	3 (100.0%)	2 (100.0%)	0.288
	No	6 (10.9%)	5 (10.4%)	1 (50.0%)	0 (0.0%)	0 (0.0%)	
Chemotherapy	No	46 (83.6%)	40 (83.3%)	2 (100.0%)	3 (100.0%)	1 (50.0%)	0.451
	Yes	9 (16.4%)	8 (16.7%)	0 (0.0%)	0 (0.0%)	1 (50.0%)	
ET	Yes	46 (83.6%)	40 (83.3%)	2 (100.0%)	2 (66.7%)	2 (100.0%)	0.702
	No	9 (16.4%)	8 (16.7%)	0 (0.0%)	1 (33.3%)	0 (0.0%)	
Drain	No	51 (92.7%)	44 (91.7%)	2 (100.0%)	3 (100.0%)	2 (100.0%)	0.89
	Yes	4 (7.3%)	4 (8.3%)	0 (0.0%)	0 (0.0%)	0 (0.0%)	
Secondary nodal surgery	ANC	4 (7.3%)	4 (8.3%)	0 (0.0%)	0 (0.0%)	0 (0.0%)	1
Outcomes							
Margin re-excision	No	50 (90.9%)	44 (91.7%)	2 (100.0%)	2 (66.7%)	2 (100.0%)	0.63
	Yes	5 (9.1%)	4 (8.3%)	0 (0.0%)	1 (33.3%)	0 (0.0%)	
Completion mastectomy	No	53 (96.4 %)	47 (97.9 %)	2 (100.0%)	3 (100.0%)	1 (50.0%)	0.118
	Yes	2 (3.6%)	1 (2.1 %)	0 (0.0%)	0 (0.0%)	1 (50.0%)	
Complications	No	46 (83.6%)	41 (85.4%)	2 (100.0%)	1 (33.3%)	2 (100.0%)	0.092
	Yes	9 (16.4%)	7 (14.6%)	0 (0.0%)	2 (66.7%)	0 (0.0%)	
Follow-up duration (days) (median IQR)		569.0 (264.5–1018.0)	591.5 (354.2–1021.0)	1001.5 (788.8–1214.2)	373.0 (299.5–719.5)	96.0 (80.0–112.0)	0.075
Recurrence	No	55 (100%)					
	Yes	0 (0%)					

NST: No special type; IDC: Invasive ductal carcinoma; LGDCIS: Low-grade ductal carcinoma *in-situ*; ILC: Invasive lobular carcinoma; HGDCIS: High-grade ductal carcinoma *in-situ*; LCIS: Lobular carcinoma in-situ; UOQ: Upper outer quadrant; LOQ: Lower outer quadrant; LIQ: Lower inner quadrant; UIQ: Upper inner quadrant; ER: Estrogen receptor; PR: Progesterone receptor; HER2: Human epidermal growth factor 2 receptor; NACT: Neo-adjuvant chemotherapy; SLNB: Sentinel lymph node biopsy; ANC: Axillary node clearance; ET: Endocrine treatment; LICAP: Lateral intercostal artery perforator; AICAP: Anterior intercostal artery perforator; MICAP: Medial intercostal artery perforator; LTAP: Lateral thoracic artery perforator; IQR: Interquartile range

1). The CWPFs are raised as a turnover flap (folded 180°), a pendulum type flap based on longer pedicles (TDAP/LTAP) or as a propeller flap to reconstruct the tumour excision defect. A drain was used according to individual intraoperative circumstances. We followed the UK Association of Breast Surgery consensus for adopting and accepting a 1 mm tumour resection margin for invasive disease and 2 mm for ductal carcinoma *in situ* (DCIS) (14).

Statistical Analysis

Data analysis was conducted using Python (version 3.14) and the pandas, numpy, and scipystats modules. Continuous variables, including age, BMI, specimen weight, radiological dimensions, tumour size, and duration of follow-up, were evaluated for normality using visual inspection and summary statistics. Because the data were not normally distributed, findings were presented as median and interquartile range, and comparisons between groups were performed using the Kruskal-Wallis test or the Mann-Whitney U test, as appropriate. Categorical characteristics (e.g., smoking status, tumour quadrant, flap type, primary versus secondary surgery, complete mastectomy, and complications) were reported as frequencies and percentages. Relationships between categorical variables were assessed using the chi-square test or Fisher's exact test when expected cell counts were below 5.

All tests were two-tailed, and a p-value <0.05 was considered statistically significant. Data were summarized in tabular form, showing group comparisons (overall and stratified by completion mastectomy, margin re-excision, and complications).

Patient-Reported Outcome Measures (PROMS)-Patient Reported Outcome Measures

As part of our routine follow up, to assess patient satisfaction the Breast-Q PROM proforma is used in our practice. For the sake of simplicity and to maintain compliance, we collected information on the following parameters: pre- and post-operative satisfaction with the breasts, sexual well-being, and psychosocial well-being. Currently, there are no validated PROMs specifically for partial breast reconstruction with CWPF. During harvesting of CWPFs, the scar extends to the back. Therefore, we also included the domain assessing satisfaction with the back, which was originally designed for patients undergoing latissimus dorsi (LD) reconstruction. As we are evaluating the procedure performed by a single surgeon, we also included domains assessing satisfaction with information provided by the breast surgeon and with the surgeon's performance to enhance the study's relevance.

Results

Patient Demographics and Tumour Factors

A total of $n = 55$ patients underwent partial breast reconstruction with CWPF; the median age was 52.0 (45.5–58). Of these, $n = 6$ (10.9%) were smokers, and $n = 21$ (38.2%) had medical comorbidities, namely hypertension ($n = 8$), hypothyroidism ($n = 4$), rheumatological conditions ($n = 3$), asthma ($n = 3$), mental health conditions ($n = 3$), diabetes ($n = 2$), and inflammatory bowel disease ($n = 1$).

The median BMI was 27.2 kg/m^2 (24.6–32.2); the most common cup sizes were C ($n = 17$, 30.9%) and D ($n = 17$, 30.9%), while larger cup sizes (DD, E, F, G) collectively made up $n = 7$ (12.7%) of the patient cohort. Most patients had no ptosis or grade 1 ptosis ($n = 47$, 85.4%).

Most tumours were left-sided ($n = 29$, 52.7%), unifocal ($n = 33$, 60%), and located in the upper outer quadrant (UOQ) ($n = 45$, 81.8%). The most common histological type was no special type ($n = 32$, 58.2%), followed equally by invasive ductal carcinoma ($n = 8$, 14.5%) and invasive lobular carcinoma ($n = 8$, 14.5%), while only $n = 6$ (11%) patients had DCIS. Most cases ($n = 50$, 90.9%) were PR+ and ER+, while only $n = 7$ (12.7%) were HER2+ (Table 1).

Treatment Factors

The most common flap performed was the LICAP ($n = 48$, 87.3%), with only $n = 3$ (5.5%) MICAP, $n = 2$ (3.6%) LTAP and $n = 2$ (3.6%) AICAP with only $n = 4/55$ (7.3%) receiving a drain. Most flaps were performed as a primary single stage procedure $n = 50$ (90.1%), while only $n = 5$ (9.1%) were performed following a previous WLE and positive margin cavity shaves.

Most patients ($n = 36$, 65.4%) underwent simultaneous sentinel lymph node biopsy, and $n = 16$ (29.1%) received an axillary node clearance during the flap reconstruction procedure. Most patients ($n = 49$, 89.1%) received radiotherapy, and endocrine treatment was received by $n = 46$ (83.6%); only $n = 9$ (16.4%) received chemotherapy (Table 1).

Outcomes Measures

Of the patient cohort, $n = 9$ (16.4%) developed complications; $n = 4$ (7.3%) were wound breakdowns, of which $n = 2$ (3.6%) required return to theatre for wound re-suturing. Three patients ($n = 3$; 5.5%) developed a surgical site infection requiring antibiotics, and $n = 2$ (3.6%) developed a seroma that was managed non-operatively. The rate of partial and complete flap loss is 0% ($n = 0$). Two patients ($n = 2$, 3.6%) required subsequent lipo-filling procedures for aesthetic purposes. Our median follow-up duration was 569 days (264.5–1018). Five patients ($n = 5$, 9.1%) required a margin re-excision, and ($n = 2$, 3.6%) required a

Table 2. Summarizes patient demographics among those who developed complications

Variable	Group	Overall (*n* = 55)	Complications: yes (*n* = 9)	No (*n* = 46)	*p*-value
Presentation	Symptomatic	29 (52.7%)	5 (55.6%)	24 (52.2%)	1
	Screen	26 (47.3%)	4 (44.4%)	22 (47.8%)	
Age [median (IQR)]		52.0 (45.5, 58.0)	48.0 (41.0, 57.0)	52.0 (46.0, 58.0)	0.284
BMI kg/m^2 [median (IQR)]		27.2 (24.6, 32.2)	27.2 (26.6, 32.4)	27.4 (24.4, 31.9)	0.393
Comorbidities	Yes	21 (38.2%)	2 (22.2%)	19 (41.3%)	0.457
	No	34 (61.8%)	7 (77.8%)	27 (58.7%)	
Smoking	Yes	6 (10.9%)	1 (11.1%)	5 (10.9%)	<0.001
	No	49 (89.1%)	8 (88.9%)	41 (89.1)	
Bra size [median (IQR)]		36.0 (34.0, 38.0)	36.0 (36.0, 38.0)	36.0 (34.0, 38.0)	0.487
Cup size	A	2 (3.6%)	0 (0.0%)	2 (4.3%)	0.459
	B	12 (21.8%)	1 (11.1%)	11 (23.9%)	
	C	17 (30.9%)	3 (33.3%)	14 (30.4%)	
	D	17 (30.9%)	3 (33.3%)	14 (30.4%)	
	DD	4 (7.3%)	1 (11.1%)	3 (6.5%)	
	E	1 (1.8%)	0 (0.0%)	1 (2.2%)	
	F	1 (1.8%)	1 (11.1%)	0 (0.0%)	
	G	1 (1.8%)	0 (0.0%)	1 (2.2%)	
Ptosis	No	23 (41.8%)	1 (11.1%)	22 (47.8%)	<0.001
	1	24 (43.6%)	5 (55.6%)	19 (41.3%)	
	2	5 (9.1%)	0 (0.0%)	5 (10.9%)	
	3	3 (5.5%)	3 (33.3%)	0 (0.0%)	
Tumour factors					
Side	Left	29 (52.7%)	4 (44.4%)	25 (54.3%)	0.721
	Right	26 (47.3%)	5 (55.6%)	21 (45.7%)	
Histology	NST	32 (58.2%)	7 (77.8%)	25 (54.3%)	0.582
	IDC	8 (14.5%)	1 (11.1%)	7 (15.2%)	
	LGDCIS	3 (5.5%)	0 (0.0%)	3 (6.5%)	
	ILC	8 (14.5%)	0 (0.0%)	8 (17.4%)	
	HGDCIS	3 (5.5%)	1 (11.1%)	2 (4.3%)	
	LCIS	1 (1.8%)	0 (0.0%)	1 (2.2%)	
Focality	Multifocal	22 (40.0%)	3 (33.3%)	19 (41.3%)	0.727
	Unifocal	33 (60.0%)	6 (66.7%)	27 (58.7%)	
Quadrant	UOQ	45 (81.8%)	6 (66.7%)	39 (84.8%)	<0.001
	LOQ	5 (9.1%)	1 (11.1%)	4 (8.7%)	
	LIQ	5 (9.1%)	2 (22.2%)	3 (6.5%)	
	UIQ	0 (0.0%)	0 (0.0%)	0 (0.0%)	
Radiological dimensions (mm) [median (IQR)]		25.0 (22.0, 33.5)	30.0 (24.0, 31.0)	25.0 (22.0, 34.2)	0.749
Tumour size (mm) [median (IQR)]		33.0 (24.0, 50.5)	41.0 (28.0, 52.0)	31.5 (24.0, 50.0)	0.569
Specimen weight (g) [median (IQR)]		63.0 (34.6, 105.0)	114.0 (47.0, 186.0)	56.5 (34.4, 84.9)	0.099
ER	Yes	50 (90.9%)	9 (100.0%)	41 (89.1%)	0.578
	No	5 (9.1%)	0 (0.0%)	5 (10.9%)	

Table 2. continued

Variable	Group	Overall (*n* = 55)	Complications: yes (*n* = 9)	No (*n* = 46)	*p*-value
PR	Yes	50 (90.9%)	9 (100.0%)	41 (89.1%)	0.578
	No	5 (9.1%)	0 (0.0%)	5 (10.9%)	
HER2	No	48 (87.3%)	8 (88.9%)	40 (87.0%)	1
	Yes	7 (12.7%)	1 (11.1%)	6 (13.0%)	
Treatment factors					
Primary *vs*. secondary flap	Primary flap	50 (90.9%)	8 (88.9%)	42 (91.3%)	<0.001
	Secondary flap	5 (9.1%)	1 (11.1%)	4 (8.7%)	
NACT	No	50 (90.9%)	8 (88.9%)	42 (91.3%)	1
	Yes	5 (9.1%)	1 (11.1%)	4 (8.7%)	
Flap	AICAP	2 (3.6%)	0 (0.0%)	2 (4.3%)	0.092
	LICAP	48 (87.3%)	7 (77.8%)	41 (89.1%)	
	MICAP	3 (5.5%)	2 (22.2%)	1 (2.2%)	
	LTAP	2 (3.6%)	0 (0.0%)	2 (4.3%)	
Primary node surgery	SLNB	36 (65.4%)	6 (66.7%)	30 (65.2%)	0.834
	ANC	16 (29.1%)	3 (33.3%)	13 (28.3%)	
	None	3 (5.5%)	0 (0.0%)	3 (6.5%)	
Drain	No	51 (92.7%)	7 (77.8%)	44 (95.7%)	0.121
	Yes	4 (7.3%)	2 (22.2%)	2 (4.3%)	
Radiotherapy	Yes	49 (89.1%)	7 (77.8%)	42 (91.3%)	0.251
	No	6 (10.9%)	2 (22.2%)	4 (8.7%)	
Chemotherapy	No	46 (83.6%)	7 (77.8%)	39 (84.8%)	0.631
	Yes	9 (16.4%)	2 (22.2%)	7 (15.2%)	
ET	Yes	46 (83.6%)	7 (77.8%)	39 (84.8%)	0.631
	No	9 (16.4%)	2 (22.2%)	7 (15.2%)	

NST: No special type; IDC: Invasive ductal carcinoma; LGDCIS: Low-grade ductal carcinoma *in-situ*; ILC: Invasive lobular carcinoma; HGDCIS: High-grade ductal carcinoma *in-situ*; LCIS: Lobular carcinoma *in-situ*; UOQ: Upper outer quadrant; LOQ: Lower outer quadrant; LIQ: Lower inner quadrant; UIQ: Upper inner quadrant; ER: Estrogen receptor; PR: Progesterone receptor; HER2: Human epidermal growth factor 2 receptor; NACT: Neo-adjuvant chemotherapy; SLNB: Sentinel lymph node biopsy; ANC: Axillary node clearance; ET: Endocrine treatment; LICAP: Lateral intercostal artery perforator; AICAP: Anterior intercostal artery perforator; MICAP: Medial intercostal artery perforator; LTAP: Lateral thoracic artery perforator; IQR: Interquartile range

Table 3. Summarizes patient-reported outcome measure scores

Breast Q domain	Range	Median
Satisfaction with breasts (preoperative)	64–100	82
Satisfaction with breasts (postoperative)	48–88	72
Satisfaction with back (postoperative)	49–90	74
Psychosocial well being	52–89	71
Sexual well-being	27–66	43 (only 21 patients answered this domain)
Satisfaction with information given by breast surgeon (postoperative)	62–91	80
Satisfaction with surgeon	70–100	86

Figure 1.1 Figure 1.2 Figure 1.3

Figure 1. Figures 1.1 and 1.2 represent clinical photographs of a 29-year-old, non-smoking female with a BMI of 30 kg/m^2 and a bra size of 34C, who underwent a single stage WLE with partial breast reconstruction using an LICAP for a left sided breast tumour with no complications. Figure 1.3 shows images is 3 months post-surgery

LICAP: Lateral intercostal artery perforator; BMI: Body mass index; WLE: Wide local excision

Figure 2.1 Figure 2.2

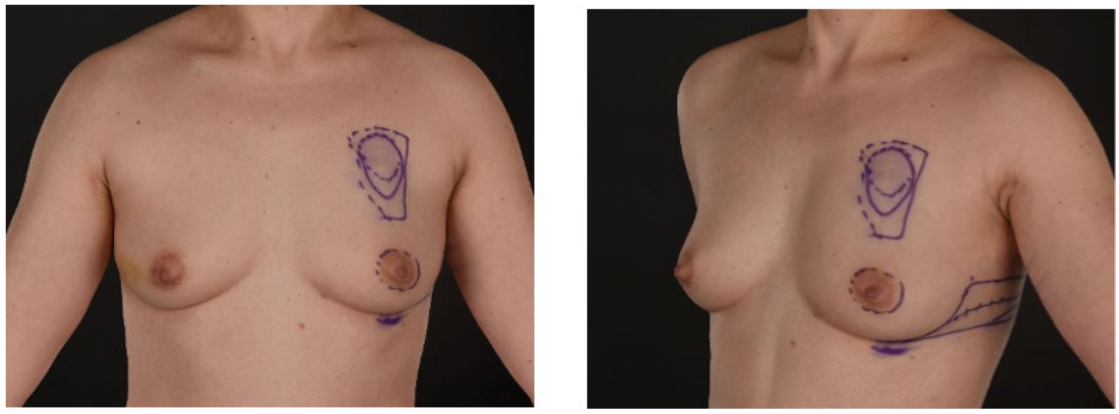

Figure 2.3 Figure 2.4

Figure 2. Figures 2.1 and 2.2 represent clinical photographs of a 34-year-old, non-smoking female with a BMI of 26 kg/m^2 and a bra size of 32B, who underwent a single stage WLE with partial breast reconstruction using an LICAP for a left sided breast tumour with no complications. Figure 2.3 and 2.4 shows images 3 months post-surgery

LICAP: Lateral intercostal artery perforator; BMI: Body mass index; WLE: Wide local excision

Figure 3.1

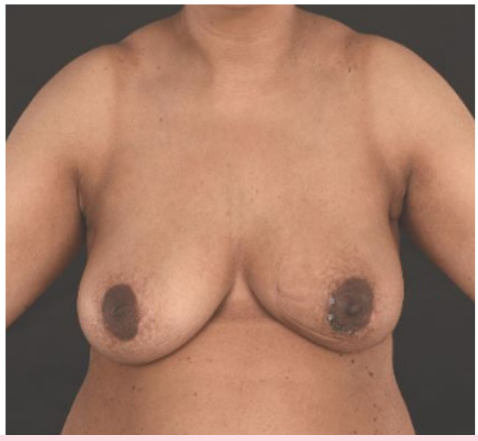

Figure 3.2

Figure 3. Figures 3.1 and 3.2 represent clinical photographs 1-month post-surgery of a 47-year-old non-smoking female with a BMI of 26.6 kg/m^2 and a bra size of 36D who underwent margin re-excision and subsequent MICAP partial breast reconstruction following a previous left sided WLE

MICAP: Medial intercostal artery perforator; BMI: Body mass index; WLE: Wide local excision

completion mastectomy (Tables 1, 2). The results of the PROMs are summarised in Table 3. Figures 1, 2, 3, 4, and 5 show clinical photographs of postoperative results.

Table 2 presents a bivariate analysis comparing patients who developed complications with those who did not. Smoking differed significantly between groups (p<0.001), suggesting a correlation between smoking exposure and the development of complications. Breast ptosis was also significantly associated with post-op complications (p<0.001). Patients with higher grades of ptosis, particularly grade 3 ptosis, were disproportionately represented among those who subsequently developed complications. Additionally, tumour location within the breast demonstrated a similarly significant association with post-op complications (p<0.001); lesions located outside the UOQ were more frequently associated with complications. Lesions in the UOQ were associated with a lower proportion of complications. Despite most patients undergoing a primary reconstruction at the time of tumour excision (n = 50, 90.9%), complications occurred more commonly following primary flap reconstruction compared with secondary procedures (p<0.001)

We have found no statistically significant differences between groups with respect to age, body mass index, comorbidities, cup size, tumour factors such as histology, focality, tumour size, specimen weight, and tumour receptor status (ER, PR, HER2), or neoadjuvant or adjuvant treatment modalities.

Discussion and Conclusion

The LD flap has long been regarded as a reliable option for breast reconstruction, particularly for patients unsuitable for microvascular procedures or those with smaller breasts (15-24). However, its use may be limited by potential complications such as shoulder dysfunction and donor site seroma, with reported incidences varying between 7% and 81% (25-28). In contrast, CWPFs preserve the underlying musculature, thereby reducing donor-site morbidity and maintaining shoulder mobility. These flaps derive their vascular supply from branches of the TDAP, LICAP, LTAP, or AICAP/MICAP (12). As muscle-sparing techniques, CWPFs have demonstrated lower morbidity than myocutaneous LD flaps, with studies reporting no impairment of shoulder function during long-term follow-up (29).

The choice of CWPF depends on the size and anatomical location of the defect following tumour excision. For instance, LTAP flaps—either alone or combined with LICAP flaps—are suitable for lateral, central, lower outer, and upper medial quadrant defects, whereas AICAP and MICAP flaps are more appropriate for lower central and inner quadrant defects (29-31). We have found that most of our reported cases presented with a tumour located in the UOQ, and that the most common flap used was the LICAP alone.

A key advantage of oncoplastic breast surgery using CWPFs is the ability to achieve oncologically safe reconstruction and favourable cosmetic results, often avoiding the need for contralateral symmetrisation procedures, particularly in women with smaller breasts (15, 16). In a large multicentre UK study by Agrawal et al. (17), symmetrisation surgery was required in only 1.2% of cases, with 2.6% undergoing minor revisions such as lipofilling or scar correction. Our findings align with the published literature: none of our patients required symmetrizing

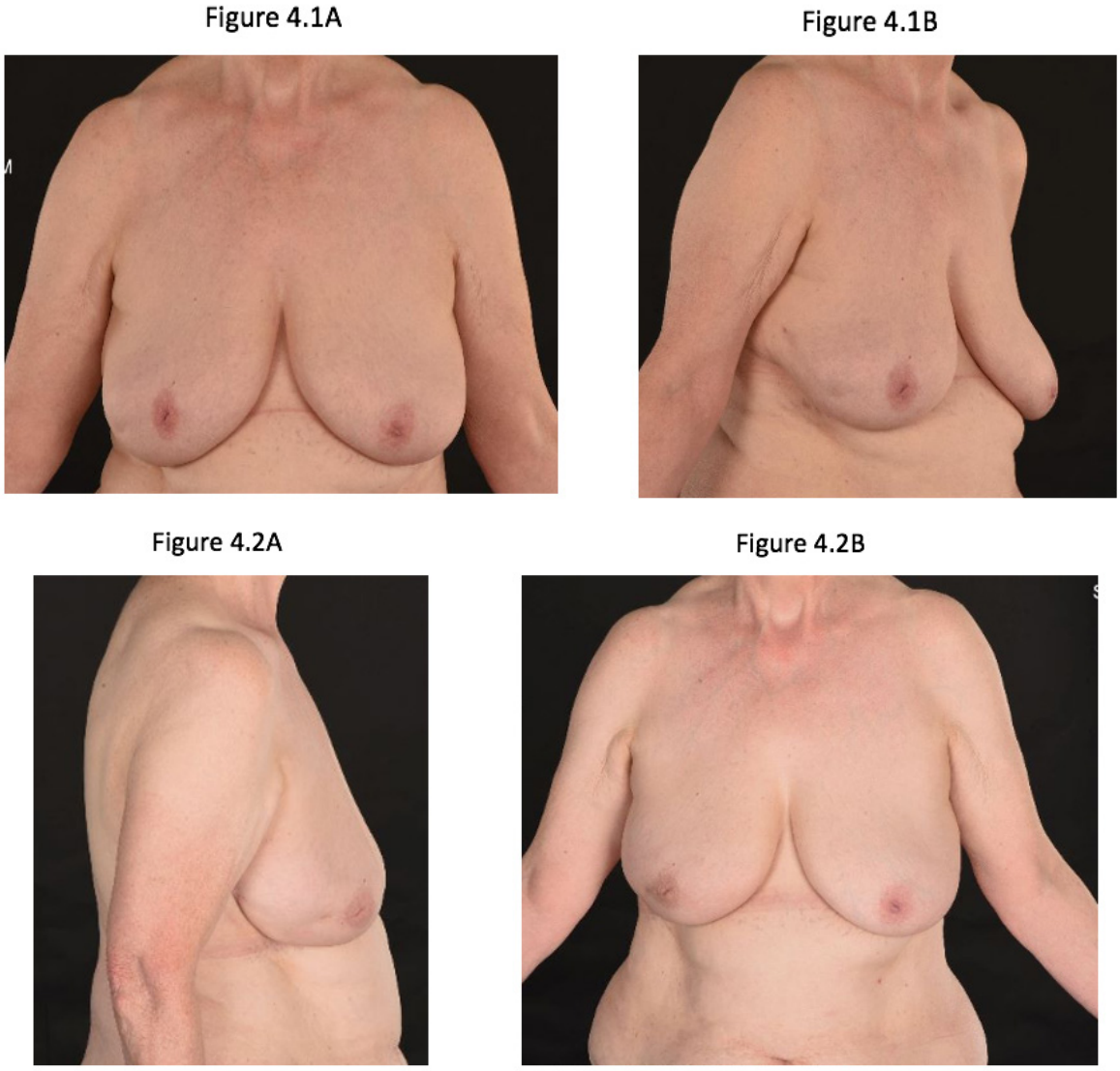

Figure 4. 4.1 A and B: represent pre-operative clinical photographs of a 69-year-old, non-smoking female with a BMI of 28 kg/m^2 and a bra size of 38C, who underwent a single stage WLE with partial breast reconstruction using an LICAP for a right sided breast tumour with no complications. She subsequently received adjuvant radiotherapy. Figures 4.2 A and B show her results 9 months post-surgery having gone through radiotherapy treatment

LICAP: Lateral intercostal artery perforator; BMI: Body mass index; WLE: Wide local excision

breast surgery, and only 2 required further procedures in the form of lipo-filling. Notably, 85.4% of our cohort had no or mild ptosis, which supports the suitability of CWPFs in this cohort.

Although outcome data are frequently reported collectively across different CWPF types, recent systematic reviews have confirmed low complication rates. Nava et al. (30) reported an overall recipient-site complication rate of 13%, a total flap loss rate of 1%, and noted that most complications—including seroma, hematoma, infection, and wound dehiscence—were managed conservatively, with only 20.5% necessitating surgical intervention. Similarly, Pujji et al. (15) documented low rates of total (0.2%) and partial (1.8%) flap necrosis. We report a comparably low rate of complications (16.4%) with only 22.2% of those experiencing complications required a surgical intervention. Additionally the rate of partial and complete flap loss is 0%. One of the common complications of breast surgery is fat necrosis, of which the rates in CWPFs seem to be around 2% in the published literature, which proves the reliability of the chest wall perforator blood supply (30).

Our findings, as represented in Table 2, indicate that smoking, breast ptosis, and tumour location show a significant correlation with the risk of developing complications. Despite the well-

Figure 5. Figure 5.1: Represents a clinical photograph of a 58-year-old, smoking female with a BMI of 32 kg/m^2 and a bra size of 36C, who underwent a single stage WLE with partial breast reconstruction using an LICAP for a right sided breast tumour with no complications. Figures 5.2 and 5.3 shows images 1-month post-surgery

LICAP: Lateral intercostal artery perforator; BMI: Body mass index; WLE: Wide local excision

known effects of smoking on flap survival, we observed a 0% rate of flap necrosis, demonstrating the robust blood supply of CWPFs. However, we found that smoking correlates with complications. In our patient cohort, $n = 9$ (16.4%) developed complications, with $n = 4$ (7.3%) being wound breakdowns, for which smoking is a well-known risk factor. Additionally, patients with higher grades of ptosis, particularly grade 3, were disproportionately represented among those who subsequently developed complications. This further reinforces that the ideal candidates for a CWPF are those with minimal or no ptosis and emphasizes the importance of appropriate patient selection. Although most of our patients had a lesion in the UOQ ($n = 45$, 81.8%), this tumour location was associated with a lower proportion of complications.

From an oncological perspective, CWPFs have demonstrated safety, whereby pooled data from Nava et al. (30) indicated a completion mastectomy rate of 1.5% and a margin re-excision rate of 13%, supporting the oncological soundness of partial breast reconstruction using CWPFs. Although we report a higher rate of completion mastectomies (3.63%), we experience a lower rate of margin re-excision (9.0%).

This study evaluates patient-reported outcomes following BCS with CWPF reconstruction, an area in which PROMs data remain limited. Our results show that postoperative satisfaction with the breasts (median 72) was lower than preoperative scores (median 82), which is expected after oncologic surgery. These values, however, remain comparable to published Breast-Q scores for standard breast-conserving therapy, such as those reported by Dahlbäck et al. (32) (median 66) and O'Connell et al. (33) (median 68).

Given the paucity of studies evaluating patient satisfaction with CWPF donor-site scars, we however, report high postoperative postoperative patient satisfaction with donor-site scars. These findings are consistent with results by Muktar et al. (34), who reported favourable donor-site outcomes after CWPF reconstruction. Psychosocial well-being (median 71) was also in line with previously reported values for breast-conserving cohorts. Tomita et al. (35) found median psychosocial well-being scores of approximately 73 following BCS. While we report lower sexual well-being scores (median 43), these may well reflect factors beyond the reconstruction itself, including adjuvant therapies and the limited number of respondents in that domain ($n = 21$).

Study Limitations

Our results show that CWPF reconstructions result in high postoperative satisfaction, acceptable donor-site outcomes, and stable psychosocial well-being, supporting their use as a safe and well-tolerated volume-replacement option in breast-conserving surgery. However, this study has limitations, including its small sample size, its unequal distribution of flap types, its short follow-up period, and its retrospective design, all of which restrict the strength and generalisability of our findings. As the data reflect the experience of a single surgeon at a single centre, outcomes may differ elsewhere due to variations in expertise and patient demographics. Larger multi-centre and long-term prospective studies using validated PROMs are needed to better assess outcomes and quality of life in this patient group.

As oncoplastic breast surgery gains popularity, partial breast reconstruction using CWPFs is a valuable technique in the oncoplastic surgeon's armamentarium. This approach is particularly well suited to patients with small- to moderate-sized

breasts and minimal or no ptosis, when a relatively large volume of tissue needs to be excised. It may also be considered for patients with larger breasts, particularly those wishing to avoid symmetrising mammoplasty. Our results align with previously published studies and support both the technical feasibility and oncological safety of CWPFs in partial breast reconstruction following breast-conserving surgery. No cases of local or distant metastasis were observed, suggesting oncological safety, although extended follow-up is necessary. Patient-reported outcomes further demonstrated high satisfaction and favourable overall aesthetic results.

Ethics

Ethics Committee Approval: This study was reviewed by the Sandwell and West Birmingham Trust Research and Development Team (R&D), and deemed exempt from Research Ethics Committee approval, and registered with the hospital's Clinical Effectiveness Team (ID 3392).

Informed Consent: Written Informed consent is obtained from patients to publish clinical photographs anonymously for academic purposes.

Footnotes

Authorship Contributions

Surgical and Medical Practices: W.B., U.S., K.S., C.X., I.J.; Concept: W.B., U.S., K.S., C.X., I.J.; Design: W.B., U.S., K.S., C.X., I.J.; Data Collection or Processing: W.B., U.S., K.S., C.X., I.J.; Analysis or Interpretation: W.B., U.S., K.S., C.X., I.J.; Literature Search: W.B., U.S., K.S., C.X., I.J.; Writing: W.B., U.S., K.S., C.X., I.J.

Conflict of Interest: No conflict of interest was declared by the authors.

Financial Disclosure: The authors declared that this study received no financial support.

References

1. Speers C, Pierce LJ. Postoperative radiotherapy after breast-conserving surgery for early-stage breast cancer: a review. JAMA Oncol. 2016; 2: 1075-1082. (PMID: 27243924) [Crossref]
2. Rajan KK, Fairhurst K, Birkbeck B, Novintan S, Wilson R, Savović J, et al. Overall survival after mastectomy versus breast-conserving surgery with adjuvant radiotherapy for early-stage breast cancer: meta-analysis. BJS Open. 2024; 8: zrae040. (PMID: 38758563) [Crossref]
3. Engel J, Kerr J, Schlesinger-Raab A, Sauer H, Hölzel D. Quality of life following breast-conserving therapy or mastectomy: results of a 5-year prospective study. Breast J. 2004; 10: 223-231. (PMID: 15125749) [Crossref]
4. Al-Ghazal SK, Fallowfield L, Blamey RW. Comparison of psychological aspects and patient satisfaction following breast conserving surgery, simple mastectomy and breast reconstruction. Eur J Cancer. 2000; 36: 1938-1943. (PMID: 11000574) [Crossref]
5. Kelsall JE, McCulley SJ, Brock L, Akerlund MTE, Macmillan RD. Comparing oncoplastic breast conserving surgery with mastectomy and immediate breast reconstruction: case-matched patient reported outcomes. J Plast Reconstr Aesthet Surg. 2017; 70: 1377-1385. (PMID: 28712883) [Crossref]
6. Kronowitz SJ, Kuerer HM, Buchholz TA, Valero V, Hunt KK. A management algorithm and practical oncoplastic surgical techniques for repairing partial mastectomy defects. Plast Reconstr Surg. 2008; 122: 1631-1647. (PMID: 19050516) [Crossref]
7. Pearce BCS, Fiddes RN, Paramanathan N, Chand N, Laws SAM, Rainsbury RM. Extreme oncoplastic conservation is a safe new alternative to mastectomy. Eur J Surg Oncol. 2020; 46: 71-76. (PMID: 31543385) [Crossref]
8. Tian R, Zheng Y, Liu R, Jiang C, Zheng H. Efficacy and safety of oncoplastic breast-conserving surgery versus conventional breast-conserving surgery: an updated meta-analysis. Breast. 2024; 77: 103784. (PMID: 39126920) [Crossref]
9. Gilmour A, Cutress R, Gandhi A, Harcourt D, Little K, Mansell J, et al. Oncoplastic breast surgery: a guide to good practice. Eur J Surg Oncol. 2021; 47: 2272-2285. (PMID: 34001384) [Crossref]
10. Agrawal SK, Shakya SR, Nigam S, Sharma A, Datta SS, Ahmed R. Chest wall perforator flaps in partial breast reconstruction after breast conservation surgery: an additional oncoplastic surgical option. Ecancermedicalscience. 2020; 14: 1073. (PMID: 32863867) [Crossref]
11. Bertozzi N, Pesce M, Santi PL, Raposio E. Oncoplastic breast surgery: comprehensive review. Eur Rev Med Pharmacol Sci. 2017; 21: 2572-2585. (PMID: 28678328) [Crossref]
12. Hamdi M, Van Landuyt K, Monstrey S, Blondeel P. Pedicled perforator flaps in breast reconstruction: a new concept. Br J Plast Surg. 2004; 57: 531-539. (PMID: 15308400) [Crossref]
13. Yamamoto T, Yamamoto N, Kageyama T, Sakai H, Fuse Y, Tsuihiji K, et al. Definition of perforator flap: what does a "perforator" perforate? Glob Health Med. 2019; 1: 114-116. (PMID: 33330765) [Crossref]
14. Association of Breast Surgery. ABS consensus margin width in breast conservation surgery. London: Association of Breast Surgery; 2015. Available link: https://associationofbreastsurgery.org.uk/professionals/information-hub/guidelines/2015/abs-consensus-statement-margin-width-in-breast-conservation-surgery [Crossref]
15. Pujji OJS, Blackhall V, Romics L, Vidya R. Systematic review of partial breast reconstruction with pedicled perforator artery flaps: clinical, oncological and cosmetic outcomes. Eur J Surg Oncol. 2021; 47: 1883-1890. (PMID: 33895022) [Crossref]
16. Hamdi M, Rasheed MZ. Advances in autologous breast reconstruction with pedicled perforator flaps. Clin Plast Surg. 2012; 39: 477-490. (PMID: 23036298) [Crossref]
17. Agrawal A, Romics L, Thekkinkattil D, Soliman M, Kaushik M, Barmpounakis P, et al; PartBreCon Collaborators. 'PartBreCon' study. A UK multicentre retrospective cohort study to assess outcomes following PARTial BREast reCONstruction with chest wall perforator flaps. Breast. 2023; 71: 82-88. (PMID: 37544090) [Crossref]
18. Gart MS, Smetona JT, Hanwright PJ, Fine NA, Bethke KP, Khan SA, et al. Autologous options for postmastectomy breast reconstruction: a comparison of outcomes based on the American College of Surgeons National Surgical Quality Improvement Program. J Am Coll Surg. 2013; 216: 229-238. Erratum in: J Am Coll Surg. 2013; 216: 1034-1035. (PMID: 23211118). [Crossref]
19. Munhoz AM, Montag E, Fels KW, Arruda EG, Sturtz GP, Aldrighi C, et al. Outcome analysis of breast-conservation surgery and immediate latissimus dorsi flap reconstruction in patients with T1 to T2 breast cancer. Plast Reconstr Surg. 2005; 116: 741-752. (PMID: 16141810) [Crossref]
20. Losken A, Schaefer TG, Carlson GW, Jones GE, Styblo TM, Bostwick J 3rd. Immediate endoscopic latissimus dorsi flap: risk or benefit in reconstructing partial mastectomy defects. Ann Plast Surg. 2004; 53: 1-5. (PMID: 15211189) [Crossref]
21. Bostwick J 3rd, Scheflan M. The latissimus dorsi musculocutaneous flap: a one-stage breast reconstruction. Clin Plast Surg. 1980; 7: 71-78. (PMID: 6988147) [Crossref]

22. Rainsbury RM. Breast-sparing reconstruction with latissimus dorsi miniflaps. Eur J Surg Oncol. 2002; 28: 891-895. (PMID: 12477482) [Crossref]

23. Losken A, Hamdi M. Partial breast reconstruction: current perspectives. Plast Reconstr Surg. 2009; 124: 722-736. (PMID: 19730292) [Crossref]

24. Mégevand V, Scampa M, McEvoy H, Kalbermatten DF, Oranges CM. Comparison of outcomes following prepectoral and subpectoral implants for breast reconstruction: systematic review and meta-analysis. Cancers (Basel). 2022; 14: 4223. (PMID: 36077760) [Crossref]

25. Steffenssen MCW, Kristiansen AH, Damsgaard TE. A systematic review and meta-analysis of functional shoulder impairment after latissimus dorsi breast reconstruction. Ann Plast Surg. 2019; 82: 116-127. (PMID: 30516558) [Crossref]

26. Losken A, Nicholas CS, Pinell XA, Carlson GW. Outcomes evaluation following bilateral breast reconstruction using latissimus dorsi myocutaneous flaps. Ann Plast Surg. 2010; 65: 17-22. (PMID: 20548235) [Crossref]

27. Sajid MS, Betal D, Akhter N, Rapisarda IF, Bonomi R. Prevention of postoperative seroma-related morbidity by quilting of latissimus dorsi flap donor site: a systematic review. Clin Breast Cancer. 2011; 11: 357-363. (PMID: 21705282) [Crossref]

28. Escandón JM, Manrique OJ, Christiano JG, Mroueh V, Prieto PA, Gooch JC, et al. Breast reconstruction with latissimus dorsi flap: a comprehensive review and case series. Ann Transl Med. 2023; 11: 355. (PMID: 37675333) [Crossref]

29. Roy PG, Mustata L, Hu J, Phillips B, Parulekar V, Bhattacharyya M, et al. Partial breast reconstruction with lateral chest wall perforator flap to facilitate breast conservation in breast cancer: first 100 cases with cancer outcomes at 8 years follow-up and the lessons learned. Cancer Manag Res. 2021; 13: 9453-9466. (PMID: 35002323) [Crossref]

30. Nava CM, Zinner G, Martineau J, Oranges CM. Chest wall perforator flaps in partial breast reconstruction: a systematic review and meta-analysis. Plast Reconstr Surg Glob Open. 2025; 13: e6996. (PMID: 40761627) [Crossref]

31. Hamdi M, Van Landuyt K, de Frene B, Roche N, Blondeel P, Monstrey S. The versatility of the inter-costal artery perforator (ICAP) flaps. J Plast Reconstr Aesthet Surg. 2006; 59: 644-652. (PMID: 16716957) [Crossref]

32. Dahlbäck C, Ullmark JH, Rehn M, Ringberg A, Manjer J. Aesthetic result after breast-conserving therapy is associated with quality of life several years after treatment. Swedish women evaluated with BCCT.core and BREAST-Q™. Breast Cancer Res Treat. 2017; 164: 679-687. (PMID: 28536951) [Crossref]

33. O'Connell RL, DiMicco R, Khabra K, O'Flynn EA, deSouza N, Roche N, et al. Initial experience of the BREAST-Q breast-conserving therapy module. Breast Cancer Res Treat. 2016; 160: 79-89. (PMID: 27637781) [Crossref]

34. Muktar S, Micha A, Farnworth S, O'Connell RL, Barry PA. Patient-reported outcomes and aesthetic assessment following chest wall perforator flap partial volume replacement for primary breast cancer. AME Surg J. 2023; 11: 81525. [Crossref]

35. Tomita S, Yoshitake T, Matsunaga N, de Kerckhove M, Fujii M, Terao Y. Patient-reported outcomes and quality of life after breast-conserving surgery, mastectomy, and breast reconstruction assessed using the BREAST-Q questionnaire. Breast Cancer Res Treat. 2024; 207: 641-648. (PMID: 38874689) [Crossref]

ORIGINAL ARTICLE

European Journal of BREAST HEALTH

DOI: 10.4274/ejbh.galenos.2026.2026-1-10
Eur J Breast Health 2026;22(3):307-317

Development and Internal Validation of a Clinical Data-Based Machine Learning Web Calculator for Predicting Recurrence in Granulomatous Lobular Mastitis: A Multicenter Retrospective Study

Jiao Feng[1], Ruiyang Wu[2], Jin Chen[2], Yi Li[1]

[1]Department of Gastrointestinal Surgery, The Affiliated Chengdu 363 Hospital of Southwest Medical University, Chengdu, China
[2]Department of Breast and Thyroid, Sichuan Provincial Hospital for Women and Children (Affiliated Women and Children's Hospital of Chengdu Medical College), Chengdu, China

ABSTRACT

Objective: Granulomatous lobular mastitis (GLM) is a disease characterized by a high recurrence rate and the absence of a standard treatment, making prognostic prediction crucial. While promising, existing machine learning models are limited by single-center data and small sample sizes. This study aimed to develop and validate machine learning models using a large multicenter dataset to predict GLM recurrence and build a clinical web calculator.

Materials and Methods: In this retrospective cohort study, data from 318 GLM patients at two tertiary hospitals (diagnosed between 2019 and 2024) were used to train and evaluate five machine learning models. Performance was assessed by accuracy, area under the curve (AUC), F1-score, sensitivity, and specificity.

Results: The five models demonstrated comparable discriminatory performance, with AUCs ranging from 0.778 to 0.808 and no statistically significant differences among them. Among them, random forest (RF) excelled in composite and sensitivity metrics (F1 score: 0.639; accuracy: 76.2%; sensitivity: 50%), whereas logistic regression achieved the top AUC (0.808), and the support vector machine achieved the best specificity (95.3%). Based on its balanced performance across multiple metrics, RF was selected for deployment to develop a publicly accessible web application platform (https://w12251393.shinyapps.io/predictGLM/). In the RF model, white blood cell count emerged as the top predictor, followed by age at diagnosis, the origin of the primary tumor, surgical excision, antitubercular therapy, corticosteroid therapy, and abscess drainage, in descending order of importance.

Conclusion: Although retrospective in design, this study developed a multicenter RF model and implemented it as an accessible web calculator, providing a valuable tool for personalized recurrence prediction and treatment decision-making in GLM. The model should be used as a risk stratification aid to support clinical decision-making rather than as a definitive predictive instrument.

Keywords: Granulomatous mastitis; machine learning; recurrence

Corresponding Author: Yi Li MD;
E-mail: wcfj123123@163.com **ORCID:** orcid.org/0009-0005-5262-1030

Received: 31.01.2026 **Accepted:** 15.03.2026 **Available Online Date:** 17.06.2026

Cite this article as: Feng J, Wu R, Chen J, Li Y. Development and internal validation of a clinical data-based machine learning web calculator for predicting recurrence in granulomatous lobular mastitis: a multicenter retrospective study. Eur J Breast Health. 2026;22(3):307-317

KEY POINTS

- This study addresses the high recurrence rate of granulomatous lobular mastitis by developing the first machine-learning-based online calculator (random forest) for predicting recurrence.
- The model, constructed from multicenter data, demonstrates balanced predictive performance and identifies seven key predictors, including white blood cell count and surgical intervention.
- The result has been translated into a freely accessible web tool that provides instant, individualized recurrence-risk assessments to support clinical decision-making and to serve as a risk-stratification aid.

Introduction

Granulomatous lobular mastitis (GLM) was a non-puerperal chronic inflammatory breast disease characterized by non-caseating granulomas and microabscesses confined to the breast lobules (1-3). Based on a significant rise in reported cases over the past decade, the incidence of GLM has increased dramatically (4). GLM typically presented with painful breast masses, redness, and abscesses that could progress to fistulas and sinus tracts, often leading to significant breast deformity and a high recurrence rate (5-7).

Given its notoriously high recurrence rate, reported in various studies to range from 24% to 40% (8-11), GLM has often been referred to as "incurable cancer" (12). This combination of a high relapse risk and the lack of standardized therapeutic guidelines makes accurate prognostic assessment crucial (13). Although some studies attempted to employ staging systems to predict patient prognosis (12, 14, 15), their predictive efficacy was largely unsatisfactory due to the disease's marked heterogeneity. For instance, in our previous work, we developed the 1st edition of GLM stage for predicting GLM prognosis; however, it yielded a suboptimal area under the curve (AUC) of only 0.642 (12). This limitation of conventional approaches highlights the need for more advanced methods, such as machine learning, which may better capture complex patterns in heterogeneous diseases. Consequently, recent research has increasingly leveraged machine learning models to integrate complex, multi-dimensional patient data, demonstrating promising predictive performance for recurrence risk (16, 17). For instance, Li et al. (16) demonstrated that the neural network model achieved higher predictive accuracy. These promising findings, however, faced substantial clinical implementation barriers. The models had not been integrated into clinical workflows for direct assessment, and their development was constrained by small, single-center datasets with incomplete metrics, which collectively limited their generalizability and immediate practical utility. To overcome these limitations, this study leveraged a large-scale, multi-center dataset to develop and compare multiple machine learning models, with the specific objective of building a web-based clinical calculator for prognostic assessment.

Materials and Methods

Data and Samples

This retrospective cohort study initially enrolled 599 patients diagnosed with GLM from two tertiary care hospitals between January 2019 and December 2024. The diagnosis of GLM requires a comprehensive assessment integrating medical history, clinical manifestations, physical examination, imaging, and laboratory findings, with definitive confirmation by histopathological examination. Among these, 575 cases were sourced from a specialized disease registry established by the Department of Breast and Thyroid Surgery at Hospital A in March 2022, which had systematically collected and followed up cases of non-puerperal mastitis since January 2017. The remaining 24 cases were obtained from Hospital B's medical records covering the same period. As of October 1, 2025, the research team extracted eligible cases from Hospital A's registry within the specified timeframe and conducted a unified retrospective review of corresponding cases from Hospital B. According to the predefined exclusion criteria, we excluded 10 patients with missing height information, 31 patients with incomplete lesion diameter records, 8 patients with an unspecified number of lesions, and 8 patients with missing white blood cell (WBC) count data. Furthermore, since the study endpoint was the one-year recurrence rate, an additional 224 patients with less than 12 months of follow-up and no recurrence were excluded. Ultimately, 318 GLM patients with diagnosis dates between January 2019 and December 2024 were included in the final analysis.

The primary endpoint of this study was the one-year recurrence rate, defined as the reappearance of non-puerperal mastitis, ipsilateral or contralateral, within 12 months of the initial diagnosis. Recurrence was defined as the re-emergence of mastitis symptoms following clinical improvement or cure achieved through surgical or conservative treatment. Clinical improvement was characterized by a reduction in lesion size, resolution of skin erythema, significant alleviation of pain, and ultrasonographic evidence of diminished inflammation. Cure was confirmed upon complete resolution of symptoms, absence of palpable masses, and normal findings on both physical and imaging examinations (18). The final follow-up was conducted on September 1, 2025.

In this retrospective design, some collected variables (detailed below) reflected assessments or interventions that occurred during the patient's management course rather than being strictly limited to the baseline state at initial diagnosis. The dataset encompassed multiple clinical variables, including age at diagnosis (years), height (cm), weight (kg), days to first visit (days), defined as the duration from symptom onset to the initial hospital consultation; laterality of the primary lesion (left, right, bilateral); maximum lesion diameter on ultrasound (cm), representing the highest value recorded during the current disease episode; ultrasound-detected lesion count (solitary, multiple); presence of mammary abscess (no, yes); WBC count (10^9/L), indicating the peak measurement observed throughout the clinical course; and documented therapeutic interventions including quinolone therapy (no, yes), penicillin therapy (no, yes), cephalosporin therapy (no, yes), macrolide therapy (no, yes), nitroimidazole therapy (no, yes), antitubercular therapy (no, yes), corticosteroid therapy (no, yes), tetracycline therapy (no, yes), abscess drainage (no, yes), and surgical excision (no, yes). These variables indicated whether a treatment was ever administered, not solely whether it was part of the initial treatment plan.

The study utilized data from two medical institutions under appropriate ethical frameworks. Hospital A's proprietary database was operated in compliance with the Declaration of Helsinki (2013 revision) and received formal approval from its Medical Ethics Committee (approval number: 20220330-024, date: 30.03.2022).

Statistical Analysis

Continuous variables were expressed as mean ± standard deviation, while categorical variables were presented as numbers and percentages. Univariate and multivariate logistic regression (LOG) analyses were performed to identify independent prognostic factors, with odds ratios (ORs) and corresponding 95% confidence intervals (CIs) reported for all significant associations.

The Boruta algorithm, implemented in the Boruta package for R, was a widely used feature selection method based on the random forest (RF) framework (19). It systematically identified all relevant features associated with the prediction target by comparing the importance of original features with randomly generated "shadow features". The primary advantages of the Boruta algorithm included its comprehensiveness, identifying all relevant features rather than identifying only an optimal subset for modeling; robustness, achieved through multiple iterations and statistical testing; and independence from preset parameters, requiring no pre-specified number of features or extensive parameter tuning. In this study, Boruta was first applied to the entire dataset to obtain a stable and interpretable set of predictors. A random seed [set.seed (123)] was set to ensure reproducibility. This fixed feature set was used consistently throughout all subsequent 5-fold cross-validation and model training steps, with no further feature selection performed within the cross-validation loop. This design ensures that all models are trained and compared within the same feature space, facilitating fair performance comparisons and clinical interpretability. To evaluate model performance and mitigate overfitting, a 5-fold cross-validation approach was employed using the caret package. The entire dataset was randomly partitioned into five folds of roughly equal size using a fixed random seed [set.seed (23)]. In each iteration, four folds served as the training subset and the remaining fold served as the validation subset. The median AUC across the five folds was used as the overall performance estimate to select the best-performing algorithm. To provide an intuitive illustration of the model's predictive ability, the fold corresponding to the median AUC (i.e., the centrally located fold representing typical performance) was selected as the representative fold. The model was retrained using the training subset of this representative fold and evaluated on the corresponding validation subset to generate the receiver operating characteristic (ROC) curve and detailed classification metrics (accuracy, sensitivity, specificity, and F1-score). This approach avoids the optimism bias that would result from selecting the best-performing fold, ensuring that the displayed performance reflects the model's typical behavior. Based on the comparative performance evaluation, the best-performing prediction model was deployed as a publicly accessible and free-to-use web calculator through the shiny package (20). This online tool, available free of charge to the research and clinical community, enables real-time recurrence risk prediction based on user-provided clinical features. Furthermore, feature importance ranking was performed on the final model's predictors to identify the most influential variables. The study process is presented in Figure 1. All statistical tests in this study adopted a two-tailed approach, with statistical significance defined at the alpha level of 0.05. The analytical procedures and data visualizations were implemented using R software (version 4.2.2; R Foundation for Statistical Computing, Vienna, Austria).

This study employed five distinct machine learning algorithms, each with its respective implementation. LOG, which estimates the probability of a binary outcome using a logistic function, was implemented with the glm function in the stats package (21). Naïve Bayes (NB), a probabilistic classifier based on Bayes' theorem with feature independence assumption, was performed utilizing the NB function within the e1071 package (22). Linear discriminant analysis (LDA), a method for projecting data into a lower-dimensional space to maximize class separability, was conducted using the LDA function in the MASS package (23). Support vector machine (SVM), which identifies optimal hyperplanes to separate classes with maximum margins, was carried out using the ksvm function from the kernlab package (24). RF, an ensemble technique constructing multiple decision

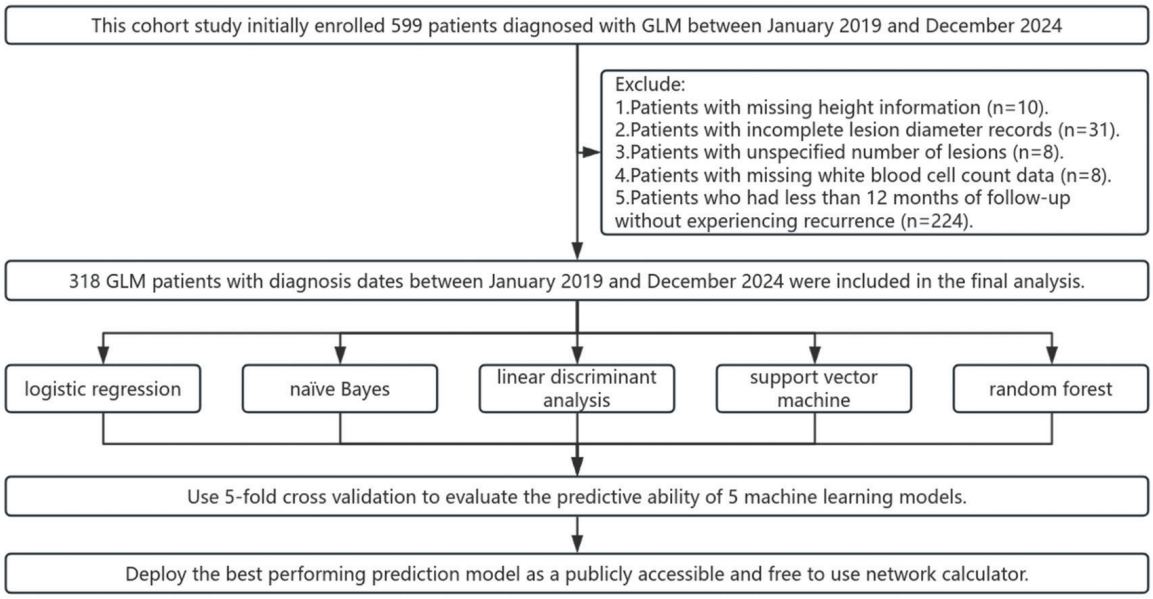

Figure 1. The process of this study
GLM: Granulomatous lobular mastitis

trees to enhance accuracy, was executed with the RF function from the RF package (25). The number of trees (ntree parameter) was set to 183 based on minimizing the out-of-bag (OOB) error rate; to determine this, we trained an initial RF model and identified the point at which the OOB error reached its minimum using the which.min [rf$err.rate (-1)] function. This analysis indicated that 183 trees provided the optimal balance between predictive performance and computational efficiency, as the error rate stabilized beyond this point. A random seed [set.seed (3)] was used for the RF to ensure reproducibility. All models were implemented using their respective packages' default parameters. This approach was adopted to provide a fair and reproducible baseline comparison of algorithmic performance on our dataset, prioritizing generalizability and mitigating the risk of overfitting given the available sample size for model training.

Results

Descriptive Characteristics and Prognostic Factor Analysis

This study included 318 female patients with granulomatous lobular mastitis. With follow-up through September 1, 2025, the cumulative one-year recurrence rate was 32.4%, corresponding to 103 patients who experienced recurrence and 215 who remained recurrence-free. Univariate LOG analysis demonstrated significant associations between GLM recurrence and several clinical factors: origin of the primary lesion ($p = 0.023$), WBC count ($p = 0.001$), antitubercular therapy ($p<0.001$), corticosteroid therapy ($p<0.001$), abscess drainage ($p = 0.002$), and surgical excision ($p = 0.008$) as detailed in Table 1. Multivariate analysis further identified independent predictors of recurrence, including days to first visit ($p = 0.006$; OR: 0.983; 95% CI: 0.971–0.995), origin of primary ($p = 0.007$), antitubercular therapy ($p = 0.002$; OR: 0.358; 95% CI: 0.190–0.676), corticosteroid therapy ($p = 0.005$; OR: 2.990; 95% CI: 1.385–6.452), abscess drainage ($p = 0.003$; OR: 0.290; 95% CI: 0.129–0.653), and surgical excision ($p< 0.001$; OR: 0.190; 95% CI: 0.084–0.428) as presented in Table 1.

Machine Learning

To enhance the prognostic prediction for GLM patients, we employed machine learning approaches, commencing with feature selection using the Boruta package in R (19). The Boruta algorithm, which evaluates feature importance by comparing original attributes with their permuted shadow copies, identified seven significant predictors: age at diagnosis, origin of the primary tumor, WBC count, antitubercular therapy, corticosteroid therapy, abscess drainage, and surgical excision (Figure 2). These seven covariates were incorporated into our subsequent machine learning models.

This study evaluated five machine learning models—LOG, NB, LDA, SVM, and RF—for predicting recurrence in GLM. The AUC values across these models ranged from 0.778 to 0.808, and ROC analysis indicated no statistically significant differences in discriminatory performance among them (Table 2, Figure 3). Among the models, RF achieved the highest F1-score (0.639), accuracy (76.2%), and sensitivity (50%), demonstrating the most balanced performance across multiple metrics. LOG yielded the highest AUC (0.808), while SVM exhibited the highest specificity (95.3%).

Table 1. Univariate and multivariate logistic regression analysis of prognostic factors for 318 patients with GLM

Factors	n (%)/X ± S	Univariate	Multivariate	
		p-value	OR (95% CI)	*p*-value
Age at diagnosis (years)	31.3±4.4	0.189	0.943 (0.883–1.007)	0.080
Height (cm)	159.6±5.1	0.246	1.059 (0.997–1.126)	0.064
Weight (kg)	61.3±11.0	0.546	0.997 (0.970–1.026)	0.850
Days to first visit (days)	26.3±74.9	0.122	0.983 (0.971–0.995)	0.006
Origin of primary		0.023		0.007
Left	164 (51.6)		Ref	
Right	146 (45.9)		1.934 (1.098–3.408)	0.022
Bilateral	8 (2.5)		15.329 (1.755–133.924)	0.014
Maximum lesion diameter on ultrasound (cm)	4.8±2.1	0.272	1.004 (0.989–1.020)	0.600
Ultrasound-detected lesion count		0.539		0.917
Solitary	41 (12.9)		Ref	
Multiple	277 (78.1)		0.951 (0.372–2.431)	
Mammary abscess		0.461		0.413
No	40 (12.6)		Ref	
Yes	278 (87.4)		1.513 (0.561–4.078)	
White blood cell (10^9/L)	10.47±3.98	0.001	1.064 (0.986–1.149)	0.112
Quinolone therapy		0.605		0.578
No	64 (20.1)		Ref	
Yes	254 (79.9)		0.790 (0.344–1.812)	
Penicillin therapy		0.579		0.653
No	306 (96.2)		Ref	
Yes	12 (3.8)		0.713 (0.164–3.108)	
Cephalosporin therapy		0.899		0.450
No	233 (73.3)		Ref	
Yes	85 (26.7)		1.292 (0.665–2.508)	
Macrolide therapy		0.936		0.672
No	303 (95.3)		Ref	
Yes	15 (4.7)		1.326 (0.359–4.888)	
Nitroimidazole therapy		0.786		0.717
No	304 (95.6)		Ref	
Yes	14 (4.4)		1.275 (0.342–4.753)	
Antitubercular therapy		<0.001		0.002
No	190 (59.7)		Ref	
Yes	128 (40.3)		0.358 (0.190–0.676)	
Corticosteroid therapy		<0.001		0.005
No	99 (31.1)		Ref	
Yes	219 (68.9)		2.990 (1.385–6.452)	
Tetracycline therapy		0.653		0.426
No	310 (97.5)		Ref	
Yes	8 (2.5)		0.482 (0.080–2.903)	
Abscess drainage		0.002		0.003
No	88 (27.7)		Ref	
Yes	230 (72.3)		0.290 (0.129–0.653)	
Surgical excision		0.008		<0.001
No	49 (15.4)		Ref	
Yes	269 (84.6)		0.190 (0.084–0.428)	

OR: Odds ratio; CI: Confidence interval; Ref: Reference; GLM: Granulomatous lobular mastitis

Web Application Development

Based on the RF model's balanced performance profile — characterized by the highest F1-score (0.639), accuracy (76.2%), and sensitivity (50%)— this study selected it as the core algorithm for developing a publicly accessible web application (https://w12251393.shinyapps.io/predictGLM/). This decision was guided by several considerations: first, RF demonstrated the most balanced performance across key classification metrics, with a high F1-score reflecting the optimal balance between precision and recall, and its highest sensitivity indicating an enhanced ability to identify true recurrence cases, which is particularly crucial for clinical early warning; second, as an ensemble learning algorithm, RF exhibited greater generalization and robustness, enabling better adaptation to new data and making it suitable for deployment as the core prediction engine in a public application. All five models achieved comparable discriminatory performance, with no statistically significant differences in AUC, and the selection of RF represents a pragmatic choice based on its multi-metric balance rather than a claim of statistical superiority. The platform automatically calculates the one-year recurrence risk based on patient characteristics entered by the user. Figure 4 displays a functional example of the interface of this web application.

Based on the RF model, feature importance ranking for the seven covariates was performed using the importance function from the RF package in R, which employs a permutation-based approach to evaluate variable significance by measuring the mean decrease in accuracy when out-of-bag data for each predictor is randomly shuffled (25). The analysis revealed the following descending order of predictive importance: WBC count, which emerged as the most influential predictor, followed by age at diagnosis, origin of the primary, surgical excision, antitubercular therapy, corticosteroid therapy, and abscess drainage (Figure 5).

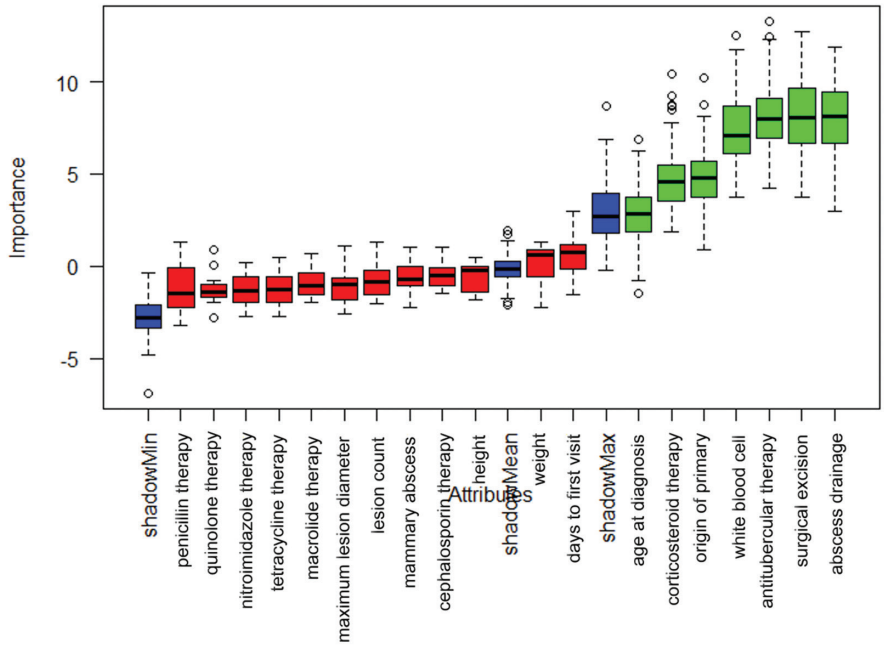

Figure 2. Predictor selection for machine learning modeling

Table 2. Performance comparison of the five machine learning models for GLM recurrence prediction in the validation set

Mode	Accuracy (%)	AUC	F1-score	Sensitivity (%)	Specificity (%)	$P_{vs\ LOG}$	$P_{vs\ NB}$	$P_{vs\ LDA}$	$P_{vs\ SVM}$
LOG	69.8	0.808	0.541	40.0	83.7	Ref	0.7129	0.9177	0.6496
NB	70.3	0.778	0.435	28.6	90.7	0.7129	Ref	0.712	0.9147
LDA	69.8	0.807	0.536	40.0	81.4	0.9177	0.712	Ref	0.662
SVM	74.6	0.787	0.456	30.0	95.3	0.6496	0.9147	0.662	Ref
RF	76.2	0.785	0.639	50.0	88.4	0.7776	0.9271	0.7868	0.9837

AUC: Area under the curve; LOG: Logistic regression; Ref: Reference; NB: Naïve bayes; LDA: Linear discriminant analysis; SVM: Support vector machine; RF: Random forest; GLM: Granulomatous lobular mastitis

Discussion and Conclusion

Studies have reported that the recurrence rate of GLM can be as high as 24–40%, making it a commonly recurring breast condition (8-11). Accurate prediction of recurrence could inform treatment decisions and follow-up strategies, ultimately improving patient outcomes. Although some studies have attempted to use staging systems to predict patient prognosis (12, 14, 15), these systems have generally demonstrated limited predictive efficacy due to the substantial heterogeneity of the condition and the wide variation in clinical manifestations among individual patients.

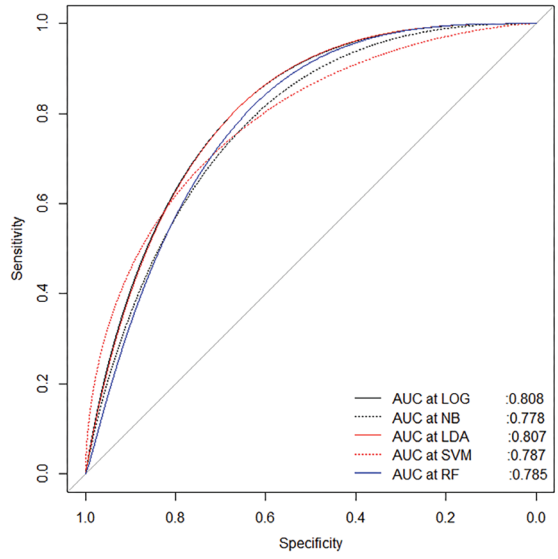

Figure 3. Comparison of ROC curves for the five machine learning models
AUC: Area under the curve; LOG: Logistic regression; NB: Naïve bayes; LDA: Linear discriminant analysis; SVM: Support vector machine; RF: Random forest; ROC: Receiver operating characteristic

Using a multicenter retrospective cohort, this study systematically compared five machine learning models for predicting one-year recurrence risk in GLM and subsequently developed a publicly accessible online calculator based on the optimally performing RF model. The results demonstrated that all models achieved comparable discriminatory performance, with AUCs ranging from 0.778 to 0.808. The RF model exhibited a balanced performance profile with an F1-score of 0.639, accuracy of 76.2%, and sensitivity of 50%, while LOG achieved the highest AUC (0.808) and the SVM exhibited the highest specificity (95.3%). Based on its balanced multi-metric performance and inherent feature importance interpretation, RF was selected as the final model for clinical deployment; this choice reflects practical considerations rather than statistical superiority, given the equivalent AUCs across models. Feature importance analysis identified WBC as the most influential predictor of recurrence, followed by age at diagnosis, origin of primary, surgical excision, antitubercular therapy, corticosteroid therapy, and abscess drainage. These findings provide novel insights and a practical tool for individualized recurrence risk assessment in GLM.

The predictive performance of our models aligns closely with previously reported machine learning applications in GLM.

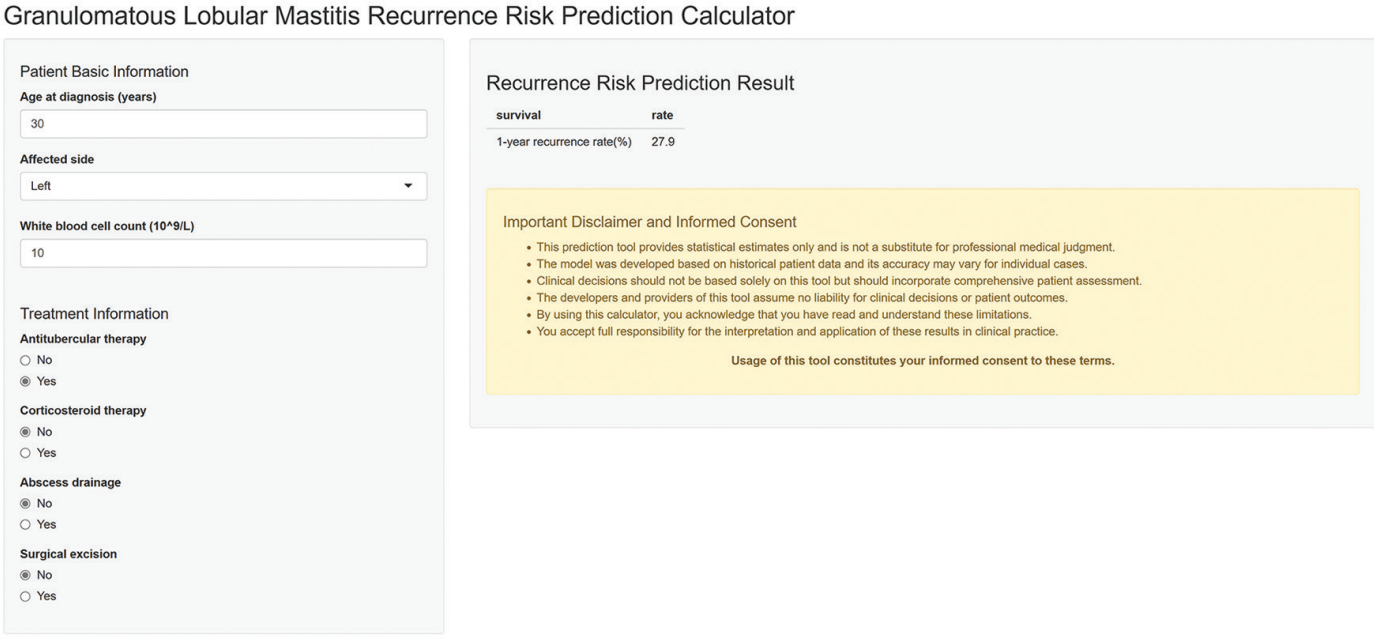

Figure 4. An example showing web function (https://w12251393.shinyapps.io/predictGLM/)

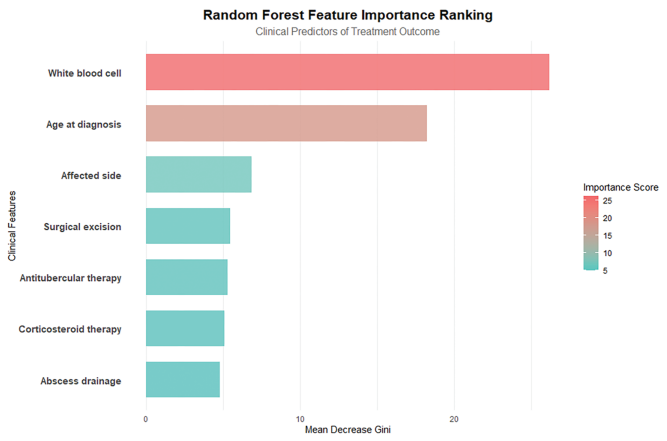

Figure 5. Feature importance ranking in the random forest model

Li et al. (16) analyzed 212 GLM patients and compared LOG, RF, and neural network models, reporting that the neural network outperformed the other models in their specific dataset, while their RF model yielded an AUC of 0.793—remarkably similar to the 0.785 AUC observed in our RF model. Similarly, Ma et al. (17) developed an XGBoost model based on contrast-enhanced ultrasound features and reported an AUC of 0.808, which is also comparable to our findings. These convergent results across studies and populations suggest that current machine learning approaches for predicting GLM recurrence consistently achieve AUCs of 0.78–0.81, reflecting the inherent complexity of GLM recurrence.

Despite comparable predictive performance, our study extends previous work in several important aspects. First, our models were developed and validated in a multicenter cohort (n = 318), enhancing generalizability compared with single-center studies with smaller samples. Second, we systematically compared five algorithms under standardized conditions, thereby providing a comprehensive benchmark for future research. Third, and most significantly, we implemented the optimal model as a freely accessible web-based calculator (https://w12251393.shinyapps.io/predictGLM/), filling a critical gap in clinical implementation that previous studies had not addressed.

The clinical deployment of any prediction model requires careful consideration of its performance characteristics. Our RF model's sensitivity of 50% warrants attention, as it indicates that approximately half of patients who ultimately experience recurrence may not be identified by the model (false negatives). In clinical practice, such false-negative predictions could lead to inadequate monitoring intensity or delayed therapeutic interventions, potentially compromising patient outcomes. Therefore, it should be emphasized that this web-based calculator is intended as a risk-stratification aid rather than a definitive predictive instrument. Clinicians should integrate model predictions with comprehensive clinical evaluation, maintaining standard follow-up protocols for all patients and exercising heightened vigilance for those with strong clinical suspicion of recurrence despite low-risk model predictions. Conversely, the model's relatively high specificity (88.4%) offers meaningful clinical value by reliably identifying patients at low risk of recurrence. This capability may facilitate more efficient resource allocation, potentially reducing unnecessarily frequent follow-up visits or overly aggressive treatment among low-risk populations. From a clinical utility perspective, the tool may be better suited to rule out low-risk patients than to definitively identify high-risk individuals—a distinction that should guide its appropriate integration into clinical workflows.

The identification of WBC as the most important predictor in our RF model warrants careful interpretation. While Sun et al. (26) similarly reported WBC as the predominant risk factor for GLM recurrence, several other studies found no significant association between WBC and recurrence (11, 27, 28). Several factors may explain these discrepancies. First, the timing of WBC measurement varied substantially across studies: our study used peak WBC during the disease course, whereas others employed baseline WBC at diagnosis or random measurements of WBC. Given that WBC can fluctuate in response to disease activity and therapeutic interventions, measurement timing critically influences its prognostic value. Second, treatment-related factors (antibiotics, corticosteroids) can directly modulate WBC levels, potentially confounding the relationship between WBC and recurrence in retrospective analyses. Third, and perhaps most importantly, the etiological heterogeneity of GLM likely influences both WBC patterns and recurrence risk. For instance, infectious etiologies (e.g., tuberculosis, Corynebacterium infection) may exhibit distinct inflammatory profiles compared with idiopathic or autoimmune variants, yet our inability to perform etiological stratification may have averaged out these differences.

The "days to first visit" variable exhibited substantial variability (mean 26.3±74.9 days), reflecting a right-skewed distribution due to a subset of patients with markedly delayed presentation. Its modest protective effect (OR: 0.983) should be interpreted cautiously, as it may reflect confounding by disease severity—patients with milder symptoms may both delay care and have a lower recurrence risk—rather than a direct causal relationship.

The inclusion of treatment-related variables—surgical excision, corticosteroid therapy, antitubercular therapy, and abscess drainage—in the final model reflects their prognostic significance. LOG revealed strong associations between recurrence and surgical excision, corticosteroid therapy, and antitubercular therapy.

These findings should be interpreted with caution due to potential confounding by indication, a common issue in observational studies where treatment assignment is influenced by disease severity. For instance, patients receiving corticosteroids may have more severe inflammation and therefore a higher risk of recurrence regardless of treatment effect. Conversely, the protective effects of surgery and antitubercular therapy may reflect patient selection rather than causal benefits. These variables may also indirectly capture etiological information—e.g., antitubercular therapy suggests tuberculous mastitis, which is characterized by distinct recurrence patterns. However, without systematic etiological confirmation, such inferences remain speculative. Therefore, these associations should be understood as observational prognostic factors and not as evidence of causal treatment effects. Prospective studies with standardized protocols and etiological stratification are needed to establish causality.

Despite the encouraging results, our study was constrained by several limitations. First, the retrospective design inherently carried a risk of selection bias. To accurately assess the one-year recurrence endpoint and avoid outcome misclassification, we excluded patients with <12 months of follow-up who had no recurrence (n = 224). While methodologically necessary, this might have limited the cohort's representativeness, as patients lost to follow-up could have differed systematically. Notably, the one-year endpoint itself represented only one aspect of this potential bias. This limitation might have affected the model's generalizability to broader populations. Second, while we evaluated several machine learning models based on structured clinical data, we did not investigate deep learning approaches or incorporate imaging-derived features (e.g., radiomic or ultrasound-derived features), which might have captured more complex patterns in the data, though at the cost of interpretability. Our deliberate focus on readily available clinical variables was intended to maximize clinical applicability and ease of implementation; however, this choice meant that potentially informative imaging data were not utilized. Future studies integrating multi-modal data may further improve predictive accuracy. Third, despite our multicenter dataset (two centers, n = 318), this study lacks external validation in an independent cohort. All data were utilized for model development and internal validation; therefore, the model's performance on entirely unseen populations remains unknown. This represents a critical limitation, as the current results may not fully reflect the model's generalizability to broader clinical settings. Future research should prioritize external validation using independent cohorts with similar or larger sample sizes. We are actively seeking collaborations with additional centers to prospectively collect validation data, which will be essential before the model can be considered for wider clinical implementation. Fifth, the lack of etiological subtyping represents an important limitation. GLM encompasses a spectrum of disorders with diverse etiologies (e.g., infectious, autoimmune, idiopathic) that have substantially different treatment responses and recurrence patterns. Due to the retrospective design and the absence of standardized etiological screening (including testing for tuberculosis, Corynebacterium, fungi, and autoimmune antibodies) in routine clinical practice, we were unable to stratify patients according to these subtypes. Consequently, our machine learning models reflect average effects across a mixed population, and heterogeneity among subtypes may have diluted certain predictive signals. Sixth, while our study focused on discrimination metrics, calibration assessment—an important aspect of model performance for clinical decision-making—was not performed. Future external validation studies should include comprehensive calibration evaluation, including calibration curves and Brier scores, to further establish the model's clinical utility.

However, this study established a multicenter, large-scale cohort and employed multiple machine learning algorithms to predict recurrence risk and subsequently developed a clinically applicable web-based calculator. This tool incorporates influential features such as treatment modalities and offers significant clinical value by supporting personalized recurrence risk assessment and treatment decision-making. Future research should aim to enhance the model's clinical utility further. Specifically, prospective studies should incorporate standardized etiological screening protocols and develop dedicated predictive models for different subtypes—especially those requiring differentiation from specific infections—to enable precision diagnosis and treatment. Key directions include improving sensitivity to reduce false-negative predictions. Potential strategies encompass prospectively collecting early or dynamic biomarkers, employing advanced machine learning techniques to handle imbalanced data, and expanding multi-center collaborations to enrich the sample size, particularly within the recurrence subgroup, thereby refining the model's ability to identify recurrence patterns.

Study Limitations

Using a multicenter cohort, this study successfully developed and validated a RF-based prediction model for GLM recurrence risk; the model was selected for its balanced performance across multiple metrics and subsequently translated into a clinically accessible web-based calculator. All five machine learning models demonstrated comparable discriminatory performance, with no statistically significant differences in AUC. The tool is intended as a risk stratification aid to support clinical decision-making, not as a definitive predictive instrument. Although the retrospective design and the absence of deep learning models represented limitations, this work provided a practical tool for personalized prognostic assessment by integrating key clinical features. External validation on larger and more diverse populations was recommended to further enhance the model's clinical utility.

Ethics

Ethics Committee Approval: The study utilized data from two medical institutions under appropriate ethical frameworks. Hospital A's proprietary database was operated in compliance with the Declaration of Helsinki (2013 revision) and received formal approval from its Medical Ethics Committee (approval number: 20220330-024, date: 30.03.2022).

Informed Consent: Retrospective study.

Footnotes

Authorship Contributions

Surgical and Medical Practices: J.F., R.W., J.C., Y.L.; Concept: J.F., R.W.; Data Collection or Processing: J.F., R.W., J.C.; Analysis or Interpretation: J.F., J.C.; Literature Search: J.F., Y.L.; Writing: J.F., R.W., J.C., Y.L.

Conflict of Interest: No conflict of interest was declared by the authors.

Financial Disclosure: The authors declared that this study received no financial support.

References

1. Ma X, Min X, Yao C. Different treatments for granulomatous lobular mastitis: a systematic review and meta-analysis. Breast Care (Basel). 2020; 15: 60-66. (PMID: 32231499) [Crossref]
2. Farouk O, Abdelkhalek M, Abdallah A, Shata A, Senbel A, Attia E, et al. Rifampicin for idiopathic granulomatous lobular mastitis: a promising alternative for treatment. World J Surg. 2017; 41: 1313-1321. (PMID: 28050664) [Crossref]
3. Li Y, Chen L, Zhang C, Wang Y, Hu J, Zhou M, et al. Clinicopathologic features and pathogens of granulomatous lobular mastitis. Breast Care (Basel). 2023; 18: 130-140. (PMID: 37261131) [Crossref]
4. Liu R, Luo Z, Dai C, Wei Y, Yan S, Kuang X, et al. Corynebacterium parakroppenstedtii secretes a novel glycolipid to promote the development of granulomatous lobular mastitis. Signal Transduct Target Ther. 2024; 9: 292. (PMID: 39428541) [Crossref]
5. Zeng W, Lao S, Jia W, Shen X, Wu L, Zhong Y, et al. Clinical features and recurrence of Corynebacterium kroppenstedtii infection in patients with mastitis. BMC Womens Health. 2022; 22: 276. (PMID: 35794560) [Crossref]
6. Wang J, Zhang Y, Lu X, Xi C, Yu K, Gao R, et al. Idiopathic granulomatous mastitis with skin rupture: a retrospective cohort study of 200 patients who underwent surgical and nonsurgical treatment. J Invest Surg. 2021; 34: 810-815. (PMID: 31818161) [Crossref]
7. Çetin K, Sıkar HE, Göret NE, Rona G, Barışık NÖ, Küçük HF, et al. Comparison of topical, systemic, and combined therapy with steroids on idiopathic granulomatous mastitis: a prospective randomized study. World J Surg. 2019; 43: 2865-2873. (PMID: 31297582) [Crossref]
8. Çetin K, Sıkar HE, Feratoğlu F, Taşdoğan B, Güllüoğlu BM. Treatment of granulomatous mastitis with steroids: should the decision to end the treatment be made radiologically? Eur J Breast Health. 2023; 20: 25-30. (PMID: 38187102) [Crossref]
9. Li S, Huang Q, Song P, Han X, Liu Z, Zhou L, et al. Clinical characteristics and therapeutic strategy of granulomatous mastitis accompanied by Corynebacterium kroppenstedtii: a retrospective cohort study. BMC Womens Health. 2023; 23: 388. (PMID: 37491234) [Crossref]
10. Karanlik H, Ozgur I, Simsek S, Fathalizadeh A, Tukenmez M, Sahin D, et al. Can steroids plus surgery become a first-line treatment of idiopathic granulomatous mastitis? Breast Care (Basel). 2014; 9: 338-342. (PMID: 25759614) [Crossref]
11. Li Q, Wan J, Feng Z, Shi J, Wei W. Predictive significance of the preoperative neutrophil-lymphocyte ratio for recurrence in idiopathic granulomatous mastitis patients. Am Surg. 2023; 89: 5577-5583. (PMID: 36880848) [Crossref]
12. Wu R, Zhang H, Wang Y, Mo Y, Hu H, Chen J, et al. A new stage for predicting the prognosis of granulomatous lobular mastitis. PLoS One. 2025; 20: e0319956. (PMID: 40106498) [Crossref]
13. Basim P, Argun D, Argun F. Risk factors for idiopathic granulomatous mastitis recurrence after patient-tailored treatment: do we need an escalating treatment algorithm? Breast Care (Basel). 2022; 17: 172-179. (PMID: 35707181) [Crossref]
14. Yılmaz TU, Gürel B, Güler SA, Baran MA, Erşan B, Duman S, et al. Scoring idiopathic granulomatous mastitis: an effective system for predicting recurrence? Eur J Breast Health. 2018; 14: 112-116. (PMID: 29774320) [Crossref]
15. Yaghan R, Hamouri S, Ayoub NM, Yaghan L, Mazahreh T. A proposal of a clinically based classification for idiopathic granulomatous mastitis. Asian Pac J Cancer Prev. 2019; 20: 929-934. (PMID: 30912417) [Crossref]
16. Li L, Yang W, Jia H. Deep learning models for predicting the recurrence of idiopathic granulomatous mastitis. J Inflamm Res. 2025; 18: 2943-2953. (PMID: 40026307) [Crossref]
17. Ma L, Du P, Sun X, Zhu L, Li Y, Li X, et al. Correlation analysis and construction of a predictive model between contrast-enhanced ultrasound features and the risk of recurrence in granulomatous mastitis. Acad Radiol. 2025; 32: 3170-3180. (PMID: 39843281) [Crossref]
18. Zhou F, Liu L, Yu ZG. Expert consensus on the diagnosis and treatment of non-puerperal mastitis. Chinese Journal of Practical Surgery. 2016;36:755-758. [Crossref]
19. Kursa MB, Rudnicki WR. Feature Selection with the Boruta Package. Journal of Statistical Software. 2010; 36: 1-13. [Crossref]
20. Chang W, Cheng J, Allaire J, Sievert C, Schloerke B, Xie Y, et al. Shiny: web application framework for R. 2022. R package version 1.7.4. Available link: https://CRAN.R-project.org/package=shiny. [Crossref]
21. R Core Team. R: a language and environment for statistical computing. 2022. R Foundation for Statistical Computing, Vienna, Austria. Available link: https://www.R-project.org/. [Crossref]
22. Meyer D, Dimitriadou E, Hornik K, Weingessel A, Leisch F. e1071: misc functions of the department of statistics, probability theory group (Formerly: E1071), TU Wien. 2023. R package version 1.7-14. Available link: https://CRAN.R-project.org/package=e1071. [Crossref]
23. Venables WN, Ripley BD. Modern applied statistics with S. Fourth Edition. Springer, New York; 2022.
24. Karatzoglou A, Smola A, Hornik K. Kernlab: kernel-based machine learning lab. 2023. R package version 0.9-32. Available link: https://CRAN.R-project.org/package=kernlab. [Crossref]
25. Liaw A, Wiener M. Classification and regression by randomforest. R News 2002; 2: 18-22. Available link: https://journal.r-project.org/articles/RN-2002-022/RN-2002-022.pdf [Crossref]
26. Sun J, Shao S, Wan H, Wu X, Feng J, Gao Q, et al. Prediction models for postoperative recurrence of non-lactating mastitis based on machine learning. BMC Med Inform Decis Mak. 2024; 24: 106. (PMID: 38649879) [Crossref]

27. Velidedeoglu M, Kundaktepe BP, Aksan H, Uzun H. Preoperative fibrinogen and hematological indexes in the differential diagnosis of idiopathic granulomatous mastitis and breast cancer. Medicina (Kaunas). 2021; 57: 698. (PMID: 34356979) [Crossref]

28. Ciftci AB, Bük ÖF, Yemez K, Polat S, Yazıcıoğlu İM. Risk factors and the role of the albumin-to-globulin ratio in predicting recurrence among patients with idiopathic granulomatous mastitis. J Inflamm Res. 2022; 15: 5401-5412. (PMID: 36158516) [Crossref]

ORIGINAL ARTICLE

European Journal of BREAST HEALTH

DOI: 10.4274/ejbh.galenos.2026.2026-2-3
Eur J Breast Health 2026;22(3):318-327

Real-World Effectiveness and Safety of Tucatinib, Trastuzumab, and Capecitabine in HER2-Positive Advanced Breast Cancer: A Multicenter Portuguese Study

Rita Quaresma Ferreira[1], Carolina Brandão Monteiro[2], Ana Catarina Dias[3], Francisca Abreu[3], Bogdana Darmits[4], Maria João Oura[5], Inês Ângelo[6], Joana Cabral[7], Alice Figueiredo[8], Ricardo Ferreira[9], Diogo Alpuim Costa[10], Maria Teresa Marques[11], Tiago Pina-Cabral[12], Filipe Araújo[13], Sandra Bento[14], Catarina Lopes Fernandes[15], Mariana Santiago[16], Bruno Silva[17], Maria Alexandra Montenegro[1], Diana Cardoso Simão[1], Leonor Fernandes[1], Sónia Duarte Oliveira[18]

[1]Department of Medical Oncology, Local Health Unit of São José, Academic Clinical Center, Lisbon, Portugal
[2]Department of Medical Oncology, Local Health Unit of Santa Maria, Lisbon, Portugal
[3]Department of Medical Oncology, Local Health Unit of Alto Ave, Guimarães, Portugal
[4]Department of Medical Oncology, Instituto Português de Oncologia de Coimbra Francisco Gentil, Coimbra, Portugal
[5]Department of Medical Oncology, Local Health Unit of São João, Porto, Portugal
[6]Department of Medical Oncology, Local Health Unit of Arco Ribeirinho, Barreiro, Portugal
[7]Department of Medical Oncology, Local Health Unit of Gaia and Espinho, Espinho, Portugal
[8]Department of Medical Oncology, Instituto Português de Oncologia de Lisboa Francisco Gentil, Lisbon, Portugal
[9]Department of Medical Oncology, Local Health Unit of Amadora/Sintra, Sintra, Portugal
[10]Oncology Functional Unit, Hospital de Cascais (Alcabideche), Cascais, Portugal
[11]Department of Medical Oncology, Local Health Unit of Arrábida, Setúbal, Portugal
[12]Department of Medical Oncology, Local Health Unit of Lisboa Ocidental, Lisbon, Portugal
[13]Department of Medical Oncology, Local Health Unit of Santo António, Porto, Portugal
[14]Department of Medical Oncology, Local Health Unit of Lezíria, Santarém, Portugal
[15]Department of Medical Oncology, Local Health Unit of Matosinhos, Matosinhos, Portugal
[16]Department of Medical Oncology, Local Health Unit of Almada/Seixal, Seixal, Portugal
[17]Department of Medical Oncology, Local Health Unit of Loures/Odivelas, Odivelas, Portugal
[18]Department of Hematology-Oncology, University Hospitals Seidman Cancer Center, Cleveland, United States

Corresponding Author: Rita Quaresma Ferreira MD
E-mail: ritaquaferreira@hotmail.com **ORCID:** orcid.org/0009-0006-7628-2886

Received: 12.02.2026 **Accepted:** 20.03.2026 **Available Online Date:** 17.06.2026
Cite this article as: Ferreira RQ, Monteiro CB, Dias AC, Abreu F, Darmits B, Oura MJ, et al. Real-world effectiveness and safety of tucatinib, trastuzumab, and capecitabine in HER2-positive advanced breast cancer: a multicenter Portuguese study. Eur J Breast Health. 2026;22(3):318-327

ABSTRACT

Objective: The HER2CLIMB trial demonstrated the benefit of tucatinib, trastuzumab and capecitabine (TTC) in human epidermal growth factor receptor 2 (HER2)-positive advanced breast cancer (ABC). However, it predated the clinical use of trastuzumab deruxtecan (T-DXd), leaving limited evidence for TTC after T-DXd exposure. This national multicenter study assessed the real-world effectiveness and safety of TTC in patients, including those previously treated with T-DXd.

Materials and Methods: This retrospective, non-interventional study included patients with HER2-positive ABC treated with TTC across 17 centers in Portugal (October 2021-May 2025). Outcomes included overall response rate (ORR), disease control rate (DCR), progression-free survival (PFS), overall survival (OS), and safety.

Results: Eighty-one patients were included (median age 54 years). Of the patients, 39.5% (n = 32) had brain metastases, and 61.7% (n = 50) had prior T-DXd exposure. Median follow-up was 21.0 months; ORR and DCR were 24.4% and 64.1%, respectively. Median PFS (mPFS) was 9.0 months (m) [95% confidence interval (CI): 5.9–12.1], and median OS (mOS) was 14.0 months (m) (95% CI: 10.5–17.5). In patients previously treated with T-DXd, the median mPFS 7.0 m (95% CI: 3.6–10.4) and 13.0 m (95% CI: 9.3–16.7), respectively. Among patients with brain metastases, mPFS was 12.0 m (95% CI: 6.7–17.3) and mOS was 17.0 m (95% CI: 12.9–21.1). The most frequent all grade adverse events were fatigue (58.0%) and diarrhea (56.8%); CTCAE grade ≥3 events occurred in 16.0%. Treatment discontinuation due to toxicity occurred in 7.4% of participants; there were no treatment-related deaths.

Conclusion: In this national real-world cohort, TTC demonstrated clinically meaningful activity and was not associated with any new safety signals in HER2-positive ABC, including patients previously exposed to T-Dxd and those with brain metastases.

Keywords: Breast cancer, HER2 protein, tucatinib, real-world data, survival analysis

KEY POINTS

- There is limited real-world evidence and a lack of prospective trial data specifically addressing the efficacy and safety of tucatinib, trastuzumab, and capecitabine (TTC) after trastuzumab deruxtecan (T-DXd) in HER2-positive advanced breast cancer.
- This national, multicenter, real-world study evaluated TTC in 81 patients who were treated at 17 oncology centers in Portugal.
- In the cohort, TTC achieved an overall response rate of 24.4%, a median progression-free survival of 9.0 months, and a median overall survival of 14.0 months.
- Clinical activity was maintained in patients previously treated with T-DXd and patients with central nervous system (CNS) metastases, including active CNS disease.
- TTC was generally well tolerated, with low rates of grade ≥3 adverse events and no treatment-related deaths.
- These findings provide real-world evidence supporting the effectiveness and safety of TTC in contemporary practice, including the post–T-DXd setting.

Introduction

Breast cancer (BC) is a major public health concern and the leading cause of cancer-related death among women worldwide, accounting for nearly one in four cancer diagnoses and one in six cancer deaths (1). In Portugal, approximately 8,950 new cases were diagnosed in 2022 (2). Although most BC are diagnosed at an early stage, 5–8% of patients present with metastatic disease at diagnosis (3).

The human epidermal growth factor receptor 2 (HER2) is encoded by the *ERBB2* gene and is a transmembrane tyrosine kinase (TK) receptor that activates multiple intracellular signaling pathways involved in cell growth and development (4). HER2 gene amplification and/or protein overexpression occurs in approximately 15–20% of BC cases (5), and is associated with a more aggressive phenotype, characterized by a higher risk of metastases—particularly to visceral organs and the central nervous system (CNS) (3).

Over the past two decades, the HER2 receptor has emerged as an effective therapeutic target, with the development of several targeted therapies. The introduction of HER2-targeted therapies, such as trastuzumab and pertuzumab, has significantly redefined the treatment of HER2-positive advanced BC (ABC), providing substantial improvements in clinical outcomes and patient survival. Nevertheless, as patients live longer, the incidence of CNS metastases has been rising, affecting up to 50% of individuals with HER2+ BC (6, 7), and it is generally associated with poor prognosis (8). Therapeutic options in this setting remain limited, largely because most HER2-targeted agents and chemotherapy demonstrate suboptimal intracranial activity (9).

Tucatinib is an oral TK inhibitor highly selective for the HER2 receptor kinase domain (10).

The pivotal phase II HER2CLIMB trial evaluated the efficacy and safety of tucatinib versus placebo, each combined with trastuzumab and capecitabine, in patients with HER2-positive ABC who had previously been treated with trastuzumab,

pertuzumab, and trastuzumab emtansine (T-DM1) (11). The study notably included patients with stable and active CNS metastases demonstrated significant improvements in progression-free survival (PFS) and overall survival (OS) in the tucatinib, trastuzumab and capecitabine (TTC) arm, including in patients with active CNS metastases. The combination was generally well tolerated, with serious adverse events (AEs) mainly related to palmar-plantar erythrodysesthesia (PPE) and diarrhea.

Given the substantial cohort of patients with CNS involvement in the HER2CLIMB trial, tucatinib has emerged as a pivotal, albeit not exclusive, therapeutic option for this patient subgroup. According to the European Society for Medical Oncology guidelines, second-line treatment for HER2-positive ABC primarily includes trastuzumab deruxtecan (T-DXd), with TTC also listed as an option, particularly for patients with CNS metastases; otherwise, it is mainly recommended in the third-line setting (12).

While the HER2CLIMB trial established the tucatinib regimen as an effective option, limited evidence exists on its real-world efficacy and safety. Furthermore, because the study predated widespread T-DXd use, there is a critical need for data on tucatinib's effectiveness in patients previously treated with T-DXd, which would better reflect current clinical practice.

This study aims to evaluate TTC therapy in a real-world setting and to provide data on its efficacy and safety in patients treated at national centers. To our knowledge, there are no previous similar studies in the Portuguese population.

Materials and Methods

Study Design and Population

This retrospective, multicenter, non-interventional study was conducted at 17 oncology centers in Portugal. It included patients aged ≥18 years with HER2-positive ABC who received at least one cycle of the TTC regimen for advanced disease until 31 May 2025. Eligibility was not restricted by Eastern Cooperative Oncology Group (ECOG) performance status (PS) or prior lines of therapy. Patients were excluded if they had not received systemic therapy for advanced disease, or if they had a history of another malignancy within 6 months before the diagnosis of ABC.

HER2 positivity was determined at each participating center and defined as either 3+ immunohistochemical (IHC) staining or 2+ IHC staining with positive fluorescence *in situ* hybridization or silver-enhanced *in situ* hybridization.

The TTC regimen comprised tucatinib (300 mg orally twice daily throughout the treatment period), trastuzumab (6 mg/kg intravenously once every 21 days, or 600 mg subcutaneously once every 21 days), and capecitabine (1,000 mg/m² orally twice daily on days 1 to 14 of each 21-day cycle). The TTC regimen was administered until disease progression, unacceptable toxicity, or patient preference.

Data Collection

Eligible patients were identified at participating centers through electronic medical records, and demographic and clinicopathological data were pseudonymized prior to analysis.

The collected baseline variables included age, ECOG (PS, metastatic sites, number of involved organs, and prior lines of therapy. CNS metastases were categorized as active—defined as untreated lesions or previously treated lesions showing progression immediately before starting TTC, without requiring urgent local intervention—or stable. Ongoing use of corticosteroids was permitted.

Histopathological characteristics were also recorded, including the BC subtype and hormone receptor (HR) status (estrogen and progesterone receptors). TTC treatment duration, clinical response, and AEs were also recorded.

Efficacy Assessment

Tumor response was assessed according to local clinical practice, based on imaging studies and clinical evaluation; radiologic response and disease progression at each center were evaluated using response evaluation criteria in solid tumors (RECIST v1.1) and response assessment in neuro-oncology brain metastases (RANO-BM). Patients who discontinued treatment or died before the first radiological assessment were considered non-evaluable for response.

Efficacy outcomes included OS, defined as the time from TTC treatment initiation to death from any cause; PFS, defined as the time from TTC treatment initiation to disease progression or death from any cause; overall response rate (ORR), defined as the proportion of patients achieving complete response (CR) or partial response (PR); and disease control rate (DCR), defined as the proportion of patients with stable disease (SD) in addition to those with an objective response. Patients who had not experienced an event by the data cut-off were censored on the date of their last documented follow-up.

Outcomes were evaluated across the overall cohort, and additional subgroup analyses were performed to explore treatment outcomes in patients with CNS metastases and in those previously treated with T-DXd.

Safety Assessment

AEs were extracted from medical records and graded on the Common Terminology Criteria for Adverse Events (CTCAE), version

5.0 (13). Safety outcomes included the incidence of grade ≥3 AEs and treatment discontinuation due to toxicity.

Statistical Analysis

All statistical analyses were performed using IBM SPSS statistics® version 25.0. Continuous variables are presented as medians with 95% confidence intervals (CIs) and interquartile ranges (IQRs); categorical variables are presented as absolute and relative frequencies. Survival outcomes (OS and PFS) were estimated using the Kaplan-Meier method, with group comparisons performed using the log-rank test, and hazard ratios (HRs) with 95% CIs were estimated using Cox proportional hazards regression. A *p*-value <0.05 was considered statistically significant.

Ethics Approval

This study was approved by the Ethics Committee of the Local Health Unit of São José (approval number: 1728/2025_MJH/MAB/NO, date: 10.10.2025).

Results

Patient Characteristics

A total of 81 patients with HER2-positive ABC were enrolled at 17 oncology centers in Portugal and received TTC. All patients were female, with a median age of 54 years (IQR 48–62); fourteen patients (17.3%) were older than 65 years. The majority (n = 76, 93.8%) had an ECOG PS of 0 or 1. Regarding tumor biology, 72.8% (n = 59) had HR–positive disease, and invasive carcinoma of no special type was the most common histologic subtype (n = 73, 90.1%). At diagnosis, approximately one- third of patients (n = 29, 35.8%) presented with metastatic disease. The most frequent metastatic sites were bone (n = 53, 65.4%), liver (n = 37, 45.7%), and lung (n = 37, 45.7%). Thirty-two patients (39.5%) had CNS metastases, of whom 62.5% (n = 20) were active. The median number of prior treatment lines for metastatic disease was 3 (IQR 2–3, range 2–8). TTC was third-line therapy in 37.0% (n = 30) and fourth-line therapy in 48.1% (n = 39) of patients. Prior exposure to anti-HER2 agents included trastuzumab in 79 patients (97.5%), pertuzumab in 71 patients (87.7%), trastuzumab emtansine (T-DM1) in 76 patients (93.8%), and trastuzumab deruxtecan (T-DXd) in 50 patients (61.7%). Additionally, 77 patients (95.1%) had previously received chemotherapy.

Among patients previously treated with T-DXd, 86.0% (n = 43) initiated TTC immediately after disease progression. In this subgroup, the median age at TTC initiation was 53.5 years (IQR 48–62), and 94.0% (n = 47) had an ECOG PS of 0 or 1. CNS metastases were present in 28.0% (n = 14), of which 57.1% (n = 8) were active. Table 1 summarizes patient characteristics.

Table 1. Baseline demographics and clinical characteristics of patients with HER2 + MBC receiving TTC

Characteristics	Overall cohort (n = 81)	Patients previously treated with T-DXd (n = 50)
Female sex, n (%)	81 (100)	50 (100)
Age at TTC initiation, median (IQR), years	54.0 (48–62)	53.5 (48–62)
ECOG Performance Status score, n (%)		
0	30 (37.0)	21 (42.0)
1	46 (56.8)	26 (52.0)
2	5 (6.2)	3 (6.0)
Hormone-receptor status, n (%)		
Positive for ER, PR, or both	59 (72.8)	38 (76.0)
Negative for ER and PR	22 (27.2)	12 (24.0)
Histology, n (%)		
No special type	73 (90.1)	44 (88.0)
Lobular	6 (7.4)	5 (10.0)
Other	2 (2.5)	1 (2.0)
Stage IV at initial diagnosis, n (%)	29 (35.8)	18 (36.0)
Sites of metastasis, n (%)[a]		
Bone	53 (65.4)	35 (70.0)
Liver	37 (45.7)	21 (42.0)
Lung	37 (45.7)	27 (54.0)
CNS	32 (39.5)	14 (28.0)
Cutaneous	16 (19.8)	9 (18.0)
Other	19 (23.5)	10 (20.0)
Previous therapies in metastatic setting, n (%)		
Trastuzumab	79 (97.5)	48 (96.0)
Pertuzumab	71 (87.7)	44 (88.0)
T-DM1	76 (93.8)	45 (90.0)
T-DXd	50 (61.7)	50 (100)
Lapatinib	8 (9.9)	6 (12.0)
Chemotherapy	77 (95.1)	49 (98.0)
Metastatic treatment line at TTC initiation, n (%)		
Third line	30 (37.0)	5 (10.0)
Fourth line	39 (48.1)	37 (54.0)
Others	12 (14.8)	8 (16.0)

ECOG: Eastern Cooperative Oncology Group; ER: Estrogen receptor; IQR: Interquartile range; PR: Progesterone receptor; T-DM1: Ado-trastuzumab emtansine; T-DXd: Trastuzumab deruxtecan; TTC: Tucatinib, trastuzumab andcapecitabine; IQR: Interquartile range; HER2: Human epidermal growth factor receptor 2; MBC: Metastatic breast cancer, a: Not mutually exclusive

Efficacy Outcomes

All patients received TTC according to the approved dosing schedule and were October 1, 2021 and May 31, 2025. The median follow-up was 21.0 months, with patients receiving a median of 7 cycles of TTC (range, 1–36). At the data cut-off (December 2025), 9 patients (11.1%) remained on active treatment, while 65 patients (80.2%) discontinued TTC due to disease progression, and 7 patients (8.6%) discontinued due to toxicity. Seventy-eight of 81 patients were evaluable for response according to RECIST v1.1 and RANO-BM. Three patients were not evaluable for response: one died from a non–treatment-related cause before the first assessment; one discontinued treatment due to toxicity; and one discontinued due to clinical deterioration.

In the overall cohort, the ORR was 24.4%, including 2 CR (2.6%) and 17 PR (21.8%). An additional 31 patients (39.7%) experienced SD, resulting in a DCR of 64.1%. Thirty-one patients (39.7%) had disease progression as their best response. Median OS (mOS) was 14.0 months (95% CI: 10.5–17.5) (Figure 1), with a 12-month OS rate of 59.1%. Median PFS (mPFS) was 9.0 months (95% CI: 5.9–12.1; Figure 2), and the 12-month PFS rate was 38.0%. Response and survival outcomes are summarized in Tables 2 and 3.

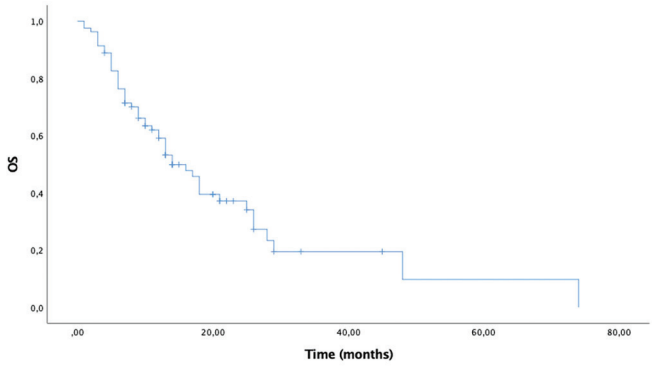

Figure 1. Kaplan-Meier curves for overall survival (OS) in the overall cohort

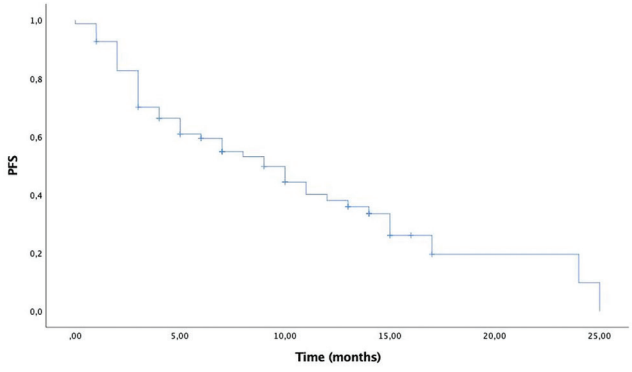

Figure 2. Kaplan-Meier curves for progression-free survival (PFS) in the overall cohort

Among patients previously treated with T-DXd, the ORR was 23.4%, including 9 patients (19.1%) with PR and 2 patients (4.3%) with CR, yielding a DCR of 61.7%. In this subgroup, mPFS was 7.0 months (95% CI: 3.6–10.4), and mOS was 13.0 months (95% CI: 9.3–16.7). In the subgroup of 31 patients who had not received T-DXd prior to TTC, the ORR was 25.8% and the DCR was 67.7%. The mOS was 28.0 months (95% CI: 11.5–44.5), and the mPFS was 12.0 months (95% CI: 6.8–17.2). The mOS was significantly longer in T-DXd–naïve patients compared with those previously treated with T-DXd ($p = 0.032$; HR: 0.52; 95% CI: 0.28–0.97) (Figure 3), whereas no statistically significant difference was detected in mPFS ($p = 0.104$; HR: 0.63; 95% CI: 0.35–1.13) (Figure 4).

Among the 32 patients with CNS metastases, the ORR was 15.6% (4 PR, 1 CR), and the DCR was 71.9%. The mPFS in patients with CNS involvement was 12.0 months (95% CI: 6.7–17.3), and the mOS was 17.0 months (95% CI: 12.9–21.1). In patients with active CNS metastases ($n = 20$), mPFS was 10.0 months (95% CI: 4.0–16.0); in those with stable CNS metastases ($n = 12$), mPFS was 14.0 months (95% CI: 4.3–23.7). The mOSs were 13.0 months (95% CI: 4.9–21.1) and 18.0 months (95% CI: 8.7–27.3), respectively.

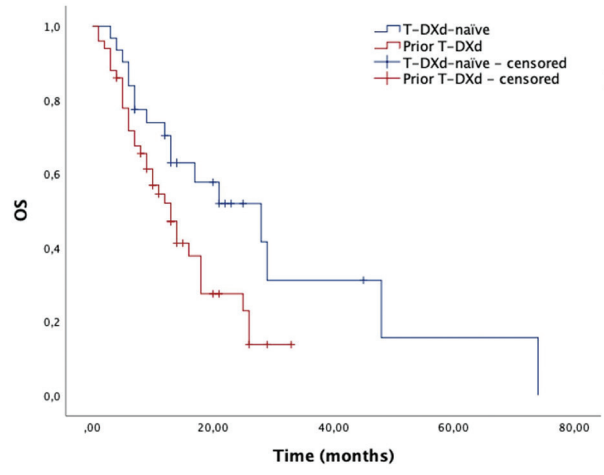

Figure 3. Kaplan-Meier curves for overall survival (OS) according to prior exposure to trastuzumab deruxtecan (T-DXd). Median OS was 28.0 months in T-DXd–naïve patients and 13.0 months in those previously treated with T-DXd (log-rank $p = 0.032$; HR: 0.52; 95% CI: 0.28–0.97)

HR: Hazard ratio; CI: Confidence interval

Table 2. Best overall response to tucatinib in combination with trastuzumab and capecitabine according to RECIST v1.1 in the overall cohort and key subgroups

Efficacy measures	Overall cohort (*n* = 81)	Patients previously treated with T-DXd (*n* = 50)	Patients with CNS metastasis (*n* = 32)
Best overall response according to RECIST v1.1[a], n (%)			
Complete response	2 (2.6)	2 (4.3)	1 (3.1)
Partial response	17 (21.8)	9 (19.1)	4 (12.5)
Stable disease	31 (39.7)	18 (38.3)	18 (56.3)
Progressive disease	31 (39.7)	21 (44.7)	9 (28.1)
Not available	3	3	0
Rate of response, (%)			
Overall response rate	24.4	23.4	15.6
Disease control rate	64.1	61.7	71.9

CNS: Central nervous system; RECIST: Response Evaluation Criteria in Solid Tumors; T-DXd: Trastuzumab deruxtecan

[a]: Responses were assessed by local investigators according to RECIST version 1.1

Table 3. Progression-free survival and overall survival outcomes in the overall cohort and predefined subgroups treated with tucatinib, trastuzumab, and capecitabine

	No of patients	PFS		OS	
		Median (95% CI), months	12-month rate (%)	Median (95% CI), months	12-month rate (%)
Overall cohort	81	9.0 (5.9–12.1)	38.0	14.0 (10.5–17.5)	59.1
Patients with no prior exposure to T-DXd	31	12.0 (6.8–17.2)	67.2	28.0 (11.5–44.5)	70.4
Patients previously treated with T-DXd	50	7.0 (3.6–10.4)	30.7	13.0 (9.3–16.7)	52.1
Duration of previous T-DXd treatment (months)					
<6	10	6.0 (2.0–10.0)	36.0	16.0 (8.8–23.2)	68.6
≥6 to ≤12	13	5.0 (0.0–11.5)	46.2	10 (1.7–18.3)	44.9
>12	27	8.0 (3.4–12.6)	28.7	12 (8.1–15.9)	49.9
TTC immediately after T-DXd treatment					
Yes	43	7.0 (3.9–10.1)	31.5	14 (11.5–16.5)	56.2
No	7	3.0 (2.2–3.8)	28.6	6.0 (3.4–8.6)	28.6
Population with CNS metastases	32	12.0 (6.7–17.3)	46.2	17.0 (12.9–21.1)	61.8
Type					
Active	20	10.0 (4.0–16.0)	41.1	13.0 (4.9–21.1)	55.0
Stable	12	14.0 (4.3–23.7)	54.7	18.0 (8.7–27.3)	72.2

CNS: Central nervous system; T-DXd: Trastuzumab deruxtecan; TTC: Tucatinib, trastuzumab and capecitabine; CI: Confidence interval; OS: Overal survival; PFS: Progression-free survival

Safety

Seventy-four patients (91.4%) experienced treatment-related AEs of any grade. The most frequent AEs were fatigue (*n* = 47, 58.0%), diarrhea (*n* = 46, 56.8%), PPE (*n* = 35, 43.2%), nausea (*n* = 29, 35.8%), and elevated liver enzymes (*n* = 23, 28.4%). Ten patients (12.3%) experienced grade 3 AEs, mainly dermatologic and gastrointestinal: the most common were PPE (*n* = 5, 6.2%) and diarrhea (*n* = 3, 3.7%). In total, 13 grade-3 events occurred, as some patients experienced multiple severe AEs. There were no grade 4 events. In patients aged ≥65 years (*n* = 14), 13 (92.9%) experienced treatment-related AEs of any grade with fatigue and PPE being the most common; 3 patients (21.4%) experienced grade 3 AEs including PPE (*n* = 2) and hyperbilirubinemia (*n* = 1).

Thirty-three patients (40.7%) received prophylaxis. Twenty-seven patients (33.3%) required dose modifications due to toxicity

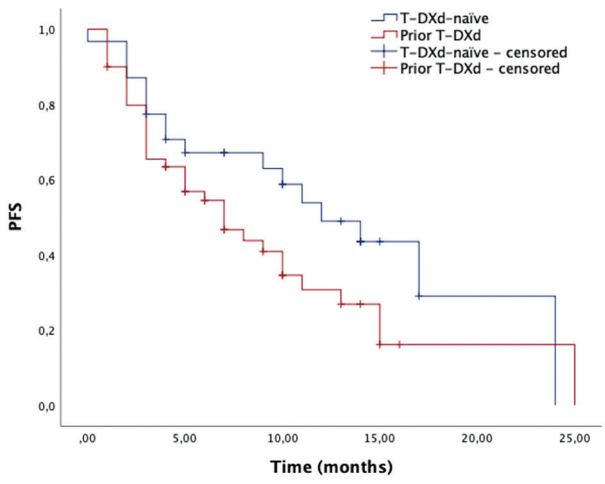

Figure 4. Kaplan-Meier curves for progression-free survival (PFS) according to prior exposure to trastuzumab deruxtecan (T-DXd). Median PFS was 12.0 months in T-DXd–naïve patients and 7.0 months in patients previously treated with T-DXd (log-rank $p = 0.104$; HR: 0.63; 95% CI: 0.35–1.13)

HR: Hazard ratio; CI: Confidence interval

and 36 (44.4%) required temporary treatment interruptions. Six patients (7.4%) discontinued treatment due to grade 3 PPE ($n = 2$), grade 3 diarrhe a ($n = 1$), grade 3 stomatitis ($n = 1$), grade 3 elevation of aspartate aminotransferase ($n = 1$), and grade 2 vomiting and diarrhea ($n = 1$). No treatment-related deaths occurred. Table 4 summarizes overall and grade 3 AEs according to CTCAE.

Discussion and Conclusion

The therapeutic landscape of HER2-positive ABC is rapidly evolving, with the emergence of multiple anti-HER2 therapies, including the TTC combination. This multicenter, real-world Portuguese study evaluated TTC in 81 patients with HER2-positive ABC at 17 oncology centers nationwide. It–expands–current evidence on the effectiveness of TTC in patients previously treated with T-DXd, now established as the standard first- or second-line therapy (14, 15). Importantly, it provides contemporary data in the post–T-DXd setting, where prospective trial evidence remains limited, and enables a pragmatic assessment of TTC sequencing after antibody–drug conjugate therapy.

Several baseline characteristics distinguish our real-world population from those in the HER2CLIMB trial and should be considered when interpreting the results. Compared with the trial population, our cohort reflects broader eligibility criteria and the heterogeneity typically seen in routine practice, including patients with ECOG PS 2 and a higher burden of visceral disease, particularly liver metastases. Conversely,

Table 4. Incidence of treatment-related adverse events of any grade and grade 3 among patients treated with tucatinib, trastuzumab, and capecitabine in the overall cohort

Adverse events	Any grade[a] n (%)	Grade 3[a] n (%)
Any adverse event	74 (91.4)	13 (16.0)
Fatigue	47 (58.0)	0 (0)
Diarrhea	46 (56.8)	3 (3.7)
PPE syndrome	35 (43.2)	5 (6.2)
Nausea	29 (35.8)	0 (0)
Aspartate aminotransferase increased	21 (25.9)	0 (0)
Alanine aminotransferase increased	20 (24.7)	2 (2.5)
Vomiting	17 (21.0)	0 (0)
Stomatitis	12 (14.8)	1 (1.2)
Decreased appetite	4 (4.9)	0 (0)
Decreased ejection fraction	4 (4.9)	0 (0)
Onycholysis	3 (3.7)	1 (1.2)
Dysgeusia	3 (3.7)	0 (0)
Neutropenia	2 (2.5)	0 (0)
Blood bilirubin increased	2 (2.5)	1 (1.2)
Anemia	1 (1.2)	0 (0)

PPE: Palmar-plantar erythrodysesthesia

[a]: Adverse events were graded according to the Common Terminology Criteria for Adverse Events, version 5.0

our cohort included a lower proportion of patients with CNS metastases and fewer active CNS lesions at treatment initiation. This may reflect differences in imaging strategies: routine brain imaging was mandatory in HER2CLIMB, whereas in routine practice imaging is often symptom-driven, potentially leading to underdiagnosis of asymptomatic disease. An additional distinguishing feature of this study is the high proportion of patients previously treated with. At the time of HER2CLIMB enrollment, T-DXd was not part of the therapeutic landscape, leaving uncertainty regarding the efficacy and safety of TTC after prior exposure, an issue addressed by this real-world analysis.

Despite these differences, TTC demonstrated clinically meaningful efficacy in this real-world cohort. When focusing on the subgroup of patients not previously exposed to T-DXd—more closely reflecting the HER2CLIMB population—both mOS and mPFS were numerically longer than those reported in the pivotal trial (mOS 28.0 *vs.* 21.9 months; mPFS 12.0 *vs.* 7.8 months), suggesting that TTC retains clinical activity in routine practice in this setting.

In the overall cohort, PFS was comparable to that observed in HER2CLIMB, with a modestly longer median PFS and 12-month PFS rate This difference likely reflects variations in prior treatment exposure—particularly the inclusion of patients previously treated with T-DXd—and a less-selective patient population. When considered alongside other real-world series, the survival outcomes in our study fall within the range reported in contemporary cohorts, including a French real-world series that enrolled patients treated with TTC after prior T-DXd exposure, despite differences in sample size, follow-up duration, and treatment sequencing (16).

Within the population previously treated with T-DXd, TTC retained clinically meaningful activity, with an mOS of 13.0 months and an mPFS of 7.0 months. These outcomes align with those reported in other real-world cohorts evaluating TTC after prior T-DXd exposure, including the aforementioned French cohort and two American real-world analyses (17, 18). In those studies, median PFS ranged from 4.7 to 5.5 months among patients receiving tucatinib-based regimens after T-DXd, with a median of three to four prior lines of therapy, reflecting that these patients were more heavily pretreated than those in our cohort. Together, these findings indicate that TTC retains activity after T-DXd exposure across different clinical settings, despite variations in cohort size, prior treatment burden, follow-up duration, and treatment sequencing. In our study, prior exposure to T-DXd was associated with worse overall survival, whereas T-DXd–naïve patients exhibited a lower risk of death (HR: 0.52; 95% CI: 0.28–0.97). Although no statistically significant difference in mPFS was detected between the two subgroups, given the limitations of the sample size ($p = 0.104$), the approximately 5-month difference in median PFS favoring T-DXd-naïve patients may still be clinically meaningful. Emerging evidence suggests that prior exposure to antibody–drug conjugates such as T-DXd, beyond representing a more heavily pretreated population, may induce biological changes—including loss of HER2 expression, altered HER2 binding, and increased drug efflux—that could attenuate, but not eliminate, sensitivity to subsequent HER2-directed therapies. These mechanisms may contribute to the reduced magnitude and durability of responses observed in the post–T-DXd setting (19-21). Given the recent shift toward the earlier use of T-DXd, the post–T-DXd subgroup in our cohort likely reflects early real-world experience following its integration into routine practice. Consequently, outcomes with TTC in this subgroup should be interpreted in the context of this evolving therapeutic landscape. In addition, survival comparisons by prior T-DXd exposure were based on univariate analyses, and multivariable adjustment was not performed due to the limited sample size and the number of events. Therefore, the observed differences in survival outcomes may have been influenced by baseline imbalances in prognostic factors, such as prior lines of therapy or disease burden, rather than representing independent treatment effects. These findings should therefore be interpreted as descriptive and hypothesis-generating.

Notably, most patients (86.0%) initiated TTC immediately after progression on T-DXd. Direct sequencing of TTC after T-DXd was associated with numerically longer mPFS and higher 12-month OS rates than in patients who received other systemic therapies between T-DXd and TTC (Table 3). The observed differences in outcomes could be due to the sequence of treatments or to a greater cumulative treatment burden among patients.

The TTC activity in CNS metastases was particularly noteworthy. In our study, mPFS among patients with CNS involvement reached 12 months, exceeding results reported in HER2CLIMB and other real-world cohorts (16, 17), and further supporting the intracranial activity of TTC. As expected, patients with stable CNS disease experienced more favorable outcomes than those with active CNS metastases. These findings support the role of TTC as a relevant therapeutic option for patients with CNS involvement, a population with historically limited therapeutic alternatives.

To our knowledge, real-world data specifically addressing the safety of TTC after T-DXd exposure remain limited. In this cohort, the tolerability of TTC was consistent with the safety profile reported in HER2CLIMB. As in the HER2CLIMB trial, the most common AEs associated with TTC were diarrhea, PPE, nausea, fatigue, and elevations in hepatic transaminases. AEs of any grade were reported in 91.4% of patients in our cohort, which is comparable to the rate reported in HER2CLIMB. Regarding grade ≥3 AEs, the reported frequency in the present cohort was 16%, which was lower than that observed in the HER2CLIMB trial (55.5%). While this difference should be interpreted with caution, the overall toxicity profile was consistent with that reported in HER2CLIMB, with grade ≥3 events predominantly consisting of PPE, diarrhea, and elevations in hepatic transaminases. Although prophylactic antidiarrheal therapy was not mandated in HER2CLIMB, 40.7% of patients in our cohort received loperamide prophylaxis, which may have contributed to a lower incidence of any-grade diarrhea compared with HER2CLIMB. No new safety signals were identified, and AEs were generally manageable with supportive care measures, dose reductions, and temporary treatment interruptions. Conversely, compared with HER2CLIMB, our study observed slightly higher rates of dose modifications and treatment discontinuation due to AEs, likely reflecting differences in patient selection, comorbidity burden, and toxicity management strategies in routine clinical practice. In HER2CLIMB, capecitabine discontinuation for treatment-related toxicity was permitted while continuing tucatinib and trastuzumab. Although not reported in our cohort, this pragmatic approach could help mitigate toxicity

and prevent premature treatment discontinuation in routine practice.

Study Limitations

Some limitations of this real-world study include inherent challenges of routine clinical practice, in which less-standardized protocols may cause clinicians to inconsistently report treatment-related AEs, potentially underestimating toxicity. In addition, heterogeneity in the timing of radiological response assessments across centers represents a significant limitation compared with centralized imaging evaluation. Survival comparisons by prior T-DXd exposure were based on univariate analyses, as the limited sample size precluded multivariable adjustment; therefore, residual confounding cannot be excluded. The retrospective nature of the study should be considered when interpreting these findings.

This national real-world cohort demonstrates that the TTC regimen has clinically meaningful activity and no unexpected safety signals in patients with HER2-positive ABC, including those with CNS metastases and prior exposure to T-DXd. These findings reinforce the clinical utility of TTC in contemporary practice, including in patients previously treated with T-DXd.

Ethics

Ethics Committee Approval: This study was approved by the Ethics Committee of the Local Health Unit of São José (approval number: 1728/2025_MJH/MAB/NO, date: 10.10.2025).

Informed Consent: Retrospective study.

Footnotes

Authorship Contributions

Surgical and Medical Practices: R.Q.F., C.B.M., A.C.D., F.A., B.D., M.J.O., I.A., J.C., A.F., R.F., D.A.C., M.T.M., T.P.C., F.A., S.B., C.L.F., M.S., B.S., M.A.M., D.C.S., L.F., S.D.O.; Concept: R.Q.F., M.A.M., D.C.S., L.F., S.D.O.; Design: R.Q.F., M.A.M., D.C.S., L.F., S.D.O., Data Collection or Processing: R.Q.F., C.B.M., A.C.D., F.A., B.D., M.J.O., I.A., J.C., A.F., R.F., D.A.C., M.T.M., T.P.C., F.A., S.B., C.L.F., M.S., B.S.; Analysis or Interpretation: R.Q.F., M.A.M., D.C.S., L.F., S.D.O.; Literature Search: R.Q.F., C.B.M., A.C.D., F.A., B.D., M.J.O., I.A., J.C., A.F., R.F., D.A.C., M.T.M., T.P.C., F.A., S.B., C.L.F., M.S., B.S., M.A.M., D.C.S., L.F., S.D.O.; Writing: R.Q.F., C.B.M., A.C.D., F.A., B.D., M.J.O., I.A., J.C., A.F., R.F., D.A.C., M.T.M., T.P.C., F.A., S.B., C.L.F., M.S., B.S., M.A.M., D.C.S., L.F., S.D.O.

Conflict of Interest: No conflict of interest was declared by the authors.

Financial Disclosure: The authors declared that this study received no financial support.

References

1. Bray F, Laversanne M, Sung H, Ferlay J, Siegel RL, Soerjomataram I, et al. Global cancer statistics 2022: GLOBOCAN estimates of incidence and mortality worldwide for 36 cancers in 185 countries. CA Cancer J Clin. 2024; 74: 229-263. (PMID: 38572751) [Crossref]
2. International Agency for Research on Cancer. Portugal fact sheet [Internet]. Lyon: International Agency for Research on Cancer; 2022 [cited 2025 Dec 3]. Report No. Available from: https://gco.iarc.who.int/media/globocan/factsheets/populations/620-portugal-fact-sheet.pdf [Crossref]
3. Gong Y, Liu YR, Ji P, Hu X, Shao ZM. Impact of molecular subtypes on metastatic breast cancer patients: a SEER population-based study. Sci Rep. 2017; 7: 45411. (PMID: 28345619) [Crossref]
4. Galogre M, Rodin D, Pyatnitskiy M, Mackelprang M, Koman I. A review of HER2 overexpression and somatic mutations in cancers. Crit Rev Oncol Hematol. 2023; 186: 103997. (PMID: 37062337) [Crossref]
5. Zhao J, Zhou Z, Saw PE, Song E. Silver Jubilee of HER2 targeting: a clinical success in breast cancer. J Natl Cancer Cent. 2025; 5: 379-391. (PMID: 40814444) [Crossref]
6. Leyland-Jones B. Human epidermal growth factor receptor 2-positive breast cancer and central nervous system metastases. J Clin Oncol. 2009; 27: 5278-5286. (PMID: 19770385) [Crossref]
7. Loibl S, Gianni L. HER2-positive breast cancer. Lancet. 2017; 389: 2415-2429. (PMID: 27939064) [Crossref]
8. Hurvitz SA, O'Shaughnessy J, Mason G, Yardley DA, Jahanzeb M, Brufsky A, et al. Central nervous system metastasis in patients with HER2-positive metastatic breast cancer: patient characteristics, treatment, and survival from systHERs. Clin Cancer Res. 2019; 25: 2433-2441. (PMID: 30593513) [Crossref]
9. Chiec L, Kumthekar P. Targeting HER2+ breast cancer brain metastases: a review of brain-directed HER2-directed therapies. CNS Drugs. 2022; 36: 167-179. (PMID: 35075602) [Crossref]
10. Moulder SL, Borges VF, Baetz T, Mcspadden T, Fernetich G, Murthy RK, et al. Phase I study of ONT-380, a HER2 inhibitor, in patients with HER2^{+}-advanced solid tumors, with an expansion cohort in HER2^{+} metastatic breast cancer (MBC). Clin Cancer Res. 2017; 23: 3529-3536. (PMID: 28053022) [Crossref]
11. Murthy RK, Loi S, Okines A, Paplomata E, Hamilton E, Hurvitz SA, et al. Tucatinib, trastuzumab, and capecitabine for HER2-positive metastatic breast cancer. N Engl J Med. 2020; 382: 597-609. Erratum in: N Engl J Med. 2020; 382: 586. (PMID: 31825569) [Crossref]
12. HER2-positive breast cancer | ESMO [Internet]. [cited 2026 Jan 31]. Available from: https://www.esmo.org/guidelines/living-guidelines/esmo-living-guideline-metastatic-breast-cancer/her2-positive-breast-cancer [Crossref]
13. U.S. Department of Health and Human Services. Common Terminology Criteria for Adverse Events (CTCAE) [Internet]. Bethesda, MD: National Cancer Institute; 2017 Nov [cited 2025 Dec 3]. Report No. Available from: https://dctd.cancer.gov/research/ctep-trials/for-sites/adverse-events/ctcae-v5-5x7.pdf [Crossref]
14. Tolaney SM, Jiang Z, Zhang Q, Barroso-Sousa R, Park YH, Rimawi MF, et al; DESTINY-Breast09 Trial Investigators. Trastuzumab deruxtecan plus pertuzumab for HER2-positive metastatic breast cancer. N Engl J Med. 2025 Oct 29. (PMID: 41160818) Epub ahead of print. [Crossref]
15. Center for Drug Evaluation and Research. FDA [Internet]. FDA; 2025 [cited 2026 Jan 31]. FDA approves fam-trastuzumab deruxtecan-nxki with pertuzumab for unresectable or metastatic HER2-positive breast cancer. Available from: https://www.fda.gov/drugs/drug-approvals-and-databases/fda-approves-fam-trastuzumab-deruxtecan-nxki-pertuzumab-unresectable-or-metastatic-her2-positive [Crossref]

16. Frenel JS, Zeghondy J, Guérin-Charbonnel C, Mailliez A, Volant E, Poumeaud F, et al. Tucatinib combination treatment after trastuzumab-deruxtecan in patients with ERBB2-positive metastatic breast cancer. JAMA Netw Open. 2024; 7: e244435. (PMID: 38568692) [Crossref]

17. Anders C, Neuberger E, Schwartz NRM, Bartley K, Wang S, Liu Y, et al. Real-world treatment patterns and clinical outcomes with tucatinib-based therapy in patients with HER2-positive metastatic breast cancer: analyses of two nationwide administrative health claims databases. Int J Clin Oncol. 2025; 30: 1982-1991. (PMID: 40768012) [Crossref]

18. Tarantino P, Lee D, Foldi J, Soulos PR, Gross CP, O'Meara T, et al. Outcomes of subsequent treatment regimens after trastuzumab deruxtecan in patients with metastatic breast cancer. J Natl Cancer Inst. 2025; 117: 2327-2335. (PMID: 40768012) [Crossref]

19. Sledge GW, Xiu J, Mahtani RL, Sandoval Leon AC, Meric-Bernstam F, Ribeiro JR, et al. Mechanisms of resistance to trastuzumab deruxtecan in breast cancer elucidated by multi-omic molecular profiling. NPJ Breast Cancer. 2025; 12: 1. (PMID: 41422323) [Crossref]

20. Zelizer S, Gallagher GB, Gonen M, Dang C, Modi S, Chandarlapaty S, et al. Evaluating post-T-DXd treatment strategies in HER2-positive metastatic breast cancer. Breast Cancer Res Treat. 2025; 215: 19. (PMID: 41307769) [Crossref]

21. Chen W, Gupta A, Mai N, Nag S, Lau JS, Singh S, et al. Trastuzumab deruxtecan resistance via loss of HER2 expression and binding. Cancer Discov. 2026; 16: 235-249. (PMID: 41212147) [Crossref]

ORIGINAL ARTICLE

European Journal of BREAST HEALTH

DOI: 10.4274/ejbh.galenos.2026.2026-2-10
Eur J Breast Health 2026;22(3):328-339

Survey of the Senologic International Society (SIS) on the Use of Preoperative Breast MRI in Early-Stage Breast Cancer: A Global Perspective on Current Practice

Alexander Mundinger[1], Carolin Mundinger[2], Darius Dian[3], Thorsten Heilmann[1], Shigeru Imoto[4], Atilla Soran[5], Wendie A Berg[6], Tolga Ozmen[7], Mitsuhiro Tozaki[8], Katja Siegmann-Luz[9], Ayfer Kamali Polat[10], Salete de Jesus Fonseca Rêgo[11], Pieter De Visschere[12], Sylvia H. Heywang-Köbrunner[13], Dionysios Koufoudakis[14], Bolivar Arboleda-Osorio[15], Maurício Magalhães Costa[16], Tadeusz Pieńkowski[17], Paula Podolski[18], Vahit Ozmen[19], Schlomo Schneebaum[20], Constanze Elfgen[21], Lydia Ioannidou-Mouzaka[22], Marianna Telesca[23], Manisha Bahl[24], Makus Müller-Schimpfle[25], Vaidotas Cesna[26], Siarhei Kharuzhyk[27], Carole Mathelin[28]

[1]Breast Center Osnabrück; Niels-Stensen-Kliniken, Franziskus-Hospital Harderberg, Georgsmarienhütte, Germany
[2]Department of Behavioural Biology, University of Muenster, Muenster, Germany
[3]Gyn-Munich and AWOgyn, Munich, Germany
[4]Kyorin University Hospital, Tokyo, Japan
[5]Magee-Womens Hospital, University of Pittsburgh Medical Center, Pittsburgh, Pennsylvania, USA
[6]Department of Radiology, University of Pittsburgh School of Medicine, Pittsburgh, Pennsylvania, USA
[7]Division of Gastrointestinal and Oncologic Surgery, Section of Breast Surgery, Department of Surgery, Massachusetts General Hospital, Massachusetts, USA
[8]Department of Radiology, Sagara Hospital Affiliated Breast Center, Kagoshima, Japan
[9]Reference Center Mammography, Berlin, Germany
[10]Department of Surgery, Ondokuz Mayıs University, Samsun, Türkiye
[11]Department of Radiology, Antonio Pedro University, Fluminense/UFF, Rio de Janeiro, Brazil
[12]Department of Radiology and Nuclear Medicine, Ghent University Hospital, Ghent, Belgium
[13]Reference Center, Munich, Germany
[14]Breast Center Nicosia General Hospital, Nicosia, Cyprus
[15]Universidad Central del Caribe School of Medicine, Puerto Rico, USA
[16]National Academy of Medicine, Rio de Janeiro, Brazil
[17]Department of Oncology and Breast Disease, Postgraduate Medical Education Center, Warsaw, Poland
[18]Croatian Senologic Society, University Hospital Centre Zagreb, Zagreb, Croatia
[19]İstanbul Florence Nightingale Hospital, İstanbul, Türkiye
[20]Department of Surgery, Tel Aviv Sourasky Medical Center, Tel Aviv, Israel
[21]Breast Center Zurich, Switzerland, University of Witten/Herdecke, Department for Human Medicine, Germany
[22]Hellenic Senologic Society, Athens, Greece

Corresponding Author: Alexander Mundinger, Prof. MD;
E-mail: mundinger.alexander@gmail.com **ORCID:** orcid.org/0000-0003-3776-4090
Received: 23.02.2026 **Accepted:** 10.04.2026 **Available Online Date:** 17.06.2026
Cite this article as: Mundinger A, Mundinger C, Dian D, Heilmann T, Imoto S, Soran A, et al. Survey of the Senologic International Society (SIS) on the use of preoperative breast MRI in early-stage breast cancer: a global perspective on current practice. Eur J Breast Health. 2026;22(3):328-339

[23]Worcestershire Acute Hospitals NHS Trust, United Kingdom
[24]Massachusetts General Hospital and Harvard Medical School, Boston, Massachusetts, USA
[25]Department of Radiology, Neuroradiology and Nuclear Medicine, Frankfurt Höchst Clinics GmbH, Frankfurt, Germany
[26]Department of Breast Surgery, Lithuanian University of Health Sciences Kauno Klinikos, Kaunas, Lithuania
[27]Department of Radiology, N.N. Alexandrov National Cancer Centre, Department of Radiodiagnostics, Institute of Posgraduate Education, Belarusian State Medical University, Minsk, Belarus
[28]Institut de Cancérologie Strasbourg, Europe (ICANS), Strasbourg, France

ABSTRACT

Objective: To map global practice patterns and disparities in the use of preoperative breast magnetic resonance imaging (MRI) for early breast cancer (EBC) among members of the Senologic International Society (SIS) and SIS Working Group.

Materials and Methods: A cross-sectional, web-based survey was distributed to SIS members worldwide. The questionnaire captured respondent demographics, center characteristics, local/national breast MRI use, guideline perceptions and personal practice, specific indications for MRI, and decision-making influences.

Results: We analyzed 114 responses from 17 countries. Significant variations were observed. While 36/46 (78.3%) of Japanese respondents perceived national guidelines as recommending preoperative MRI, only 18/60 (30%) of Europeans did. Overall, 96/114 (84.2%) of all respondents believed preoperative MRI provided a patient benefit, with none believing it caused harm. The most frequent indications in the total cohort were invasive lobular carcinoma (106/114, 93.0%), mammographic/sonographic suspicion of multifocality/multicentricity (96/114, 84.2%) and planned neoadjuvant therapy (89/114, 78.1%), while in Japan ductal carcinoma *in situ* (DCIS) or accompanying DCIS component was the most frequent indication (45/46, 97.8%). Half of respondents stated that national guidelines recommend preoperative breast MRI for EBC (57/114, 50%). Furthermore, 30/57 (52.6%) of these "guideline-positive" respondents reported performing more MRIs than advised while most guidelines recommending only selected preoperative indications such as invasive lobular histopathology, dense breasts, suspicion of multifocality/multicentricity or imaging inconsistencies. Key influencing factors included specialty, reimbursement, and time to access preoperative MRI.

Conclusion: This SIS-based international survey revealed heterogeneous global adoption of preoperative breast MRI for EBC, highlighting a significant gap between evidence-based guidelines and real-world practice. Clinical decisions are heavily influenced by geography, culture and resources, and belief in patient benefit. These findings highlight the need to tailor guidelines to local contexts, and strengthen awareness and dissemination efforts, together with further research to clarify the role of MRI in the modern multidisciplinary management of EBC.

Keywords: Early breast cancer; magnetic resonance imaging; preoperative staging; practice patterns; guidelines; international survey

KEY POINTS

- Early breast cancer
- Magnetic resonance imaging
- Preoperative staging
- Practice patterns
- Guidelines
- International survey

Introduction

The preoperative assessment of early breast cancer (EBC) aims to achieve complete tumor resection with optimal cosmetic outcomes. EBC represents stage I and stage II invasive cancers according to a narrow definition and includes ductal carcinoma *in situ* (DCIS) and stage IIIA or even operable stage IIIB according to a broader oncological definition. While mammography and ultrasound are standard imaging modalities to assess disease extent, breast magnetic resonance imaging (MRI) offers superior sensitivity, with a median incremental cancer detection rate of 16% compared to conventional imaging (1). This has fueled a rising trend in preoperative MRI use, particularly in the United States, where preoperative breast MRI application rates in EBC reached 60% for women under 65 years of age in 2020 (2-4).

The clinical benefit of routine preoperative MRI, however, remains controversial. While it improves surgical planning, randomized trials have shown it can increase mastectomy rates by 8% without demonstrating a significant improvement in local relapse-free or overall survival (5-8). Other studies suggest this initial increase in mastectomies may be balanced by a reduction in reoperation rates (9-12). The largest and most recent meta-analysis demonstrated both improved recurrence-free survival (hazard ratio = 0.77) and better overall survival (hazard ratio = 0.89) with the use of pre-operative contrast-enhanced MRI

Table 1. Summary table comparing national and international key guidelines on preoperative breast MRI in early breast cancer, with a focus on routine breast MRI in EBC and recommended selected indications

Organization/ country	Routine breast MRI recom-mended?	Recommended indications for preoperative use of breast MRI	Notes/latest update
ACR (USA)	No	Ipsilateral and contralateral DCIS and invasive carcinoma, particularly invasive lobular carcinoma (ILC), invasion of underlying fascia and muscle, neoadjuvant treatment response assessment	American College of Radiology 2025
AGO (Germany)	No	ILC, dense breasts, multifocal or contralateral suspicion, discrepancy Mx/ultrasound and histologic tumor extent	Arbeitsgemeinschaft Gynäkologische Onkologie (AGO). Breast Committee of the AGO 2024
ASBrS (USA)	No	ILC, young women, dense breasts, inconclusive imaging	The American Society of Breast Surgeons (ASBrS). ASBrS Resource Guide 2023
CACA (China)	No	Find multifocal and multicentric tumors, and evaluate the tumor's infiltration of the skin, pectoralis fascia, pectoralis major muscle, and chest wall	China Anti-Cancer Association (CACA). CACA Guidelines for Holistic Integrative Management of Breast Cancer 2022
EUSOBI (Europe)	No	ILC, dense breasts, multifocal/ multicentric suspicion	European Society of Breast Imaging (EUSOBI). EUSOBI 2008
ESMO (Europe)	No	ILC, imaging discrepancy, high-risk patients	European Society for Medical Oncology (ESMO). ESMO Early Breast Cancer Guidelines 2023
German S3 Guidelines (Germany)	No	ILC, dense breasts, multifocal suspicion	Evidence-based Guideline for the Early Detection, Diagnosis, Treatment and Follow-up of Breast Cancer. German S3 Guideline 2025*
INCa (France)	No	ILC, young women, dense breasts, inconclusive findings	Institut National du Cancer (INCa). INCa 2023
JBCS (Japan)	No	MRI is recommended in determining diagnosis and treatment policies for intra-breast lesions	Japanese Breast Cancer Society. Clinical Practice Guidelines for breast cancer screening and diagnosis 2022
NCCN (USA)	No	ILC, high-risk patients, inadequate conventional imaging	National Comprehensive Cancer Network (NCC). NCCN Breast Cancer Guidelines 2025
NICE (UK)	No	ILC, diagnostic uncertainty	National Institute for Health and Care Excellence (NICE). NICE NG101 2025
SBI (USA)	No	ILC, dense breasts, diagnostic uncertainty	Society of Breast Imaging (SBI). SBI Position Statements 2024

*Note: ILC: Invasive lobular cancer; DCIS: Ductal carcinoma *in situ*; MRI: Magnetic resonance imaging; EBC: Early breast cancer

(13), though some of this benefit may reflect patient selection (with healthier women having MRI). This conflicting evidence is reflected in heterogeneous national and international guidelines, which largely advise against routine use, reserving it for specific scenarios, such as histologically-proven invasive lobular carcinoma, dense breasts, suspicion of multifocality/ multicentricity or imaging inconsistencies (Table 1). This creates clinical ambiguity. While national trends for preoperative MRI are documented for the United States, comprehensive data on global practice patterns are lacking. The present study aimed to map current global practices, perceived benefits, and challenges associated with preoperative breast MRI in EBC among members of the Senologic International Society (SIS) and SIS Working Group to identify key drivers and areas for improvement.

Materials and Methods

Study Design and Survey Distribution

This study was performed according to the principles of the Declaration of Helsinki. After reviewing several international guidelines, a cross-sectional, web-based survey was conducted. The authors developed a 20-question English-language questionnaire, designed to be completed within 10 minutes. The questionnaire was distributed via email to members of the SIS and its working groups. A total of 120 recipients at an expert level were asked to answer and to forward the survey to other experienced colleagues. Communicative hubs among the experts helped to extend the reach of the survey. However, due to data protection regulations, we were not given information

on the number or identities of the experts contacted, making it impossible to calculate an exact response rate. The SIS is a worldwide federation of over 100 societies devoted to breast care, and its associated SIS working group comprise groupings of individual experts.

Data Collection

The survey was hosted online using a survey and feedback platform named PM+ (Performance Management Plus), and responses were collected over 14 days (October 28-November 11, 2024).

Statistical Analysis

Data from 114 respondents were analyzed using SPSS, version 31 (IBM Inc., Armonk, NY, USA). Analyses included descriptive statistics, chi-square test, Kruskal-Wallis tests, cross-tabulation and ordinal logistic regression (PLUM, Polytomous Universal Model). The threshold for significance was $p<0.05$.

Survey Content

The survey was divided into five sections: Section A: Respondent demographics (specialty, continent, country). Section B: Affiliation and center characteristics (certification status, type of institution, annual breast cancer operation volume). Section C: Local and national MRI use (annual MRI volume, national infrastructure, reporting, reimbursement, access times). Section D: MR policy and guidelines (guideline recommendations, personal adherence, perceived patient benefit, comparison with other modalities, eg CEM). Section E: Specific indications (patient characteristics, risk factors, and planned treatment options qualifying for MRI). All questions included in the questionnaire are shown in Table 1 of the Supplementary Material.

Results

Guideline Recommendation

Several international guidelines have been reviewed and judged whether they recommend routine preoperative breast MRI. The summarized results are shown in Table 1. All guidelines were judged to indicate that preoperative MRI was appropriate but only in specific circumstances with none recommending routine use in all patients. These guidelines suggest preoperative MRI for specific conditions, where conventional mammographic and ultrasound imaging is limited, and/or the risk for additional cancers is increased, such as in invasive lobular carcinoma, dense breasts, suspicion of multifocality/multicentricity, or larger size on ultrasound than mammography. Further, most guidelines require that centers should also have the facilities to perform correlation with prior breast imaging, to offer MRI-guided biopsy, and to have the capacity for multidisciplinary discussion and assessment of imaging-pathology concordance. We did not review protocol specifications such as abbreviated MRI or inclusion of diffusion-weighted imaging.

Respondent Characteristics, Heterogeneous Distribution

Of 114 respondents, 50.0% ($n = 57$) were radiologists and 46.5% ($n = 53$) were breast surgeons and 3.5% ($n = 4$) oncologists (Table 2). Most participants were from Europe (52.6%, $n = 60$) or Asia (40.4%, $n = 46$), all of whom were from Japan. The countries with the highest numbers of respondents were Japan (40.4%, $n = 46$), Germany (28.9%, $n = 33$), Belgium (9.6%, $n = 11$), the USA (3.5%, $n = 4$) and Türkiye (3.5%, $n = 4$). The majority (89.5%, $n = 102/114$) worked in certified breast centers, distributed across community-based hospitals (33.3%, $n = 38$), university hospitals (31.6%, $n = 36$), and private

Table 2. Respondent characteristics-specialty, continent, breast center certification

Characteristic	Surgical specialties ($n = 53$)	Radiology ($n = 57$)	Others ($n=4$)	Total cohort* ($n = 114$)
Continent				
Europe	10 (18.9%)	47 (82.5%)	3 (100%)	60 (52.6%)
Asia (all from Japan)	41 (77.4%)	5 (8.8%)	-	46 (40.4%)
North America	1 (1.9%)	3 (5.3%)	-	4 (3.5%)
Latin America	1 (1.9%)	2 (3.5%)	-	3 (2.6%)
No answer	-	-	1 (33.3%)	1 (0.9%)
Certified breast center				
Yes	50 (94.3%)	49 (86.0%)	3 (100%)	102 (89.5%)
No	3 (5.7%)	8 (14.0%)	-	11 (9.6%)
No answer	-	-	1 (33.3%)	1 (0.9%)

*Note: Total cohort represents all responding specialties including medical oncology, radiation oncology. Three gynecological breast surgeons are classified under surgical specialties

institutions (29.8%, *n* = 34) or other institutions (5%, *n* = 5, and one missing answer). In general, the answers to all questions were significantly heterogeneously distributed (all $p<0.05$).

Center Volume, Breast MRI Turnaround Times and MRI Infrastructure

Center Volumes: The mean number of annual breast cancer operations per center was 355. The mean number of annual breast MRI examinations was 514. In Europe and North America, MRI use was concentrated in fewer centers with high annual examination volumes ("high-volume, concentrated use"). In contrast, Asia (Japan) showed broader diffusion, with more centers adopting preoperative MRI but each performing fewer examinations ("low-volume, diffuse adoption") (Table 2 of the Supplementary Material).

MRI Turnaround Times: 98% (*n* = 112/114) of total respondents reported a significant variation across continents in timespan between request of the breast MRI to the MRI report (Kruskal-Wallis $p = 0.002$). Rapid access to MRI results (within 7 days) was reported by 67.5% (*n* = 77/114) of respondents, with 19.6% (*n* = 9/46) in Japan having access on the same day.

MRI Infrastructure: The knowledge about national MRI infrastructure was limited, with 38.6% (*n* = 44/114) of respondents not answering this question. Reimbursement by the public health system was more comprehensive in Japan (79.5%, *n* = 35/44 public health coverage) than in Europe (64.4%, *n* = 58/90).

Indications for Preoperative MRI

Indications are detailed in Table 3. Overall, the most common indications based on patient characteristics were invasive lobular carcinoma (93.0%, *n* = 106/114) and suspicion of multifocality/multicentricity on conventional imaging (84.2%, *n* = 96/114). For risk factors, family history of breast cancer (76.3%, *n* = 87/114)

Table 3. Preoperative patient characteristics that qualify for preoperative breast MRI in early breast cancer in daily routine (following to non-invasive biopsy and after imaging by other modalities than breast MRI)

Preoperative patient characteristics	Absolute numbers and percentual frequency (total cohort *n* = 114)*
Lobular invasive cancer histology	106/114 (93.0%)
Multicentricity at imaging	96/114 (84.2%)
Multifocality at imaging	96/114 (84.2%)
DCIS or accompanying DCIS component	77/114 (67.5%)
Other invasive histology than lobular invasive cancer	62/114 (54.4%)
Additional B3 lesions at non-invasive biopsy	42/114 (46.8%)
T2 stage at basic complimentary imaging	50/114 (43.9%)
T3 stage at basic complimentary imaging	46/114 (40.4%)
T1 stage at basic complimentary imaging	45/114 (39.5%)
Lymph node metastasis at biopsy	37/114 (32.5%)
Grading at biopsy	18/114 (15.8%)
Systemic metastasis at imaging	10/114 (8.8%)
Additional risk factors	
Family breast cancer history	87/114 (76.3%)
High breast density	84/114 (73.7%)
Previous breast cancer	71/114 (62.3%)
Age <50	67/114 (58.8%)
Age ≥50	16/114 (14.0%)
Age >75	8/114 (7.0%)
Planned treatment options	
Planned neoadjuvant therapy	89/114 (78.1%)
Planned breast conservative therapy	81/114 (71.1%)
Planned oncoplastic surgery	59/114 (51.8%)
Planned modified radical mastectomy	21/114 (18.4%)

DCIS: Ductal carcinoma *in situ*; MRI: Magnetic resonance imaging

and high breast density (73.7%, *n* = 84/114) were the most cited. In terms of treatment planning, neoadjuvant therapy (78.1%, *n* = 89/114) and breast-conserving therapy (71.1%, *n* = 81/114) were the primary drivers. Significant variation was seen for T1 staging, supported by 76.1% (*n* = 35/46) of Japanese respondents but only 13.3% (*n* = 8/60) of Europeans ($p<0.001$). Detailed cross calculations are included in the Supplementary Material.

Guideline Perceptions and Personal Practice

Guideline Perception: Half of the respondents (50.0%, *n* = 57/114) reported that their national guidelines recommend preoperative MRI for EBC. This perception was more frequent among breast surgeons (67.9%, *n* = 36/53) than radiologists (31.6%, *n* = 18/57). Further, this perception was stronger in Japan (78.3%, *n* = 36/46) compared to Europe (30.0%, *n* = 18/60) (Table 4), a remarkable contrast to the actual guideline positions shown in Table 1. The practice guidelines of the American College of Radiology (ACR) and the Japanese are liberal in evaluating the extent of disease with newly diagnosed breast cancer and both include DCIS as an indication. However, most guidelines at the time of the survey suggest limiting the use of preoperative MRI to only a few select patient populations.

Personal Practice: Strikingly, among those 57 respondents who perceived guidelines as supportive, 52.6% (*n* = 30/57) reported performing more MRIs than guidelines recommend, 36.8% (*n* = 21/57) reported strictly following the guideline indications and 8.8% (*n* = 5/58) performed fewer MRIs than recommended (Table 5). These liberal or restrictive personal practice patterns could not systematically be explained by continent, specialty, payer, institution type or MR examination numbers in logistic models.

Personal Judgement: A majority (84.2%, *n* = 96/114) believed preoperative MRI provided patient benefit, with none believing it caused harm. This belief was positively correlated with the perception of positive guideline support for the practice ($p<0.05$) (Table 6). This divergence between widespread perception of guideline endorsement in daily practice and restrained guideline content (Table 1) was a key finding.

Associations with perceived positive guidelines recommendations: Centers in countries where guideline endorsement was perceived for preoperative EBC MRI demonstrated shorter MRI turnaround times compared to those without such ($p<0.02$). This association between perceived guideline endorsement and

Table 4. Perceived national guideline recommendations for preoperative breast MRI

Do national guidelines recommend preoperative breast MRI for early breast cancer?	Japan (*n* = 46)	Europe (*n* = 60)	Total cohort* (*n* = 114)
Yes	36 (78.3%)	18 (30.0%)	57 (50.0%)
No	10 (21.7%)	42 (70.0%)	57 (50.0%)

*Note: Total cohort represents all respondents; MRI: Magnetic resonance imaging

Table 5. Strict adherence, liberal or restrictive application of national guidelines in a subgroup perceiving positive guidelines on preoperative breast MRI for EBC

Compared to indications of national guidelines, how restrictive or liberal do you request preoperative breast MRI? (Filter: positive national guidelines recommendation)	Japan (*n* = 36)	Europe (*n* = 18)	Subgroup* (*n* = 57)
Strictly following the guidelines	15 (41.7%)	5 (27.8%)	21 (36.8%)
Performing more MRIs than recommended	18 (50.0%)	11 (61.1%)	30 (52.6%)
Performing fewer MRIs than recommended	3 (8.3%)	2 (11.1%)	5 (8.8%)
No answer	0 (0.0%)	0 (0.0%)	1 (1.8%)

*Note: Subgroup represents respondents (*n* = 57) from countries with positive guidelines that makes 50% of total cohort (*n* = 114). MRI: Magnetic resonance imaging; EBC: Early breast cancer

Table 6. Subjective perceived patient benefit of preoperative MRI among all respondents

According to your subjective opinion, is the patient benefit by preoperative MRI the same, better than or worse than without preoperative MRI?	Japan (*n* = 46)	Europe (*n* = 60)	Total cohort* (*n* = 114)
Better	43 (93.5%)	48 (80.0%)	96 (84.2%)
Same	3 (6.5%)	10 (16.7%)	15 (13.2%)
Worse	0 (0.0%)	0 (0.0%)	0 (0.0%)
No answer	0 (0.0%)	2 (3.3%)	3 (2.6%)

*Note: Total cohort represents all respondents. MRI: Magnetic resonance imaging

reporting efficiency does not imply causality because structural or resource-related factors may also contribute.

Availability of Preoperative Staging Tools

The availability of staging tools is detailed in Table 7. Overall, ultrasound (97.4%, *n* = 111/114) and mammography (93.9%, *n* = 107/114) were nearly universally available. Digital breast tomosynthesis (DBT) was less often available (58.8%, *n* = 67/114) and contrast-enhanced mammography (CEM) was even less often available (21.9%, 25/114). Among the Japanese respondents, more than half reported availability of dedicated breast CT (54.3%, *n* = 25/46) compared to the whole collective (26.3%, *n* = 30/114), while CEM was not used for preoperative staging at all in Japan. For the small subgroup of 25 (21.9% of all respondents) CEM users in Europe, USA and Latin America, preoperative MRI was judged to be more beneficial than CEM by 56% (*n* = 14/25), equal to CEM in 32% (*n* = 8/25) and worse in 12% (*n* = 3/25).

Discussion and Conclusion

Preoperative breast MRI consistently detects additional cancers that remain occult on mammography and ultrasound. Whether these additional findings translate into improved clinical outcomes in EBC had been a matter of debate until 2024. In that year, the largest metaanalyses available to date reported improved recurrence-free and overall survival associated with the use of preoperative MRI (1, 12, 13). Our SIS global survey was performed in 2024 and reveals both striking variation and notable consensus. The most prominent finding was the profound interdisciplinary and intercontinental disparity in guideline perception and practice: 50% of respondents reported that guidelines in their region positively recommended preoperative MRI in EBC. At the same time, more than four fifths (84.2%, 96/114) of all respondents expressed belief in a patient benefit, a sentiment transcending geography and specialty. Clinical decisions appear to be driven not only by the reported survey indications and the traditional guideline interpretation, but also by local culture and resources, health system organization, and deeply held personal conviction that often diverge in our survey respondents from the guidelines recommendations, which were out of date after the publication of the 2024 meta-analysis (13).

The Evidence-Guideline-Practice Gap: The observed global heterogeneity underscores a fundamental disconnect between guideline recommendations and clinical practice. Most international guidelines advise against routine preoperative MRI, citing historical concerns about increased mastectomy rates and the absence of level-1 evidence for a survival benefit if they do not respect newest evidence (13). The American Society of Breast Surgeons (ASBrS) Choosing Wisely® Campaign is the most explicit, stating: “Don’t routinely order breast MRI in new breast cancer patients” (14). In contrast, responses from Japan suggest a different picture. A majority (78.3%, 36/46) of Japanese respondents reported that national guidelines recommend preoperative breast MRI in EBC, compared with 30% (18/60) of European and 50% (2/4) of U.S. respondents. What do the Japanese guidelines actually say? The 2013 Japanese Breast Cancer Society guidelines do not advocate routine use of MRI and do not mention EBC at all but recommend (Grade B) MRI for three scenarios: to determine diagnosis and treatment policies for intra-breast lesions, to diagnose the extent of breast cancer and to detect multifocal breast cancer undetectable by mammography and ultrasound (15). The Japanese breast cancer society clinical practice guidelines for breast cancer screening and diagnosis, 2022 edition, adds: “For MRI-detected lesions that are suspected to be malignant on preoperative contrast-enhanced breast MRI, histological examination should be performed if there is an impact on the surgical procedure”. The rationale has been outlined; the decision on the surgical approach should not be based on preoperative MRI findings alone (16). This recommendation to perform additional biopsy prior to surgery is shared by all current guidelines. Today, in Japan, treatment policies for T1 stage cancers include radiofrequency ablation (RFA). MRI is required not only to select and monitor patients for RFA versus breast-conserving therapy (BCT), but also as a prerequisite for reimbursement under public health insurance (17).

Table 7. Frequency of imaging tools for preoperative staging among all respondents

Modality	Absolute numbers and percentual frequency (total cohort *n* = 114)*
Ultrasound	111/114 (97.4%)
Mammography	107/114 (93.9%)
Digital breast tomosynthesis (DBT)	67/114 (58.8%)
Dedicated breast CT	30/114 (26.3%)
Contrast enhanced mammography (CEM)	25/114 (21.9%)
Positron emission tomography (PET)	18/114 (15.8%)
Single photon emission computed tomography (SPECT)	5/114 (4.4%)

*Note: Total cohort represents all respondents. CT: Computed tomography

This is the reason for widespread acceptance of MRI in EBC in Japan. This national context likely explains the sharp contrast in acceptance of T1 stage as an indication for preoperative MRI, observed in 76% (35/46) of Japanese respondents compared with only 13% (8/60) of Europeans.

The 2026 published German S3-Guidelines emphasize the better recurrence-free and overall survival after preoperative MRI according to the latest meta-analysis (13) and justify the routine use of MRI, or alternatively CEM in all patients with newly diagnosed, locally limited breast cancer in the setting of dense beasts or difficult assessment with mammography and ultrasound (18).

Reported clinical practice across continents exceeds the authors' expectations. Clinical adoption of preoperative MRI in EBC appears more liberal than guideline recommendations, as reflected in our survey for Japan 50% (18/36), Europe 61.1% (11/18), and reported real-world rates in the literature of 60% preoperative breast MRI of EBC in USA for women under 65 years of age (2-4).

The Drivers for Use of Preoperative MRI beyond Guideline Recommendations: Firstly, although our survey answers do not provide a clear explanation for the overuse of preoperative MRI compared to guideline intentions, it is reasonable to assume that general resources, financial aspects and rapid access to MRI may encourage the willingness to perform a preoperative MRI examination.

Secondly, the evidence base continues to evolve and is open to interpretation. While early trials raised concerns, recent meta-analyses by Eisen et al. (13) indicate that preoperative MRI significantly reduces re-operation rates (odd ratio = 0.73), re-excisions (odd ratio = 0.63), and increases recurrence-free survival (hazard ratio = 0.77) and overall survival (hazard ratio = 0.89). The benefit in preventing re-excisions may outweigh the initial increase in mastectomy rates, particularly in invasive lobular carcinoma and non-calcified DCIS (13, 19-21). Moreover, improved detection of synchronous contralateral breast cancers has been associated with a reduction in metachronous contralateral disease (hazard ratio = 0.71) (13).

Thirdly, this nuanced benefit where the outcome metric has shifted from survival to surgical precision and patient burden resonates strongly with clinicians, as reflected in the 84.2% (96/114) belief in patient benefit reported in our survey. Historically, pioneers of BCT achieved survival outcomes equivalent to mastectomy through wider excisions and radiotherapy, relying solely on mammography for breast staging (22). Contemporary surgical paradigms, however, favor smaller excisions to optimize cosmesis and multimodal preoperative breast staging. In this context, MRI is increasingly perceived as a modern tool to offset reduced surgical margins, enabling "first-pass" clear margins in an era of precision surgery. Combined with advances in systemic therapy that improve overall survival, this reframes the value of MRI not as a determinant of survival, but as a tool of enhancing surgical quality and reducing patient burden, a rationale not fully captured by traditional evidence hierarchies (12, 13).

Fourthly, emerging data on molecular subtypes further complicate a one-size-fits-all guideline approach. For example, MRI has been shown to reduce mastectomy rates in HER2-positive disease (21). Respondent comments and recent publications emphasize that the indication for preoperative MRI in hormone-negative HER2+ and triple-negative cancers is driven more by planned neoadjuvant systemic therapy than by biological aggressivity alone (23-25). Both subtypes are prone to multiple occult ipsilateral invasive lesions, higher local recurrence rates and nearly all patients with HER2+ or triple-negative disease, as well as those with invasive lobular carcinoma, are potential guideline candidates to undergo preoperative breast MRI in U.S. centers. Currently the Alliance A11104/ACRIN 6694 phase III trial is examining the hypothesis that preoperative breast MRI improves staging and selection of stage I and II patients with ER/PR- negative tumors for BCT, thus lowering rates of local regional recurrence (26).

The Drivers of Decision-Making: Survey Indications and "Fast Thinking": Our data show that the decision for preoperative breast MRI in EBC varies by the traditional patient and tumor characteristics, but now also depends on medical specialty, subjective beliefs and local infrastructure. The strong contrast between Japan (predominantly surgeon respondents) and Europe (predominantly radiologist respondents) suggests the perceived value of MRI is viewed through different professional lenses. The reliance on risk factors such as previous history of breast cancer, despite their limited evidence base for preoperative planning, illustrates the influence of intuitive "fast thinking" in clinical decision-making. Nobel laureate Kahneman (27) examined this "fast thinking mode" in economic contexts and demonstrated that it is prone to several systematic biases, including optimism bias and a tendency to overestimate benefits while underestimating costs. Breast MRI remains the most sensitive modality for detecting breast cancer in high-risk women and as supplemental screening in those with extremely dense breasts (28-30). Given this sensitivity, it is understandable that breast surgeons may favor MRI in a proven cancer; to determine tumor size, identify additional foci in either breast, and assess potential extension to the chest wall or lymph nodes. In the absence of precise risk stratification for preclinical and clinical scenarios, surgeons and radiologists seem to intuitively prioritize the anticipated individual benefit for the patient over restrictive guideline recommendations. Practical factors further reinforce this decision pattern, including rapid access to

breast MRI, reimbursement policies, and the ease of achieving interdisciplinary consensus for performing preoperative MRI (30). We hypothesize that intuitive reasoning and contextual facilitators shape practice beyond the boundaries of still valid guidelines that are not adapted to the latest evidence.

The Continent-Specific Context: The underlying geographic differences are shaped by the distinct ways in which guidelines are interpreted, contextualized, and implemented across continents (31).

Japan represents a model where perceived guideline support, favorable reimbursement, rapid MRI access, and a strong belief in technological advancement converge. The frequent application of preoperative MRI may explain the moderate use of DBT (26.1%, 12/46) and absence of CEM in our survey.

Europe embodies a more restrictive approach, more closely aligned with the intention of the guidelines, likely influenced by cost-control and a higher reliance on radiologists as gatekeepers. Overall availability of ultrasound (100%, 60/60) and high dissemination of DBT (80%, 48/60) and to a lesser degree CEM (31.7%, 39/60) substituting breast MRI may explain this pattern. In Europe, a milestone survey conducted by the European Society of Breast Imaging on the use of clinical breast MRI has reported a restrictive approach of north European countries as far back as 2016 (32). In Southern European countries, preoperative breast MRI was more frequently performed in all breast cancer patients rather than being limited to those with invasive lobular carcinoma (32.1% versus 6% in northern Europe) (32). A similar pattern has been observed for patients with DCIS, where 50.9% of respondents in southern Europe reported routinely using preoperative MRI, compared with 22.2% in northern European countries (32).

United States: Although our U.S. survey data remain limited, the reported studies provide a coherent picture. In the United States, preoperative breast MRI continues to be used at comparatively high rates in EBC, despite divergent professional recommendations (2-4). The ACR quite generously supports preoperative MRI for evaluating disease extent, characterizing additional ipsilateral and contralateral lesions including DCIS and invasive lobular carcinoma and assessing chestwall involvement or response to neoadjuvant therapy (33). In contrast, surgical guidelines from the ASBrS strictly has argued against any routine use of preoperative MRI dating back to 2018 (14). Today MRI is most frequently requested for women with dense breasts in Australia (34). To the best of our knowledge, none of the major U.S. studies or registries (SEER, NCDB, Medicare datasets) report a national percentage of preoperative MRI use stratified by breast density. In the U.S., however, levels of public and provider awareness is high regarding the masking effect of dense breast tissue and its associated increased cancer risk. This awareness has been actively shaped by scientific societies, advocacy groups, and dedicated educational platforms, exemplified by DenseBreastInfo.org, which disseminate information on breast density, supplemental screening, and statelevel legislation (35). The recent Food and Drug Administration National Dense Breast Reporting requirement, mandating that all mammography facilities inform patients whether their breast tissue is “dense” or “not dense” and include an official density assessment in clinician reports, has further institutionalized this awareness (36). The authors hypothesize that these expectations on supplemental imaging in women with dense breasts may extend beyond screening and influence decisionmaking in the preoperative setting, contributing to higher preoperative MRI use in the United States compared with other countries. Realworld surveys suggest that feeforservice reimbursement structures, defensive medical practices, and a strong emphasis on individualized surgical planning further contribute to this persistent utilization pattern (2-4).

Guidelines themselves are complex instruments balancing evidence, harm, benefit, and socio-economic factors aiming to provide support for physicians and patients to utilize shared decision making (31, 33). When evidence for a clear survival benefit is weak, as is the case with preoperative MRI before the time of the 2024 survey, recommendations naturally lean towards case-by-case discussion. This inherent ambiguity creates space for “instinctive judgement”, as described above (27). A clinician’s perspective can shift the historic calculus from “no survival benefit” (arguing against MRI) to “prevents reoperations and optimizes cosmesis” (arguing for MRI), especially for subtypes like invasive lobular carcinoma or in patients planned for neoadjuvant therapy. This survey confirms that in practice, the indications often extend beyond the core scenarios incorporating best subjective intentions (assumed patient benefit), risk factors such as dense breasts, planned neoadjuvant therapy and a desire for comprehensive pre-surgical mapping.

Implications for Future Guidelines and Research

Scientifically, such ambiguity can be resolved and nuanced by subgroup analysis with reference to metanalysis or new trial data, such as the current phase III Alliance A011104/ACRIN 6694 study, which to date does not suggest an oncologic benefit from routine preoperative MRI in early-stage hormone-negative cancers, i.e. HER2+ and triple negative disease (13, 26). This is not surprising in the era of powerful radiation oncology and improving adjuvant/neoadjuvant therapy, both of which can eliminate residual malignant lesions in patients without preoperative MRI. Future trials need to focus on stage-specific surgical endpoints as re-resection and conversion from breast-conservative surgery to mastectomy, and whether deescalation of surgical therapy will progress further with improvement in

systemic therapy. The Breast Imaging Reporting and Data System (BI-RADS) 2025 manual represents a major step forward to obtain up-scaled real-world data (37). By recommending audits of breast MRI examinations after cancer diagnosis (BI-RADS MR 6), it provides a unified framework to define and validate expected performance parameters of preoperative MRI (38). Those data are needed for more nuanced, international guidelines that explicitly address stage dependent specific clinical scenarios (e.g., molecular subtypes) for oncoplastic planning. The final goal will be harmonizing preoperative imaging guidelines with preexisting treatment guidelines, updated evidence on survival benefit for early and advanced breast cancer within an integrated holistic concept (39-41).

Study Limitations

This study has several limitations. All data are self-reported, and the survey format primarily captures "fast-thinking" clinical judgments. As the term EBC was not explicitly defined in the questionnaire, respondents may have interpreted it differently. A standard definition of EBC shared by most guidelines refers to invasive breast cancer confined to the breast and/or axillary lymph nodes without distant metastases (stage I to IIIA). However, some experts favor broader or narrower borders divergent to the mainstream and include DCIS (stage 0) or operable stage IIIB or restrict EBC to nodenegative or small T1 or T2 tumors. These divergent definitions complicate international comparisons and may influence how clinicians interpret survey questions related to EBC.

Although international, the sample size is too small to be representative for most countries, and a selection bias toward clinicians using breast MRI in certified centers is likely. A substantial proportion of respondents came from Japan and Europe. This uneven geographic distribution limits the global generalizability of the results, particularly for less developed regions. Imbalances in respondent specialties between Japan and Europe, together with low participation from other continents, may further skew the findings. All statistical analyses assess associations only; they do not establish causation. For example, a positive perception of guidelines may correlate with faster reporting, but structural factors such as resources, workflow, or infrastructure could equally account for this difference. Another limitation is that, unlike therapy guidelines with stage- or subtype-specific recommendations, most preoperative breast MRI guidelines remain broad and do not differentiate between early and advanced disease. Our survey did not attempt to define a universal standard for what constitutes the presence or absence of preoperative MRI guidance in EBC, acknowledging differing interpretive traditions. A more holistic reading, common in some Asian contexts, may treat broad recommendations as implicitly inclusive of early-stage disease, whereas a more selective, scenario-driven interpretation, typical of Western scientific traditions, may conclude that no explicit recommendation exists. This distinction aligns with established findings in cultural psychology, which demonstrate that East Asian cognition tends to be more holistic and context-oriented, whereas Western cognition is typically more analytic and object-focused (42).

In conclusion, this SIS survey maps the current global practices and demonstrates that the use of preoperative breast MRI is shaped more by geography, different cultural approaches and resources, and clinical interpretation of evolving evidence than by strict adherence to the current guidelines. Overall, 84.2% of all respondents believed preoperative MRI provided a patient benefit, with none believing it caused harm. The most frequent overall indications were invasive lobular carcinoma (93.0%, 106/114), mammographic/sonographic suspicion of multifocality/multicentricity (84.2%, 96/114), and planned neoadjuvant therapy (78.1%, 89/114), and in Japan, assessing the extent of DCIS (97.8%, 45/46). Among respondents who reported using positive guidelines, 52.6% (30/57) performed more MRI examinations than the guidelines advised. Key influencing factors included specialty reimbursement, and rapid access to MRI. These findings highlight the need for standardized guidelines including the newest evidence and further research to clarify the role of MRI in the modern multidisciplinary management of EBC. Functional and abbreviated MR specifications and CEM should be integrated in future international guidelines updates (42, 43).

Ethics

Ethics Committee Approval: Not necessary.

Informed Consent: No personal patient data were used for this survey. No informed consent necessary.

Footnotes

Acknowledgements

We thank the market research institute Produkt + Markt GmbH & Co. KG for providing the electronic questionnaire and link, and Ms. Kaja Böneker for the data preparation.

Authorship Contributions: Surgical and Medical Pracites: A.M., C.M., D.D., T.H., S.I., A.S., W.A.B., T.O., M.T., K.S-L., A.K.P., S.D.J.F.R., P.D.V., S.H.H-K., D.K., B.A-O., M.M.C., T.P., P.P., V.O., S.S., C.E., L.I-M., M.Te., M.B., M.M-S., V.C., S.K., C.Ma.; Concept: A.M., C.M., D.D., T.H., S.I., A.S., W.A.B., T.O., M.T., K.S-L., A.K.P., S.D.J.F.R., P.D.V., S.H.H-K., D.K., B.A-O., M.M.C., T.P., P.P., V.O., S.S., C.E., L.I-M., M.Te., M.B., M.M-S., V.C., S.K., C.Ma.; Design: A.M., C.M., D.D., T.H., S.I., A.S., W.A.B., T.O., M.T., K.S-L., A.K.P., S.D.J.F.R., P.D.V., S.H.H-K., D.K., B.A-O., M.M.C., T.P., P.P., V.O., S.S., C.E., L.I-M., M.Te., M.B., M.M-S., V.C., S.K., C.Ma.; Data Collection and/or Processing: A.M., C.M., D.D., T.H., S.I., A.S., W.A.B., T.O., M.T., K.S-L., A.K.P., S.D.J.F.R., P.D.V., S.H.H-K., D.K., B.A-O., M.M.C., T.P., P.P., V.O., S.S., C.E., L.I-M., M.Te.,

M.B., M.M-S., V.C., S.K., C.Ma.; Analysis and/or Interpretation: A.M., C.M., D.D., T.H., S.I., A.S., W.A.B., T.O., M.T., K.S-L., A.K.P., S.D.J.F.R., P.D.V., S.H.H-K., D.K., B.A-O., M.M.C., T.P., P.P., V.O., S.S., C.E., L.I-M., M.Te., M.B., M.M-S., V.C., S.K., C.Ma.; Literature Search: A.M., C.M., D.D., T.H., S.I., A.S., W.A.B., T.O., M.T., K.S-L., A.K.P., S.D.J.F.R., P.D.V., S.H.H-K., D.K., B.A-O., M.M.C., T.P., P.P., V.O., S.S., C.E., L.I-M., M.Te., M.B., M.M-S., V.C., S.K., C.Ma.; Writing: A.M., C.M., D.D., T.H., S.I., A.S., W.A.B., T.O., M.T., K.S-L., A.K.P., S.D.J.F.R., P.D.V., S.H.H-K., D.K., B.A-O., M.M.C., T.P., P.P., V.O., S.S., C.E., L.I-M., M.Te., M.B., M.M-S., V.C., S.K., C.Ma.

Conflict of Interest: The authors have no conflicts of interest to declare.

Financial Disclosure: The authors declared that this study has received no financial support.

Supplementary Material Table 1: https://d2v96fxpocvxx.cloudfront.net/ae2c7771-39a2-40bf-a837-aa639bcdd123/content-images/3e14feb4-d21b-48e1-b7fd-8b2a16b2eb7c.pdf

Supplementary Material Table 2: https://d2v96fxpocvxx.cloudfront.net/58770459-5a06-4076-a747-5b73e24cd7c0/content-images/ce826b1e-0fe6-4712-9dcc-152da729ec03.pdf

References

1. Houssami N, Hayes DF. Review of preoperative magnetic resonance imaging (MRI) in breast cancer: should MRI be performed on all women with newly diagnosed early stage breast cancer? CA Cancer J Clin. 2009; 59: 290-302. (PMID: 19679690) [Crossref]
2. Wang SY, Virnig BA, Tuttle TM, Jacobs DR Jr, Kuntz KM, Kane RL. Variability of preoperative breast MRI utilization among older women with newly diagnosed early-stage breast cancer. Breast J. 2013; 19: 627-636. (PMID: 24011145) [Crossref]
3. Pak LM, Banaag A, Koehlmoos TP, Nguyen LL, Learn PA. Non-clinical drivers of variation in preoperative MRI utilization for breast cancer. Ann Surg Oncol. 2020; 27: 3414-3423. (PMID: 32215756) [Crossref]
4. Pan IW, Yen TWF, Bedrosian I, Shih YT. Current trends in the utilization of preoperative breast magnetic resonance imaging among women with newly diagnosed breast cancer. JCO Oncol Pract. 2023; 19: 446-455. (PMID: 37071025) [Crossref]
5. Turnbull L, Brown S, Harvey I, Olivier C, Drew P, Napp V, et al. Comparative effectiveness of MRI in breast cancer (COMICE) trial: a randomised controlled trial. Lancet. 2010; 375: 563-571. (PMID: 20159292) [Crossref]
6. Houssami N, Turner RM, Morrow M. Meta-analysis of pre-operative magnetic resonance imaging (MRI) and surgical treatment for breast cancer. Breast Cancer Res Treat. 2017; 165: 273-283. (PMID: 28589366) [Crossref]
7. Sardanelli F, Trimboli RM, Houssami N, Gilbert FJ, Helbich TH, Álvarez Benito M, et al. Magnetic resonance imaging before breast cancer surgery: results of an observational multicenter international prospective analysis (MIPA). Eur Radiol. 2022; 32: 1611-1623. (PMID: 34643778) [Crossref]
8. Mota BS, Reis YN, de Barros N, Cardoso NP, Mota RMS, Shimizu C, et al. Effects of preoperative magnetic resonance image on survival rates and surgical planning in breast cancer conservative surgery: randomized controlled trial (BREAST-MRI trial). Breast Cancer Res Treat. 2023; 198: 447-461. (PMID: 36786946) [Crossref]
9. Peters N, Van Esser S, Van Den Bosch M, Storm RK, Plaisier PW, Van Dalen T, et al. Preoperative MRI and surgical management in patients with nonpalpable breast cancer: the MONET–randomised controlled trial. Eur J Cancer. 2011; 47: 879-886. (PMID: 21195605) [Crossref]
10. Gonzalez V, Sandelin K, Karlsson A, Åberg W, Löfgren L, Iliescu G, et al. Preoperative MRI of the breast (POMB) influences primary treatment in breast cancer: a prospective, randomized, multicenter study. World J Surg. 2014; 38: 1685-1693. (PMID: 24817517) [Crossref]
11. Balleyguier C, Dunant A, Ceugnart L, Kandel M, Chauvet MP, Chérel P, et al. Preoperative breast magnetic resonance imaging in women with local ductal carcinoma in situ to optimize surgical outcomes: results from the randomized phase III trial IRCIS. J Clin Oncol. 2019; 37: 885-892. (PMID: 30811290) [Crossref]
12. Christensen DM, Shehata MN, Javid SH, Rahbar H, Lam DL. Preoperative breast MRI: current evidence and patient selection. J Breast Imaging. 2023; 5: 112-124. (PMID: 38416933) [Crossref]
13. Eisen A, Fletcher GG, Fienberg S, George R, Holloway C, Kulkarni S, et al. Breast magnetic resonance imaging for preoperative evaluation of breast cancer: a systematic review and meta-analysis. Can Assoc Radiol J. 2024; 75: 118-135. (PMID: 37593787) [Crossref]
14. The American Society of Breast Surgeons. Resource guide: diagnostic and screening magnetic resonance imaging of the breast. Columbia (MD): The American Society of Breast Surgeons; 2018. [Crossref]
15. Tozaki M, Isomoto I, Kojima Y, Kubota K, Kuroki Y, Ohnuki K, et al.; Japanese Breast Cancer Society. The Japanese Breast Cancer Society Clinical Practice Guideline for screening and imaging diagnosis of breast cancer. Breast Cancer. 2015; 22: 28-36. (PMID: 25085808) [Crossref]
16. Kubota K, Nakashima K, Nakashima K, Kataoka M, Inoue K, Goto M, et al. The Japanese breast cancer society clinical practice guidelines for breast cancer screening and diagnosis, 2022 edition. Breast Cancer. 2024; 31: 157-164. Erratum in: Breast Cancer. 2024; 31: 165. (PMID: 37973686) [Crossref]
17. Takayama S, Kinoshita T, Shiino S, Jimbo K, Watanabe KI, Fujisawa T, et al. Patients offer radiofrequency ablation therapy for early breast cancer as local therapy (PO-RAFAELO) study under the patient-proposed health services. JMA J. 2023; 6: 505-512. (PMID: 37941717) [Crossref]
18. Hahn M, Schulz-Wendtland R, Banys-Paluchowski M, Bee M, Fallenberg E, Gerber B, et al. Kap.4.1 Diagnostics for the clarification of abnormal findings and pre-therapeutic staging diagnostics. Guideline program oncology (German Cancer Society, German Cancer Aid, AWMF): S3 guideline early detection, diagnosis, therapy and follow-up care of breast cancer, long version 5.02, 2025, AWMF registry number: 032-045OL. [Crossref]
19. Kuhl CK, Strobel K, Bieling H, Wardelmann E, Kuhn W, Maass N, et al. Impact of preoperative breast MR imaging and MR-guided surgery on diagnosis and surgical outcome of women with invasive breast cancer with and without DCIS component. Radiology. 2017; 284: 645-655. (PMID: 28445683) [Crossref]
20. Gommers JJJ, Duijm LEM, Bult P, Strobbe LJA, Kuipers TP, Hooijen MJH, et al. The impact of preoperative breast MRI on surgical margin status in breast cancer patients recalled at biennial screening mammography: an observational cohort study. Ann Surg Oncol. 2021; 28: 5929-5938. (PMID: 33796997) [Crossref]
21. Cozzi A, Di Leo G, Houssami N, Gilbert FJ, Helbich TH, Álvarez Benito M, et al. Preoperative breast MRI reduces reoperations for unilateral invasive lobular carcinoma: a patient-matched analysis from the MIPA study. Eur Radiol. 2025; 35: 3990-4000. (PMID: 40016317) [Crossref]
22. Fricker J. Breast cancer surgery: the journey from mastectomy to conserving treatment. Oncopedia; 2022. [Crossref]
23. Eom HJ, Choi WJ, Sun YJ, Kim HJ, Chae EY, Shin HJ, et al. Preoperative breast MRI in HER2-positive/hormone receptor-negative breast cancer: surgical outcomes using propensity score matching. Eur Radiol. 2025; 35: 5648-5657. (PMID: 40108012) [Crossref]
24. Eom HJ, Cha JH, Choi WJ, Chae EY, Shin HJ, Kim HH. Predictive clinicopathologic and dynamic contrast-enhanced MRI findings for tumor

response to neoadjuvant chemotherapy in triple-negative breast cancer. AJR Am J Roentgenol. 2017; 208: W225-W230. (PMID: 28350486) [Crossref]

25. Coşkun Bilge A, Bulut ZM. The predictive role of mammography, dynamic contrast-enhanced breast magnetic resonance imaging and diffusion-weighted imaging in hormone receptor status of pure ductal carcinoma in situ lesions. Eur J Breast Health. 2024; 20: 241-250. (PMID: 39323287) [Crossref]
26. The ASCO Post Staff. Phase III trial shows no oncologic benefit from routine preoperative MRI for some early breast cancers. The ASCO Post. 2025. [Crossref]
27. Kahneman D. Thinking, fast and slow. New York: Farrar, Straus and Giroux; 2011. [Crossref]
28. Choi WJ, Chae EY, Shin HJ, Cha JH, Kim HH. The role of preoperative breast MRI in patients with early-stage breast cancer. Investig Magn Reson Imaging. 2025; 29: 23-30. [Crossref]
29. Gilbert FJ, Payne NR, Allajbeu I, Yit L, Vinnicombe S, Lyburn I, et al. Comparison of supplemental breast cancer imaging techniques-interim results from the BRAID randomised controlled trial. Lancet. 2022; 405: 1935-1944. (PMID: 40412427) [Crossref]
30. Expert Panel on Breast Imaging; McDonald ES, Scheel JR, Lewin AA, Weinstein SP, Dodelzon K, et al. ACR appropriateness criteria® imaging of invasive breast cancer. J Am Coll Radiol. 2024; 21: S168-S202. (PMID: 38823943) [Crossref]
31. Yamamoto Y, Yamauchi C, Toyama T, Nagai S, Sakai T, Kutomi G, et al. The Japanese Breast Cancer Society Clinical Practice Guidelines for breast cancer, 2022 edition: changes from the 2018 edition and general statements on breast cancer treatment. Breast Cancer. 2024; 31: 340-346. Erratum in: Breast Cancer. 2024; 31: 736-737. (PMID: 38570435) [Crossref]
32. Clauser P, Mann R, Athanasiou A, Prosch H, Pinker K, Dietzel M, et al. A survey by the European Society of Breast Imaging on the utilisation of breast MRI in clinical practice. Eur Radiol. 2018; 28: 1909-1918. (PMID: 29168005) [Crossref]
33. American College of Radiology. ACR practice parameter for the performance of contrast-enhanced magnetic resonance imaging (MRI) of the breast. Revised 2023 (Resolution 8). Reston (VA): American College of Radiology; 2023. [Crossref]
34. Marinovich ML, Houssami N, Spillane A, Mann GB, Taylor D, Reintals M, et al. Changes in patient management after preoperative MRI for newly diagnosed breast cancer: a multicentre prospective observational study. Med J Aust. 2025; 223: 602-610. (PMID: 40993756) [Crossref]
35. DenseBreast-info.org. Dense breast tissue information resource [Internet]. Deer Park (NY): DenseBreast-info, Inc.; [cited 2026 Feb 5]. [Crossref]
36. Berg WA, Seitzman RL, Pushkin J. Implementing the national dense breast reporting standard, expanding supplemental screening using current guidelines, and the proposed find it early act. J Breast Imaging. 2023 Nov 30; 5: 712-723. (PMID: 38141231) [Crossref]
37. DeMartini WB, Strigel RM, Pinker K, Rahbar H, Wang LC. Magnetic resonance imaging. In: ACR BI-RADS v2025 Manual. Reston (VA): American College of Radiology; 2025. [Crossref]
38. Cohen EO, Tso HH, Shin K, Martaindale SR, Bragg AC, Phalak KA, et al. Feasibility of auditing preoperative breast for extent-of-disease evaluation using the BI-RADS v2025 Manual. Radiology. 2025; 317: e243803. Erratum in: Radiology. 2025; 317: e259018. (PMID: 41085394) [Crossref]
39. Wu J, Fan D, Shao Z, Xu B, Ren G, Jiang Z, et al.; Committee of Breast Cancer Society, Chinese Anti-Cancer Association. CACA guidelines for holistic integrative management of breast cancer. Holist Integr Oncol. 2022; 1: 7. (PMID: 37520336) [Crossref]
40. Müller-Schimpfle M, Bader W, Baltzer P, Bernathova M, Fuchsjäger M, Golatta M, et al. Consensus meeting of breast imaging: BI-RADS® and beyond. Breast Care (Basel). 2019; 14: 308-314. (PMID: 31798391) [Crossref]
41. Nisbett RE. The geography of thought: how Asians and Westerners think differently—and why. London: Nicholas Brealey Publishing; 2005. [Crossref]
42. Mounir AM, Shokeir FA, Abd Elraouf GH. Breast imaging: correlation between axillary lymph nodes apparent diffusion coefficient and pathological lymphovascular invasion in patients with invasive breast cancer. Eur J Breast Health. 2025; 21: 141-153. (PMID: 40079346) [Crossref]
43. Kuhl CK. Abbreviated breast MRI: state of the art. Radiology. 2024; 310: e221822. (PMID: 38530181) [Crossref]

ORIGINAL ARTICLE

European Journal of BREAST HEALTH

DOI: 10.4274/ejbh.galenos.2026.2026-3-1
Eur J Breast Health 2026;22(3):340-349

Grisotti versus Wise-Pattern Oncoplastic Reconstruction in Central Breast Cancer: A Randomized Controlled Study

Ismail Ahmed Shafik[1], Sherif Mohamed Mokhtar[1], Kerolos A. Barsoum[1], Abdelrahman Lotfy[1], Abdelrahman M. Mohamed[1], Muhammed Hussein Khalifa[1], Ahmed Shafik Jr.[2], Mahmoud Ali Abdel-Mohsen[1]

[1]Department of General Surgery, Cairo University Faculty of Medicine, Cairo, Egypt
[2]Department of Surgery, New Giza University (NGU), Cairo, Egypt

ABSTRACT

Objective: Central breast tumors requiring excision of the nipple-areola complex present a reconstructive challenge in breast-conserving surgery. Volume-displacement oncoplastic techniques, including the Grisotti flap and reduction-based Wise-pattern reconstruction, allow breast preservation while maintaining oncological safety. This study compares the short-term oncological and aesthetic outcomes of these two techniques.

Materials and Methods: A randomized controlled trial was conducted, enrolling 40 patients with centrally located breast cancer who underwent breast-conserving surgery between March 2023 and November 2024. Patients were randomized to reconstruction using either the Grisotti technique (n = 20) or the Wise-pattern technique (n = 20). The primary outcome was surgical margin status. Secondary outcomes included postoperative complications and aesthetic satisfaction. The mean follow-up duration was 6.9 months.

Results: Mean tumor size was 3.2±1.5 cm in the Grisotti group and 2.6±0.8 cm in the Wise-pattern group (p = 0.327). The mean tumor-to-nipple-areola complex distance was 2.17±1.01 cm in the Grisotti group and 2.90±1.04 cm in the Wise-pattern group (p = 0.428). Negative surgical margins were achieved in 90% and 100% of cases, respectively (p = 0.487), with re-excision required in two Grisotti cases. Postoperative complications did not differ significantly between groups; seroma was the most frequent complication (25% *vs.* 20%, p = 1.0). Patient satisfaction was rated as good or excellent in 85% of Grisotti cases and 90% of Wise-pattern cases (p = 0.549). Mean surgeon satisfaction scores were 7.55±1.39 and 8.10±0.72, respectively (p = 0.128). No cases of flap necrosis were observed.

Conclusion: Both the Grisotti and Wise-pattern techniques demonstrated comparable short-term oncological safety and satisfactory aesthetic outcomes in breast-conserving surgery for central breast tumors. Differences in patient and surgeon satisfaction did not reach statistical significance. The Grisotti technique is most suitable for patients with small-to-moderate breast volumes and mild-to-moderate ptosis, while the Wise-pattern technique offers advantages in macromastia, significant ptosis, or when contralateral symmetrisation is planned. These findings support individualized technique selection based on breast volume and anatomical considerations, while highlighting the need for larger studies with longer follow-up to assess long-term oncological and aesthetic outcomes, and prospective use of validated aesthetic outcome instruments.

Keywords: Oncoplastic breast surgery; breast-conserving surgery; central breast cancer; nipple-areola complex excision; Grisotti flap; Wise-pattern oncoplastic reconstruction; aesthetic outcomes; surgical margins

Corresponding Author: Ahmed Shafik Jr., MD;
E-mail: shafikahmed@me.com; ahmed.shafik@ngu.edu.eg **ORCID:** orcid.org/0009-0002-8035-066X

Received: 31.03.2026 **Accepted:** 17.05.2026 **Available Online Date:** 17.06.2026
Cite this article as: Shafik IA, Mokhtar SM, Barsoum KA, Lotfy A, Mohamed AM, Khalifa MH, et al. Grisotti versus Wise-pattern oncoplastic reconstruction in central breast cancer: a randomized controlled study. Eur J Breast Health. 2026;22(3):340-349

KEY POINTS

- This randomized study compares the Grisotti flap and Wise-pattern therapeutic mammoplasty for centrally located breast cancer.
- Both techniques demonstrated comparable short-term oncologic safety and acceptable aesthetic outcomes.
- Margin status, complication rates, and patient satisfaction did not differ significantly between groups.
- Technique selection may be guided by anatomical considerations and surgeon expertise.

Introduction

Breast-conserving surgery (BCS) is a cornerstone of contemporary breast cancer management, offering oncological outcomes equivalent to those of mastectomy while preserving breast form and patients' quality of life. Landmark randomised trials have established that BCS with radiotherapy achieves long-term survival and local control equivalent to mastectomy in eligible patients (1, 2). Over the past two decades, the integration of reconstructive techniques into breast-conserving procedures has led to the development of oncoplastic BCS (OPBCS), which combines oncologic resection with volume displacement or volume replacement techniques to optimize aesthetic outcomes without compromising oncological safety (3). International consensus statements and practice guidelines now recognize OPBCS as a standard component of breast cancer surgery when performed in accordance with established oncologic principles (4-6).

Multiple observational studies and pooled analyses have demonstrated that OPBCS achieves rates of negative margins, local recurrence, and survival comparable to conventional BCS, despite being applied to patients with larger tumors or less favorable tumor-to-breast ratios (5-7). Importantly, available evidence suggests that OPBCS does not increase the risk of postoperative complications or delay adjuvant therapy when appropriately planned and executed, supporting its oncological safety in routine clinical practice (5-7).

Centrally located breast cancers, particularly those requiring excision of the nipple-areola complex (NAC), represent a distinct reconstructive challenge in BCS. Although tumor location alone is no longer considered a contraindication to breast conservation, resection of the NAC can result in significant central breast deformity if reconstruction is inadequate. Contemporary oncoplastic approaches have therefore focused on restoring breast shape and symmetry following central excision, allowing breast conservation in selected patients who might otherwise undergo mastectomy (8, 9).

Among the volume-displacement techniques described for centrally located tumors, the Grisotti flap is a well-established approach that enables immediate reconstruction of the central defect using local glandular tissue. Favorable oncological and aesthetic outcomes have been reported with this technique, particularly in patients with small-to-moderate breast volumes and mild to moderate ptosis (8-10). However, several studies have highlighted limitations of the classical Grisotti technique in patients with large or markedly ptotic breasts, short nipple–inframammary fold distances, or unfavorable breast morphology, prompting the development of technical modifications and alternative oncoplastic strategies (8, 11).

Therapeutic reduction mammoplasty and mastopexy-based techniques, commonly employing a Wise-pattern skin incision, represent established level II volume-displacement oncoplastic procedures. These techniques allow wider resections, improved reshaping of the breast mound, and contralateral symmetrization in appropriately selected patients, particularly those with larger breast volumes or significant ptosis (5, 6, 8). Current guidelines emphasize that selection of oncoplastic technique should be individualized, taking into account breast size, degree of ptosis, tumor characteristics, and patient preferences, rather than adhering to a single reconstructive approach (4-6).

Despite the widespread adoption of both the Grisotti technique and reduction-based oncoplastic approaches, existing evidence directly comparing specific oncoplastic techniques remains limited. Most available comparative studies remain retrospective or descriptive in nature, and comparative data are often confounded by heterogeneity in patient selection, tumor characteristics, and outcome assessment (4, 7, 12). In addition, while patient-reported outcomes and aesthetic satisfaction are increasingly recognized as essential endpoints in oncoplastic surgery, few studies have incorporated both surgeon-reported and patient-reported assessments within a comparative framework (6, 12).

This randomized controlled trial was designed to compare the short-term oncological and aesthetic outcomes of the Grisotti technique and Wise-pattern oncoplastic reconstruction in patients undergoing BCS for centrally located breast cancer. By directly comparing two commonly used volume-displacement techniques within a randomized design, this study aims to contribute higher-level evidence to inform technique selection and to optimize individualized surgical planning for this challenging patient population.

Materials and Methods

Study Design

This prospective randomized controlled trial was conducted at Kasr Al-Ainy Teaching Hospitals, Faculty of Medicine, Cairo University between March 2023 and November 2024. The study included 40 patients diagnosed with centrally located breast cancer who underwent BCS. Patients were randomized into two equal groups: Group A (Grisotti technique, $n = 20$) and Group B (Wise-pattern technique, $n = 20$).

Ethics Approval and Trial Registration

The study protocol was approved by the Research Ethics Committee of the Faculty of Medicine, Cairo University (approval code: MD-266-2023, approved on 10 September 2023), prior to patient enrollment. The study design, eligibility criteria, and primary and secondary outcomes were prospectively defined before recruitment commenced in March 2023. The trial was retrospectively registered with the ISRCTN registry (ISRCTN16836500) on 20 May 2025; prospective registration was not mandated by the institutional ethics committee at the time of study initiation. All procedures were conducted in accordance with the Declaration of Helsinki and relevant national regulations. Written informed consent was obtained from all participants prior to enrollment.

The study was conducted in accordance with the pre-approved protocol throughout; no amendments to the study design, eligibility criteria, or outcome definitions were made after patient enrollment commenced.

Inclusion and Exclusion Criteria

Inclusion Criteria

- Patients with early-stage, centrally located breast cancer (cT1–2) suitable for BCS.
- Centrally located breast cancer cases downgraded to cT1–2 following neoadjuvant therapy.

Exclusion Criteria

- Breast cancer not centrally located.
- Inflammatory breast cancer (cT4d).
- Metastatic or multicentric breast cancer.
- Patients with small breast size (cup size C or smaller).

Preoperative Assessment

All patients underwent comprehensive preoperative evaluation, including:

- Detailed medical history, including family history, prior breast irradiation, and symptoms suggestive of metastatic disease.
- Complete clinical examination of the breasts and axillae.
- Bilateral sonomammography.
- Histopathological confirmation via ultrasound-guided core needle biopsy.
- Breast magnetic resonance imaging (MRI) to evaluate NAC involvement.
- Routine laboratory investigations and metastatic workup.

All cases were discussed in a multidisciplinary setting prior to surgical intervention.

The decision to excise the NAC was based on a multidisciplinary assessment and was not determined by tumor-to-NAC distance alone. Indications included clinical nipple involvement (retraction or ulceration), MRI-documented subareolar extension, and pathological subtypes associated with increased risk of NAC involvement, such as Paget disease and centrally located invasive carcinoma with subareolar ductal spread.

Molecular Classification and Receptor Status

All tumors were analyzed for hormone receptor and HER2 status via immunohistochemistry. Estrogen receptor (ER) and progesterone receptor (PR) positivity were defined as ≥1% of tumor cell nuclei with nuclear staining. HER2 status was determined by immunohistochemistry (0, 1+, 2+, 3+) and confirmed by fluorescence in situ hybridization (FISH) when IHC was 2+. Tumors were classified into five molecular subtypes based on receptor status and Ki-67 proliferation index: Luminal A (ER+ and/or PR+, HER2-, Ki-67 <14%), Luminal B1 (ER+ and/or PR+, HER2-, Ki-67 ≥14%), Luminal B2 (ER+ and/or PR+, HER2+, any Ki-67), HER2-enriched (ER-, PR-, HER2+), and triple-negative breast cancer (ER-, PR-, HER2-). Classification was performed according to American Society of Clinical Oncology and College of American Pathologists guidelines (13).

Randomization

Eligible patients were randomized 1:1 to the Grisotti technique group or the Wise-pattern technique group. Randomization was performed using a computer-generated randomization sequence. Due to the nature of the surgical interventions, blinding of the operating surgeons was not feasible.

Surgical Techniques

Grisotti Technique

Preoperatively, the NAC was marked for circular excision. Following central lumpectomy with removal of the NAC,

Figure 1. Circular excision of the nipple-areola complex is outlined, with inferiorly based dermoglandular flap design and planned skin island for neo-areola reconstruction

Figure 2. Postoperative appearance demonstrating central defect reconstruction with advancement of the dermoglandular flap and formation of the neo-areola

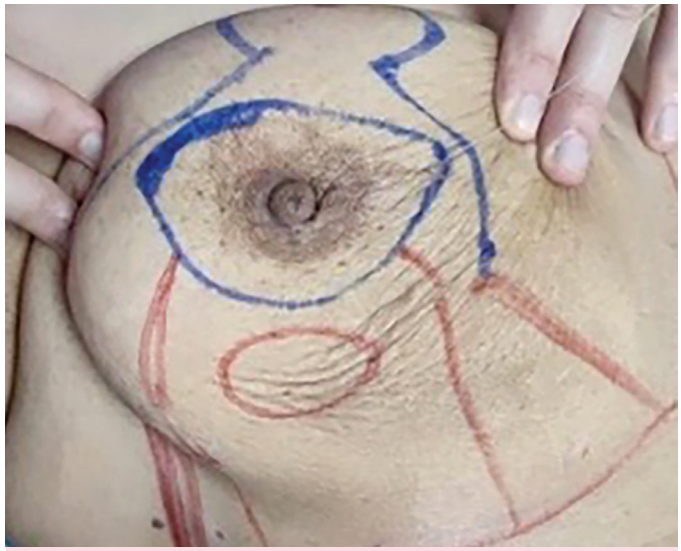

Figure 3. Standard Wise-pattern skin markings outlining central excision and planned reduction-based parenchymal reshaping

reconstruction was performed using a dermoglandular flap incorporating a skin island to recreate the neo-NAC. The flap was mobilized and advanced into the central defect, and glandular reshaping was performed to restore breast contour (Figures 1 and 2).

Wise-Pattern Technique

In the Wise-pattern group, reconstruction was performed using a therapeutic mammoplasty approach. After central tumor excision with NAC removal, a Wise-pattern incision was used to permit adequate tumor resection and parenchymal reshaping. Glandular redistribution was performed to restore breast contour and symmetry. Contralateral symmetrization was performed when indicated (Figures 3 and 4).

All procedures adhered to oncological principles with the goal of achieving clear surgical margins.

Outcome Measures

Primary outcomes included:

- Surgical margin status.
- Postoperative complications.
- Aesthetic satisfaction.

Margin status was determined from the final histopathological examination. Postoperative complications included seroma formation and wound infection.

Aesthetic outcomes were assessed using both patient-reported satisfaction (categorized as excellent/good versus fair/poor) and surgeon-reported visual analog scale (VAS) scoring. A surgeon-reported VAS (0–10) was selected as a complementary continuous measure of overall aesthetic outcome alongside the categorical patient satisfaction scale. We acknowledge that validated instruments, such as the Harvard Breast Cosmesis Scale and the BREAST-Q, would have provided a more standardised assessment; their absence is recognised as a limitation of the current study. VAS was selected for its simplicity and feasibility in routine clinical practice.

Follow-up

Patients were followed postoperatively according to institutional protocols. The mean follow-up duration was 6.9 months. Follow-up duration was reported as the mean because individual patient-level data required to calculate the median and range were unavailable. Clinical assessment included evaluation of wound healing, postoperative complications, and early oncological outcomes. No patients were lost to follow-up.

Figure 4. Intraoperative view demonstrating parenchymal redistribution and closure using the Wise-pattern technique after nipple-areola complex excision

Statistical Analysis

Statistical analysis was performed using SPSS version 28 (IBM Corp., Armonk, NY, USA). Continuous variables were expressed as mean ± standard deviation. Normality of data distribution was assessed using the Shapiro-Wilk test. Tumor diameter and NAC distance were non-normally distributed and were therefore analyzed using the Mann-Whitney U test; normally distributed variables were compared using independent-samples t-tests. Categorical variables were analyzed using chi-square or Fisher's exact tests where appropriate. A p-value <0.05 was considered statistically significant.

Results

Patient Characteristics

Forty patients were randomized into two equal groups: the Grisotti group (n = 20) and the Wise-pattern group (n = 20).

The mean age was 52.95±9.79 years in the Grisotti group and 54.90±6.50 years in the Wise-pattern group (p = 0.463) (Table 1). Marital status (p = 0.438), medical comorbidities (p = 0.739), and family history (p = 0.661) were comparable between groups (Table 2).

Tumor characteristics were similar between groups. The mean largest tumor diameter was 3.21±1.48 cm in the Grisotti group and 2.60±0.82 cm in the Wise-pattern group (p = 0.327, Mann-Whitney U test). The mean distance from the NAC was 2.17±1.01 cm in the Grisotti group and 2.90±1.04 cm in the Wise-pattern group (p = 0.428, Mann-Whitney U test) (Table 3). One patient in the Grisotti group had an initial tumor diameter of 6.8 cm (clinical T3); this patient received neoadjuvant chemotherapy, resulting in downstaging to ypT2 prior to enrollment, consistent with the study's inclusion criteria.

The distribution of pathological types showed no significant differences between groups (p = 0.220). Invasive ductal carcinoma was the most common subtype in both groups (70% in the Grisotti group *vs.* 80% in the Wise-pattern group). Hormonal receptor subtypes were similarly distributed (p = 0.829) (Table 4). All randomized patients were included in the final analysis.

Treatment Characteristics

Neoadjuvant chemotherapy was administered more frequently in the Wise-pattern group (70%) than in the Grisotti group (25%) (p = 0.004). Regarding axillary management, sentinel lymph node biopsy was performed in 70% of Grisotti patients and 40% of Wise-pattern patients, whereas axillary lymph node dissection was required in 30% of Grisotti patients and 60% of Wise-pattern patients (p = 0.057) (Table 5).

Among the 19 patients who received neoadjuvant chemotherapy (5 in the Grisotti group, 14 in the Wise-pattern group), invasive ductal carcinoma was the predominant histological subtype. Pre-treatment tumor sizes in the Grisotti NCT subgroup ranged from 1.9 to 6.8 cm, and molecular subtypes included Luminal B1, Luminal A, HER2-enriched, and Luminal AB1. One patient in this subgroup was downstaged from cT3 to ypT2 following treatment.

Table 1. Age distribution of participants

	Grisotti					Wise pattern					*p*-value
	Mean	SD (±)	Median	Min.	Max.	Mean	SD (±)	Median	Min.	Max.	
Age	52.95	9.79	51.00	37.00	74.00	54.90	6.50	54.50	43.00	66.00	0.463

SD: Standard deviation; Min.: Minimum; Max: Maximum

Table 2. Demographic data

Count		Grisotti		Wise pattern		*p*-value
		%	Count	%		
Marital status	Married	16	80.0%	12	60.0%	0.438
	Widow	3	15.0%	6	30.0%	
	Divorced	1	5.0%	2	10.0%	
Medical condition	Cardiac	1	5.0%	2	10.0%	0.739
	CKD	1	5.0%	0	0.0%	
	DM	2	10.0%	0	0.0%	
	HTN	3	15.0%	4	20.0%	
	HTN, DM	3	15.0%	2	10.0%	
	Free	10	50.0%	12	60.0%	
Family history	Positive	2	10.0%	4	20.0%	0.661
	Negative	18	90.0%	16	80.0%	

CKD: Chronic kidney disease; DM: Diabetes mellitus; HTN: Hypertension

Table 3. Tumor characteristics: diameter and distance from nipple-areola complex (NAC)

	Grisotti					Wise pattern					*p*-value
	Mean	SD	Median	Min.	Max.	Mean	SD	Median	Min.	Max.	
Largest diameter of the tumor	3.21	1.48	2.80	1.40	6.80*	2.60	0.82	2.75	1.50	4.00	0.327
Distance from the NAC (cm)	2.17	1.01	2.15	0.50	4.00	2.90	1.04	2.20	0.00	3.5	0.428

*: This value represents a patient who was initially clinical T3 and was downstaged to ypT2 following neoadjuvant chemotherapy prior to surgical enrollment, in accordance with the study's inclusion criteria. *P*-values: tumor diameter $p = 0.327$; NAC distance $p = 0.428$ (Mann-Whitney U test). SD: Standard deviation; Min.: Minimum; Max.: Maximum

Table 4. Histopathological and immunohistochemical characteristics of tumor

Count		Grisotti		Wise pattern		*p*-value
		%	Count	%		
Pathological type	Paget	2	10.0%	4	20.0%	0.220
	ILC	3	15.0%	0	0.0%	
	IDC	14	70.0%	16	80.0%	
	DCIS	1	5.0%	0	0.0%	
Clinical involvement of the nipple	Ulceration	2	10.0%	4	20.0%	0.458
	Retraction	7	35.0%	4	20.0%	
	No clinical involvement	11	55.0%	12	60.0%	
Hormonal status	HER2 enriched	2	10.0%	2	10.0%	0.829
	Luminal A	9	45.0%	6	30.0%	
	Luminal B1	5	25.0%	8	40.0%	
	Luminal B2	1	5.0%	2	10.0%	
	Luminal AB1	1	5.0%	0	0.0%	
	Triple negative	2	10.0%	2	10.0%	

Molecular subtypes were determined based on immunohistochemistry (IHC) for estrogen receptor (ER), progesterone receptor (PR), and human epidermal growth factor receptor 2 (HER2), and Ki-67 proliferation index, classified as follows: Luminal A (ER+ and/or PR+, HER2-, Ki-67 <14%), Luminal B1 (ER+ and/or PR+, HER2-, Ki-67 ≥14%), Luminal B2 (ER+ and/or PR+, HER2+, any Ki-67), HER2-enriched (ER-, PR-, HER2+), and Triple-negative (ER-, PR-, HER2-) (13). ER status was considered positive if ≥1% of tumor cell nuclei stained positive; PR and HER2 were scored according to American Society of Clinical Oncology/College of American Pathologists guidelines. ILC:

ILC: Invasive lobular carcinoma; IDC: Invasive ductal carcinoma; DCIS: Ductal carcinoma *in situ*

In the Wise-pattern NCT subgroup, pre-treatment tumor sizes ranged from 1.5 to 4.0 cm, with Luminal B1 being the most frequent subtype, followed by triple-negative, HER2-enriched, and Luminal B2. The higher proportion of NCT recipients and higher rate of axillary lymph node dissection in the Wise-pattern group suggest a greater initial tumor burden at presentation, which may have influenced surgical planning and technique selection.

Surgical Outcomes

Negative margins were achieved in 90% of patients in the Grisotti group and 100% in the Wise-pattern group ($p = 0.487$). Two patients in the Grisotti group required re-excision because of positive margins on initial surgery; clear margins were subsequently obtained.

Postoperative Complications

Postoperative complications did not differ significantly between groups. Seroma occurred in 25% of patients in the Grisotti group and in 20% of patients in the Wise-pattern group ($p = 1.0$). Wound infection was reported in 10% of Grisotti patients and in none of the Wise-pattern patients ($p = 0.487$). Wound dehiscence occurred in 5% of Grisotti patients and was not observed in the Wise-pattern group ($p = 1.0$). No cases of flap necrosis were observed in either group (Table 6).

Aesthetic Outcomes

Patient-reported satisfaction did not differ significantly between groups ($p = 0.549$). In the Grisotti group, outcomes were rated

Table 5. Surgical approach and procedure details

Count		Grisotti		Wise pattern		*p*-value
		%	Count	%		
Neoadjuvant therapy	Yes	5	25.0%	14	70.0%	0.004
	No	15	75.0%	6	30.0%	
Surgery to axilla	SLNB	14	70.0%	8	40.0%	0.057
	ALND	6	30.0%	12	60.0%	
Margin status	Infiltrated	2	10.0%	0	0.0%	0.487
	Free	18	90.0%	20	100.0%	

SLNB: Sentinel lymph node biopsy; ALND: Axillary lymph node dissection

Table 6. Postoperative complications and their incidence

Count		Grisotti		Wise pattern		*p*-value
		%	Count	%		
Seroma	Yes	5	25.0%	4	20.0%	1.000
	No	15	75.0%	16	80.0%	
Wound infection	Yes	2	10.0%	0	0.0%	0.487
	No	18	90.0%	20	100.0%	
Flap necrosis	No	20	100.0%	20	100.0%	N/A
Wound dehiscence	Yes	1	5.0%	0	0.0%	1.000
	No	19	95.0%	20	100.0%	

Table 7. Aesthetic outcomes according to surgical technique

Outcome	Grisotti ($n = 20$)	Wise pattern ($n = 20$)	*p*-value
Surgeon satisfaction (mean ± SD)	7.55±1.39	8.10±0.72	0.128
Patient satisfaction category, n (%)			0.549
Fair	3 (15%)	2 (10%)	
Good	6 (30%)	10 (50%)	
Excellent	11 (55%)	8 (40%)	

SD: Standard deviation

as excellent, good, and fair in 55%, 30%, and 15% of patients, respectively. In the Wise-pattern group, 40% rated the outcomes as excellent, 50% as good, and 10% as fair.

Surgeon satisfaction scores were 7.55±1.39 in the Grisotti group and 8.10±0.72 in the Wise-pattern group ($p = 0.128$) (Table 7).

Follow-up

The mean follow-up duration was 6.9 months. No early local recurrences were observed during the follow-up period.

Discussion and Conclusion

The present randomized study compared the Grisotti technique and Wise-pattern therapeutic mammoplasty in patients undergoing BCS for centrally located breast cancer. Both techniques demonstrated acceptable short-term oncological and aesthetic outcomes.

OPBCS has been widely adopted as a safe alternative to conventional lumpectomy, integrating oncologic resection with reconstructive principles to optimize cosmetic results without compromising cancer control (4-6). Pooled analyses have demonstrated comparable rates of margin negativity and local recurrence between OPBCS and conventional BCS (7). Negative margins were achieved in the majority of patients in both groups, and no statistically significant difference was observed between groups. Although two patients in the Grisotti group required re-excision, clear margins were ultimately obtained in all cases. No early local recurrences were detected during follow-up; however, the limited duration of monitoring precludes conclusions regarding long-term oncologic safety.

Centrally located breast cancers requiring excision of the NAC represent a distinct reconstructive challenge. Several oncoplastic techniques, including the Grisotti flap and reduction-based approaches, have been described to facilitate breast conservation in such cases (8, 9). Contemporary consensus statements emphasize that technique selection should be individualized based on breast size, degree of ptosis, tumor characteristics, and surgeon expertise rather than adherence to a single reconstructive strategy (4-6). In this context, the absence of significant differences in margin status or complication rates between the groups in our study suggests that both approaches can be applied safely when patients are appropriately selected.

Based on our findings and current consensus guidelines, technique selection should be tailored to the individual patient's breast morphology and tumor characteristics. The Grisotti technique is most appropriate for patients with small-to-moderate breast volumes and mild-to-moderate ptosis (Regnault grade I–II), where the central defect can be reliably reconstructed by rotation and advancement of an inferiorly based dermoglandular flap, without requiring extensive parenchymal redistribution. It offers a technically straightforward approach with limited scarring and is particularly useful when the contralateral breast does not require symmetrisation. Its principal limitations include restricted applicability in cases of macromastia or significant ptosis (grade III), where flap reach and capacity for reshaping may be insufficient to achieve satisfactory aesthetic outcomes, and the potential for central breast flattening if parenchymal volume is inadequate.

The Wise-pattern technique is best suited to patients with larger breast volumes, significant ptosis, or those in whom wide parenchymal redistribution is required to fill a larger central defect. It simultaneously achieves breast reduction, mastopexy, and oncological resection and is advantageous when contralateral symmetrisation is planned. Its limitations include a more complex inverted-T scar pattern, longer operative time, and a theoretical risk of wound-healing complications at the T-junction, although these complications were not observed in our series. When breast morphology is intermediate, patient preference, surgeon expertise, and the intended adjuvant treatment plan should guide the final decision. Both techniques should be performed within a multidisciplinary oncoplastic framework with clear margin achievement as the primary oncological endpoint (4-6). These findings reinforce the importance of individualized oncoplastic planning rather than technique standardization.

A significant imbalance in neoadjuvant chemotherapy administration was observed between groups, with higher rates in the Wise-pattern cohort. While tumor diameter and biological subtype distribution were comparable at the time of surgery, the higher pre-treatment tumor burden, as suggested by the NCT distribution, may reflect selection bias toward the Wise-pattern technique for patients with initially larger or more advanced tumors requiring greater parenchymal reshaping. The potential impact of neoadjuvant therapy on surgical complexity and aesthetic outcomes should be considered when interpreting results.

Postoperative complications were infrequent and comparable between groups. Seroma formation was the most common complication, while wound infection and dehiscence were uncommon. No cases of flap necrosis occurred. Previous series evaluating oncoplastic techniques have reported low rates of major complications, with most events managed conservatively and without delay to adjuvant therapy (5, 12). Our findings are consistent with these reports and support the safety of both reconstructive strategies in the early postoperative period.

Aesthetic outcomes were evaluated using both patient-reported and surgeon-reported measures. Patient satisfaction did not differ significantly between groups, and surgeon satisfaction

scores were comparable. Increasing emphasis has been placed on the importance of patient-reported outcomes in oncoplastic breast surgery (6, 12). The comparable satisfaction rates observed in this study align with prior literature suggesting that both local flap and reduction-based techniques can achieve acceptable cosmetic results when carefully planned (8, 10).

The Wise-pattern technique has been described as advantageous in patients with larger or ptotic breasts due to broader parenchymal reshaping and improved symmetry (5, 8). Conversely, the Grisotti technique remains a valuable option in selected cases with moderate breast volume and central defects (8, 9). The absence of statistically significant differences in short-term outcomes within this randomized cohort suggests that both techniques remain viable options for centrally located tumors when applied to appropriately selected patients. Reduction-based techniques employing Wise-pattern skin incisions have also demonstrated reliable reconstructive outcomes in breast surgery, supporting their versatility in managing complex breast defects (14).

Study Limitations

Several limitations should be acknowledged. The sample size was relatively small, limiting statistical power to detect modest differences. The follow-up was too short to assess long-term recurrence, radiation-related changes, or late cosmetic outcomes. Individual patient follow-up data to calculate the median and range were not available for this report. Additionally, the imbalance in neoadjuvant therapy distribution represents a potential confounding factor. Aesthetic outcomes were assessed using a surgeon-reported VAS and a categorical patient satisfaction scale rather than validated instruments such as the Harvard Breast Cosmesis Scale or BREAST-Q. This limits direct comparability with published literature and reduces the robustness of conclusions regarding aesthetic outcomes. The absence of a validated patient-reported outcome measure such as the BREAST-Q—which encompasses multiple domains including satisfaction with breasts, psychosocial well-being, and physical well-being—represents a further limitation, and future studies should incorporate such instruments prospectively. The retrospective registration of the trial was acknowledged as a further limitation; however, the study design, eligibility criteria, and outcomes were defined prior to enrollment, and ethical approval was obtained before the first patient was recruited. Larger, multicenter studies with extended follow-up and prospective use of validated outcome measures are warranted to further evaluate comparative effectiveness.

In this randomized cohort of patients undergoing BCS for centrally located breast cancer, both the Grisotti and Wise-pattern techniques demonstrated comparable short-term oncological safety and acceptable aesthetic outcomes. Margin status, complication rates, and patient- and surgeon-reported satisfaction did not differ significantly between groups. Within the limitations of sample size and follow-up duration, both approaches appear to be viable reconstructive options when selected according to patient anatomy and tumor characteristics with the Grisotti technique preferred in small-to-moderate-volume breasts with mild-to-moderate ptosis and the Wise-pattern technique offering advantages in macromastia, significant ptosis, or when contralateral symmetrisation is required. Further studies with larger populations and longer follow-up are warranted to confirm long-term oncologic and cosmetic outcomes.

Ethics

Ethics Committee Approval: The study protocol was approved by the Research Ethics Committee of the Faculty of Medicine, Cairo University (approval code: MD-266-2023, approved on 10 September 2023), prior to patient enrollment.

Informed Consent: Written informed consent was obtained from all participants prior to enrollment.

Footnotes

Authorship Contributions

Concept: I.A.S., K.A.B., A.L., M.H.K., A.S.J.; Design: I.A.S., S.M.M., A.L., M.A.A-M.; Data Collection and/or Processing: A.L., A.M.M., M.H.K., A.S.J., M.A.A-M.; Analysis and/or Interpretation: I.A.S., S.M.M., K.A.B., A.M.M., A.S.J., M.A.A-M.; Literature Search: A.L., A.M.M., A.S.J.; Writing: I.A.S., S.M.M., K.A.B., A.L., A.M.M., M.H.K., A.S.J., M.A.A-M.

Conflict of Interest: The authors have no conflicts of interest to declare.

Financial Disclosure: The authors declared that this study has received no financial support.

References

1. Fisher B, Anderson S, Bryant J, Margolese RG, Deutsch M, Fisher ER, et al. Twenty-year follow-up of a randomized trial comparing total mastectomy, lumpectomy, and lumpectomy plus irradiation for the treatment of invasive breast cancer. N Engl J Med. 2002; 347: 1233-1241. (PMID: 12393820) [Crossref]

2. Veronesi U, Cascinelli N, Mariani L, Greco M, Saccozzi R, Luini A, et al. Twenty-year follow-up of a randomized study comparing breast-conserving surgery with radical mastectomy for early breast cancer. N Engl J Med. 2002; 347: 1227-1232. (PMID: 12393819) [Crossref]

3. Clough KB, Lewis JS, Couturaud B, Fitoussi A, Nos C, Falcou MC. Oncoplastic techniques allow extensive resections for breast-conserving therapy of breast carcinomas. Ann Surg. 2003; 237: 26-34. (PMID: 12496527) [Crossref]

4. Weber WP, Soysal SD, El-Tamer M, Sacchini V, Knauer M, Tausch C, et al. First international consensus conference on standardization of oncoplastic breast-conserving surgery. Breast Cancer Res Treat. 2017; 165: 139-149. (PMID: 28578506) [Crossref]

5. Gilmour A, Cutress R, Gandhi A, Harcourt D, Little K, Mansell J, et al.

Oncoplastic breast surgery: a guide to good practice. Eur J Surg Oncol. 2021; 47: 2272-2285. (PMID: 34001384) [Crossref]

6. Thompson PW, Chatterjee A, Losken A. Standards in oncoplastic breast-conserving surgery. Ann Breast Surg. 2022; 6: 37. [Crossref]
7. Hasan MT, Hamouda M, Khashab MKE, Elsnhory AB, Elghamry AM, Hassan OA, et al. Oncoplastic versus conventional breast-conserving surgery in breast cancer: a pooled analysis of 6941 female patients. Breast Cancer. 2023; 30: 200-214. (PMID: 36622565) [Crossref]
8. Karoobi M, Yazd SMM, Aminolroaya F, Mahram H, Saghafinia S, Pompei S, et al. Introducing an oncoplastic approach for centrally located breast cancer patients. World J Surg Oncol. 2025; 23: 249. (PMID: 40551172) [Crossref]
9. Kijima Y, Yoshinaka H, Shinden Y, Hirata M, Nakajo A, Arima H, et al. Oncoplastic breast surgery for centrally located breast cancer: a case series. Gland Surg. 2014; 3: 62-73. (PMID: 25083497) [Crossref]
10. Chen Y, Chen Q, Dong J, Liu D, Huang L, Xie F, et al. Modified Grisotti flap technique in centrally located breast cancer: case report. Gland Surg. 2021; 10: 2867-2873. (PMID: 34733734) [Crossref]
11. Chatterjee A, Gass J, Burke MB, Kopkash K, El-Tamer MB, Holmes DR, et al. Results from the American Society of Breast Surgeons Oncoplastic Surgery Committee 2017 survey: Current practice and future directions. Ann Surg Oncol. 2018; 25: 2790-2794. (PMID: 30003450) [Crossref]
12. Mysuria S, McKevitt E, Warburton R, Bazzarelli A, Bovill E, Isaac K, et al. Oncoplastic breast reconstruction: complications and patient-reported outcomes. Plast Surg (Oakv). 2025: 22925503251350906. (PMID: 40607202) [Crossref]
13. Hammond ME, Hayes DF, Dowsett M, Allred DC, Hagerty KL, Badve S, et al. American Society of Clinical Oncology/College of American Pathologists guideline recommendations for immunohistochemical testing of estrogen and progesterone receptors in breast cancer. Arch Pathol Lab Med. 2010; 134: 907-922. Erratum in: Arch Pathol Lab Med. 2010; 134: 1101. (PMID: 20516735) [Crossref]
14. Cheong SC, Maliekal J, Tung WS, Saadya A, Awad GA. Wise versus vertical mastopexy pattern skin-reducing mastectomy with immediate breast reconstruction: systematic review and meta-analysis. Plast Reconstr Surg Glob Open. 2025; 13: e6584. (PMID: 40092505) [Crossref]

ORIGINAL ARTICLE

European Journal of BREAST HEALTH

DOI: 10.4274/ejbh.galenos.2026.2026-1-9
Eur J Breast Health 2026;22(3):350-357

Interim Breast MRI for Predicting Pathologic Complete Response After Neoadjuvant Chemotherapy in Early Breast Cancer

Eri Kato[1], Hideo Shigematsu[1], Ai Amioka[1], Shinsuke Sasada[1], Takayuki Kadoya[1,2], Morihito Okada[1]

[1]Department of Surgical Oncology, Hiroshima University, Research Institute for Radiation Biology and Medicine, Hiroshima, Japan
[2]Department of Breast Center, Shimane University Hospital, Izumo, Japan

ABSTRACT

Objective: Accurate prediction of pathological complete response (pCR) to neoadjuvant chemotherapy (NAC) is essential for treatment decision-making in breast cancer. The value of integrated prediction models combining interim magnetic resonance imaging (MRI) findings with clinicopathological factors remains uncertain. This study aimed to compare interim and post-NAC MRI in predicting pCR and to assess the performance of prediction models integrating MRI and clinicopathological variables.

Materials and Methods: We retrospectively analyzed 249 patients with early-stage breast cancer who underwent MRI before, during (interim), and after NAC. Clinicopathological variables were selected via stepwise regression based on the minimum Akaike information criterion. Four predictive models were developed: Model A used clinicopathological variables alone; Model B added interim MRI; Model C added post-NAC MRI; and Model D incorporated both interim and post-NAC MRI. Model performance was assessed using receiver operating characteristic curve analysis, calibration plots, and decision curve analysis.

Results: Sixty-two (25%) patients achieved pCR. Independent predictors in Model A included hormone receptor status, human epidermal growth factor receptor 2 status, and clinical tumor size. The areas under the curves were 0.721 (Model A), 0.819 (Model B), 0.847 (Model C), and 0.848 (Model D). Model B (interim MRI) demonstrated the highest sensitivity (0.99) and negative predictive value (0.97), enabling early identification of pCR, while Models C and D showed only modest improvements. In decision curve analysis, calibration and clinical utility were superior in models incorporating MRI compared with Model A.

Conclusion: Interim MRI demonstrated pCR-predictive performance comparable to that of post-NAC MRI, supporting its potential utility as a clinically meaningful tool for early treatment decision-making. However, its relatively high false-positive rate suggests that caution is warranted when applying it to guide surgical de-escalation.

Keywords: Breast neoplasms; neoadjuvant therapy; magnetic resonance imaging; pathologic complete response; predictive value of tests

Corresponding Author: Hideo Shigematsu, MD, PhD;
E-mail: shigematu1330@hiroshima-u.ac.jp **ORCID:** orcid.org/0000-0001-9393-9655
Received: 10.02.2026 **Accepted:** 19.05.2026 **Available Online Date:** 17.06.2026
Cite this article as: Kato E, Shigematsu H, Amioka A, Sasada S, Kadoya T, Okada M. Interim breast MRI for predicting pathologic complete response after neoadjuvant chemotherapy in early breast cancer. Eur J Breast Health. 2026;22(3):350-357

KEY POINTS

- Interim magnetic resonance imaging (MRI), performed during neoadjuvant chemotherapy (NAC) treatment, demonstrated significant predictive ability for post-NAC pathological complete response (pCR) in patients with breast cancer.
- Combining interim MRI findings with clinicopathological factors improved predictive accuracy for pCR.
- Interim MRI may contribute to early identification of non-responders and support treatment decision-making.
- This study provides real-world evidence supporting the clinical utility of interim MRI in patients with breast cancer undergoing NAC.

Introduction

Although surgery-first has traditionally been the standard approach in early-stage breast cancer, neoadjuvant chemotherapy (NAC) is increasingly used and represents a standard treatment option in selected subtypes, particularly human epidermal growth factor receptor 2 (HER2)-positive and triple-negative breast cancer, in the context of surgical de-escalation and response-guided therapy (1). With advances in systemic therapy, treatment response rates have improved, and the number of patients achieving pathological complete response (pCR) has increased. With these improvements, clinical trials investigating the omission of surgery in responders are underway, but the development of surgical de-escalation strategies requires accurate and less invasive identification of pCR in patients with breast cancer undergoing NAC (2).

Among imaging modalities used to assess response to NAC, contrast-enhanced magnetic resonance imaging (MRI) is considered to be the most reliable technique (3). However, MRI alone has limited accuracy in predicting pCR, and its diagnostic performance varies according to breast cancer subtype, with lower accuracy reported in hormone receptor (HR)-positive/HER2-negative breast cancer and higher accuracy in HER2-positive and triple-negative subtypes (3, 4). To address these limitations, several integrated prediction models that combine MRI features with clinicopathological variables (e.g., tumor size, HR status, HER2 status, and Ki-67 index) have been proposed, demonstrating superior and less invasive pCR prediction compared with MRI alone (5, 6).

Recent studies have further suggested that pCR may be predicted more accurately based on MRI performed during NAC treatment (interim MRI) than on post-NAC MRI (7). Quantitative longitudinal parameters, such as changes in tumor size, apparent diffusion coefficient values on diffusion-weighted imaging, and background parenchymal enhancement, have also shown promise in detecting early treatment response (8-10). Nevertheless, studies comparing the diagnostic accuracy of interim and post-NAC MRI or evaluating the clinical utility of integrated prediction models that incorporate clinicopathological variables remain limited (6, 11). Moreover, previous studies defined pCR as the absence of residual invasive cancer in the breast, whereas only a few have adopted the stricter criterion of no residual invasive or non-invasive carcinoma in either the breast or lymph nodes (ypT0, ypN0) (6, 8, 11, 12).

Therefore, we conducted a retrospective cohort study of patients with early-stage breast cancer who underwent MRI during and after NAC. The aim of this study was to compare the predictive performance of interim and post-NAC MRI in predicting pCR (defined as ypT0, ypN0) and to evaluate the diagnostic performance and clinical usefulness of integrated prediction models combining MRI findings with clinicopathological factors.

Materials and Methods

Study Design and Patients

This single-center, retrospective, observational study was conducted at Hiroshima University Hospital using data derived from a multicenter database; however, only patients treated at our institution were included in the present analysis. This is because interim MRI was not routinely performed at all participating institutions, and including data from multiple centers would have resulted in substantial heterogeneity and potentially missing data in MRI assessments. To ensure consistency and completeness of imaging data and uniformity in clinical management and MRI interpretation, we limited the analysis to a single-center cohort. The study included patients with breast cancer who underwent NAC between April 2010 and December 2020. All women with invasive breast cancer were eligible if they underwent MRI at three time points: before NAC, during the early phase of treatment (interim MRI, i.e., after completion of the first half of chemotherapy), and after completion of NAC (post-NAC MRI). Both imaging and pathological evaluation data were required for patient inclusion.

The exclusion criteria were as follows: (1) presence of distant metastasis; (2) discontinuation of NAC before completion; and (3) absence of MRI or insufficient image quality for evaluation at any of the three time points. Clinical data were obtained from electronic medical records and the picture archiving and communication system.

This study was approved by the Ethics Committee for Epidemiology of Hiroshima University (approval number: E2014-

1157-06, date: 25.07.2023) and was conducted in accordance with the Declaration of Helsinki. Formal patient consent was not required for this retrospective study.

Clinicopathological Factors

The candidate predictors for pCR included clinical tumor size (T category), clinical nodal status (N category), HR status, HER2 expression, and nuclear grade. T and N categories were determined according to the 8th edition of the American Joint Committee on Cancer TNM staging system based on tumor size and clinical nodal status (13).

HR-positivity was defined as positive staining for either the estrogen receptor (ER) or the progesterone receptor. Tumors with ≥1% positively stained tumor cells on immunohistochemistry (IHC) were considered HR-positive. HER2 status was determined in accordance with the American Society of Clinical Oncology/College of American Pathologists guidelines and was defined as positive if scored as IHC 3+ or confirmed as amplified by fluorescence *in situ* hybridization (14, 15). All clinicopathological assessments were based on needle biopsy specimens and imaging findings obtained before initiation of NAC. pCR was defined as no residual invasive or non-invasive carcinoma in both the breast and axillary lymph nodes (ypT0, ypN0).

NAC Regimen

NAC was administered according to standard institutional protocols consisting of sequential anthracycline- and taxane-based chemotherapy regimens. Dose-dense schedules were also adopted in selected cases. For patients with HER2-positive breast cancer, trastuzumab was administered concurrently with taxanes. Pertuzumab was additionally incorporated after its approval for early breast cancer in 2013 (16).

MRI Acquisition and Evaluation

Breast MRI examinations were performed using a 1.5-Tesla scanner (Achieva; Philips Healthcare, Best, the Netherlands) with a dedicated breast coil. A gadolinium-based contrast agent (0.1 mmol/kg) was administered intravenously at a rate of 2.0 mL/s using a bolus injection, followed by a saline flush of at least 10 mL.

The imaging protocol included axial diffusion-weighted imaging (b-value: 1500 s/mm^2), axial T1-weighted imaging, axial fat-suppressed T2-weighted imaging, and dynamic contrast-enhanced, fat-suppressed T1-weighted imaging using a 3D turbo field echo sequence (e-THRIVE). Dynamic images were acquired at 0, 1, 2, and 5 minutes after contrast administration. Additional sagittal contrast-enhanced T1-weighted images were acquired separately for each breast.

The slice thickness ranged from 1.6 to 5.0 mm depending on the sequence, and fat suppression was performed using SPAIR. MRI was performed at three time points: before NAC, during NAC, and after NAC.

MRI assessments were based on final radiological reports, documented by board-certified radiologists in the electronic medical records. MRI examinations were interpreted under a double-reading system by two board-certified radiologists. All radiologists had experience in breast MRI interpretation. MRI examinations were interpreted with access to clinical information, including the treatment course, as part of routine clinical practice. The readers were not fully blinded to pathological outcomes owing to the retrospective design of the study. Using information on the presence or absence of residual lesions and on the degree of contrast enhancement described in the reports, the investigators determined the final MRI findings for this study. Radiologic complete response (rCR) was defined as the complete disappearance of contrast enhancement at the tumor site on contrast-enhanced MRI.

Statistical Analysis

Logistic regression models were constructed with pCR (ypT0, ypN0) as the dependent variable. First, Model A was developed using only clinicopathological variables, without MRI findings. Variable selection was performed using a stepwise method based on the minimum Akaike information criterion (AIC). The assessments of rCR on interim and post-NAC MRI were sequentially added to the clinicopathological factors to construct Models B and C, respectively. Model D included both interim and post-NAC MRI assessments to evaluate their combined predictive value.

Model performance was compared using the area under the receiver operating characteristic (ROC) curve (AUC) as the primary metric. Internal validation was performed using bootstrap resampling with 1,000 iterations to assess model discrimination. Sensitivity and specificity were also calculated to evaluate discriminative ability. To assess clinical usefulness, decision curve analysis was conducted to compare net benefits across a range of threshold probabilities.

All statistical analyses were performed using R statistical software (version 4.5.0; the R foundation for statistical computing, Vienna, Austria). A two-sided p-value <0.05 was considered statistically significant. There were no missing data for the variables included in the regression analysis. Analyses were performed by breast cancer subtype (HR-positive/HER2-negative, HER2-positive, and triple-negative). Diagnostic performance metrics, including sensitivity, specificity, positive predictive value (PPV), and negative predictive value (NPV), were evaluated within each subtype.

Comparison of Diagnostic Performance Metrics

Diagnostic performance of each prediction model was evaluated using sensitivity, specificity, PPV, NPV, false-positive rate (FPR), and overall accuracy. All metrics were calculated to assess the ability of each model to predict pCR.

Sensitivity was defined as the proportion of patients with pCR correctly identified by the model. Specificity was defined as the proportion of patients without pCR who were correctly predicted as not having pCR. PPV and NPV were calculated from the counts of true-positive, true-negative, false-positive, and false-negative cases. FPR was defined as the proportion of patients without pCR who were incorrectly predicted to have pCR (1-specificity), and accuracy the proportion of correctly classified cases among all patients.

Results

Patient Characteristics

A total of 249 patients with invasive breast cancer were included in the analysis. The median age was 52 years. Clinical T1–2 tumors were present in 195 (78%) patients, and 133 (53%) had clinically positive lymph nodes. pCR was observed in 62 patients (25%; Table 1).

Logistic Regression Analysis of Clinicopathological Predictors of pCR

Multivariable logistic regression analysis identified three independent predictors associated with pCR for Model A: HR status, HER2 expression, and clinical T category. Clinical T category ≥3 [odds ratio (OR) 0.32; 95% confidence interval (CI) 0.10–0.79; $p = 0.023$] and HR-positivity (OR 0.42; 95% CI 0.22–0.80; $p = 0.008$) were significantly associated with non-pCR, whereas HER2-positivity (OR 2.38; 95% CI 1.27–4.51; $p = 0.007$) was significantly associated with pCR. Nuclear grade 3 showed a trend toward significance (OR 1.97; 95% CI 0.98–4.14; $p = 0.063$). The overall model remained statistically significant (likelihood ratio test, $p<0.001$; Table 2).

ROC Analysis and Comparison of Models' Diagnostic Performance

ROC curve analysis showed that the AUCs were 0.721 (95% CI 0.661–0.796) for Model A, 0.819 (95% CI 0.752–0.881) for Model B, 0.847 (95% CI 0.791–0.903) for Model C, and 0.848 (95% CI 0.791–0.906) for Model D. Compared with Model A, all MRI-based models (Models B-D) showed significantly improved discrimination (DeLong test, $p<0.0001$). However, no significant differences were observed among Models B-D ($p = 0.23$–0.95; Figure 1). Bootstrap resampling yielded a mean AUC of 0.829 (95% CI, 0.762–0.891) for Model B, indicating stable model discrimination.

Table 1. Baseline characteristics of the study population ($n = 249$)

Characteristic	*n* (%)
Age (y), median (range)	52 (22–76)
Menopausal status	
Premenopausal	129 (52%)
Postmenopausal	106 **(43%)**
Unknown	**14 (5%)**
Clinical T stage	
T1/T2	195 (78%)
T3/T4	54 (22%)
Clinical N stage	
N-negative	116 (47%)
N-positive	133 (53%)
HR status	
Positive	112 (45%)
HER2 status	
Positive	79 (32%)
Nuclear grade	
Grade 1/2	88 (35%)
Grade 3	161 (65%)
pCR	
Achieved	62 (25%)
Not achieved	187 (75%)
Surgery	
Breast-conserving surgery	91 (37%)
Mastectomy	157 (63%)
Axillary surgery	
Sentinel node biopsy only	104 (42%)
Axillary dissection	144 (58%)

HER2: Human epidermal growth factor receptor 2; HR: Hormone receptor; pCR: Pathological complete response

Table 2. Clinicopathological factors associated with pathological complete response selected by AIC-based stepwise logistic regression (Model A)

Variables	Odds ratio	95% CI	*p*-value
T3 or higher (*vs.* T1–2)	0.32	0.10–0.79	0.023
HR-positive (*vs.* HR-negative)	0.42	0.22–0.80	0.008
HER2-positive (*vs.* HER2-negative)	2.38	1.27–4.51	0.007
Nuclear grade 3 (*vs.* nuclear grade 1–2)	1.97	0.98–4.14	0.063

AIC = 259.19; Pseudo-R^2 = 0.108 (McFadden's R^2). Overall significance of the logistic regression model (likelihood ratio test): $p = 0.0000084$. CI: Confidence interval; AIC: Akaike information criterion; HER2: Human epidermal growth factor receptor 2; HR: Hormone receptor

Calibration

Calibration curve analysis demonstrated that Models B, C, and D, which incorporated MRI information, had better agreement between predicted and observed probabilities than Model A (Figure 2). Model B exhibited good calibration in the low-to-intermediate probability range, whereas Model C tended to slightly underestimate predicted probabilities in the higher-probability range. Model D demonstrated the most consistently favorable calibration across the full range of predicted probabilities.

Clinical Utility based on Decision Curve Analysis

All prediction models demonstrated greater net benefit than did the treat-all and treat-none strategies. Model B provided the greatest net benefit in the higher threshold probability range (≥0.6), whereas Model C showed relatively higher clinical utility in the lower threshold probability range (≤0.3; Figure 3).

Comparison of Diagnostic Accuracy Metrics

Model B demonstrated the highest sensitivity (0.99) and NPV (0.97), indicating an excellent ability to identify patients who achieve pCR. However, Model B also showed the lowest specificity (0.45) and the highest FPR (0.55), suggesting a substantial risk of misclassifying non-pCR cases as pCR.

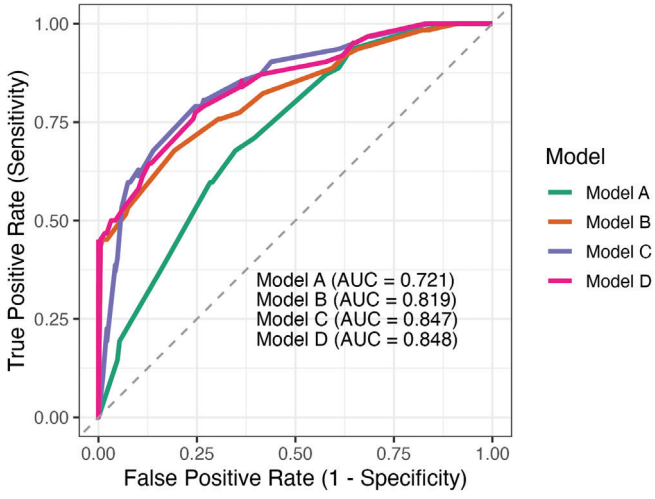

Figure 1. ROC curves of four logistic regression models for predicting pCR. The AUC values were 0.721 for Model A, 0.819 for Model B, 0.847 for Model C, and 0.848 for Model D. Models incorporating MRI information (Models B-D) demonstrated markedly better predictive performance than that of Model A, whereas differences among the MRI-based models were minimal

ROC: Receiver operating characteristic; MRI: Magnetic resonance imaging; pCR: Pathological complete response; AUC: Area under the curve

Model A showed the highest specificity (0.73) and the lowest FPR (0.27). Model C yielded the highest PPV (0.88), while Models C and D demonstrated comparable overall accuracy (0.83), slightly lower than that of Model B (0.86).

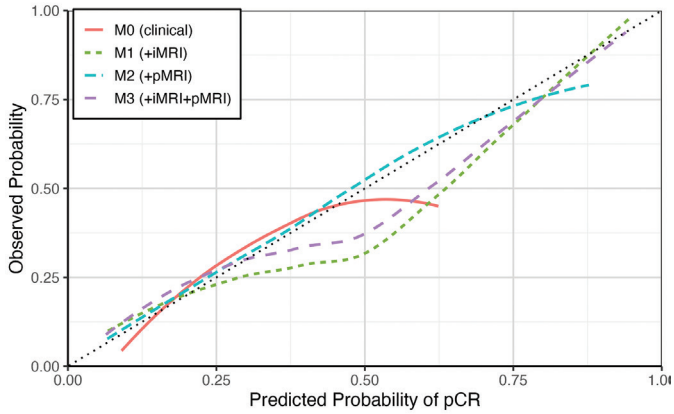

Figure 2. Calibration curves of four prediction models for pCR. Models incorporating MRI information (Models B-D) showed better agreement between predicted and observed probabilities than did Model A, with Model D demonstrating the most consistent calibration across a wide range of predicted probabilities

MRI: Magnetic resonance imaging; pCR: Pathological complete response

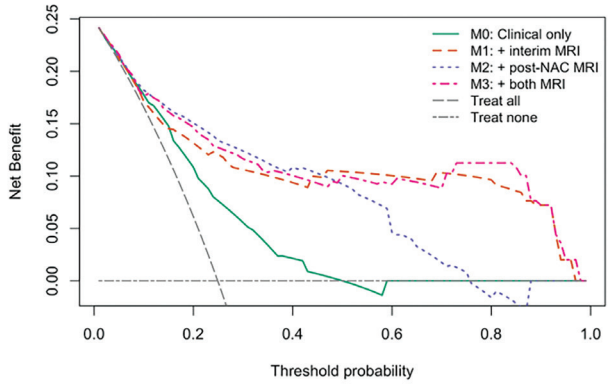

Figure 3. Decision curve analysis of four logistic regression models for predicting pCR. Decision curve analysis of the four prediction models: The vertical axis indicates net benefit, and the horizontal axis indicates the threshold probability for pCR. All models provided greater net benefit than did the treat-all and treat-none strategies. Model B showed the highest clinical utility in the higher threshold probability range (≥0.6), whereas Model C showed relatively greater utility in the lower threshold probability range (≤0.3)

pCR: Pathological complete response; NAC: Neoadjuvant chemotherapy; MRI: Magnetic resonance imaging

These findings indicate that although Model B is highly sensitive and useful for identifying responders, its high FPR may limit its applicability for safely guiding surgical de-escalation (Table 3).

Subtype-Specific Analysis

Subtype-specific analyses revealed differences in diagnostic performance among the models across breast cancer subtypes (HR-positive/HER2-negative, HER2-positive, and triple-negative breast cancer).

Model B showed higher specificity in subtype analyses and lower FPRs across subtypes, whereas Models C and D showed more balanced performance with higher sensitivity. These subtype-specific results are presented in Supplementary Tables 1A-C.

Discussion and Conclusion

In this study, the interim MRI-based pCR prediction model demonstrated a diagnostic performance comparable to that of post-NAC MRI, indicating its potential usefulness for clinical decision-making at an early-stage of treatment. Although Model B achieved the highest sensitivity (0.99) and NPV (0.97), this benefit was associated with the highest FPR (0.55), raising concerns about the risk of overtreatment when applied to surgical de-escalation. Models C and D demonstrated slightly superior overall discrimination with the highest AUC values (0.847 and 0.848); however, the improvement over Model B was marginal, and their FPRs remained moderately high.

Calibration curve analysis showed that MRI-integrated models provided better agreement between predicted and observed probabilities than did Model A, with Model D demonstrating the most stable calibration across all ranges. Decision curve analysis indicated that Model B provided the greatest net benefit at higher threshold probabilities (≥0.6), supporting its value when prioritizing pCR detection for early treatment intensification. Conversely, Model C was more beneficial at lower thresholds (≤0.3), suggesting that these models may have complementary roles depending on specific clinical goals. Taken together, interim MRI offers clinically meaningful predictive performance comparable to that of post-NAC MRI while enabling earlier therapeutic intervention. However, the relatively high FPR indicates that interim MRI alone may not be a safe guide for surgical de-escalation and that integration with post-NAC MRI remains essential to reduce unnecessary undertreatment and to optimize individualized patient care.

Previous prospective studies have also suggested the value of interim MRI for early assessment of treatment response. However, many of these studies were limited by small sample sizes or focused on specific molecular subtypes (e.g., ER-positive/HER2-negative), which may have restricted generalizability to real-world practice (8, 12). In contrast, the present study included all molecular subtypes and incorporated diverse treatment sequences reflective of contemporary clinical practice. Thus, our results provide evidence that the utility of interim MRI can be extrapolated to a broader patient population.

Response-adapted treatment strategies guided by MRI have recently gained attention in NAC. For example, the TRAIN-3 trial evaluated an MRI-guided early termination strategy based on rCR, demonstrating reduced treatment burden without compromising pCR rates (17). The I-SPY 2 trial incorporated early MRI response into its adaptive trial design, reporting a strong association between interim MRI response and pCR (18). These findings highlight the role of interim MRI not only as a predictive imaging biomarker but also as a key component in optimizing treatment duration and regimen selection. Our study supports this concept by demonstrating that combining interim MRI findings with clinicopathological factors can facilitate effective response-adapted clinical decision-making.

The strengths of this study include (1) a relatively large, single-institution cohort of 249 patients; (2) MRI evaluation at three standardized time points (pre-NAC, interim, and post-NAC), covering a broad range of molecular subtypes and treatment regimens reflecting real-world practice; (3) use of a strict definition of pCR (ypT0, ypN0); and (4) comprehensive evaluation

Table 3. Diagnostic performance for predicting pathological complete response in each prediction model

Parameter	Model A	Model B	Model C	Model D
Sensitivity	0.59 (0.52–0.66)	0.99 (0.97–1.00)	0.90 (0.85–0.94)	0.91 (0.86–0.95)
Specificity	0.73 (0.60–0.83)	0.45 (0.32–0.58)	0.63 (0.50–0.75)	0.60 (0.46–0.72)
PPV	0.87 (0.80–0.92)	0.85 (0.79–0.89)	0.88 (0.82–0.92)	0.87 (0.82–0.92)
NPV	0.37 (0.29–0.46)	0.97 (0.82–1.00)	0.67 (0.54–0.79)	0.69 (0.54–0.80)
FPR	0.27 (0.17–0.40)	0.55 (0.42–0.68)	0.37 (0.25–0.50)	0.40 (0.28–0.54)
Accuracy	0.63 (0.56–0.69)	0.86 (0.81–0.90)	0.83 (0.78–0.88)	0.83 (0.78–0.88)

Values are shown as estimates with 95% confidence intervals in parentheses.

FPR: False-positive rate (1-specificity); NPV: Negative predictive value; PPV: Positive predictive value

of discrimination, calibration, and clinical usefulness using decision curve analysis. These features reinforce the clinical applicability of the developed prediction models.

Some limitations should also be acknowledged. First, as this was a single-center retrospective study, potential selection and information biases cannot be excluded. Second, patients were treated between 2010 and 2020, and updated analyses incorporating more recent standard-of-care regimens, including immunotherapy for triple-negative breast cancer, are warranted (19). Third, variable selection was performed using an AIC-based stepwise procedure, which may have introduced data-driven selection bias and potential overfitting. However, internal validation using bootstrap resampling suggested that the model performance was relatively stable, although external validation is warranted.

Fourth, subgroup analyses by breast cancer subtype were performed; however, the results should be interpreted with caution due to the limited sample size in each subgroup. This study did not assess the absolute clinical consequences of false positives (undertreatment) or true positives (benefit), as the primary objective was to compare relative usefulness among models. Future investigations should incorporate regimen-specific toxicity and patient preferences when defining clinically meaningful decision thresholds.

Future Perspectives

External validation using independent cohorts is necessary to confirm the generalizability of our findings. Standardization of MRI acquisition and interpretation criteria should also be pursued. Additionally, incorporating quantitative MRI-derived parameters (e.g., volumetric tumor shrinkage, signal intensity changes) may further improve objectivity and reproducibility in prediction models (20). Ultimately, integration of these predictive models into routine clinical workflows to guide response-adapted strategies and to dynamically optimize treatment duration and regimens based on interim MRI responses will be essential. Such an approach may enhance personalized breast cancer care by maximizing therapeutic benefit while minimizing unnecessary treatment-related toxicities.

In this study, we showed that interim MRI demonstrated predictive performance for pCR in patients with breast cancer that was comparable to that of post-NAC MRI and enabled earlier clinical decision-making, indicating its potential utility as a decision-support tool that can be implemented early in the management of breast cancer.

Ethics

Ethics Committee Approval: This study was approved by the Ethics Committee for Epidemiology of Hiroshima University (approval number: E2014-1157-06, date: 25.07.2023) and was conducted in accordance with the Declaration of Helsinki.

Informed Consent: Formal patient consent was not required for this retrospective study.

Acknowledgements

We would like to thank Dr. Naoyuki Kitamura and Mr. Eikoh Ueda for their valuable support in providing detailed information on MRI acquisition protocols and imaging procedures.

Footnotes

Authorship Contributions

Surgical and Medical Practices: E.K., H.S., A.A., S.S., T.K.; Concept: E.K., H.S., A.A., S.S., T.K., M.O.; Design: E.K., H.S., A.A., S.S., T.K., M.O.; Data Collection and/or Processing: E.K., H.S., A.A., S.S., T.K.; Analysis and/or Interpretation: E.K., H.S.; Literature Search: E.K., H.S.; Writing: E.K., H.S.

Conflict of Interest: The authors have no conflicts of interest to declare.

Financial Disclosure: The authors declared that this study has received no financial support.

Supplementary Tables Link: https://d2v96fxpocvxx.cloudfront.net/e1c28131-4444-460a-9703-9fa751c405df/content-images/ecdea770-ab1b-4d99-a7fe-7248d779e1fc.pdf

References

1. Loibl S, André F, Bachelot T, Barrios CH, Bergh J, Burstein HJ, et al. Early breast cancer: ESMO Clinical Practice Guideline for diagnosis, treatment and follow-up. Ann Oncol. 2024; 35: 159-182. (PMID: 38101773) [Crossref]
2. Johnson HM, Lin H, Shen Y, Diego EJ, Krishnamurthy S, Yang WT, et al. Patient-reported outcomes of omission of breast surgery following neoadjuvant systemic therapy: a nonrandomized clinical trial. JAMA Netw Open. 2023; 6: e2333933. (PMID: 37707811) [Crossref]
3. Janssen LM, den Dekker BM, Gilhuijs KGA, van Diest PJ, van der Wall E, Elias SG. MRI to assess response after neoadjuvant chemotherapy in breast cancer subtypes: a systematic review and meta-analysis. NPJ Breast Cancer. 2022; 8: 107. (PMID: 36123365) [Crossref]
4. Marinovich ML, Houssami N, Macaskill P, Sardanelli F, Irwig L, Mamounas EP, et al. Meta-analysis of magnetic resonance imaging in detecting residual breast cancer after neoadjuvant therapy. J Natl Cancer Inst. 2013; 105: 321-333. (PMID: 23297042) [Crossref]
5. Zhang Y, Cai J, Cui C, Qi S, Zhao D. Predicting breast cancer response to neoadjuvant therapy by integrating radiomic and deep-learning features from early-and-peak phases of DCE-MRI. BMC Cancer. 2025; 25: 1747. (PMID: 41219899) [Crossref]
6. Hajri R, Aboudaram C, Lassau N, Assi T, Antoun L, Ribeiro JM, et al. Prediction of breast cancer response to neoadjuvant therapy with machine learning: a clinical, MRI-qualitative, and radiomics approach. Life (Basel). 2025; 15: 1165. (PMID: 40868813) [Crossref]
7. Fangberget A, Nilsen LB, Hole KH, Holmen MM, Engebraaten O, Naume B, et al. Neoadjuvant chemotherapy in breast cancer—response evaluation and prediction of response to treatment using dynamic contrast-enhanced and

diffusion-weighted MR imaging. Eur Radiol. 2011; 21: 1188-1199. (PMID: 21127880) [Crossref]

8. Hylton NM, Blume JD, Bernreuter WK, Pisano ED, Rosen MA, Morris EA, et al. Locally advanced breast cancer: MR imaging for prediction of response to neoadjuvant chemotherapy—results from ACRIN 6657/I-SPY TRIAL. Radiology. 2012; 263: 663-672. (PMID: 22623692) [Crossref]

9. Suo S, Yin Y, Geng X, Zhang D, Hua J, Cheng F, et al. Diffusion-weighted MRI for predicting pathologic response to neoadjuvant chemotherapy in breast cancer: evaluation with mono-, bi-, and stretched-exponential models. J Transl Med. 2021; 19: 236. (PMID: 34078388) [Crossref]

10. You C, Peng W, Zhi W, He M, Liu G, Xie L, et al. Association between background parenchymal enhancement and pathologic complete remission throughout neoadjuvant chemotherapy in breast cancer patients. Transl Oncol. 2017; 10: 786-792. (PMID: 28806712) [Crossref]

11. Henderson SA, Muhammad Gowdh N, Purdie CA, Jordan LB, Evans A, Brunton T, et al. Breast cancer: influence of tumour volume estimation method at MRI on prediction of pathological response to neoadjuvant chemotherapy. Br J Radiol. 2018; 91: 20180123. (PMID: 29641224) [Crossref]

12. Rigter LS, Loo CE, Linn SC, Sonke GS, van Werkhoven E, Lips EH, et al. Neoadjuvant chemotherapy adaptation and serial MRI response monitoring in ER-positive HER2-negative breast cancer. Br J Cancer. 2013; 109: 2965-2972. (PMID: 24149178) [Crossref]

13. Giuliano AE, Edge SB, Hortobagyi GN. Eighth edition of the AJCC cancer staging manual: breast cancer. Ann Surg Oncol. 2018; 25: 1783-1785. (PMID: 29671136) [Crossref]

14. Allison KH, Hammond MEH, Dowsett M, McKernin SE, Carey LA, Fitzgibbons PL, et al. Estrogen and progesterone receptor testing in breast cancer: American Society of Clinical Oncology/College of American Pathologists Guideline update. Arch Pathol Lab Med. 2020; 144: 545-563. (PMID: 31928354) [Crossref]

15. Wolff AC, Hammond MEH, Allison KH, Harvey BE, McShane LM, Dowsett M. HER2 testing in breast cancer: American Society of Clinical Oncology/College of American Pathologists Clinical Practice Guideline focused update summary. J Oncol Pract. 2018; 14: 437-441. (PMID: 29920138) [Crossref]

16. Gianni L, Pienkowski T, Im YH, Roman L, Tseng LM, Liu MC, et al. Efficacy and safety of neoadjuvant pertuzumab and trastuzumab in women with locally advanced, inflammatory, or early HER2-positive breast cancer (NeoSphere): a randomised multicentre, open-label, phase 2 trial. Lancet Oncol. 2012; 13: 25-32. (PMID: 22153890) [Crossref]

17. van der Voort A, Louis FM, van Ramshorst MS, Kessels R, Mandjes IA, Kemper I, et al. MRI-guided optimisation of neoadjuvant chemotherapy duration in stage II–III HER2-positive breast cancer (TRAIN-3): a multicentre, single-arm, phase 2 study. Lancet Oncol. 2024; 25: 603-613. (PMID: 38588682) [Crossref]

18. Li W, Newitt DC, Wilmes LJ, Jones EF, Arasu V, Gibbs J, et al. Additive value of diffusion-weighted MRI in the I-SPY 2 TRIAL. J Magn Reson Imaging. 2019; 50: 1742-1753. (PMID: 31026118) [Crossref]

19. Schmid P, Cortes J, Dent R, McArthur H, Pusztai L, Kümmel S, et al. KEYNOTE-522 investigators. overall survival with pembrolizumab in early-stage triple-negative breast cancer. N Engl J Med. 2024; 391: 1981-1991. (PMID: 39282906) [Crossref]

20. Tang W, Jin C, Kong Q, Liu C, Chen S, Ding S, et al. Development and validation of an MRI spatiotemporal interaction model for early noninvasive prediction of neoadjuvant chemotherapy response in breast cancer: a multicentre study. EClinicalMedicine. 2025; 85: 103298. (PMID: 40584836) [Crossref]

CASE REPORT

European Journal of BREAST HEALTH

DOI: 10.4274/ejbh.galenos.2025.2025-9-11
Eur J Breast Health 2026;22(3):358-362

Axillary Lymph Node Calcifications due to Tattoo Pigment: A Radiologic-Pathologic Correlation

Manuel López-Herrero[1], Mireia Pitarch[2], Mario Giner[3], David López-Segura[3], Rodrigo Alcantara[2,4]

[1]Department of Radiology, Hospital Clínico San Carlos, Madrid, Spain
[2]Department of Radiology, DIBI-Hospital del Mar, Barcelona, Spain
[3]Department of Pathology, DIBI-Hospital del Mar, Barcelona, Spain
[4]Department of Medicine, Universitat Autònoma de Barcelona, Barcelona, Spain

ABSTRACT

Tattoo pigment may migrate to regional lymph nodes and appear as dense deposits and/or calcifications, mimicking malignant axillary findings on breast imaging. We report a breast imaging case with apparent axillary lymph node calcifications detected on mammography and ultrasound, in which image-guided sampling and histopathology demonstrated tattoo pigment-related deposits without malignancy. Awareness of this benign mimic, combined with careful correlation with the clinical history and multimodality imaging, can prevent unnecessary escalation of care. Additionally, confirming imaging-pathology concordance supports accurate diagnosis and helps avoid overtreatment.

Keywords: Tattoo; axillary lymph node; calcifications; breast imaging

KEY POINTS

- Tattoo pigment migration can mimic calcifications in axillary lymph nodes, potentially simulating malignant disease on breast imaging.
- Careful correlation of imaging features with clinical history and pathology, when required, helps to avoid unnecessary invasive procedures.
- Awareness of this benign mimic is important to prevent overtreatment and patient anxiety.

Introduction

Axillary lymph node calcifications are uncommon findings on mammography and ultrasound, with a differential diagnosis that includes both benign and malignant conditions. In recent decades, the migration of tattoo pigments to regional lymph nodes has been increasingly recognized as a potential diagnostic pitfall, particularly in light of the rising prevalence of both tattoos and breast cancer screening. The first case report describing tattoo pigment mimicking mammographic calcifications was published by Honegger et al. (1) in 2004, and since then, several additional reports have documented similar findings, underscoring the challenge of distinguishing pigment deposits from true pathology (2-5). These deposits can closely resemble calcifications and, in some cases, may be mistaken for metastatic disease, creating significant diagnostic difficulties.

The aim of this case report is to raise awareness of this imaging pitfall and to emphasize the importance of correlating radiological findings with clinical history to avoid misdiagnosis

Corresponding Author: Rodrigo Alcantara MD
E-mail: ralcantara@hmar.cat **ORCID:** orcid.org/0000-0003-4365-5640
Received: 15.10.2025 **Accepted:** 21.12.2025 **Available Online Date:** 17.06.2026
Cite this article as: López-Herrero M, Pitarch M, Giner M, López-Segura D, Alcantara R. Axillary lymph node calcifications due to tattoo pigment: a radiologic-pathologic correlation. Eur J Breast Health. 2026;22(3):358-362

and unnecessary interventions, such as biopsies. However, when clinical and radiological findings are inconclusive, histological examination may be required for a definitive diagnosis.

Case Presentation

A 50-year-old woman attended routine screening mammography. Images demonstrated hyperdense foci, simulating coarse heterogeneous calcifications, within two right axillary lymph nodes (Figure 1), which had otherwise normal size and morphology. No suspicious findings were observed in either breast. The patient was recalled for ultrasound, which confirmed the presence of echogenic foci within two lymph nodes of preserved morphology, including an intact fatty hilum and cortical thickness less than 3 mm (Figure 2). Given the absence of breast abnormalities, a contrast-enhanced breast magnetic resonance imaging (MRI) was performed to rule out occult disease. MRI revealed no suspicious breast lesions and showed magnetic susceptibility artifacts inside two right lymph nodes (Figure 3). Despite this, an ultrasound-guided core-needle biopsy was performed to exclude malignancy or extramammary metastasis (Figure 4). Radiography of the biopsy specimen confirmed the retrieval of dense material (Figure 5). Histopathology demonstrated lymphoid tissue containing greenish-black pigment deposits, with no evidence of carcinoma or calcifications (Figures 6, 7). On further clinical questioning, the patient reported a tattoo on the right arm (Figure 8), within the drainage territory of the axillary lymph nodes. Written informed consent was obtained from the patient for publication of this case and accompanying images.

Figure 1. Digital screening mammogram shows hyperdense foci in two right axillary lymph nodes (arrows) simulating calcifications. The breast parenchyma shows no abnormalities, despite the breast being categorized by breast composition c (heterogeneously dense). Technique: Synthesized 2-dimensional mammogram (mediolateral oblique views)

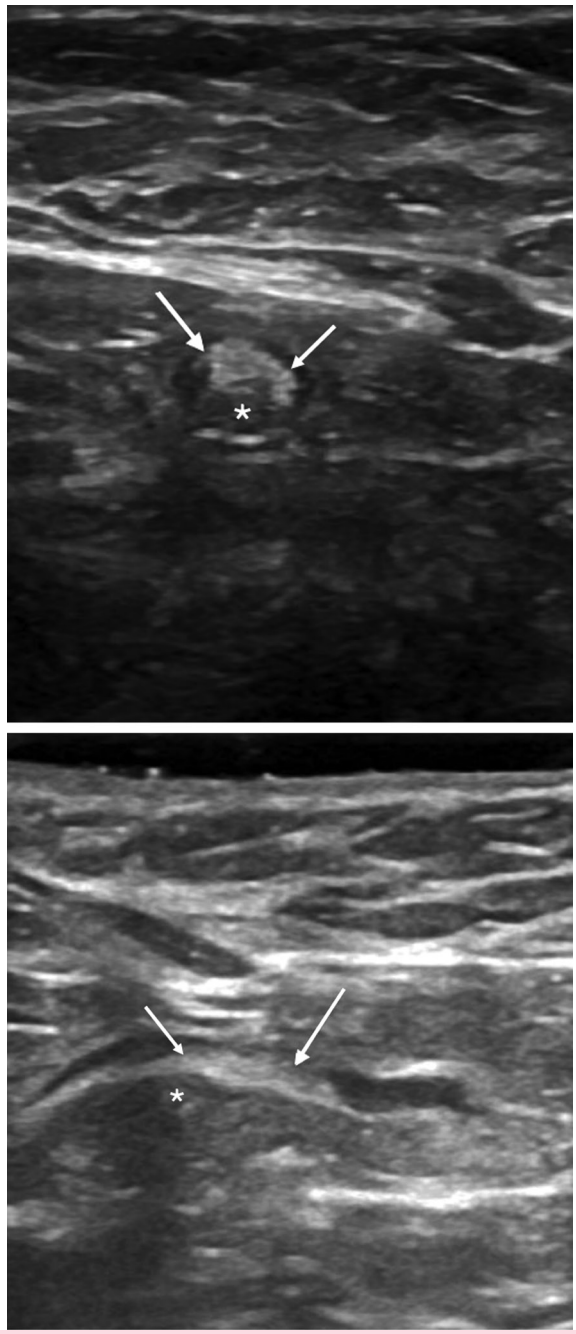

Figure 2. Right axillary ultrasound confirms the presence of apparent calcifications in two axillary lymph nodes (arrows). They have oval shape with a preserved fatty hilum (asterisks) and cortical thickness less than 3 mm. Technique: High frequency linear probe ultrasound, 14 MHz

Eur J Breast Health
2026;22(3):358-362

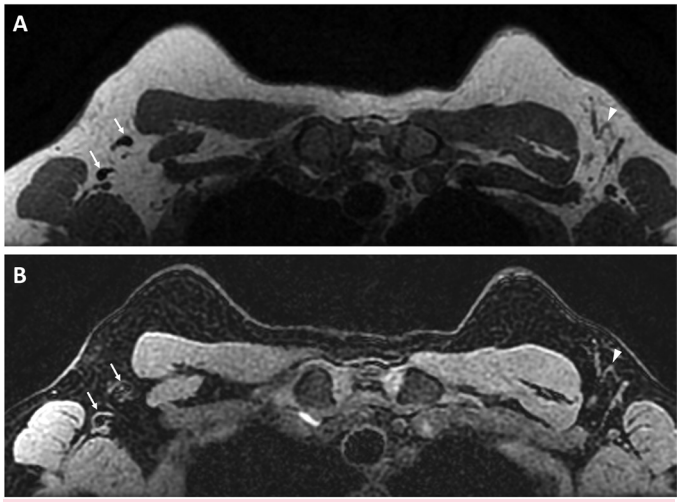

Figure 3. (A) Axial T1-weighted and (B) T1-weighted fat-suppressed magnetic resonance images show magnetic susceptibility artifacts within two right lymph nodes (arrows), which are not observed in the contralateral nodes (arrowhead). No abnormalities were found in the breast parenchyma. Technique: Bilateral breast magnetic resonance imaging (axial) using a 1.5T magnet

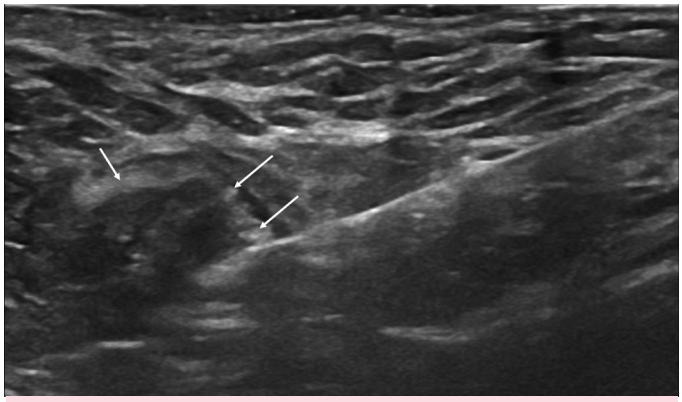

Figure 4. An ultrasound-guided core-needle biopsy was performed. The image depicts the needle passing through the cortex. Notice the hyperechogenic foci within it, corresponding to the apparent calcifications (arrows). Technique: High frequency linear probe ultrasound, 14 MHz

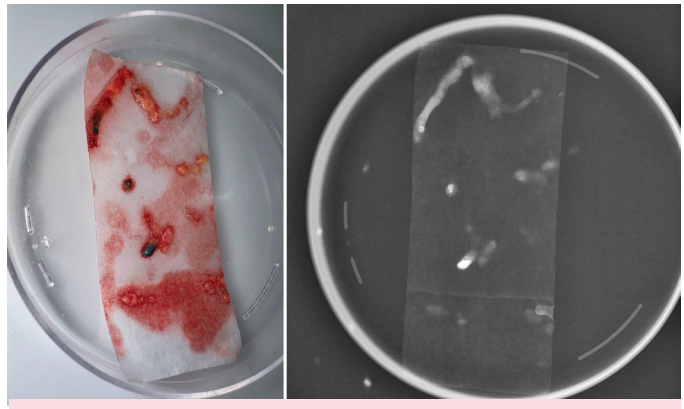

Figure 5. Photograph of the core-needle biopsy specimen with X-ray correlation. Note the darkest areas (due to ink), which correspond to regions of calcification density

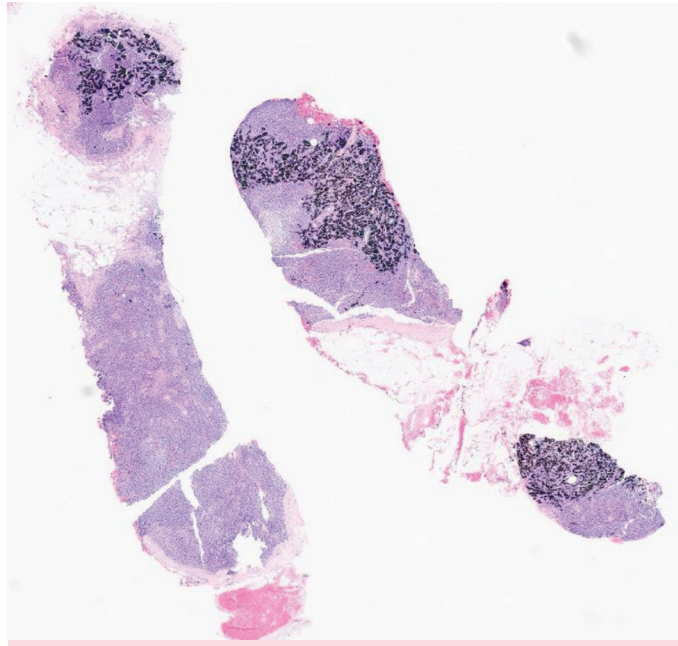

Figure 6. Two lymph node cylinders are observed with blackish areas suggestive of ink marking. Technique: Hematoxylin-eosin stain

Discussion and Conclusion

The presence of calcifications in the axillary lymph nodes is an unusual finding. The deposition of tattoo ink within axillary lymph nodes may mimic calcifications, as the color pigments are commonly mixed with or derived from various heavy metal oxides (6). The most widely accepted theory regarding its etiopathogenesis is that repeated intradermal injection of ink during tattooing initiates an inflammatory response driven by macrophages. These macrophages phagocytose some of the metal fragments, which are then slowly transported to the axillary lymph nodes via lymphatic vessels, where they remain for years (7). The accumulation of tattoo pigment in lymph nodes can also resemble the appearance of blue dye used for sentinel node identification, which may result in unnecessary removal of additional axillary nodes (8).

On mammography, tattoo ink deposits are usually seen as foci of calcification density within the lymph node, which may mimic true calcifications. These deposits may sometimes appear as punctate (5), coarse heterogeneous (2), which was similar to the findings in the presented case, or amorphous (3, 4) calcifications on imaging,

all of which can raise suspicion of malignancy, especially in the case of a personal history of breast cancer (4) or if the lymph node shows other concerning signs, such as enlargement (1). Mammographic features suggestive of abnormal axillary lymph nodes include loss of the fatty hilum, a round rather than oval morphology, poorly defined margins, and increased size or density compared to previous imagind studies (1, 9). However, in most reported cases, lymph nodes with tattoo ink deposits have maintained normal size and morphology (3, 4).

These ink deposits can also be seen on ultrasound, usually as echogenic foci suggestive of calcifications (1). Sonography allows a better assessment of the lymph nodes. In breast cancer, axillary lymph nodes are commonly classified based on cortical morphologic features. The identification of asymmetric focal hypoechoic cortical lobulation or a completely hypoechoic lymph node should prompt cytological or histopathological evaluation (10).

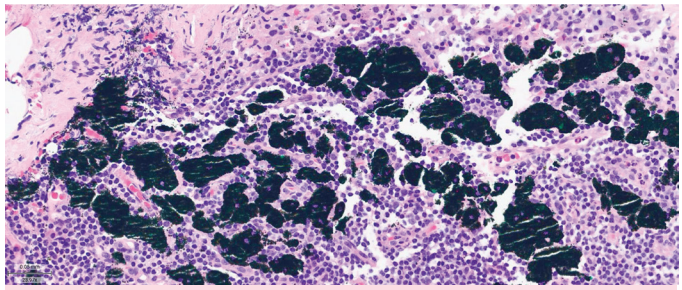

Figure 7. At higher magnification, dark greenish pigment is seen trapped within cellular components in the lymph node tissue. Technique: Hematoxylin-eosin stain

Figure 8. Photograph of the patient's arm tattoo

There are other etiologies that can cause calcified lymphadenopathies, both benign and malignant. The benign causes include, for example, tuberculosis, sarcoidosis, histoplasmosis and prior Bacillus Calmette-Guerin vaccination. These granulomatous calcifications typically exhibit a coarse appearance (5, 11). Long-term chrysotherapy, which involves the administration of gold salts for the treatment of rheumatoid arthritis, can result in their accumulation in the lymph nodes, potentially simulating calcifications. This deposition may persist for up to 20 years after discontinuation of therapy (5, 12). A similar phenomenon occurs with certain drugs, such as cocaine, due to talc deposition. Another benign etiology to consider is fat necrosis, especially when calcifications are located in the axillary tail and the patient has a history of prior trauma (13). Talc powder from certain deodorants may also mimic calcified lymph nodes on mammography, particularly when the calcifications are bilateral (3).

The most common malignant cause of axillary lymph node calcifications is metastasis from breast carcinoma (5, 14). These calcifications are usually unilateral and present as pleomorphic and/or amorphous microcalcifications, similar to those seen in breast cancer lesions, in contrast to the coarse and large calcifications commonly associated with benign processes (14). In cases of occult carcinoma, however, axillary calcifications may be more difficult to differentiate.

Non-breast neoplasms that can occasionally cause calcified adenopathy in the axilla (often bilaterally) include those that produce mucin, such as ovarian serous-papillary adenocarcinoma (4,9), mucinous adenocarcinoma of the colon and papillary thyroid carcinoma. These calcifications typically appear amorphous and peripheral, due to the presence of psammoma bodies (9). In addition, patients with lymphoma undergoing treatment (either chemotherapy or radiotherapy) may exhibit calcification of axillary lymphadenopathy, which, in this context, is associated with a favorable therapeutic response (5, 15).

Both clinical history and physical examination, together with imaging findings, are essential for narrowing the differential diagnoses. In cases of suspicious calcifications in axillary lymph nodes and negative results on conventional imaging (mammography/ultrasound), contrast-enhanced breast MRI may be performed to identify an occult primary tumor (16). In patients where benign status can be confidently established, unnecessary biopsies can be avoided. Nevertheless, if tissue sampling is performed, accurate clinical and radiologic-pathologic correlations are required.

In summary, the presented case report described an uncommon mammographic finding of calcification in axillary lymph nodes resulting from migration and deposition of pigment after

tattooing. This condition, likely unfamiliar to most radiologists, should be considered in the differential diagnosis to avoid unnecessary escalation of care.

Ethics

Informed Consent: Written informed consent was obtained from the patient for publication of this case and accompanying images.

Footnotes

Authorship Contributions

Surgical and Medical Practices: M.P., M.G., R.A.; Concept: M.L-H., M.P., R.A.; Design: M.L-H., M.P.; Data Collection or Processing: M.L-H., M.G., D.L-S., R.A.; Analysis or Interpretation: M.L-H., M.P., M.G., D.L-S., R.A.; Literature Search: M.L-H., R.A.; Writing: M.L-H., M.P., R.A.

Conflict of Interest: No conflict of interest was declared by the authors.

Financial Disclosure: The authors declared that this study received no financial support.

References

1. Honegger MM, Hesseltine SM, Gross JD, Singer C, Cohen JM. Tattoo pigment mimicking axillary lymph node calcifications on mammography. AJR Am J Roentgenol. 2004; 183: 831-832. (PMID: 15333377) [Crossref]
2. Paul Litton T, Vijay Ghate S. Tattoo pigment mimicking axillary lymph node calcifications on mammography. Radiol Case Rep. Elsevier Inc; 2020; 15: 1194-1196. [Crossref]
3. Heaney RM, Sweeney L, Smith C, O'Brien A. Much 'tattoo' about nothing; tattoo pigment mimicking breast microcalcifications on mammography. Radiol Case Rep. 2021; 16: 1833-1835. (PMID: 34040686) [Crossref]
4. Aguillar VLN, Tucunduva TCM, Carvalho FM, Mazucato MB, Viana MP, Torres US, et al. Tattoo pigment mimicking calcifications in axillary lymph nodes: a pitfall in mammographic imaging evaluation. Breast J. 2020; 26: 764-766. (PMID: 31595606) [Crossref]
5. Yactor AR, Michell MN, Koch MS, Leete TG, Shah ZA, Carter BW. Percutaneous tattoo pigment simulating calcific deposits in axillary lymph nodes. Proc (Bayl Univ Med Cent). 2013; 26: 28-29. (PMID: 23382606) [Crossref]
6. Timko AL, Miller CH, Johnson FB, Ross E. In vitro quantitative chemical analysis of tattoo pigments. Arch Dermatol. 2001; 137: 143-147. (PMID: 11176685) [Crossref]
7. Sperry K. Tattoos and tattooing. Part II: gross pathology, histopathology, medical complications, and applications. Am J Forensic Med Pathol. 1992; 13: 7-17. (PMID: 1585890) [Crossref]
8. Soran A, Menekse E, Kanbour-Shakir A, Tane K, Diego E, Bonaventura M, et al. The importance of tattoo pigment in sentinel lymph nodes. Breast Dis. 2017; 37: 73-76. (PMID: 28697552) [Crossref]
9. Singer C, Blankstein E, Koenigsberg T, Mercado C, Pile-Spellman E, Smith SJ. Mammographic appearance of axillary lymph node calcification in patients with metastatic ovarian carcinoma. AJR Am J Roentgenol. 2001; 176: 1437-1440. (PMID: 11373209) [Crossref]
10. Bedi DG, Krishnamurthy R, Krishnamurthy S, Edeiken BS, Le-Petross H, Fornage BD, et al. Cortical morphologic features of axillary lymph nodes as a predictor of metastasis in breast cancer: in vitro sonographic study. AJR Am J Roentgenol. 2008; 191: 646-652. (PMID: 18716089) [Crossref]
11. Burdeny DA, Reed MH, Ferguson CA. Calcification of axillary lymph nodes following BCG vaccination. Can Assoc Radiol J. 1989; 40: 92-93. (PMID: 2702508) [Crossref]
12. Bruwer A, Nelson GW, Spark RP. Punctate intranodal gold deposits simulating microcalcifications on mammograms. Radiology. 1987; 163: 87-88. (PMID: 3823464) [Crossref]
13. Hooley R, Lee C, Tocino I, Horowitz N, Carter D. Calcifications in axillary lymph nodes caused by fat necrosis. AJR Am J Roentgenol. 1996; 167: 627-628. (PMID: 8751666) [Crossref]
14. Mooney S, Dutmers J, Jameel Z, Weinfurtner RJ. Calcified axillary lymph nodes in a case of de novo metastatic breast cancer. Radiol Case Rep. 2023; 19: 483-488. (PMID: 38046920) [Crossref]
15. Lyou CY, Yang SK, Choe DH, Lee BH, Kim KH. Mammographic and sonographic findings of primary breast lymphoma. Clin Imaging. 2007; 31: 234-238. (PMID: 17599616) [Crossref]
16. Chotai N, Xu GG, Tan HW. Bilateral axillary node calcifications: a case report and revisiting causes. Radiol Case Rep. 2022; 18: 581-583. (PMID: 36452892) [Crossref]

CASE REPORT

European Journal of BREAST HEALTH

DOI: 10.4274/ejbh.galenos.2026.2025-10-12
Eur J Breast Health 2026;22(3):363-367

Bilateral Myeloid Sarcoma of Breast: A Case Report and Discussion

Lian Li, Zhi Liu, Huiling Zhang, Yudie Zou, Yingjia Li

Department of Ultrasound, Nanfang Hospital, Southern Medical University, Guangzhou, Guangdong, China

ABSTRACT

Myeloid sarcoma (MS) involving the breast is rare. We reviewed a case of a 21-year-old female with palpable masses in the bilateral breasts without medullary acute myeloid leukemia. Ultrasound revealed irregular, indistinct, and complex hypoechoic masses with internal blood flow and hyperechoic halos in the bilateral breasts. A biopsy was subsequently recommended, and MS was confirmed. Further cytogenetic evaluation of breast biopsy specimens demonstrated positive t(16;16)(p13.1;q22) translocation. The patient was admitted for chemotherapy. Subsequent follow-up breast ultrasound following chemotherapy revealed a notable treatment response. This report aims to delineate the ultrasound characteristics of breast MS and the utilization of ultrasound in the evaluation of early response to chemotherapy.

Keywords: Myeloid sarcoma; breast; ultrasonography

KEY POINTS

- Myeloid sarcoma (MS) involving bilateral breast is rare but aggressive.
- Ultrasound plays a certain role in the initial evaluation of breast MS.
- The assessment of therapeutic response involves the use of ultrasound.

Introduction

Myeloid sarcoma (MS), also known as granulocytic sarcoma or chloroma, is a rare subtype of acute myeloid leukemia (AML) that involves the extramedullary proliferation of myeloid blasts. It often occurs concomitantly with AML or myelodysplastic diseases, and rarely without bone marrow involvement (1, 2). MS involving the breast is even rarer. Imaging knowledge of breast MS remains limited due to its rarity. This study aims to enhance the understanding of ultrasound characteristics of the disease.

Case Presentation

A 21-year-old female presented to our breast clinic with a 6-month history of rapidly enlarging palpable and painless breast masses in January 2024. She denied any other notable medical history. A physical examination revealed firm lumps measuring 60×55 mm and 20×15 mm, respectively, in the left and right subareolar areas. The presence of light skin edema was observed in the central retroareolar region of both breasts.

Corresponding Author: Yingjia Li Prof. Dr.
E-mail: lyjia@smu.edu.cn **ORCID:** orcid.org/0009-0004-1206-8608
Received: 16.11.2025 **Accepted:** 26.01.2026 **Available Online Date:** 17.06.2026
Cite this article as: Li L, Liu Z, Zhang H, Zou Y, Li Y. Bilateral myeloid sarcoma of breast: a case report and discussion. Eur J Breast Health. 2026;22(3):363-367

The ultrasound revealed two distinct masses in the right breast. The first mass, measuring 50×42 mm, was identified in the central retroareolar region, while the second, measuring 50×21 mm, was located in the upper outer quadrant (Figure 1). The masses were irregularly shaped with indistinct margins, a non-homogeneous hypoechoic central portion, and a hyperechoic peripheral halo. Relatively rich internal blood flow signals with a resistance index of 0.57 were observed. Concurrently, in the left breast, a substantial hypoechoic mass was identified in the central retroareolar region, measuring approximately 74×50 mm. Additionally, a smaller hypoechoic mass was detected in the upper inner quadrant (Figure 2). These masses presented similarly in appearance on ultrasound. Furthermore, an abnormal lymph node measuring 15×8 mm was identified in the left axilla, characterized by cortical thickening, loss of lymphoid follicles, and a hyperechoic peripheral halo (Figure 2). The patient was given a breast imaging-reporting and data system classification of 4b. In light of the potential radiation exposure, the recommendation was made to opt for an ultrasound-guided biopsy over mammography.

Pathology showed breast tissue with diffuse infiltrate of blasts, consistent with MS (Figure 3). The neoplastic cells were strongly positive for myeloperoxidase, CD33, CD43, and CD34, and partially positive for CD117 and CD68. The patient went on to have a bone marrow biopsy, yielding no clear evidence of medullary ALM. Subsequent cytogenetic testing of breast biopsy specimens demonstrated positive t(16;16)(p13.1;q22) translocation (*GBFβ-MYH11* gene). Fluorine-18 fluorodeoxyglucose positron emission tomography-computed tomography (PET-CT) imaging revealed multiple metabolically active masses in both breasts, as well as metabolic activity in lymph nodes, intestinal wall at the terminal ileum, uterus, bilateral ovaries, left perineum, and left parieto-occipital subcutaneous tissue and muscles.

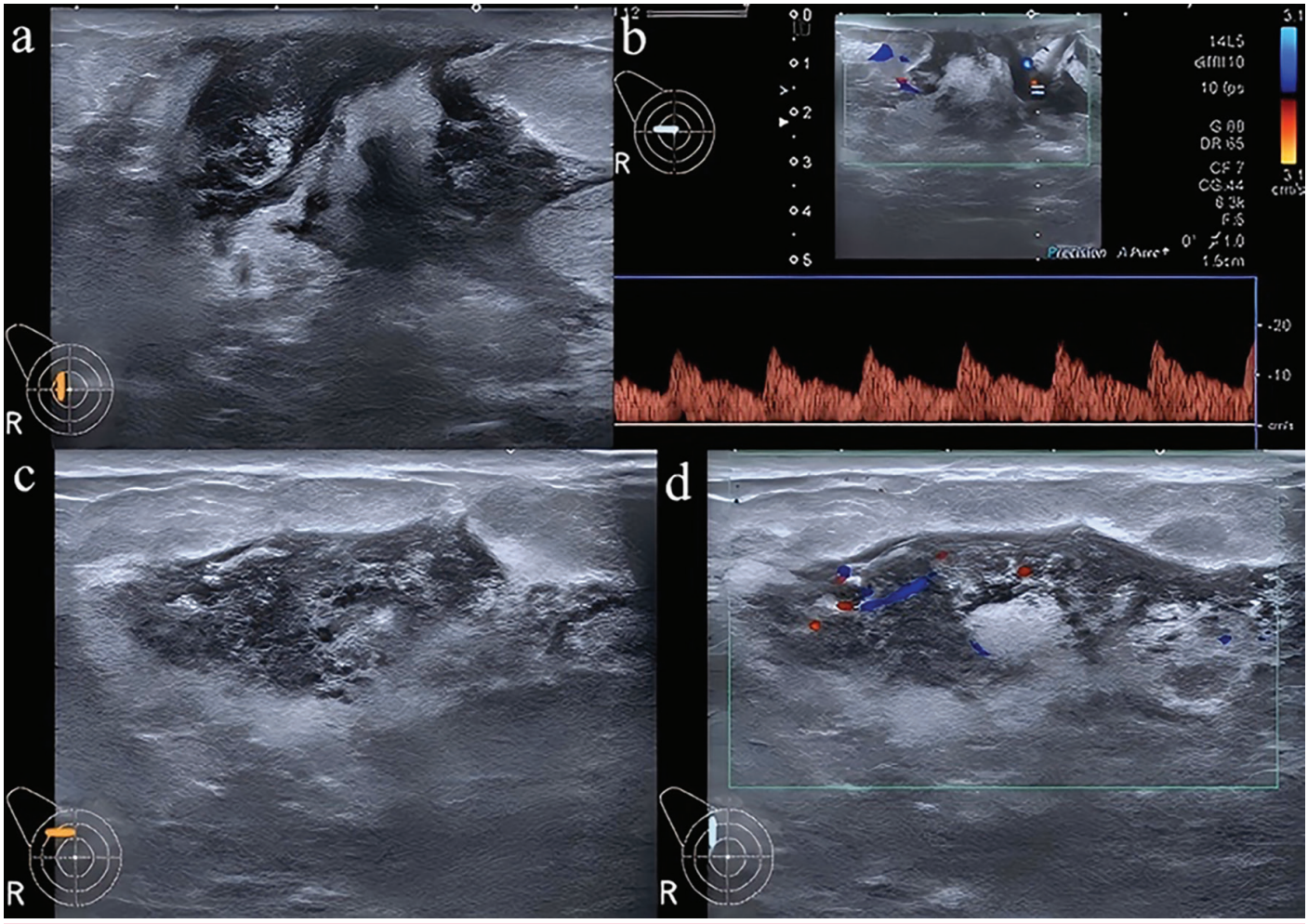

Figure 1. Ultrasound images of the right breast. Ultrasound revealed a non-homogeneous hypoechoic mass in the central retroareolar region (a). Doppler ultrasound revealed that the mass exhibited internal blood flow with a moderate resistance index (b). The second mass was located in the upper outer quadrant (c), with relatively rich internal blood flow signals (d)

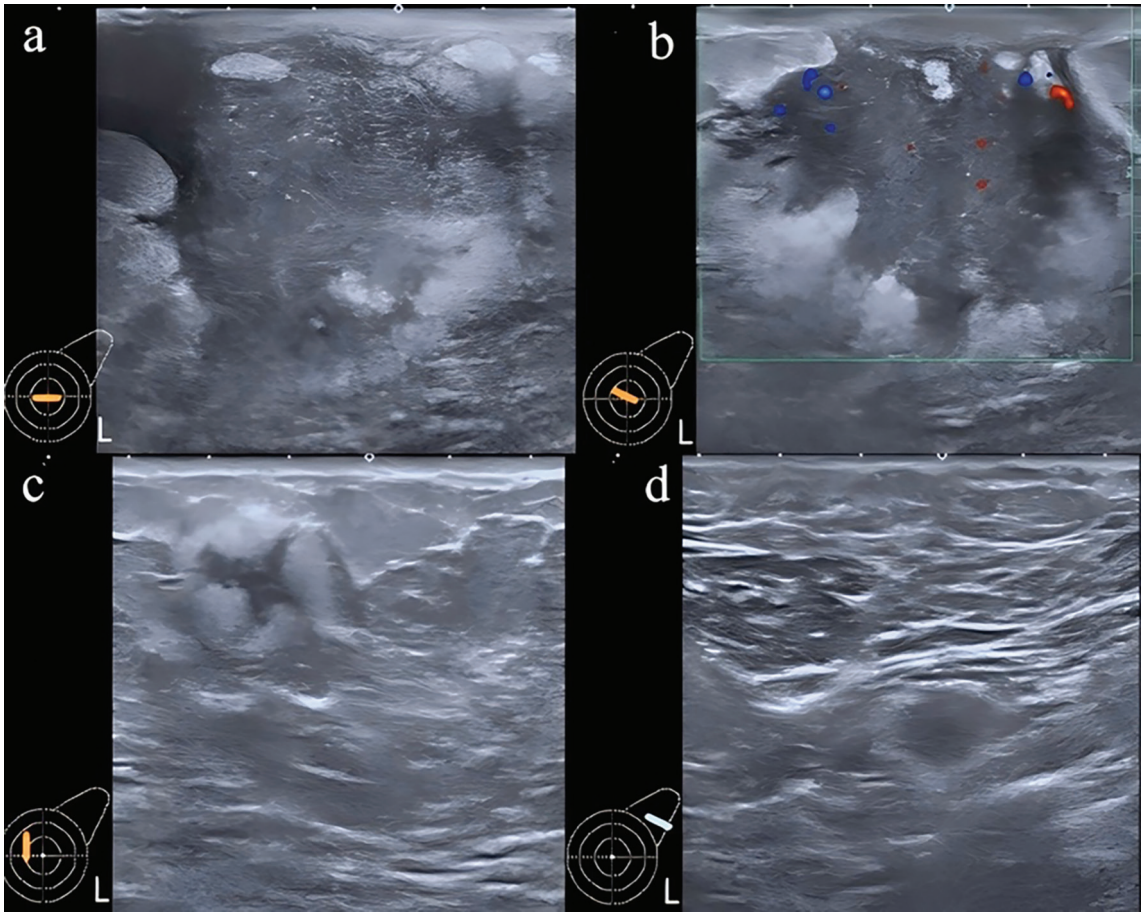

Figure 2. Ultrasound images of the left breast and left axilla. A substantial hypoechoic mass was revealed by ultrasound in the central retroareolar region (a), accompanied by relatively rich internal blood flow signals (b). The second mass was located in the upper inner quadrant (c). An abnormal lymph node was identified in the left axilla (d)

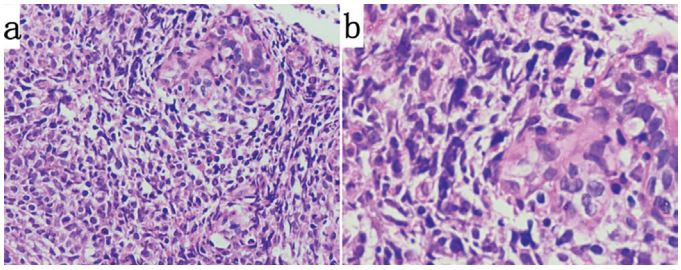

Figure 3. Hematoxylin and eosin-stained sections of the core biopsy showed a diffuse infiltration of intermediate-sized atypical mononuclear cells with ovoid to irregular nuclear contours (a, 200x; b, 400x)

The patient was referred to hematological oncology, where she underwent six cycles of chemotherapy comprising cytarabine and sorafenib. Following the first cycle of chemotherapy, ultrasound imaging demonstrated a notable treatment response (Figure 4). The mass in the upper inner quadrant of the left breast and the left axillary lymph node disappeared. A PET-CT scan, conducted after four cycles of chemotherapy, revealed no evidence of residual tumors. At the latest follow-up in May 2025, the patient was thriving and disease-free.

Discussion and Conclusion

MS is a distinct entity among myeloid neoplasms. It is characterized by the development of tumor masses, consisting of immature myeloid cells at extramedullary sites. MS involving the breast is rare. Breast MS is characterized by the presence of masses in the breast with rapid enlargement. Patients typically present to breast clinics, and breast ultrasound is most frequently utilized.

We reviewed prior literature. Breast MS is always characterized by irregular shape, indistinct margin, and hypoechoic pattern (3-14). Furthermore, the presentation of breast MS may manifest as an oval form with a circumscribed margin (15). The current case adds additional imaging evidence to the limited literature. In this case, the internal echo pattern of the lesions in the left breast was completely hypoechoic, while the lesions in the right breast manifested as non-homogeneous hypoechoic. We

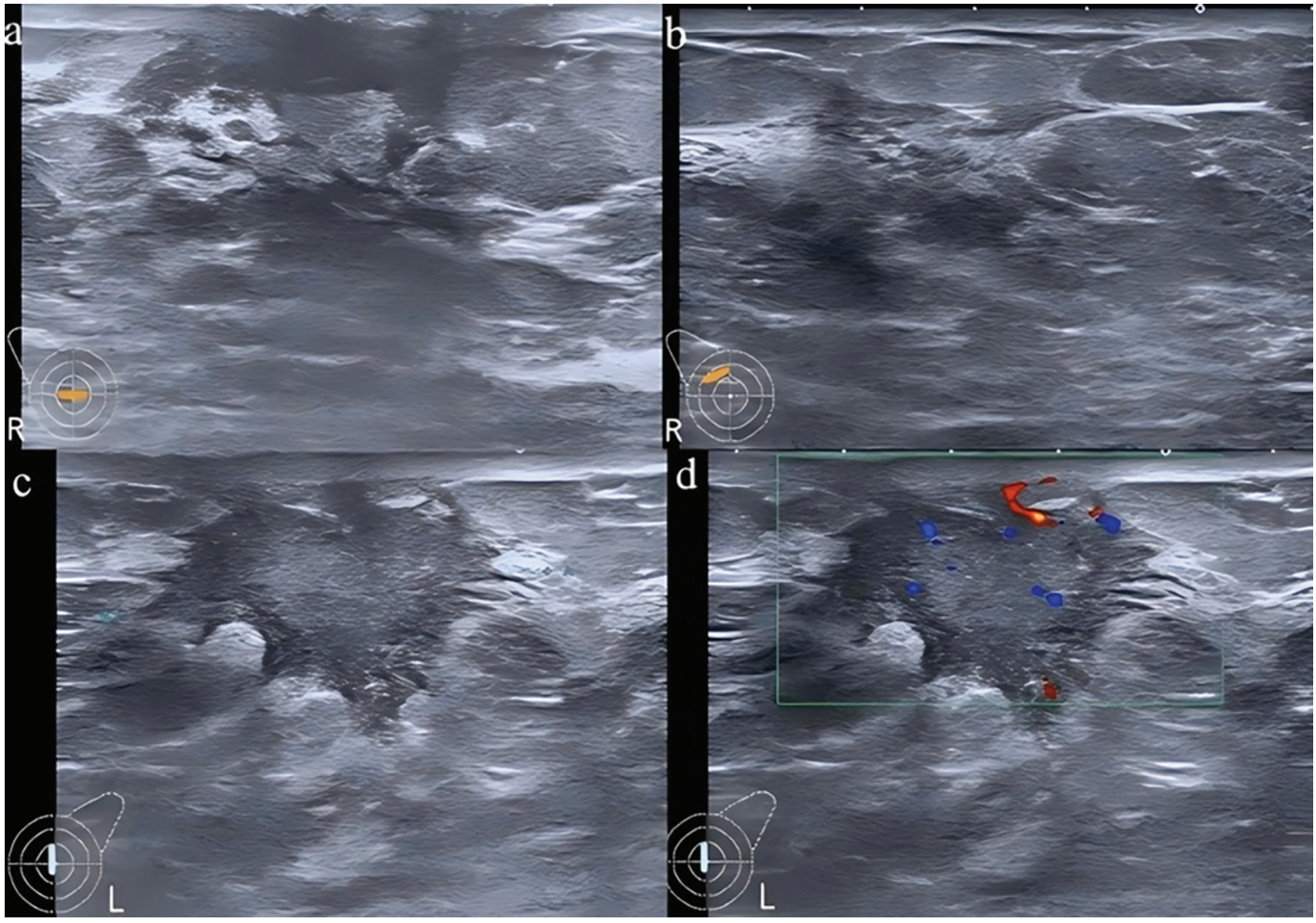

Figure 4. Following the first cycle of chemotherapy, ultrasound imaging demonstrated a notable treatment response in the right breast masses (a, b), as well as a reduction in the size of the central retroareolar mass in the left breast (c). Notably, rich blood flow signals remained observable in the latter (d)

speculated that the internal echo pattern exhibited variability due to the extent of infiltration by immature myeloid cells and the presence of residual lobules and ducts.

Though the relatively non-specific imaging characteristics of breast MS, ultrasound may play a certain role in the initial evaluation. Bilateral breast involvement with multiple masses is comparatively common in breast MS (3, 5, 9-12, 15). Interestingly, in cases involving multiple lesions, ultrasound mass characteristics demonstrate a tendency to manifest similarly (3, 5, 9-12, 15). Echogenic halo is common in breast MS (3-5, 9, 11-14). While calcification is rare in breast MS. Histopathological and immunohistochemical examinations are necessary for confirming the final diagnosis. Following admission to chemotherapy, breast ultrasound is a simple and effective modality for assessing the early therapeutic response.

Though relatively non-specific, breast MS tends to present as irregular, indistinct, and complex hypoechoic masses with internal blood flow on ultrasound. Hyperechoic halos are common. Ultrasound may play a certain role in the initial evaluation and follow-up therapeutic response assessment of breast MS.

Ethics

Informed Consent: The patient provided written informed consent for publication of the data and images in this case report.

Footnotes

Authorship Contributions

Concept: L.L.; Design: L.L., Y.L.; Data Collection or Processing: Z.L., H.Z., Y.Z.; Analysis or Interpretation: Z.L., H.Z., Y.Z.; Literature Search: L.L.; Writing: L.L., Y.L.

Conflict of Interest: No conflict of interest was declared by the authors.

Financial Disclosure: The authors declared that this study received no financial support.

References

1. Cunningham I. A clinical review of breast involvement in acute leukemia. Leuk Lymphoma. 2006; 47: 2517-25126. (PMID: 17169796) [Crossref]
2. Ramia de Cap M, Chen W. Myeloid sarcoma: an overview. Semin Diagn Pathol. 2023; 40: 129-139. (PMID: 37149396) [Crossref]
3. Minoia C, de Fazio V, Scognamillo G, Scattone A, Maggialetti N, Ferrari C, et al. Long-lasting remission in de novo breast myeloid sarcoma treated with decitabine and radiotherapy. Diagnostics (Basel). 2019; 9: 84. (PMID: 31357576) [Crossref]
4. Amiraian D, McDonough M, Geiger X. Bilateral myeloid sarcoma of the breast: a case report with radiological and pathological correlation. Cureus. 2022; 14: e24731. (PMID: 35686262) [Crossref]
5. Zhang Z, Chen Y, Zhang R, Liu M. Primary breast myeloid sarcoma: a case report and literature review. Oncol Lett. 2024; 29: 58. (PMID: 39606566) [Crossref]
6. Naamo S, Naamo S, Sarker S, Vasconez M, Froicu M. Breast manifestation of extramedullary myeloid sarcoma: a case report. Radiol Case Rep. 2022; 17: 4660-4665. (PMID: 36204411) [Crossref]
7. Kim SJ, Kim WG. Sonographic features of a myeloid sarcoma of the breast as a relapse of acute myeloid leukemia after stem-cell transplantation: a case report. Am J Case Rep. 2019; 20: 612-619. (PMID: 31030205) [Crossref]
8. Nia ES, Leung JWT. Solitary palpable breast mass as the initial presentation of clinically silent extramedullary acute myeloid leukemia. Breast J. 2020; 26: 267-268. (PMID: 31486164) [Crossref]
9. Sosa YJ, Pope D, Monetto FEP, Robinson A, Klimberg VS. Hematologic malignancies of the breast: report of three cases. Radiol Case Rep. 2022; 17: 1384-1390. (PMID: 35309379) [Crossref]
10. Ozsoy A, Akdal Dolek B, Barca N, Aktas H, Araz L, Kulacoglu S. Ultrasound findings in a case of myeloid sarcoma of the breast. J Belg Soc Radiol. 2016; 100: 15. (PMID: 30151441) [Crossref]
11. Nalwa A, Nath D, Suri V, Jamaluddin MA, Srivastava A. Myeloid sarcoma of the breast in an aleukemic patient: a rare entity in an uncommon location. Malays J Pathol. 2015; 37: 63-66. (PMID: 25890617) [Crossref]
12. Myers CB, Ene A, Clark A. A rare presentation of myeloid sarcoma as symmetrical bilateral breast masses. Clin Imaging. 2022; 85: 94-98. (PMID: 35276439) [Crossref]
13. Le Y, Leng X. Primary granulocytic sarcoma of the breast. Lancet Oncol. 2025; 26: e331. (PMID: 40449507) [Crossref]
14. Wu S, Lin Z, Shang Q, Pang Y, Chen H. Use of 68Ga-FAPI PET/CT for detecting myeloid sarcoma of the breast and assessing early response to chemotherapy. Clin Nucl Med. 2022; 47: 549-550. (PMID: 35025784) [Crossref]
15. Huang C, Fei S, Yao J, Chen P, Luo J, Wang Y, et al. Breast myeloid sarcoma presenting as a palpable breast lump after allogeneic stem cell transplantation for acute myelomonocytic leukemia: a rare case report. World J Surg Oncol. 2021; 19: 289. (PMID: 34579724) [Crossref]

LETTER TO EDITOR

European Journal of BREAST HEALTH

DOI: 10.4274/ejbh.galenos.2026.2025-12-10
Eur J Breast Health 2026;22(3):368-369

Axillary De-Escalation: Precision Matters

Wiebren A. Tjalma[1-3]

[1]Multidisciplinary Breast Clinic, Unit Gynecologic Oncology, Antwerp University Hospital, Edegem, Belgium
[2]Department of Obstetrics and Gynecology, Antwerp University Hospital, Edegem, Belgium
[3]University of Antwerp Faculty of Medicine, Wilrijk, Belgium

Dear Editor,

We read with interest the review by Mukherjee et al. (1) on omission of sentinel lymph node biopsy (SNB) in early-stage breast cancer. The topic is important and evolving. However, several key elements essential for safe clinical implementation are insufficiently defined or omitted in their review. This becomes apparent when the review is considered alongside contemporary guideline recommendations (2).

First, current recommendations do not support a broad or biologically vague omission strategy. They define a highly selected patient population in whom SNB may be safely omitted: postmenopausal women aged ≥50 years, with unifocal invasive ductal carcinoma ≤2 cm, Nottingham grade 1–2, hormone receptor-positive/human epidermal growth factor receptor 2-negative disease, a negative preoperative axillary ultrasound (or a single suspicious node with benign concordant biopsy), planned adjuvant endocrine therapy, and upfront breast-conserving surgery followed by whole-breast radiotherapy (2). In contrast, Mukherjee et al. (1) refer to "low-risk" or "favourable" disease without consistently presenting these criteria as mandatory conditions, thereby risking overextension of the concept.

Second, omission of SNB is explicitly conditioned on the assumption that nodal information would not change adjuvant systemic or radiotherapy decisions. Preoperative multidisciplinary discussion is therefore essential. This safeguard is not highlighted in the review, despite its central role in preventing undertreatment.

Third, the contemporary American Society of Clinical Oncology (ASCO) guideline introduces an important age-specific nuance (2). In patients ≥65 years who otherwise meet omission criteria, radiotherapy after breast-conserving surgery is not mandatory. This distinction, derived from CALGB 9343 and PRIME II, has direct implications for shared decision-making (3, 4). Mukherjee et al. (1) do not address this age-specific consideration and implicitly present radiotherapy as standard, thereby overlooking an established opportunity for further treatment de-escalation in selected older patients.

Fourth, ASCO defines surgery-specific axillary pathways after mastectomy (2). Patients with one to two positive sentinel nodes may omit completion axillary dissection only if postmastectomy regional nodal irradiation is planned. In the absence of such radiotherapy, axillary dissection remains recommended. These decision pathways are only superficially discussed in the review, despite their clear clinical relevance.

Finally, ASCO is explicit about what should not be done: routine SNB for ductal carcinoma in situ treated with breast-conserving surgery is discouraged (2). SNB should not be performed solely to evaluate internal mammary nodes. Nor should SNB replace axillary dissection in inflammatory breast cancer or in the presence of biopsy-proven palpable axillary disease (2). These explicit "red lines" are not systematically highlighted.

Corresponding Author: Wiebren Tjalma MD, PhD, FEBS (Hon), Prof (full);
E-mail: wiebren.tjalma@gmail.com **ORCID:** orcid.org/0000-0002-6618-045X
Received: 31.12.2025 **Accepted:** 07.01.2026 **Available Online Date:** 17.06.2026
Cite this article as: Tjalma WA. Axillary de-escalation: precision matters. Eur J Breast Health. 2026;22(3):368-369

In summary, the review by Mukherjee et al. (1) is timely and informative. However closer alignment with the prescriptive structure of the current recommendations would improve its clinical precision. In axillary de-escalation, nuance is not optional. Precision is the safety net. Clear eligibility criteria, explicit contraindications, and treatment-altering decision points are essential to ensure that "less" surgery truly remains "no less" care.

Footnotes

Financial Disclosure: The author declare that he's received no financial support for this study.

References

1. Mukherjee R, Ranjan P, Singh BK. It is not an obituary of sentinel lymph node biopsy or surgery to axilla, it's a de-escalation of surgery to axilla in early breast cancer: a traditional review. Eur J Breast Health. 2025; 22: 19-24. (PMID: 41447642) [Crossref]
2. Park KU, Somerfield MR, Anne N, Brackstone M, Conlin AK, Couto HL, et al. Sentinel lymph node biopsy in early-stage breast cancer: ASCO guideline update. J Clin Oncol. 2025; 43: 1720-1741. (PMID: 40209128) [Crossref]
3. Hughes KS, Schnaper LA, Bellon JR, et al. Lumpectomy plus tamoxifen with or without irradiation in women age 70 years or older with early breast cancer: long-term follow-up of CALGB 9343. J Clin Oncol. 2013; 31: 2382-2387. (PMID: 23690420) [Crossref]
4. Kunkler IH, Williams LJ, Jack WJL, Cameron DA, Dixon JM. Breast-conserving surgery with or without irradiation in early breast cancer. N Engl J Med. 2023; 388: 585-594. (PMID: 36791159) [Crossref]

LETTER TO EDITOR

European Journal of BREAST HEALTH

DOI: 10.4274/ejbh.galenos.2026.2026-4-6
Eur J Breast Health 2026;22(3):370-371

Comment on: "Robotic and Endoscopic Minimally Invasive Breast Surgery: A Narrative Synthesis on Divergent Global Adoption and Emerging Trends"

Vasileios Kalles[1], Antonio Toesca[2], Apostolos Mitrousias[1], Ioannis Papapanagiotou[1]

[1]Breast Unit, Mediterraneo Hospital, Glyfada, Greece
[2]Division of Breast Surgical Oncology, Candiolo Cancer Institute FPO-IRCCS, Candiolo, Italy

Keywords: Endoscopic mastectomy; handx; learning curve; minimally invasive mastectomy; robotic mastectomy

Dear Editor,

We read with great interest the narrative synthesis by Vidya et al. (1) on divergent global adoption patterns in minimally invasive breast surgery (MIBS). Their review is both timely and important, as it shifts the discussion beyond feasibility, safety, and oncologic non-inferiority toward a more clinically relevant question: how minimally invasive nipple-sparing mastectomy (NSM) can be disseminated effectively across different healthcare systems. The authors demonstrate that minimally invasive mastectomy is not a single entity but a family of procedures shaped by infrastructure, training, the integration of reconstruction, cost, and institutional priorities. This classification provides a valuable framework for understanding robotic and endoscopic NSM as context-dependent solutions.

A particularly insightful aspect is the contrast between robotics-driven adoption in high-income countries and endoscopic innovation at scale in upper-middle-income settings. Robotic NSM, while enabled by advanced platforms and institutional investment, remains resource-intensive and concentrated in specialized centers. In contrast, endoscopic NSM represents a more scalable and cost-conscious solution adaptable to high procedural volumes. This distinction highlights that the evolution of MIBS is driven as much by system-level constraints as by technical capability.

This raises an important implication: the future of MIBS may not rest on a binary choice between conventional endoscopy and full robotic surgery, but on developing intermediate solutions that address the ergonomic limitations of rigid endoscopic instruments without imposing the full infrastructural burden of robotic platforms. This intersects with a key yet underexplored question in breast surgery: whether reproducible, ergonomically improved, and scalable techniques can be developed that bridge the extremes of rigid endoscopy and high-cost robotics.

In our recent technical report, we described single-port endoscopic NSM using a handheld motorized articulating system in selected patients (2). The rationale was straightforward: straight laparoscopic instruments remain limiting, whereas articulating instruments improve angulation and facilitate dissection in constrained planes while preserving direct manual control. We therefore positioned this approach as an intermediate, minimally invasive technique between fully robotic systems and endoscopic techniques." In subsequent work, we emphasized that the central challenge in minimal-access NSM is no longer

Corresponding Author: Vasileios Kalles, MD
E-mail: vassilis_kalles@yahoo.gr **ORCID:** orcid.org/0000-0001-9856-8152
Received: 16.04.2026 **Accepted:** 17.05.2026 **Available Online Date:** 17.06.2026
Cite this article as: Kalles V, Toesca A, Mitrousias A, Papapanagiotou I. Comment on: "robotic and endoscopic minimally invasive breast surgery: a narrative synthesis on divergent global adoption and emerging trends". Eur J Breast Health. 2026;22(3):370-371

feasibility alone, but technical reproducibility and ergonomic sustainability (3).

This perspective is also consistent with contemporary outcome data. Minimally invasive NSM has been shown to achieve oncologic outcomes comparable to conventional approaches (4), while emerging prospective data suggest non-inferior—and in some analyses lower—early postoperative complication rates (5). These findings extend the relevance of minimal-access techniques beyond cosmetic benefit, reinforcing the importance of expanding access through reproducible and scalable approaches.

Seen through the lens of Vidya et al. (1), the "middle-ground" concept is not a niche technical curiosity, but a direct response to the health-system challenges they describe. If robotic NSM remains concentrated in well-resourced centers and endoscopic NSM represents the more scalable option, technologies that enhance endoscopic ergonomics without requiring a full robotic program may facilitate broader dissemination.

Importantly, this relevance is not purely economic. The authors highlight that learning curves, structured training pathways, and institutional experience are central to safe adoption (1). Outcomes improve with experience, yet training frameworks and reporting remain inconsistent. This underscores that the challenge is not whether the procedure can be performed but whether it can be standardized, taught, and reproduced beyond early-adopter centers.

For this reason, ergonomics and reproducibility should be viewed as global safety issues rather than technical refinements. A technically elegant operation that cannot be reliably reproduced will have limited impact. In contrast, reproducible workflows that integrate into existing endoscopic infrastructure may expand access to safe surgery more broadly (3).

Another strength of the study is its avoidance of technological triumphalism. By highlighting that the evolution of MIBS is driven "not only by technical feasibility but increasingly by system-level determinants," the authors redirect attention from platforms to processes (1). In this context, intermediate articulating technologies should be viewed not as alternatives to robotics, but as complementary tools within a spectrum of solutions.

Ultimately, we agree with the authors that the future of MIBS will depend on more than technical proof of concept. Reproducibility, training, and context-sensitive implementation will be equally important. Between rigid endoscopy and full robotics, there exists a space where ergonomically improved and scalable solutions may help extend the benefits of minimally invasive NSM more safely and globally.

Footnotes

Authorship Contributions

Surgical and Medical Pracites: V.K., A.T., A.M., I.P.; Concept: V.K., A.T., A.M., I.P.; Design: V.K., A.T., I.P.; Data Collection and Processing: V.K., A.M., I.P.; Analysis and/or Interpretation: V.K., A.T., A.M., I.P.; Literature Search: V.K., A.M., I.P.; Writing: V.K., A.T.

Conflict of Interest: The authors have no conflicts of interest to declare.

Financial Disclosure: The authors declared that this study has received no financial support.

References

1. Vidya R, Yadav SK, Bipte S, Ryu JM, Ning Goh SS. Robotic and endoscopic minimally invasive breast surgery: a narrative synthesis on divergent global adoption and emerging trends. J Robot Surg. 2026; 20: 412. (PMID: 41933257) [Crossref]
2. Kalles V, Mitrousias A, Vlachogiorgos A, Tsoti SM, Kaklamanis L, Gkiaourakis M, et al. Single-port endoscopic nipple-sparing mastectomy using a handheld motorized articulating system: technical description and initial outcomes. Ann Surg Oncol. 2026. (PMID: 41832360) [Crossref]
3. Kalles V, Mitrousias A, Vlachogiorgos A, Toesca A, Papapanagiotou I. ASO author reflections: enhancing technical reproducibility and ergonomics in single-port endoscopic nipple-sparing mastectomy. Ann Surg Oncol. 2026; 33: 5620-5621. (PMID: 41913019) [Crossref]
4. Kim JH, Ryu JM, Bae SJ, Ko BS, Choi JE, Kim KS, et al.; Korea Robot-endoscopy Minimal Access Breast Surgery Study Group. Minimal access vs conventional nipple-sparing mastectomy. JAMA Surg. 2024; 159: 1177-1186. Erratum in: JAMA Surg. 2025; 160: 115. (PMID: 39141399) [Crossref]
5. Park HS, Ryu JM, Lee J, Lee J, Ko B, Kim JH, et al. Postoperative complication rates of minimally invasive mastectomy compared to conventional mastectomy: a prospective multicenter cohort study (MARRES) [abstract]. In: Proceedings of the San Antonio Breast Cancer Symposium 2025; 2025; San Antonio, TX, USA. Philadelphia (PA): American Association for Cancer Research (AACR). Clin Cancer Res. 2026; 32(4 Suppl): Abstract RF1-01. [Crossref]